CELLULAR AND MOLECULAR STUDIES OF POSTEMBRYONIC MUSCLE FIBRE RECRUITMENT IN ZEBRAFISH (*DANIO RERIO* L.)

Hung-Tai Lee

A Thesis Submitted for the Degree of PhD
at the
University of St. Andrews

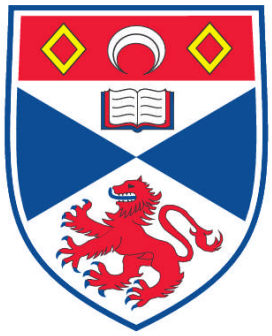

2010

Cellular and Molecular Studies of Postembryonic Muscle Fibre Recruitment in Zebrafish (*Danio rerio* L.)

Submitted to the University of St. Andrews for the degree of Doctor of Philosophy

by

Hung-Tai Lee (BSc., MSc.)

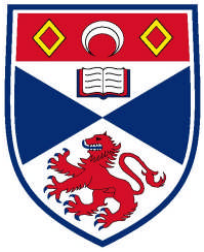

Thesis Supervisor
Professor Ian Alistair Johnston
Scottish Oceans Institute
School of Biology
University of St. Andrews
St. Andrews
Fife KY16 8LB

January 2010

Table of contents

Declaration

I, Hung-Tai Lee, hereby certify that this thesis, which is approximately 42,000 words in length, has been written by me, that it is the record of work carried out by me and that it has not been submitted in any previous application for a higher degree.

I was admitted as a research student in Oct, 2003 and as a candidate for the degree of Doctor of Philosophy in Oct, 2004; the higher study for which this is a record was carried out in the University of St Andrews between 2003 and 2009.

date ……. signature of candidate ……..

I hereby certify that the candidate has fulfilled the conditions of the Resolution and Regulations appropriate for the degree of Doctor of Philosophy in the University of St Andrews and that the candidate is qualified to submit this thesis in application for that degree.

date……. signature of supervisor ……..

In submitting this thesis to the University of St Andrews we understand that we are giving permission for it to be made available for use in accordance with the regulations of the University Library for the time being in force, subject to any copyright vested in the work not being affected thereby. We also understand that the title and the abstract will be published, and that a copy of the work may be

made and supplied to any bona fide library or research worker, that my thesis will be electronically accessible for personal or research use unless exempt by award of an embargo as requested below, and that the library has the right to migrate my thesis into new electronic forms as required to ensure continued access to the thesis. We have obtained any third-party copyright permissions that may be required in order to allow such access and migration, or have requested the appropriate embargo below.

The following is an agreed request by candidate and supervisor regarding the electronic publication of this thesis:

Access to Printed copy and electronic publication of thesis through the University of St Andrews.

date……

signature of candidate ……

signature of supervisor ……

Acknowledgements

Firstly, I would like to thank Professor Ian Johnston for offering me the opportunity to carry out this interesting PhD project under his supervision. I sincerely appreciate for all his patience, guidance, and full support as always.

Secondly, I would like to thank all past and current members of Fish Muscle Research Group / Physiological and Evolutionary Genomics Laboratory for all their kind helps. More specifically, I would like to express my gratitude to the following colleagues: Dr. Jorge Fernandes for his guidance to molecular biology techniques and valuable discussion; Dr. Daniel Macqueen for improving the quality of this thesis with his incredible patience and critical comments; Dr. Ørjan Hagen for generously inviting me as a guest speaker to share my studies at Bodø University College in Norway; Dr. Xuejun Li for offering me a comfortable place to keep me in a good shape during my writing up; Mrs. Marguerite Abercromby for her guidance to my cell biology techniques as well as inviting me to join Christmas dinner with her family; Dr. Vera Vieira-Johnston for her positive and warm messages as always.

Thirdly, I would also like to thank Dr. Shin-Chieh Tzeng, Dr. Chih-Mei Kao, Dr. Shu-Ying Ye, Ms. Chi-Ling Chen, Ms. Chien-Yu Huang, Ms. Lin-Ye Cao, Ms. I-Chun Chou, Dr. Ewan Drylie, and Ms. Margaret Humfrey for sharing numerous memorable moments together and making me feel more confident with my studies in St. Andrews. Additionally, I would like to thank Dr. Bao-Quey Huang, Dr. Shoou-Jeng, Dr. Ming-An Lee, Dr. Cheng-Hsin Liao, Mr. Shang-Chien Li, Dr. Yuan-Chih Lin, Dr. Hua-Hsun Hsu, and Ms. Shu-Min Tseng for their continous encouragements and supports from Taiwan.

Finally, my deepest gratitude goes to my parents (Wen-Ching and Mei-Yueh), sister (Meng-Jen), and brother (Sheng-Feng) for their endless love, encouragement, and support.

Abstract

Cellular and molecular mechanisms of postembryonic muscle fibre recruitment were investigated in zebrafish (*Danio rerio* L.), a standard animal model for developmental and genetic studies.

Distinct cellular mechanisms of postembryonic muscle fibre recruitment in fast and slow myotomal muscles were found. In slow muscle, three overlapping waves of stratified hyperplasia (SH) from distinct germinal zones sequentially contributed to a slow and steady increase in fibre number (FN) through the life span. In fast muscle, SH only contributed to an initial increase of FN in early larvae. Strikingly, mosaic hyperplasia (MH) appeared in late larvae and early juveniles and remained active until early adult stages, accounting for >70% of the final fibre number (FFN).

The molecular regulation of postembryonic muscle fibre recruitment was then studied by characterising *myospryn* and *cee*, two strong candidate genes previously identified from a large scale screen for genes differentially expressed during the transition from hyperplastic to hypertrophic muscle phenotypes. Zebrafish *myospryn* contained very similar functional domains to its mammalian orthologues, which function to bind to other proteins known to regulate muscle dystrophy. Zebrafish *myospryn* also shared a highly conserved syntenic genomic neighbourhood with other vertebrate orthologues. As in mammals, zebrafish *myospryn* were specifically expressed in striated muscles. Zebrafish *cee* was a single-copy gene, highly conserved among metazoans, ubiquitously expressed across tissues, and did not form part of any wider gene family. Its protein encompassed a single conserved domain (DUF410) of unknown function although knock-down of *cee* in *C. elegans* and yeast have suggested a role in regulating growth patterns. Both *myospyrn* and *cee* transcripts were up-regulated concomitant

with the cessation of postembryonic muscle fibre recruitment in zebrafish, indicating a potential role in regulating muscle growth. Furthermore, a genome-wide screen of genes involved in the regulation of postembryonic muscle fibre recruitment was performed using microarray. 85 genes were found to be consistently and differentially expressed between growth stages where muscle hyperplasia was active or inactive, including genes associated with muscle contraction, metabolism, and immunity. Further bioinformatic annotation indicated these genes comprised a complex transcriptional network with molecular functions, including catalytic activity and protein binding as well as pathways associated with metabolism, tight junctions, and human diseases.

Finally, developmental plasticity of postembryonic muscle fibre recruitment to embryonic temperature was characterised. It involved transient effects including the relative timing and contribution of SH and MH, plus the rate and duration of fibre production, as well as a persistent alteration to FFN. Further investigation of FFN of fish over a broader range of embryonic temperature treatments (22, 26, 28, 31, 35°C) indicated that 26°C produced the highest FFN that was approximately 17% greater than at other temperatures. This finding implies the existence of an optimal embryonic temperature range for maximising FFN across a reaction norm. Additionally, a small but significant effect of parental temperature on FFN (up to 6% greater at 24 and 26°C than at 31°C) was evident, suggesting some parental mechanisms can affect muscle fibre recruitment patterns of progeny.

This work provides a comprehensive investigation of mechanisms underlying postembryonic muscle fibre recruitment and demonstrates the power of zebrafish as an ideal teleost model for addressing mechanistic and practical aspects of postembryonic muscle recruitment, especially the presence of all major phases of muscle fibre production in larger commercially important teleost species.

Chapter 1.0 General Introduction

1.1 Zebrafish (*Danio rerio* L.)

1.1.1 The emergence of zebrafish in the scientific world

During the past few decades, zebrafish has emerged as one of the most important and popular experimental animals for the scientific community. According to the zebrafish information network (ZFIN) (Sprague et al., 2001, 2006), there are more than 500 world-wide research groups that use this animal as a model system to address various research topics ranging from basic to applied science (Fig. 1.1).

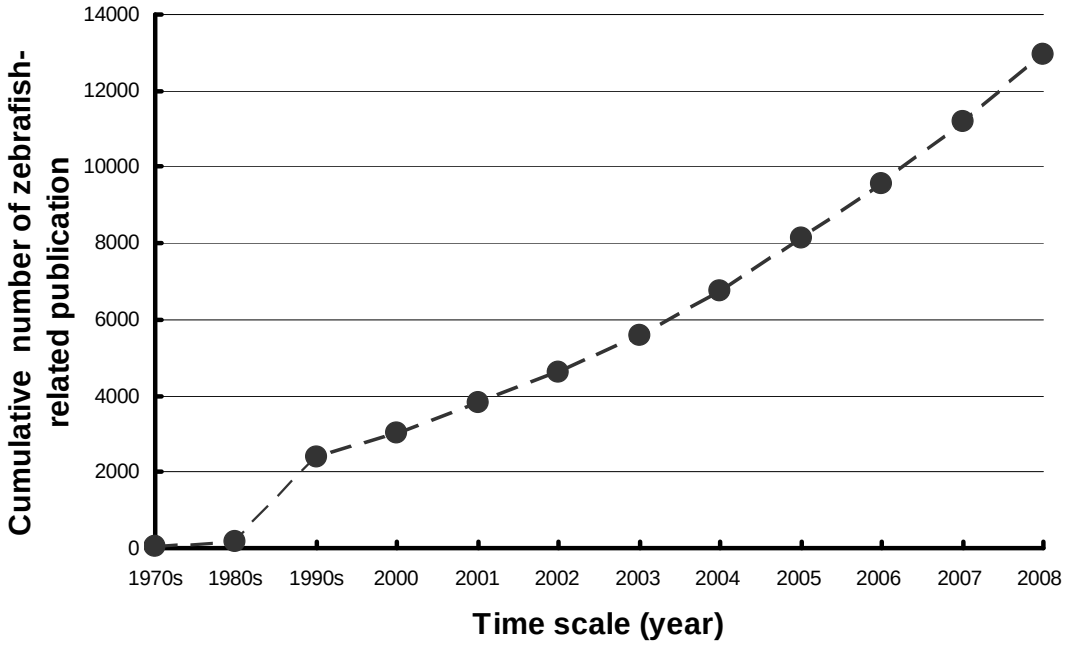

Fig. 1.1 The cumulative number of zebrafish-related publications between 1970 and 2008 searched from ISI Web of Knowledge database using zebrafish as the keyword. A notable increase in the number of zebrafish-related publication occurred in the 1990s and this trend has continued.

1.1.2 Geographic distribution and natural habitats

Zebrafish is a tropical species taxonomically classified as a member of the Cyprinidae family representing the largest family of freshwater fish and vertebrates with over 2000 species (Nelson, 1994, 2006). Despite its global availability, wild zebrafish has a natural geographic distribution centred near river basins in north-eastern India, Bangladesh and Nepal (Fig. 1.2).

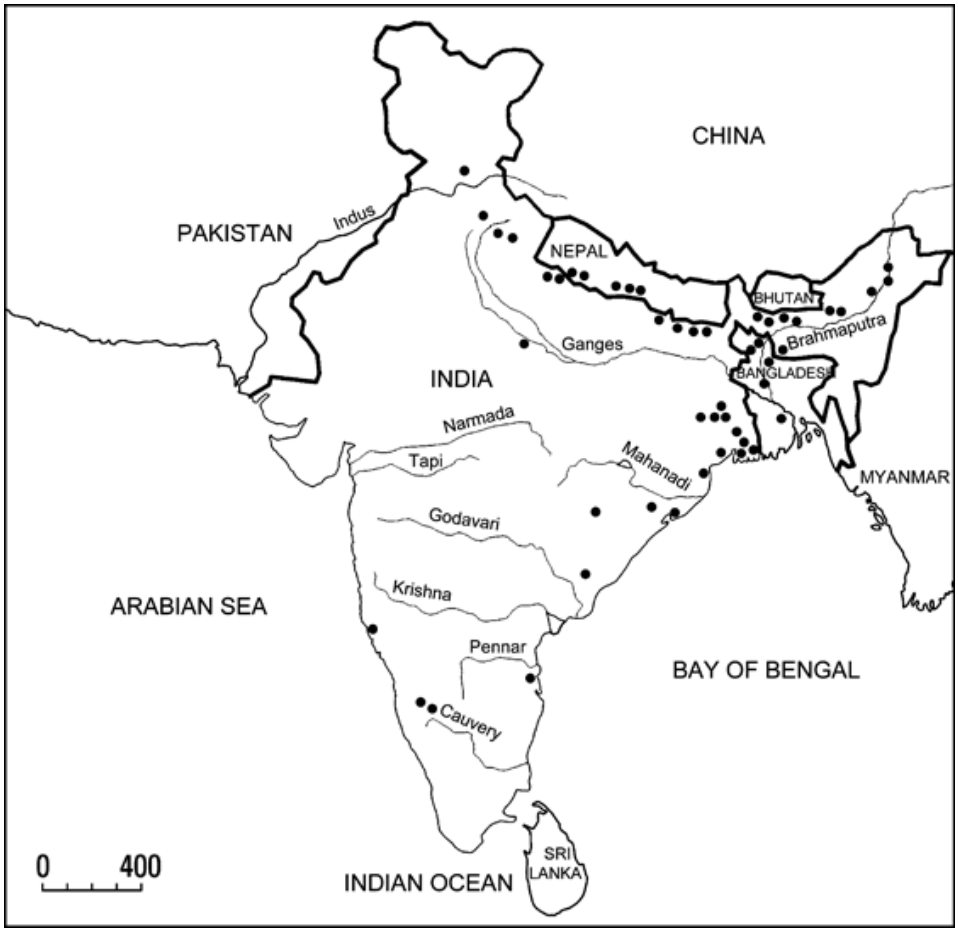

Fig. 1.2 Geographic distribution of zebrafish. Black dots indicate recorded occurrences of zebrafish (Taken from from Spence et al., 2008).

In the wild, zebrafish generally inhibits in shallow and slow-moving water varying between 16.0 and 38.6ºC (Engeszer et al., 2007; Spence et al., 2008). These habitats generally contain aquatic vegetation and a slity substratum in floodplains (McClure, 2006; Spence, 2006; Engeszer et al., 2007). Wild zebrafish can grow to 4-5 cm in standard length (SL) although they often tend to grow even bigger and faster when being maintained in captivity (Spence et al., 2008).

1.1.3 Zebrafish as a model vertebrate

There are several important features of zebrafish making it an ideal experimental animal (Fig. 1.3). Differences in the appearance between male and female zebrafish are easily distinguishable (Fig. 1.3A). In the laboratory, a pair of zebrafish can produce approximately 30-50 embryos per spawning, possible 2-3 times a week, throughout the whole year depending on the level of maturity (Fig. 1.3A). Zebrafish eggs are transparent and relative large (~0.7 mm in diameter) compared to other teleost of a similar size (Fig. 1.3A). Embryogenesis is rapid and all major organs develop within 24 hr (Fig. 1.3A). The generation time is also relatively short requiring 3-4 months (Fig. 1.3A). Therefore, it was possible use to zebrafish for the first vertebrate large-scale genetic screens which generated a large number of mutants with various phenotypes (Fig. 1.3B) (Driever et al., 1996; Haffter et al., 1996). A comprehensive range of powerful tools and research resources specific to zebrafish have been established and are publicly available through the World Wide Web (Table 1.1).

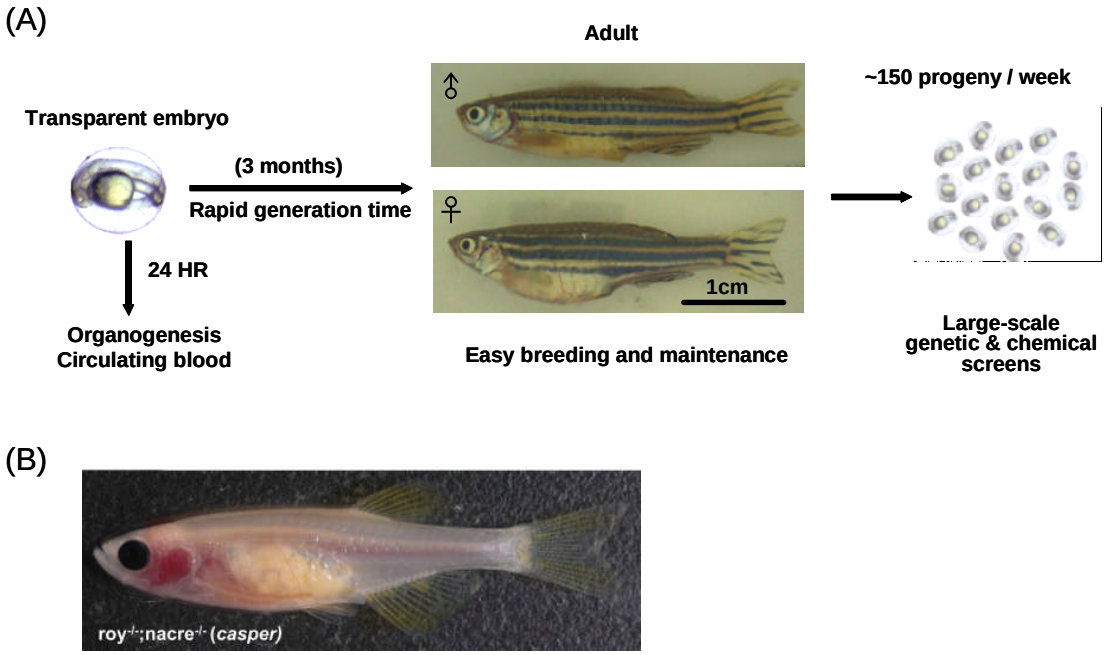

Fig. 1.3 The utilisation of zebrafish as model system. (A) General features of zebrafish that make them excellent laboratory models. (B) Transparent adult zebrafish mutant (named *casper*) with the combined features of *nacre* (complete lack of melanocytes) and *roy* mutants (complete lack of iridophores, uniformly pigmented eyes, sparse melanocytes, and a translucency of the skin) (Adapted from White et al, 2008).

Table 1.1 Representive zebrafish resources avaliable in the world wide web

Host/resource	Description	Website
Animals		
Mutant and transgenic	Mutant and transgenic zebrafish via ZFIN database	http://zfin.org/cgi-bin/webdriver?MIval=aa-fishselect.apg&line_type=mut
Strains	Zebrafish strains via ZFIN database	http://zfin.org/cgi-bin/webdriver?MIval=aa-wtlist.apg
Mutant stocks	Zebrafish stock center (Max Plank Institute)	http://www.eb.tuebingen.mpg.de/services/stockcenter/zebraf_stockcenter.h
Genes/clones/genomic maps		
Genes, markers, clones	Searchable by accession number and name via ZFIN	http://zfin.org/cgi-bin/webdriver?MIval=aa-newmrkrselect.apg
Zebrafish gene collection	NIH initiative that provides full length ORF sequences and cDNA clones of expressed sequences via NCBI database	http://zgc.nci.nih.gov/
Genome sequencing	The Sanger Institutevia the Ensembl website.	http://www.ensembl.org/Danio_rerio/
Genetic maps	Graphical views of genetic, radiation hybrid or consolidation maps via ZFIN	http://zfin.org/cgi-bin/mapper_select.cgi
miRBase	microRNA database	http://www.mirbase.org/
Expression profiling		
Gene expression	Searchable using a range of parameters viz ZFIN database	http://zfin.org/cgi-bin/webdriver?MIval=aa-xpatselect.apg
Norwegian microarray consortium (NMC)	Academically developed zebrafish oligonucleotide microarray: 16399 oligos probes (65-mers).	http://www.microarray.no
Anatomy		
Anatomy database	Searching zebrafish anatomical ontology via ZFIN database	http://zfin.org/cgi-bin/webdriver?MIval=aa-anatdict.apg&mode=search
Anatomical maps	Anatomical and developmental maps via ZFIN database	http://zfin.org/zf_info/anatomy/dict/sum.html
General/newsgroups		
Zebrafish book	Online version of 'The Zebrafish Book: A guide for the laboratory use of Zebrafish (Danio rerio)' 4th edn, Westerfield, 2000.	http://zfin.org/zf_info/zfbook/zfbk.html
Zebrafish information network	A scientific newsgroup dedicated to discussion of Zebrafish.	http://groups-beta.google.com/group/bionet.organisms.zebrafish?hl=en
Zebrafish	The only peer-reviewed journal to focus on the zebrafish model.	http://www.liebertonline.com/loi/zeb
ZF-MODELS IP (EU FP6)	A resource that acquires knowledge and technology in the form of disease models, drug targets and insight into pathways of gene regulation applicable to human development and disease.	http://www.zf-models.org/

1.2 Fish muscle as an important food resource

Skeletal muscle is the most abundant tissue in teleost that accounts for up to 60~70% of the body mass (Weatherly and Gill, 1985) and constitutes the main edible part. The latest reports indicate that more than 110 million tonnes (77%) of world fish production is used for direct human consumption and the remaining 33 million tonnes is used for non-food products, particularly the manufacture of fishmeal and fish oil (FAO, 2008). Furthermore, fish has also been reported to be an important source of food providing high-value protein as well as offering a wide range of essential micronutrients, minerals and fatty acids. In general, the Food and Agriculture Organization (FAO) estimates that fish supplies more than 1.5 billion people with approximately 20% of their average per capita intake of animal protein and nearly 3.0 billion people with 15% of such protein. Remarkably, fish contributes at least 50 % of total animal protein intake in some countries and areas such as Bangladesh, Cambodia, and Equatorial Guinea (FAO, 2008). While capture fisheries has provided a major contribution to world fish production in the past 4 decades, the world fish production from aquaculture has dramatically risen from less than 1 million tonnes per year in the early 1950s to 51.7 million tonnes in 2006, and currently accounts for 47% of world fish production (FAO, 2006, 2008) and this proportion is increasing year by year.

1.3 General features of myotomal muscle of teleost fish

1.3.1 Structure and arrangement of teleost muscle

In teleosts, skeletal muscle is arranged into segmental myotomes in a complex three-dimensional structure (Fig. 1.4A). Muscle fibres located at the lateral surface of the myotomes run parallel to the body axis whilst fibres in deeper region of the myotomes have a helical arrangement (Fig. 1.4A). This distinct arrangement of muscle fibres is related to the requirement to produce equal shortening of sacromeres at different body flexures (Alexander, 1969; Rome and Sosnicki, 1990).

1.3.2 Muscle fibre types

In general, teleost muscle can be broadly classified as slow, intermediate or fast based on different morphological and physiological characteristics (reviewed in Sanger and Stoiber, 2001). The majority of myotomal muscle is composed of slow and fast muscle fibres (Fig. 1.4Bi, ii, iii). Intermediate muscle fibres, are found in some teleost species during the juvenile and adult stages (Fig. 1.4B iii),

The slow muscle, or “red” muscle, is composed of “slow twitch” fibres, which are usually comparatively smaller in diameter than the other types of myotomal muscle fibres (Greer-Walker and Pull, 1975; Altringham and Johnston, 1988). Slow muscle fibres are located in a narrow superficial strip adjacent to the lateral line with a wedge-shaped thickening in the region of the horizontal septum (HS) (Fig. 1.4B).

They constitute a relatively small proportion of the total cross-sectional area of the myotome in any given teleost species (Greer-Walker and Pull, 1975). The proportion of the cross-sectional area containing slow muscle fibres varies along the fish length. For example, the largest cross-sectional area of slow muscle fibres occurs at 60% of total body length in scup (*Stenostomus chrysops*) where the proportion of the cross-sectional area varies from 1.37% to 8.42% moving caudally along the length of the scup (Zhang et al., 1996). Furthermore, a higher proportion of slow muscle is mostly present in teleosts exhibiting a more active mode of life (Greer-Walker and Pull, 1975). In addition, slow muscle fibres are also widely found to contract slowly (Altringham and Johnston, 1982; Johnston and Salmonski, 1984; Langfeld et al., 1989), contain high volume densities of mitochondria (Johnston, 1982; Egginton and Sidell, 1989; Sanger and Stoiber, 2001), and are supplied with a dense capillary network (Egginton and Sidell, 1989; Sanger and Stoiber, 2001). All these distinct features of slow muscle fibres reflect their functional role in steady and sustained swimming activities fuelled by aerobic metabolism (Johnston et al., 1977; Rome et al., 1984; Altringham and Ellerby, 1999).

The fast muscle, termed white muscle, is composed of fast twitch fibres, which are usually larger in diameter than slow muscle fibres and constitute the majority of myotomes (70-100%) in teleosts (Greer-Walker and Pull, 1975; Altringham and Johnston, 1988). In contrast to slow muscle fibres, the fast muscle fibres contain a low density of mitochondria (Johnston, 1982; Egginton and Sidell, 1989; Sanger and Stoiber, 2001) and have a sparse capillary network (Johnston, 1982; Egginton and Sidell, 1989; Sanger and Stoiber, 2001). Fast muscle fibres contract and fatigue

faster than other fibre types (Altringham and Johnston, 1982; Johnston and Salmonski, 1984; Langfeld et al., 1989). They are recruited to power rapid bursts of movement e.g. escape responses when a predator appears (Altringham et al., 1993; Altringham and Ellerby, 1999).

The intermediate, or pink muscle, is composed of intermediate twitch muscle fibres, which are usually intermediate in diameter and constitute 10%~20% of total teleost myotomal cross-sectioned area (Johnston et al., 1977; Langfeld et al., 1989). They are located between the slow and fast muscles and have intermediate contraction speeds and fatigue-resistance compared to slow and fast muscle fibres (Altringham et al., 1993; Altringham and Ellerby, 1999). Intermediate muscles power high speed sustained swimming usually less than 200 min duration (Altringham et al., 1993; Altringham and Ellerby, 1999).

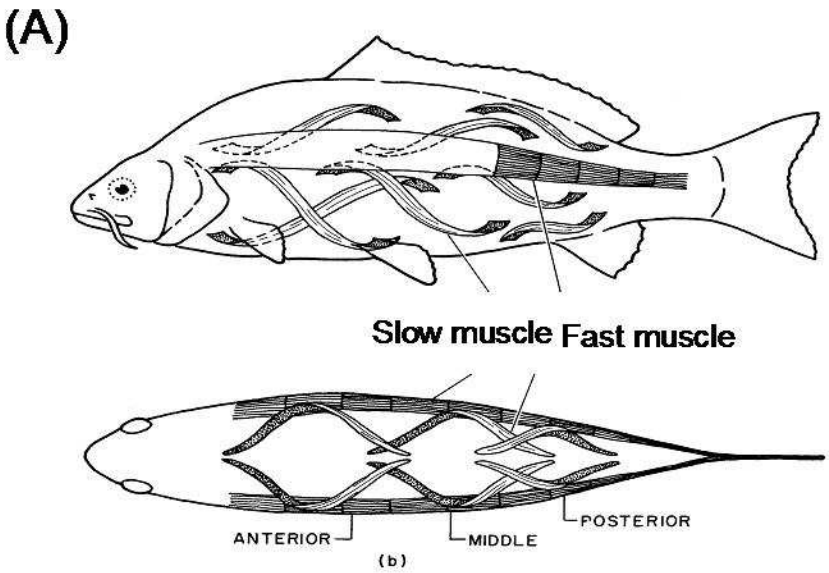

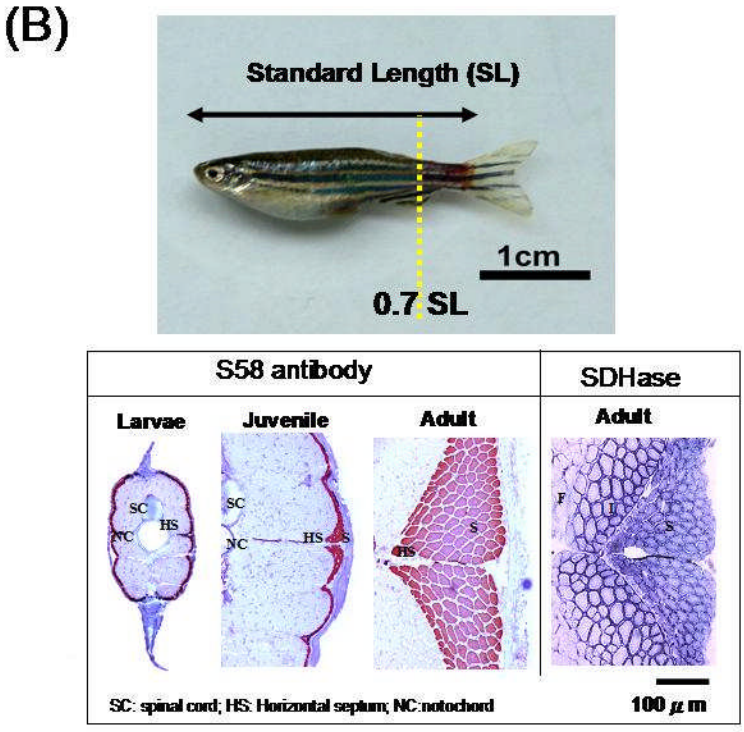

Fig. 1.4 Structure and composition of teleost muscle. (A) Arrangement of muscle fibres with the myotome (Adapted from Rome and Sosnicki, 1990). (B) An example of different muscle fibre types within teleost myotome muscle. Slow, intermediate, and fast muscle fibres from zebrafish myotome at 70% of standard length are revealed and distinguished by their specificities of S58 antibody (specific to slow muscle fibres) and SDHase enzyme (strong, morderate, and weak activity in slow, intermediate, and fast muscle fibres, respectively). Slow (S), Intermediate (I), and fast muscle (F).

1.4 Teleost myogenesis

1.4.1 Introduction

Myogenesis refers to the process required for muscle development and growth, which involves the generation of new muscle fibres (hyperplasia) and expansion of existing muscle fibres (hypertrophy). This process is common to all vertebrates and consists of serial complex cell events, including the specification, activation, proliferation, differentiation, migration and fusion of the cells (Fig. 1.5).

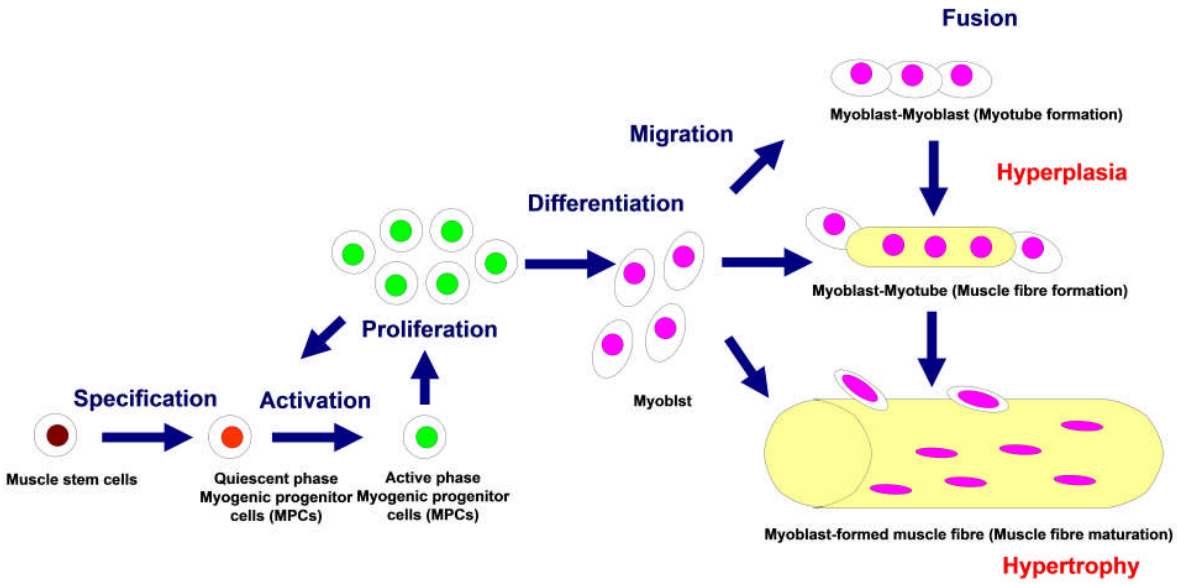

Fig. 1.5 A simple and general model for vertebrate myogenesis (Adapted from Johnston, 2006).

Three major phases of myogenesis have been observed in a variety of teleost species, namely embryonic myogenesis, stratified hyperplasia (SH), and mosaic hyperplasia (MH) (Rowlerson and Veggetti 2001; Johnston, 2006). The relative

timing and importance of individual phases vary considerably between species. In species with determinate growth that have a small maximum body size such as guppies (*Poecilia reticulate*) (Veggetti et al. 1993), the first two phases of myogenesis give rise to the majority of muscle fibres. On the other hand, MH gives rises to the majority of muscle fibres in species which show indeterminate growth and reach a large body size (Johnston, 2006). Current understandings of these three major phases of myogenesis are reviewed in the followining sections.

1.4.2 Embryonic myogenesis: Somite formation

Skeletal muscle of the vertebrate body is initially derived from the somites, segmental blocks of paraxial mesoderm, with the exception of the anterior head muscles, which are derived from perchordal and paraxial head mesoderm (Noden, 1991; Couly et al., 1992). The process of somitogenesis in teleosts is similar to that in amphibians, birds, and mammals that is highly conserved within these vertebrates (Kimmel et al., 1995; Pourquié 2001). In teleost, “shield cells” of the embryo, functionally equivalent to the “Spearmann organizer” of amphibians and “Hensen’s node cells” in the chick, first give rise to notochord and precaudal plate in the axial mesoderm (Hill and Johnston, 1997; Stickney et al., 2000). Then the paraxial mesoderm, the mesoderm adjacent to the central body axis, develops from cells around the margin of the germ ring that migrate toward dorsal side, where the somites form and condense (Kimmel et al., 1990). Further diversification of the paraxial mesoderm, and its segmentation into somites, are highly dependant on the axial structures (Lassar and Munsterberg 1996). The onset of somitogenesis varies with respect to epiboly between different species, the process proceeds in a

rostral-caudal gradient as the paraxial mesoderm is segmented into bilaterally symmetrical, epithelial-bound blocks of cells (Kimmel et al., 1995; Stickney et al., 2000; Pourquié 2001). In normal vertebrate embryonic development, somites form from the segmental plate (presomitic mesoderm) and rapidly divide to give rise to two main substructures, a ventral sclertome compartment and a dorsally located epithelial dermomyotome (Pourquié 2001). Within the teleost somite, however, the ventral sclerotome, which will form the axial bone and cartilage of the embryo, is greatly reduced compared with terrestrial vertebrates (Kimmel et al., 1995; Stickney et al., 2000). This may reflect the reduced demand for the supporting skeleton as well as an increased locomotory requirement for axial muscle rather than appendicular muscle in an aqueous environment (Bone, 1966).

1.4.3 Embryonic myogenesis: Embryonic slow and fast muscle fibre formation

Pioneering work establishing patterns of teleost embryonic muscle development was largely performed in zebrafish. Devoto *et al.* (1996) firstly demonstrated the spatial separatation of teleost muscle types occur in the embryo, where slow and fast muscle fibres originate from two separate subpopulations of muscle pioneers (adaxial cells and lateral presomitic cells) in the somites. These two cell populations, the adaxial and lateral presomitic cells, can be distinguished in the segmental plate on the basis of their position and morphologies (Devoto et al., 1996) as well as the expression of genes such as *snail* (Thisse et al., 1993) and *myod* (Weinberg et al., 1996). Initially, adaxial cells can be identified at each side of the notochord prior to segmentation at the level of the horizontal septum (HS) as a epithelia-like sheet monolayer flanking each side of the notochord (Devoto et al.,

1996). Adaxial cells are notably larger and more regularly shaped than the surrounding lateral presomitic cells that surround them (Devoto e al., 1996). Recent studies further indicate that the region previously thought to contain lateral presomatic cells (Devoto et al., 1996) are composed of two distinct cell populations, lateral-anterior and lateral-posterior somite cells (Fig. 1.6A). These three distinct cell populations are rearranged through a series of whole somite rotation events in order to give rise to embryonic slow and fast muscle fibres as well as the myogenic progenitor cells (MPCs) used for subsequent myogenesis (Fig. 1.6-E). During the whole somite rotation, lateral anterior and posterior cells are rearranged into the lateral-external and later-medial cell layer (Fig. 1.5B). The adaxial cells still remain inner, but begin to express slow myosin heavy chain isoforms (Crow and Stockdale, 1986; Devoto et al., 1996; Blagden et al., 1997; Roy et al., 2000) and elongate through the whole somite longitudinally (Fig. 1.6B). At late segmentation the 90 degree somite rotation is completed leading to the formation of a distinct external cell layer (ECL) sourced from the lateral anterior somite cells (Fig. 1.6C). Additionally, the adaxial cells start to migrate both laterally and radially (Fig. 1.6C). The lateral-medial cells also begin to express fast myosin heavy chain isoforms and elongate though the whole somite (Fig. 1.6C). The migrated adaxial cells eventually form a single layer of embryonic slow muscle fibres between ECL and embryonic fast muscle fibres (Fig. 1.6D). Subsequently, some cells from ECL migrate into the myotome though the slow muscle layer giving rise to fast muscle fibres in distinct zones as stratified hyperplasia (Fig. 1.6E) (Rowlerson and Veggetti, 2001). It has been suggested that ECL plays an important role in other subsequent postembryonic muscle fibre production although this remains to be proven.

Functional studies of embryonic myogenesis in zebrafish embryos have revealed some distinct signaling pathways required for the formation of both slow and fast muscle fibres. For example, sonic hedgehog protein (Shh), the hedgehog family (Hh) of glycoproteins secreted from the notochord and floor plate, play an important role in the pattering of the embryonic slow muscle layer. Sonic hedgehog protein (Shh), one family member, influences these adaxial cells of the segmental plate mesoderm to become determined as myoblasts of the slow muscle lineage (Blagden, 1997). Zebrafish mutants that lack a differentiated notochord show defects in their paraxial mesoderm, including the lack of a horizontal septum, muscle pioneer cells and abnormalities in myotome shape. Injection of *shh* sense mRNA into eggs results in the activation of *myom* expression throughout the presomitic paraxial mesoderm and the subsequent differentiation of the entire myotome into embryonic slow muscle (Hammerschmidt et al. 1996; Barresi et al. 2000). Analysis of the *sonic you* (*syu*) mutant, which is homozygous for a disruption in the *Shh* gene, show a drastic reduction in the number of slow fibres (Schauerte et al. 1998). However, the analysis of other notochord deficient mutants (*ntl* and *flh*) that lack muscle pioneers has led to the suggestion that another member of the hedgehog family of proteins, Echidna hedgehog (Ehh), may be required for muscle pioneer cell formation (Currie and Ingham, 1996; Barresi et al. 2000). Whereas *shh* is expressed in both the notochord and floorplate, *ehh* is confined exclusively to the notochord. A third hedgehog family transcript Tiggywinkle hedgehog (*Twhh*) is expressed in the floorplate early in development (Ekker et al. 1995, Currie and Ingham 1996). In contrast to the formation of slow muscle, the lateral presomitic cells, the pioneer of the fast muscle fibre (Devoto *et al.*, 1996) are not controlled by *Shh* expression (Blagden, 1997). *In-situ*

hybridisation and ectopic expression studies have demonstrated that *Shh* is necessary for normal expression of *myod* and *myf-5* in the adaxial slow muscle precursors, but not in the lateral paraxial mesoderm (Coutelle et al. 2001).

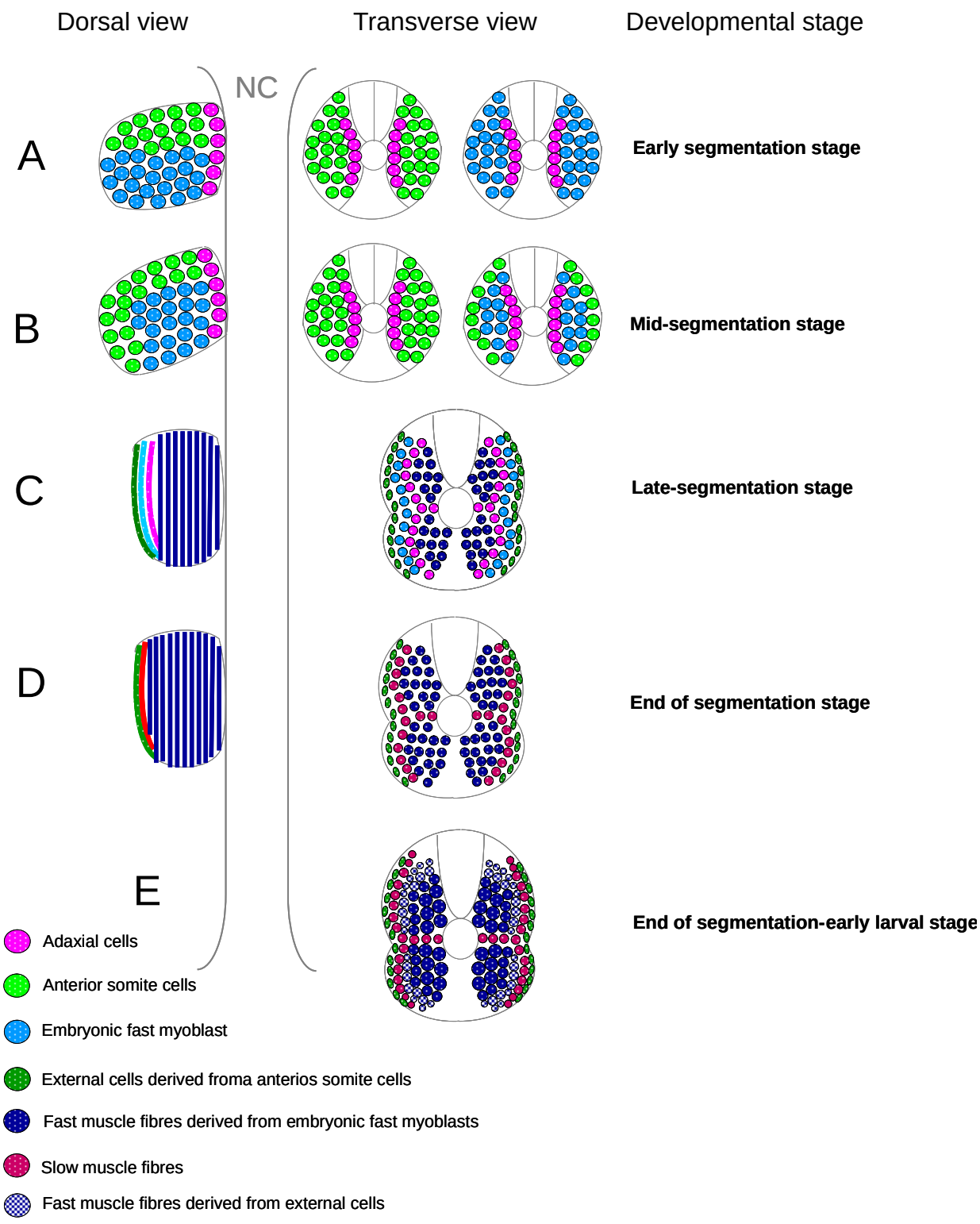

Fig. 1.6 Schematic illustration of the patterning of slow and fast muscle fibres during embryonic and early postembryonic stages based on the evidence presented by Devoto et al., 1996; Hollway et al., 2007; Stellabotte and Devoto, 2007; Stellabotte et al., 2007. The tranverse views of somites during early and mid segmentation stage indicate the distinct origins of anterior somite cells (anterior) and embryonic fast myoblast (posterior).

1.4.4 Stratified hyperplasia (SH)

Following embryonic myogenesis, new muscle fibres are continued to be added from the so-called “germinal zones” by a distinct process termed SH (Fig. 1.7). SH gives rise to distinguishable gradients in muscle fibre diameter from the peripheral to the deep myotomes (Rowlerson and Veggetti, 2001).

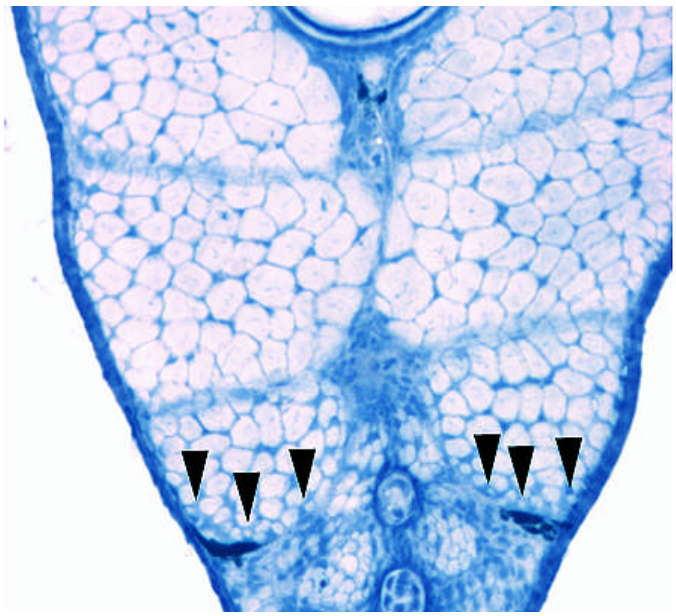

Fig. 1.7 Illustration of SH identified by small diameter fibres observed in germinal zones of ventral part of myotomes in a fish of 6.0 mm SL (arrowheads). Scale bar = 200 μm.

SH occurs after the complete of segmentation according to the identification of new muscle fibres by their gene expression pattern in zebrafish (Barresi et al, 2001), pearlfish (Steinbacher et al., 2006) and brown trout (Steinbacher, 2007). Initially, new slow muscle fibres are mostly added into the dorsal-ventral extremities of the existing single slow muscle layer (Barresi et al, 2001) whereas new fast muscle fibres are widely added at the border of the slow muscle layer, the periphery of the existing fast myotome and dosal-ventral extremities of the

myotome (Steinbacher et al., 2006, 2007).

Recent cell labeling studies have provided strong evidence that fast muscle fibres added through SH are soursed from ECL derived from the anterior somite compartments following the whole somite rotation (Hollway et al., 2007; Stellabotte et al., 2007) although these studies provide no evidence for the exact origin for slow muscle fibres. Some studies have previously suggested that the addition of new fibres into slow muscle through SH might be sourced from ECL since the horizontal expansion of single slow muscle layer occurs during late larval stage (Veggetti et al., 1990; Patruno et al., 1998). In addition, the identification of SH of slow muscle fibres from zebrafish mutants lacking Hedgehog signaling also showed this process is regulated by a distinct mechanism independent of Hedgehog signaling, which is required for the formation of those embryonic slow muscle fibre derived from the adaxial cells (Barresi et al., 2001).

SH has been widely identified in many species (review in Rowlerson and Veggetti, 2001) and provides the major source of new muscle fibres during late embryonic and early postembryonic growth. Interestingly, a temporary cessation of muscle fibre production is reported to occur in some species such as Atlantic herring (*Clupea harengus*) where there is complete cessation of muscle fibre production following the initial embryonic myogenesis and total fibre number remains constant to allow the hypertrophic growth of existing muscle fibres until hatched (Johnston 1993; Johnston et al, 1998).

1.4.5 Mosaic hyperplasia

Following SH, the final phase of hyperplasia occurs through MH (Rowlerson and Veggetti, 2001). In contrast to SH, MH involves the proliferation of a population(s) of precursor cells which subsequently migrate and fuse to form myotubes on the scaffold of existing fibres to produce a mosaic of muscle fibre diameters in a myotome across section (Fig. 1.8) (Rowlerson et al., 1995).

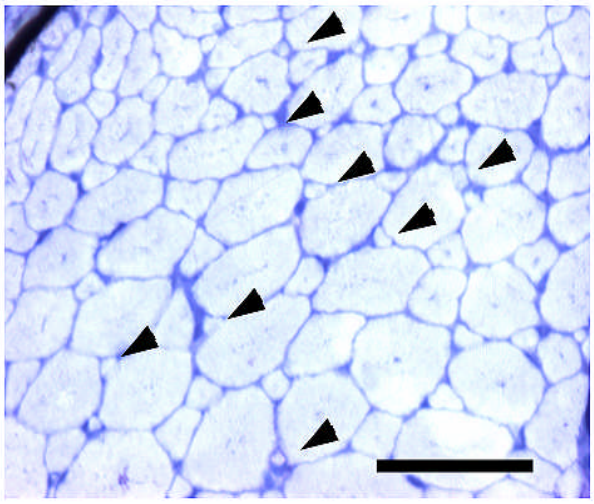

Fig. 1.8 Illustration of MH identified by small diameter muscle fibres formed on the surface of existing fibres throughout the fast muscle (arrowheads). Scale bar = 200 μm.

Comparing to the SH sourced from ECL, the origin of MH is still extremely unclear although the latest finding suggests ECL also possibly gives rise to at least some MPCs required for MH (Hollway et al., 2007). In fast muscle, muscle fibre recruitment continues until ~40% of the maximum fork length (FLmax) (Weatherley et al., 1988; Johnston et al., 2003; 2004). In teleost which are larger than 40 % FLmax, muscle fibre recruitment is stopped unless the muscle becomes damaged in which case new fibre formation is initiated to repair the injury

(Rowlerson et al., 1997). Following the end of muscle fibre recruitment all subsequent growth is by fibre hypertrophy alone, which requires the accretion of additional nuclei to maintain the myonuclear domain size within certain limits (Johnston et al., 2003, 2004). In contrast, slow fibre number continues to increase with body length to the maximum body size (Raamsdonk et al., 1983; Johnston et al., 2004).

1.5. Teleost genomics

1.5 .1 Teleost genome sequencing and its applications

Teleost genomes have recently received much attention and a large amount of genomic sequence information has become available (Table 1.2). The initial phase of teleost genomes sequencing mainly attempted to establish an ideal vertebrate model genome i.e. small-sized, less complexity, and highly homologous to human genome. Tiger pufferfish (*Takifugu rubripes*) has the smallest known vertebrate genome (380Mb) containing short introns and less than 10% of repetitive sequences (Brenner et al., 1993). The green spotted pufferfish (*Tetraodon nigroviridis*), a closely-related species with a similar compact genome, can be relatively easy obtained and maintained in freshwater environment making it as an alternative ideal model for a species with a compact genome (Crnogorac-Jurcevic et al., 1997; Crollius et al., 2000). The availability of the whole genome drafts from two pufferfish species allowed a series of following comparative studies for understating vertebrate genome biology, particularly the structure and organisation of the genes and genomes relevant to development and evolution (Miller et al., 2004; Mulley and Holland, 2004; Venkatesh et al., 2005).

Although two pufferfish species represent excellent models for comparative genome studies, their applications for functional genomic studies were found to be largely limited by the difficulties of routinely rearing and breeding them in the laboratory compared to other experimental teleost models such as zebrafish (Alestrom et al., 2006) and medaka (Mitani et al., 2006). In 2001, the Welcome

Trust Sanger Institute began to sequence the whole genome of the zebrafish, the most well-established teleost model for studying gene functions as illustrated in Chapter 1, section 1.3. The sequencing of zebrafish genome is extremely valuable for functional genomic studies since it accelerates the investigation of the functional role of genes associated with a given phenotype through forward and reverse genetics approaches (Amsterdam and Hopkins, 2006; Skromne and Prince, 2008). Medaka is another emerging teleost model ideal for functional genomics studies (Wittbrodt et al., 2002). Medaka is less related to zebrafish since their common ancestor was thought to have been diverged in 110–160 million years ago (Hedges and Kumar, 2002; Wittbrodt et al., 2002). Therefore, the comparison of these two ideal experimental models for functional genomics can offer more insights into the mechanisms underlying convergent and divergent evolution of gene function (Furutani and Wittbrodt, 2004).

The stickleback genome has also been sequenced, a teleost species that has undergone a rapid evolution (10,000-15,000 years ago) leading to thousands of phenotypic populations with a great diversity of morphologies, behaviours and habitats (Bell and Foster, 1994; Bell and Stamps, 2004). Therefore, sticklebacks have received much attention for investigating the mechanisms underlying the diversity of populations. Genome resources from other teleost species are also increasingly becomes available, particularly species of importance to aquaculture such as the Atlantic salmon, Atlantic cod, and European sea bass (Table 1.2).

Table. 1.2 The fish genome projects registered in the NCBI database as of Sep' 2009).

ProjectID	Organism Subgroup	Genome Size (Mb)	Chr No	Status	Method	List of Center/Consortium (pipe separated)
12880	Sea lamprey (Petromyzon marinus)	N.A.	N.A.	In Progress	N.A.	Genome Sequencing Center (GSC) at Washington University (WashU) School of Medicine
18361	Elephant shark (Callorhinchus milii)	0.91	N.A.	In Progress	WGS	Institute of Molecular and Cell Biology, Singapore
38195	White spotted clarias (Clarias fuscus CLFUWH01)	17	N.A.	In Progress	N.A.	Institute of Bioinformatics, Anhui Normal University, China|Shanghai Sangon Biological Engineering Technology & Services Co. Ltd
38187	Japanese grenadier anchovy (Coilia nasus COECWH01)	17	N.A.	In Progress	N.A.	Institute of Bioinformatics, Anhui Normal University, China|Shanghai Sangon Biological Engineering Technology & Services Co. Ltd
39737	Grass Carp (Ctenopharyngodon idella)	N.A.	N.A.	In Progress	N.A.	Chinese Academy of Sciences
11776	Zebrafish (Danio rerio Tuebingen)	1700	25	In Progress	WGS & Clone-based	Welcome Trust Sanger Institute
38201	Zebrafish (Danio rerio Wild)	1700	25	In Progress	Clone-based	University of Manitoba|University Core DNA Services
39865	European sea bass Dicentrarchus labrax Adriatic clade, male 57	600	N.A.	In Progress	WGS & Clone-based	European seabass sequencing consortium|Max-Planck-Institute for Molecular Genetics, Ihnestr 63/73, D-14197 Berlin, Germany
13579	Stickleback (Gasterosteus aculeatus)	450	22	In Progress	WGS	The Genome Assembly Team|Broad Institute
20429	Stickleback (Gasterosteus aculeatus)	450	22	In Progress		Baylor College of Medicine
29479	African Cichlids (Labeotropheus fuelleborni Domwe Island)	N.A.	N.A.	Assembly	WGS	Cichlid Genome Consortium|School of Biology, Georgia Institute of Technology|Joint Genome Institute
38197	Japanese sea bass (Lateolabrax japonicus LAJAWH01)	17	N.A.	In Progress	N.A.	Institute of Bioinformatics, Anhui Normal University, China|Shanghai Sangon Biological Engineering Technology & Services Co. Ltd
38001	Coelacanth (Latimeria menadoensis Indonesian)	2400	N.A.	In Progress	WGS & Clone-based	Broad Institute
38185	Chinese longsnout catfish (Leiocassis longirostris LELOWH01)	17	N.A.	In Progress	N.A.	Institute of Bioinformatics, Anhui Normal University, China|Shanghai Sangon Biological Engineering Technology & Services Co. Ltd
13631	Little Skate (Leucoraja erinacea)	N.A.	N.A.	In Progress	N.A.	Genome Sequencing Center (GSC) at Washington University (WashU) School of Medicine
29483	Lake Malawi cichlid (Maylandia zebra Mazinzi Reef)	N.A.	N.A.	Assembly	WGS	Cichlid Genome Consortium|School of Biology, Georgia Institute of Technology|Joint Genome Institute
29477	Lake Malawi cichlid (Mchenga conophoros Otter Point)	N.A.	N.A.	Assembly	WGS	Cichlid Genome Consortium|School of Biology, Georgia Institute of Technology|Joint Genome Institute
29481	Lake Malawi cichlid (Melanochromis auratus Domwe Island)	N.A.	N.A.	Assembly	WGS	Cichlid Genome Consortium|School of Biology, Georgia Institute of Technology|Joint Genome Institute
40115	Striped Bass (Morone saxatilis NCSU 1)	N.A.	N.A.	In Progress	N.A.	North Carolina State
29535	Killifish (Nothobranchius furzeri GRZ)	1.5	19	Assembly	WGS	Leibniz Institute for Age Research - Fritz Lipmann Institute (FLI)|Kathrin Reichwald|Dept. of Genome Analysis
33315	killifish (Nothobranchius furzeri MZM-0403)	1.5	19	Assembly	WGS	Leibniz Institute for Age Research - Fritz Lipmann Institute, Jena, Germany|Dept. of Genome Analysis
33401	Killifish (Nothobranchius kuhntae)	1.5	19	Assembly	Clone-based	Leibniz Institute for Age Research - Fritz Lipmann Institute, Jena, Germany|Dept. of Genome Analysis
20433	Nile Tilapia (Oreochromis niloticus)	N.A.	N.A.	In Progress		Broad Institute
19569	Medaka (Oryzias latipes HNI)	800	N.A.	Assembly	WGS	Medaka genome sequencing project|University of Tokyo, Chiba , Japan
16702	Medaka (Oryzias latipes Hd-rR)	800	N.A.	Assembly	WGS	Medaka genome sequencing project|University of Tokyo, Chiba , Japan
38199	White amur bream (Parabramis pekinensis PAPEWH01)	17	N.A.	In Progress	N.A.	Institute of Bioinformatics, Anhui Normal University, China|Shanghai Sangon Biological Engineering Technology & Services Co. Ltd
38005	Paralabidochromis chilotes Lake Victoria	N.A.	N.A.	In Progress	Clone-based	Broad Institute
38193	Yellow catfish (Pelteobagrus fulvidraco PEFUWH01)	17	N.A.	In Progress	N.A.	Institute of Bioinformatics, Anhui Normal University, China|Shanghai Sangon Biological Engineering Technology & Services Co. Ltd
38189	European Turbot (Psetta maxima SCMAWH01)	17	N.A.	In Progress	N.A.	Institute of Bioinformatics, Anhui Normal University, China|Shanghai Sangon Biological Engineering Technology & Services Co. Ltd
29485	Lake Malawi cichlid (Rhamphochromis esox Otter Point)	N.A.	N.A.	Assembly	WGS	Cichlid Genome Consortium|School of Biology, Georgia Institute of Technology|Joint Genome Institute
1434	Tiger pufferfish (Takifugu rubripes)	340	N.A.	Assembly	WGS	The Fugu Genome Sequencing Consortium|DOE Joint Genome Institute|Institute of Molecular and Cell Biology, Singapore
12350	Spotted green pufferfish (Tetraodon nigroviridis)	342.4	N.A.	Assembly	WGS	Genescope

N.A.: Not available; WGS: Whole genome shot gun; Mb: millions of base pairs

1.5.2 Teleost-specific whole genome duplication (WGD)

Duplication of genes and/or whole genomes are now generally considered as the major mechanism for increasing complexity of organisms during evolution as first proposed by Ohno (1970). In earlier studies, the evolution of the vertebrate genomes was firstly suggested to follow the "1-2-4" rule, indicating the vertebrate genome underwent two rounds of WGD (Pebusque et al., 1998; Meyer and Schart, 1999). However, this rule was inconsistent with the identification of more than seven Hox gene clusters in the zebrafish (Amores et al., 1998), suggesting an expanded "1-2-4-8" rule for the additional round of WGD in teleost lineages. This finding also led to a hypothesis that an additional WGD occurred after the divergence of ray-finned and lobe-finned fishes but before the teleost radiation and was also supported by the evidence from gene mapping (Gates et al. 1999; Barbazuk et al. 2000; Postlethwait et al. 2000) and phylogenetic studies (Prince et al., 1998; Meyer and Schart, 1999; Taylor et al., 2001). Moreover, this teleost-specific WGD was clearly confirmed after several teleost whole genome draft sequences became available and the additional round of whole genome duplication (WGD) led to some duplicate genes being specific to teleost (Fig. 1.9A) (Aparicio et al., 2002; Jaillon et al., 2004; Kasahara et al., 2007). In addition to the whole genome duplication events, a given duplicate gene could also be derived from lineage-specific gene duplication events. For example, Macqueen and Johnston (2008) recently demonstrated two *myod* genes (*myod1* and *myod2*) were duplicated from the teleost specific WGD event. *Myod2* was lost in some teleost species such as zebrafish and Atlantic salmon. Despite the presence of three myod genes (*myod1a*, *myod1b*, *myod1c*) in Atlantic salmon, none of these myod genes

were derived from the basal teleost WGD and were phylogenetically distinct from *myod2* of other teleost species (Fig. 1.9B).

(A)

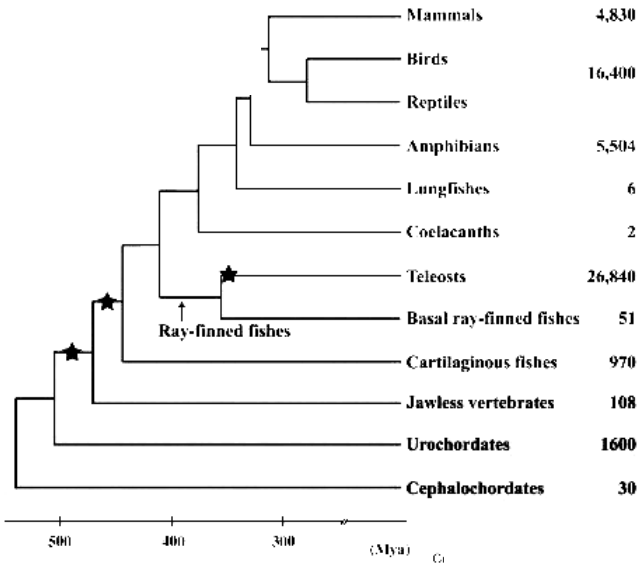

(B)

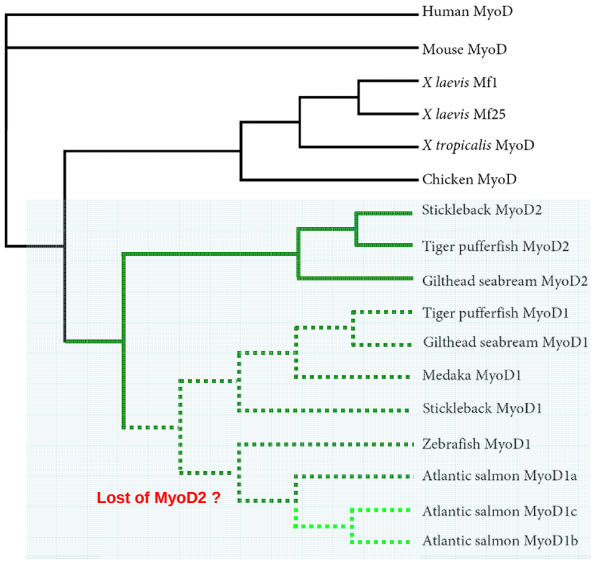

Fig. 1.9 Gene and genome duplication in chordates. (A) Three rounds of whole genome duplication (WGD) occurred during chordate evolution. Stars represent the WGD events. The first round of WGD occurred before the divergence of jawless vertebrate. The second round of WGD occurred before the divergence of cartilaginous fishes. The third round of WGD occurred in the ancestral teleost (adapted from Ravi and Venkatesh, 2008). (B) Evolution of *myod* in chordates *Myod2* was arose from a teleost-specific WGD event (dark green line), but lost in some teleost species (dotted line). Additional salmon myod paralogues were also arose from the lineage-specifc duplication (adapted from Macqueen and Johnston, 2008).

1.6. Developmental plasticity of teleost muscle phenotypes and temperature

1.6.1 The concept of developmental plasticity

Developmental plasticity (or phenotypic plasticity) can be generally defined as the ability of an organism with a given genotype to alter its phenotype when subjected to environmental change (Smith-Gill, 1983; Stearns, 1989; West-Eberhard, 2003). While developmental plasticity and phenotypic plasticity are interchangeable terms, the former one is often specifically referred to as influences of environmental change during early development and the latter one is generally referred to as influcences of environmental change at late stages and is typically reversible. Various phenotypic variations, including the molecular, chemical, morphological, physiological, behavioural alternations, have been intensively documented in a broad range of organisms, such as the alternation of muscle cellularity (e.g. fibre number, size and type) in teleosts (Johnston, 2006), metamorphosis in amphibians (Newman, 1992), reproduction physiology and offspring size in reptiles (Shine, 2005), song learning in birds (Marler and Nelson, 1993), visual acuity in mammals (Prusky and Douglas, 2003), body pigmentation in insects (Gibert et al., 2000), and leaf angle, stomatal aperture and photosynthetic rate in plants (Sultan, 2000). Plasticity of a given phenotype is considered to be adaptative when it is beneficial for increasing environmental fitness (Gotthard, 1995). It is believed that developmental (or phenotypic) plasticity might have an important role in increasing the environmental fitness and/or driving the diversity of organisms during evolution (Price et al., 2003; West-Eberhard, 2003).

Plasticity of a given phenotype over a certain range of environmental changes is often described as a reaction norm. As shown in Fig1.10, developmental plasticity of a given phenotype can potentially occur within either a short or wide range of environmental changes depending on different traits. Morever, it could be more complex when different genotypes are also considered as variable factors. In addition, the reaction norm for a given phenotype can also be restricted to a specific developmental stage. Therefore, the investigation of an interesting phenotype over a wide range of environmental conditions and a complete life span is vital for drawing an appropriate conclusion.

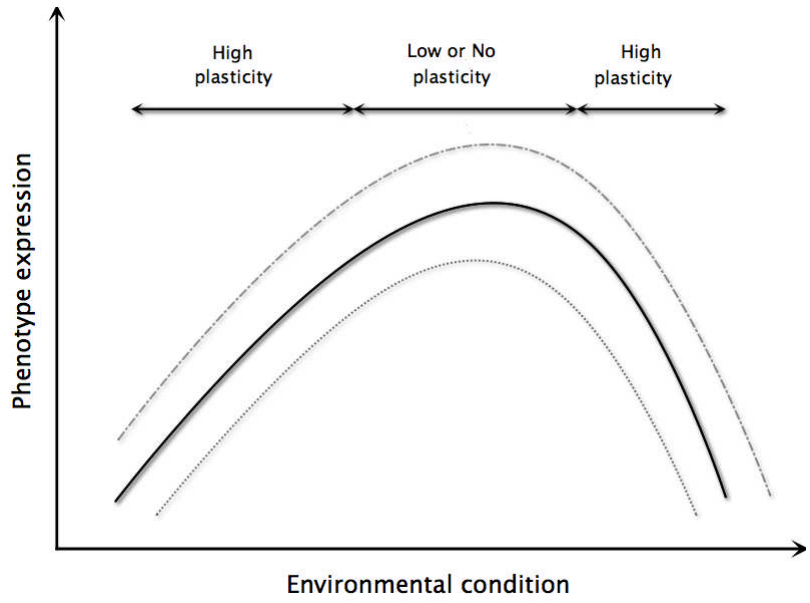

Fig. 1.10. Schematic illustration for the concept of a reaction norm. The phenotype expression of a given organism might exhibit no, low, or high plasticity over different ranges of environmental condition. Each individual curve represents a reaction norm for an organism with a given genotype.

1.6.2 Developmental plasticity of teleost muscle phenotypes

The skeletal muscle of teleost fishes is highly plastic in relation to changing environment (abiotic and biotic factors) (Fig. 1.11). The influences of environmental change on teleost muscle can be direct or indirect through a single or multiple systems (Fig. 1.11). Plasticity of muscle phenotypes can subsequently reflect on various physiological responses (Fig. 1.11).

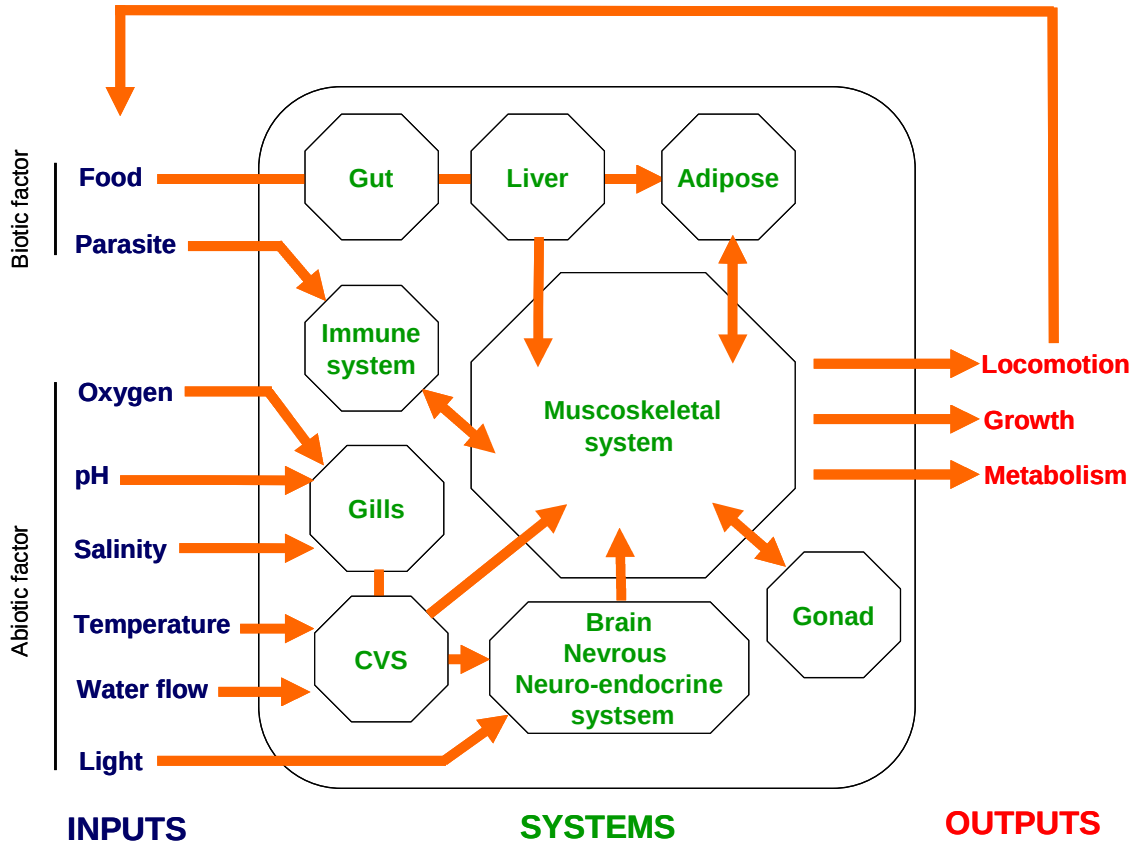

Fig. 1.11 The influences and consequences of environmental changes on teleost muscle (Adapted from Johnston, 2006)

Plasticity of fish muscle plasticity in response to temperature has received much attention since teleost fishes are ectotherms. The early experience of ambient temperature changes is considered to be crucial and significant for teleost species since their embryos are generally produced through the external fertilisation and subsequently restricted to a confined habitat during their early development.

Transient effects of embryonic temperature on muscle phenotypes include the timing of muscle innervation (Johnston et al., 1993; Johnston et al., 1997; Johnston et al., 1998; Johnston and Hall, 2004) and myofibrillar protein expression (Johnston et al., 1997; Johnston et al., 1998) as well as muscle mitochondria abundance (Johnston et al., 1992; Galloway et al., 1998; Sänger and Stoiber, 2001; Johnston and Hall, 2004). Persistent effects of temperature include the size and number of muscle fibres (Vieira and Johnston, 1992; Johnston et al., 2003b; Martel and Kieffer, 2007; Macqueen et al., 2008).

Developmental plasticity of muscle fibre recruitment is an important issue to be investigated since it is potentially related to growth traits of teleosts from the aquaculture perspective (Johnston, 1999). Additionally, it can also provide the insights into the mechanisms underlying myogenesis. Notably, persistent effects of embryonic temperature on postembryonic muscle growth have been demonstrated in a few teleost species, these studies were mainly restricted to either larval or exogenous feeding stages (Johnston, 2006) and very few studies has investigated the development plasticity of muscle fibre recruitment to temperature over the full range of temperatures found in nature or the complete life cycle (Johnston et al., 2003b; Macqueen et al., 2008; López-Albors et al., 2008).

1.6.3 Developmental plasticity and parental (maternal and/or paternal) effects

While developmental plasticity is commonly reported to occur in a given organism subjected to environmental changes, additional evidence also has been shown that developmental plasticity of some phenotypes can be induced in the offspring rather than in the parents. For example, an interesting finding from daphnia (*Daphnia cucullata*), a freshwater crustacean, indicates that offsprings of daphnia are hatched with a defensive helmet structure for the protection when their parents are exposed to the chemical traces of a predator (Agrawal et al., 1999). However, this distinct structure is redundant in a predator-free environment since the extra cost for this structure reduces competitive successes relative to non-helmeted daphnia (Agrawal et al., 1999). Thus, the importance of development plasticity to parental effects has been highlighted (Mousseau and Fox, 1998; Uller, 2008)

Maternal gene effects are part of potential mechanisms underlying developmental plasticity. Maternal genes refer to those genes originally stored in the eggs during oogenesis and necessary for all developmental processes prior to the initiation of zygotic transcription (Lindeman and Pelegri, 2010). Large scale genetic screens have identified several maternal genes associated with zebrafish mutants (Dosch et al., 2004; Pelegri et al., 2004; Wagner et al., 2004). Interestingly, maternal genes are not restricted to act prior to zygotic transcription but also function beyond this stage (Pelegri et al., 2004; Wagner et al., 2004). For example, the deficiencies of maternal genes such as *Blistered*, *Ichabod* and *Hecate* can lead to the disruption of body plan occurring during the embryogenesis (Wagner et al., 2004). Therefore, it is very likely that developmental plasticity in offspring can be induced through the

influences of maternal gene expression although the mechanisms are poorly investigated.

1.7 Objectives of the present study

1. To determine whether zebrafish can be utilized as a teleost model for postembryonic muscle fibre recruitment by investigating the pattern of muscle fibre recruitment and fibre number in both slow and fast muscle. Specifically, to establish the parameters for postembryonic muscle growth, including the number, diameter, and nuclear content of muscle fibres in relation to body size (Chapter 3).

2. To characterise the expression of two genes, *myospryn* and *cee*, previously identified as involved in postembryonic muscle fibre recruitment of tiger pufferfish (Fernandes et al., 2005) (Chapter 4 and 5).

3. To perform a genome-wide screen for genes involved in postembryonic muscle fibre recruitment using a zebrafish whole genome microarray (Chapter 6).

4. To investigate the effects of embryonic and parental temperature on postembryonic muscle fibre recruitment in zebrafish and to determine whether it could be utilised as a model for developmental plasticity of teleost muscle phenotype (Chapter 7).

Chapter 2.0 General Materials and Methods

2.1 Introduction

In this chapter, general experimental procedures performed in this thesis are described, including the animal handling as well as cell biology, molecular biology, and bioinformatics techniques. Those procedures specific to individual experiments are described separately in the appropriate experimental chapters (Chapter, 3, 4, 5, 6, and 7).

2.2 Animal handling

2.2.1 Fish strain

The juvenile and adult zebrafish used in this thesis were obtained in Ultimate Discount Aquatics (Cupar, UK) originally sourced from a Singapore fish farm. Fish were maintained in a temperature-controlled room at the Gatty Marine Laboratory (St. Andrews, UK) for the subsequent growing and breeding experiments.

2.2.2 Fish maintenance and breeding

The first generation (F1), Zebrafish were maintained on a 12-h light and 12-h dark photoperiod at 26 °C. Fish were fed twice daily, the larvae with artemia and fry dry food (ZM Ltd) and juvenile and adult stages with a propriety flake food supplemented with blood worm. Embryos were obtained from 5 pairs of adult fish

by natural spawning and raised at 28.5 °C in tank water.

2.2.3 Fish collection and tissue sampling

The offspring of zebrafish were sampled at regular intervals from 3.5 to 40.0 mm standard length (SL). All specimens were sacrificed by the administration of an anesthetic overdose of MS-222 and by severing the spinal cord (Schedule 1 Killing, UK Home office Regulations). All animals used for the experiments were processed according to the UK Home Office regulations (Guidance on the Operation of Animals, Scientific Procedures Act 1986).

2.3 Cell biology techniques

2.3.1 Frozen section

A steak through the trunk muscle was prepared at 0.7 SL and rapidly frozen in isopentane cooled to near its freezing point (-159 °C) using liquid nitrogen. Sections were cut at 7~10 μm thickness in a cryostat (Leica Microsystems, CM1850) and mounted on microscope slides coated with poly-L-Lysine (Sigma). Slides prepared for antibody staining were stored at -80 °C until use.

2.3.2 Histology

Haematoxylin staining was utilised as the regular staining in the present work, particular for visualising fast muscle fibres and their nuclei. Slides prepared from

frozen section were air-dried for 10 min or at least 30 min if previously stored at -80 °C before staining with Haematoxylin (Sigma) for 10 min. Stained slides were then washed thoroughly in water for 10 min and mounted in glycerol gelatin (Sigma).

2.3.3 Histochemistry

Succinate dehydrogenase (SDHase) staining was performed to visualize intermediate muscle fibres to distinguish them from slow and fast muscle layers. Developing solution was prepared by adding 2mg/ml nitroblue tetrazolium to an aliquot of pre-made 50 mM Phosphate Buffer/80 mM Sodium Succinate Solution (0.1 M solution of di-sodium hydrogen orthophosphate (Na_2HPO_4) (BDH), 0.1 M solution of sodium di-hydrogen orthophosphate (NaH_2PO_4) (BDH), 80 mM of sodium succinate (succinic acid) (Sigma), pH 7.6). Frozen section slides were then incubated with developing solution in the dark for 1.5~2 hr and subsequently washed in distilled water and mount in glycerol gelatin (Sigma).

2.3.4 Immunochemistry

Primary and secondary antibodies and ExtrAvdin Peroxidase (Sigma) were diluted in 1% (v/v) TritonX100 (Sigma), 1.5% (m/v) BSA (Sigma) in PBS. The following primary antibodies were used: S58 monoclonal mouse IgA (S58) (diluted 1:10 v/v) (Crow and Stockdale, 1988), and rabbit IgG polyclonal antibodies to Paired Box 7 protein (Pax7) (diluted 1:1000 v/v) and Forkhead Box protein K1-α (Foxk1α) (diluted 1:2000 v/v) (Johnston et al., 2004).

Sections were fixed in acetone for 10 min, air dried for 10 min and then were place in block solution (5 % (v/v) normal goat serum (Sigma, Poole, UK), 1 % (v/v) tritonX100 (Sigma), 1.5% (m/v) bovine serum albumin (BSA) (Sigma) in phosphate buffer saline (PBS) (Sigma)) for 1hr at room temperature. Sections were washed in PBS for 5 min and incubated in the primary antibodies overnight at 4°C. Sections were washed three times for 3 min each in PBS. Background was reduced by incubation in peroxidase blocking reagent (DAKO Corp) for 10 min. Secondary antibodies, anti-mouse IgA biotin conjugate (Sigma), ant-rabbit IgG biotin conjugate were diluted into 1:40 (v/v) and 1:800 (v/v), respectively and applied for 1 h at room temperature. Sections were washed three times for 3 min each in PBS and incubated in ExtrAvidin-Peroxidase (Sigma) (diluted 1:50 v/v) for 30 min. 3-amino-9-ethylcarbazole (AEC) was used as the chromogen for the peroxidase staining to develop the final signal. Sections were counterstained with Mayer's hematoxylin (Sigma). Control sections were performed by omitting the primary or secondary antibodies.

For double staining with S58 and Pax7 antibodies, two different chromogens, AEC (red colour) and NBT (blue colour) were used to distinguish their signals. Sections were firstly stained with S58 by following the same procedure described above until the end of ExtrAvidin-Peroxidase incubation. Subsequently, Pax7 antibodies were applied to the section followed by the above antibody statining procedure with a minor modification, where ExtrAvidin-Peroxidase was replaced by ExtrAvidin-Phosphotase (Sigma) (diluted 1:150 v/v) for 30 min. NBT (Sigma) was used as the chromogen for phosphotase staining to development the final signal.

2.4 Molecular Biology techniques

2.4.1 General guidelines

Bacteria and RNase are potentially existed and distributed in the working place that can cause some major problems, including the degradation of RNA and the amplification of non-specific PCR products. The bench and routinely used equipment, such as the pipettes, were regularly cleaned with 70 % (v/v) ethanol and RNase Zap® (Ambion). Milli-Q water (Millipore) was used in all reagents and procedures required for the following molecular biology protocols. Additional Milli-Q water (Millipore) autoclaved with 0.1 % diethylpyrocarbonate (DEPC) (Sigma) was also prepared for those works associated with RNA. All glass and plasticware were either autoclaved or manufacturer-certified sterile prior to use.

2.4.2 Total RNA extraction

Total RNA was extracted from 30~100 mg of tissue. Each sample was firstly homogenized in a Lysing Matrix D tube (FastPrep® Kits) with 1 ml of Tri-regent (Sigma) using FastPrep® instrument for 20 sec at speed setting of 4.0. The homogenized sample was then centrifuged at x 12,000 g for 5 min at 4ºC and transferred the aqueous upper phase into a new tube to avoid matrix and cell debris. An extra 5 min incubation at room temperature for 5 min was made to allow complete dissociation of nucleoprotein complexes. RNA was further separated from DNA by adding 300 µl of chloroform, vortexing for 10 sec ,and incubating for 5 min at room temperature before centrifuging the mixture at 12,000g for 15

min at 4ºC. Following the centrifuge the mixture was separated into an upper aqueous phase (colourless), an interface phase (white), and a lower phenol-chloroform phase (red). The aqueous phase of mixture was transferred into a new 2ml tube for further RNA precipitation. A 500 µl of pre-cooled 100 % (v/v) ethanol (Sigma) was added and incubated for at least 1h at -20 ºC before centrifuging at 12,000g for 5 min at 4ºC. Following the centrifuge a white RNA pellet was formed in the bottom of the tube. The supernatant was discarded and added 750 µl of pre-cooled 75 % (v/v) ethanol (Sigma) to wash and resuspend the pellet. To suspend the RNA centrifuged at 12,000g for 5 min at 4 ºC, discarded the supernatant and air-dried the pellet at room temperature for 5-10 min to remove the ethanol. The pellet was finally dissolved with 30-50 µl of RNase free water and incubated at 50 ºC for 10 min or until the pellet responded completely. To remove the potential genomic DNA all RNA samples were further treated with DNase using TURBO DNA-free™ Kit (Ambion) according to manufacturers instruction. All RNA samples were stored at -80 °C until use.

2.4.3 Assessment of total RNA quality

2 µl of each sample was incubated at 85 ºC for 3 min to denature RNA before running on a 1% RNase free agarose gel with an RNA size marker (New England Biolabs) to identify if any degradation of RNA occurred. The clear integrity of 18 and 28S ribosomal RNA bands was used to indicate that the total RNA was not degraded.

2.4.4 Quantification of total RNA concentration

Total RNA concentration was quantified by two approaches in the present study. The first one was using the RiboGreen RNA quantitation reagent kit (Invitrogen) to quantify the concentration of RNA used for qPCR assay (Chapter4 and 5) following a modified version of the manufacturers 'high range' protocol and using a FluoStar fluorimeter (BMG Lab Technologies). Each reaction was performed in triplicate and contained 100 µl of total RNA of unknown concentration and 100 µl of RiboGreen working solution. A standard curve was established using a series of RNA standard dilutions (1000, 500, 100, 20 and 0 ng/ml RNA standard diluted in TE). Alternatively, a NanoDropTM 1000 spectrophotometer (Thermo Scientific) was used to directly quantify 1 µl of RNA sample. The purify of all RNA samples were confirmed by having the optimal ratio of absorbance at 260 nm/280 nm (1.9-2.3) and 260 nm: 230 nm (>2.2).

2.4.5 Gel electrophoresis

Electrophoresis was performed to separate, identify, and purify nucleic acids (DNA and RNA). Agarose gels were prepared by dissolving agarose powder (Bioline) in Tris-Acetate-EDTA buffer (TAE, 40 mM Tris base (Sigma), 20 mM acetic acid (Sigma), 1 mM EDTA (Sigma)). 1-2 % (m/v) agarose gels were used depending on the size of the PCR amplicon. Agarose was melt in TAE by heating in a microwave and ethidium bromide (EtBr) (Sigma) was later added to obtain a final concentration of 0.5 µg/ml when the molten agarose had cooled to 50 ˚C. Gels were solidified and then submerged with TAE buffer in a gel apparatus (Bio-Rad).

Before being loaded into the gel, 1xloading dye (Promega) was added into each sample and a Quantitative DNA (Promega) or RNA ladder (New England Biolab). An electrical current was applied to the gel tank at 100 volt (Bio-Rad) until nucleic acids were appropriately separated. The gels were then visualised under ultraviolet light and recorded the images using a VersaDoc 3000 image system (Bio-Rad).

2.4.6 Gel extraction and purification

Agarose gels containing PCR products were placed under UV light to select the bands of interest and isolate them using a sterile disposable scapel. Isolated gels were transferred into new tubes and purified using a QIAquick gel extraction kit (Qiagen) according to the manufacturers protocol.

2.4.7 Complementary DNA (cDNA) synthesis

First strand cDNA was synthesised from total RNA using RETROscript kit (Ambion) following by the manufactures procedure. The concentration of total RNA varied with different samples and thus the equal amount of total RNA from each sample was estimated prior to cDNA synthesis. RNA was denatured with oligo (DT) primers at 85 ˚C and then single strand cDNA was synthesised for 1hr in a mix containing 100U of reverse transcriptase (MMLV-RT), 2 mM dNTPs, 10U of RNase inhibitor and 2 µl 10X reverse transcription buffer (100 mM Tris-HCl (pH 8.3), 750 mM KCl, 30 mM $MgCl^{+2}$, 50 mM dithiothreitol). The reaction was halted by denaturing the MMLV-RT at 92 ˚C for 10 min. cDNA was stored at -20 ˚C and diluted 5-10 times in sterile milli-Q water. cDNA prepared (normalized to

represent the same amount reverse transcribe total RNA in each sample).

2.4.8 Polymerase chain replication (PCR) and Reverse transcription-PCR (RT-PCR)

Nucleic acid sequences of interest were amplified by PCR using DNA as the template or RT-PCR using cDNA as the template. The standard mixtures (25 µl) for the regular PCR reaction in this work were prepared by the following recipe:

a. 1 µl cDNA (RT-PCR) or 1 µl DNA (PCR)

b. 1.25 U of BioTaqTM DNA polymerase (Bioline)

c. 2.5 µl of the supplied 10 x NH4 buffer (Bioline)

d. 1.25 µl 50 mM $MgCl^{+2}$ (Bioline)

e. 0.1mM dNTPs (Bioline)

f. 4 µM of forward and reverse primer

Reactions were carried out in microcentrifuge tubes in a themocycler (Bio-Rad) with a range of cycling conditions, specific to each primer set. In general, the reactions were performed by the following cycling parameters:

a. Initial denaturation: 1 cycle of 95 ˚C for 10 min

b. Amplification: 20-35 cycles of 95 ˚C for 30 s, 55 ˚C for 30 s (annealing temperature, depending on the primer and its application, optimal temperature can be determined by applying a temperature gradient), 72 ˚C for 30 s-5 min (1000 bp per min are typically required)

c. Final extension: 10 min at 72 ˚C.

2.4.9 DNA cloning

10-20 ng of PCR products were ligated to a pCR©4- TOPO vector (Invitrogen) followed by a heat-shock (42 ˚C) to transform them into a chemically competent One Shot®TOP10 *Escherichia coli* cells (Invitrogen) and subsequently mixed with a SOC medium (2 % tryptone, 0.5 % yeast extract, 10 mM sodium chloride, 2.5 mM KCl, 10 mM MgCl, 10 mM magnesium sulfate, 20 mM glucose) (Invitrogen) to incubate on a horizontal shaking platform at 200 rpm for 1hr before spreading 50-200 µl culture mixture on fresh LB agar plates containing 100 mg/ml ampicillin (Sigma) and left overnight at 37 ˚C. Clearly and isolated colonies were picked up by hands with a sterile toothpick or pipette tip.

2.4.10 Plasmid purification, digestion and screening

Plasmid DNA was purified from *E. coli* cells using the QiaPrep spin Miniprep kit (Qiagen) according to the manufacturers instruction. Plasmid DNA was digested by a *Eco*R1 restrictive enzyme (Promega) at 37 ˚C for 3 hr. Digested products were run on a 1.2 % agarose gel with a quantitative 1kb DNA marker (New England Biolabs) and visualised under UV light, to quantify plasmid DNA mass and to confirm the presence and size of expected insert. Alternatively, a PCR the T3/T7 or M13F/R primers from TOPO T/A Cloning® kit can be used to screen expected inserts from the plasmid. Plasmid containing the expected insert were then stored at –20 ˚C until sent for sequencing.

2.4.11 Sequencing

Two clones of each plasmid were sequenced in both sense and antisense directions with T3 and T7S by the University of Dundee (UK) sequencing service using Applied Biosystems Big-Dye ver 3.1 chemistry on an Applied Biosystems model 3730 automated capillary DNA sequencer (Applied Biosystems).

2.4.12 Quantitative PCR (qPCR)

The expression of genes of interest was quantified by qPCR using an ABI PRISM® 7000 Sequence Detection System (Applied Biosystems) and the QuantiTect SYBR Green PCR Kit (Qiagen). Each reaction mixture contained 1x QuantiTect SYBR Green PCR master mix, 1 µl cDNA (normalized to represent the equal amount of reverse-transcribed total RNA in each sample), 0.4 µM each primer and RNase-free water (Qiagen) to a final volume of 25 µl. Each reaction was performed in duplicate in 96-well plates (Applied Biosystems) under the following thermocycling conditions: 15 min at 95 °C for initial activation and then 40 cycles of 15 s at 94 °C, 30 s at 56 °C and 30 s at 72 °C. The fluorescent dye ROX was used as an internal reference for normalisation of SYBR Green fluorescence. A dissociation protocol ranging from 60 °C to 90 °C was performed to investigate the specificity of the primer and the presence of primer dimers after the final amplification cycle. The controls, including –RTs (no reverse transcriptase) and NTC (no template control), produced no amplification.

2.4.13 Whole mount in situ hybridisation

Whole-mount *in situ* hybridisation was performed following a standard procedure (Fernan) with a mirnor modification. Embryos were fixed in 4% (m/v) paraformaldehyde (PFA) (Sigma) /PBS at 4°C overnight. Next, fixed embryos were washed in PBT (PBS + 0.1 % Tween 20), dechorionated and staged according to the standard criteria (Kimmel et al., 1995). Embryos were then dehydrated with a series of 25, 50, 75, 100 % (v/v) methanol/PBS before being stored at -20 °C until use.

Six embryos from each developmental stage were used for both antisense and sense hybridisation (control). Stored embryos were rehydrated with a series of 75, 50, 25 % (v/v) methanol/PBS and PBT. Embryos were then permeabilised with 1:1000 dilution of proteinase K (Roche) in PBT for 30 s to 2 min at room temperature (depending on their developmental stages). After the digestion treatments, embryos were refixed in 4% (m/v) PFA /PBS for 20 min and washed 4 x 5 min in PBT.

The probe for *in situ* hybridisation was amplified by PCR with T3 and T7 primers from a pCR4-TOPO plasmid containing an appropriate insert of gene of interest. PCR products were used as the templates to in vitro synthesize sense and antisense DIG-labeled myospryn RNA probes by in vitro transcription with T3 or T7 RNA polymerases (Roche), according to the manufacturer's instructions. Final signals of bound DIG-labeled probes were detected with alkaline phosphatase conjugated to anti-DIG Fab fragments (Roche) using nitroblue tetrazolium (Roche). Cryosections

were prepared by snap freezing embryos mounted in Cryomatrix (Thermo Electron Corp) in isopentane cooled to near freezing (−159 °C) by liquid nitrogen. A series of 18-μm sections were cut on a cryostat. Images of whole-mount embryos and sections were photographed using a Leica DMRB compound or Leica MZ7.5 binocular microscope attached to a Nikon Cool-Pix camera.

2.5 Bioinformatics techniques

2.5.1 Blast search

The basic local alignment search tool (BLAST) (Altschul et al, 1990) was used to compare sequences of interest against various gene and genome databases, such as Ensembl (http://www.ensmbl.org) and NCBI (http://www.ncbi.nlm.nih.gov). BLASTn compares nucleotide sequences to a nucleotide database, BLASTp compares protein sequences to a protein database and tBLASTn compares a translated nucleotide sequence to a database of nucleotides translated in all six open reading frames.

2.5.2 Primer design

Primers for PCR experiments were designed according the following standard. The length of each primer was ranged from 18-25 nucleotides with a >50% of guanine/cytosine (GC) content greater than 50% in order to result in a melting temperature (Tm) from 50-65 ˚C. The web-based software NetPrimer (http://www.premierbiosoft.com/netprimer/) was used to check and avoid the

secondary structure, hairpin, primer dimmer, cross-dimmer caused by designed primers. Specifically, primers for quantitativereal-time PCR need to have a Tm greater than 60 ˚C and were predicted to produce no secondary structure, hairpin, primer dimmer, cross-dimme to amplify a desired 150-250 bp in size amplicon. Additionally, at least one primer per pair spanned an exon/intron junction to minimize the amplification from contaminating genomic DNA.

2.5.3 Predication of gene structure

To characterise the intron-exon organization, corresponding cDNA and genomic DNA sequences were extracted from genome database via Ensembl or NCBI when both of them were available, which was the case in this work. The intronic splice sites were characterised by loading these sequences into Spidey (Wheelan et al., 2001) at http://www.ncbi.nlm.nih.gov/spidey/ with default settings.

2.5.4 Prediction of functional domain

To identify the potential functional motif encoded by a given gene, its deduced amino acid sequence was analysed using Simple Modular Architecture Research Tool (SMART) (http://smart.embl-heidelberg.de/) (Schultz et al., 1998; Letunic et al., 2008).

Chapter 3.0 Postembryonic fibre recruitment and growth in slow and fast myotomal muscle of zebrafish

3.1 Abstract

The mechanism by which fibre number increased in the larval and adult stages differed between slow and fast muscles. In slow muscle, three overlapping waves of fibre recruitment were observed involving three anatomically distinct germinal zones termed, SG1, SG2, and SG3. The number of slow fibres per myotomal cross-section increased from ~100 in hatched larvae of 4 mm standard length (SL) to 750 in adults of 40 mm SL, which is close to the maximum body size. In fast muscle, fibres were added from a single germinal zone from 4 to 8 mm SL by stratified hyperplasia (SH) and throughout the myotome from 7 to 17 mm SL by mosaic hyperplasia (MH). The number of fast muscle fibres per myotomal cross-section increased from ~300 at 4mm to ~3,500 at 17mm SL, largely via MH. Further growth involved increases in fibre diameter and length accompanied by nuclear accretion and ~1,700 myonuclei per cm were evident in fast muscle fibres of 80 μm diameter. Maximum fibre diameter (Dmax) of slow and fast muscle fibres reached a limiting value in zebrafish larger than 32 mm SL, at 40 and 80 μm, respectively. The densities of myogenic progenitor cells (MPCs) expressing the Paired Box 7 protein (Pax7) and Forkhead Box protein K1-α (Foxk1-α) decreased with boy size although no strong correlation was evident with the rate of muscle fibre recruitment. The presence of all phases of muscle fibre production evident in other teleost species in zebrafish suggests it can be an excellent model to examine postembryonic myogenesis.

3.2 Introduction

Fish myotomes contain slow and fast muscle fibre types arranged in anatomically discrete layers, each with different metabolic and contractile profiles and roles in swimming (reviewd in Chapter 1, section 1.3). Fast and slow muscle fibres have different embryonic origins and patterns of postembryonic growth (reviewed in Chapter 1, section 1.4). In teleosts, three distinct phases of muscle fibre recruitment can be identified during embryonic and postembryonic muscle growth (described in Chapter 1, section 1.4.3-1.4.5). In fast muscle, muscle fibre recruitment continues until ~40% of the maximum fork length (FLmax) (Weatherley et al., 1988; Johnston et al., 2003, 2004) unless the muscle becomes damaged in which case new fibre formation is initiated to repair the injury (Rowlerson et al., 1997). Following the end of muscle fibre recruitment all subsequent growth is by fibre hypertrophy alone, which requires the accretion of additional nuclei to maintain the myonuclear domain size within certain limits (Johnston et al., 2003, 2004). In contrast, slow fibre number continues to increase with body length to the maximum body size (Raamsdonk et al., 1983; Johnston et al., 2004).

Myogenic progenitor cells (MPCs), representing the muscle stem cell population and their progeny committed to differentiation, play a central role in both hyperplastic and hypertrophic growth processes. Recently, a novel population of myogenic progenitor cells expressing both transcription factors Pax3 and its paralogue Pax7 (paired box proteins 3 and 7) have been found in the dermoyomtome and suggested to be the source of those MPCs required for the myogenesis of fetal and postnal muscle growth in chick and mouse (Gros et al.,

2005; Relaxi et al., 2005). These findings highlight the importance of the dermomyotome for muscle growth. In teleosts, the external cells previous described anatomically (Waterman, 1969) have recently been shown to be functionally equivalent to the dermomyotome in amniotes. The external cells can later give rise to the appendicular, hypaxial, and axial muscles during development (Hollway et al., 2007; Stellabotte et al., 2007).

There is considerable interest in the mechanisms regulating these phases of myogenesis especially in aquaculture species, e.g. salmonids because muscle fibre density is an explanatory variable for the growth rate and flesh texture (Johnston et al., 2000, 2003, 2004, 2006). However, the long life cycle and lack of genome sequences in these valuable species impede studies on the underlying cellular and genetic mechanisms. Zebrafish, on the other hand, is an ideal model system for genetic and developmental research due to several laboratory advantages, most notably their relatively short life span (3-4 months), easy maintenance and large egg clutches all year round (reviewed in Chapter 1, section 1.1.3). The aim of this chapter was to investigate patterns of slow and fast muscle growth in zebrafish from hatching until the maximum body size. Another aim was to determine if zebrafish is a useful model for postembryonic growth in larger commercially important teleost species.

3.3 Materials and methods

3.3.1 Fish maintenance and breeding

All the experitmental procedures performed in this section were described in Chapter 2, section 2.2.1-2.2.3.

3.3.2 Section preparation

A steak through the trunk muscle was prepared at 0.7 SL and rapidly frozen in isopentane cooled to near its freezing point (-159 °C) using liquid nitrogen. Sections were cut at 7~10 μm thickness and mounted on slides coated with poly-L-Lysine (Sigma).

3.3.3 Immunohistochemistry

Antibody staining was performed according to a standard procedure as previous described in Chapter 2 (Section 2.3). Different antibodies, including S58 monoclonal mouse IgA (S58) (diluted 1:10 v/v) was used to identify slow fibres, and rabbit IgG polyclonal antibodies to Pax7 (diluted 1:1000 v/v) and Foxk1-α (diluted 1:2000 v/v) were used as reprective markers for myogenic progenitor cells (MPCs) that were quiescent and active or solely active phase of MPCs. Additionally, double staining of S58 and Pax7 antibodies was performed in adultfish following the same procedure described in Chapter 2 (section 2.3.4).

3.3.3 Quantification of muscle fibre number and diameter

S58-stained slides were counterstained with haematoxylin and photographed using a microscope (Axioskop2 plus, Karl Zeiss) fitted with a digital camera (AxioCam, Karl Zeiss). The total and individual cross-sectional area of $S58^{+}$ and $S58^{-}$ muscle fibres were measured using image-analysis application software (Sigma Scan Pro5, SPSS INC). All individual slow muscle fibres, in a half side of the trunk cross-section, were measured in each fish. For the fast muscle, the cross-sectional areas of a minimum 400 of fibres were measured except in fish less then 10.0 mm SL where a half trunk cross-section was measured.

Fibre number was estimated as previously described (Johnston et al., 1999). A kernel function was fitted to the measured fibre diameters to obtain a smoothed probability density function (Johnston et al., 1999). The kernel estimate can expressed as $f(y) = \sum_{i=1}^{n} w(y - yi; hi)$, where f is the estimated probability function, yi is the ith observation from the list of n, h is the smoothing parameter, and w is the kernel function. The smallest size class of fibres observed was approximately ~5 μm in diameter. The absence of fibres in this size class served as an objective criterion to determine the end of the recruitment phase of growth. The maximum number of fast muscle fibres (FNmax) was estimated from fish that had finished recruiting muscle fibres. Dmax for each was estimated from the average of the top 3% of measured fibre diameters.

3.3.4 Quantification of MPCs density

The densities of mononuclear cells in fast muscle stained with antibodies specific to Pax-7 and FoxK1-α was determined from fish ranging from 6.0 to 33.0 mm SL. All positive stained cells were counted at magnification of 40x in 1 to 25 of $0.028mm^{-2}$ fields depending on fish size. For fish less than 10.0 mm SL, the whole cross-sectional area of fast muscle was measured.

3.3.5 Quantification of the myonuclei in single muscle fibres

Small bundles of fast muscle fibres were isolated from the dorsal and ventral myotomes at 0.7 SL. Fibre bundles were pinned at the resting length in Sylgard (RS Ltd), fixed in 4 % (m/v) paraformaldehye in PBS at 4 °C for 8 hr and washed in PBS. Single muscle fibres were isolated under a dissecting microscope (Zeiss) using dark field illumination. The fibres were placed in 1% (m/v) saponin (Sigma) in PBS for 3 hr, washed 3 times in PBS and 3 times in 2x SSC (300mM NaCl, 30mM sodium citrate, pH 7.0). Myonuclei were stained with SYTOX Green (Molecular Probes Inc) at a dilution of 1:300 (v/v) in 2x SSC for 5 min in the dark. Fibres were washed 3 times (5 min each) in 2x SSC and mounted on glass slides using fluorescent mounting medium (DAKO Corp). All fibres were observed with a laser confocal microscope (BioRad Radiance 2000). The number of myonuclei was quantified using a z-series image collection of 2 μm thick sections and LaserPix vs 4.0 software (BioRad).

3.4 Results

3.4.1 Muscle fibre composition

Slow and fast muscle fibre, were identified in myotomal cross-sections on the basis of S58 antibody staining (Fig. 3.1A). A distinct population of intermediate muscle fibres could be further distinguished among the S58 negative muscle fibres adjacent to the slow muscle layers on the basis of their intermediate staining for SDHase activity (Fig. 3.1.B) as well as myosin ATPase activity (not shown). The intermediate layer was excluded from the analysis. Double stained section with S58 and pax7 antibodies showed the superficial slow muscle fibres were surrounded by a layer of $pax7^{+}$ cells (Fig. 3.1).

3.4.2 Postembryonic fibre recruitment in slow muscle

The total number of slow muscle fibres (SN) per trunk cross-section increased consistently with increasing fish length (SL) from approximately ~100 at 5.0 mm SL to ~700 at 40.0 mm SL (Fig. 3.2). Analysis of fibre diameters revealed three distinct germinal zones in slow muscle that appeared sequentially at different developmental stages (Fig. 3.3). In early larvae (~5.0 mm SL), a single layer of slow fibres was expanded in dorsal and ventral regions by a germinal zone producing new fibres that was named SG1 (Fig. 3.3A). A second germinal zone (SG2) was found to be active in late larvae (~8.0 mm SL) along the major HS (Fig. 3.3B). A third germinal zones (SG3) overlapped with SG2 and was activated in early juvenile fish (~10.0 mm SL) (Fig. 3.3C) at the internal edge of the embryonic

slow muscle layer along the major HS. Additionally, a distinct wedge-shaped region of slow muscle appeared at the level of the lateral line following the addition of slow muscle fibres produced from SG2 and SG3. SG2 started to become exhausted in early adult stages (20.0 mm SL) (Fig. 3.3D) whereas SG3 persisted late into the life cycle (20.0 & 35.0 mm SL) (Fig. 3.3D, E). On rare occasions, small diameter fibres were observed outside these principal germinal zones.

Next the relative contribution of germinal zones to slow muscle was further demonstrated. As shown in Fig. 3.4, SG1 made the major contribution to fibre recruitment in slow muscle of larvae (4.0-6.0 mm SL). In early-juvenile stages (7.0-9.0 mm SL), SG2 was main source of new fibres (Fig. 3.4). By mid-juvenile stages (10.0-12.0 mm SL), SG2 remained the main source of new muscle fibres although the contribution of SG3 was increased (Fig. 3.4). By late-juvenile stages (13.0-15.0 mm SL), both SG2 and SG3 made a similar contribution to fibre recruitment (Fig. 3.4). By early-adult stages (18.0-20.0 mm SL), the SG2 contribution decreased and SG3 was the main source of new fibres (Fig. 3.4). New muscle fibres production was reduced from all germinal zones during mid (23-25 mm SL) and late adult stages (33-35 mm SL) (Fig. 3.4).

3.4.3 Postembryonic fast muscle fibre recruitment

The number of fast muscle fibres per trunk cross-section increased from 400 at 5.8 mm SL to 3400 at 17.0 mm SL and then remained constant until the maximum length at 40.0 mm SL (Fig. 3.5). Both SH and MH were identified (Fig. 3.6). SH

occurred in germinal zones at the dorsal and ventral edges of the myotome in larvae from 3.5 to 6.0 mm SL (Fig. 3.6A). The germinal zones were exhausted at approximately 8.0 mm SL. MH occurred in fish between 7.0 and 17.0 mm SL and was observed as small muscle fibres forming on the surface of existing fibres throughout the myotome (Fig. 3.6B). Examination of the smooth distribution of fast muscle fibre diameters revealed the absence of <4.5 μm in diameter fibres in fish larger than 17.0 mm SL (Fig. 3.7A). A dramatic increase in fast muscle FN occurred concomitant with the onset of MH and 60~70 % of the FFN was obtained from 8.0 to 17.0 mm SL. After FFN was reached, fast fibre production ceased and existing fibres were observed to increase in diameter until the maximum body length (Fig. 3.7B).

3.4.4 Muscle fibre hypertrophy

A non-linear regression equation was fitted to establish the relationship between Dmax of fast and slow fibres and standard length (SL) (Fig. 3.8). In slow muscle, Dmax increased from ~10 μm at 5.0 mm SL to ~16 μm at 10.0 mm SL and then remained constant in fish of 10.0 to 15.0 mm SL (Fig. 3.8). Subsequently, a consistent increase in Dmax from ~20 to 40 μm was evident in fish ranging from 20.0-30.0 mm SL (Fig. 3.8). Dmax of fast muscle remained relatively constant at 35 μm between fish of 10.0 and 17.0 mm SL, concomitant with the major phase of MH (Fig. 3.8). It then increased until a limiting value of ~80.0 μm was reached in fish larger than 30.0 mm SL (Fig. 3.8).

3.4.5 Myonuclei content

Most of the nuclei in isolated single fast muscle fibres were found in the sub-sarcolemmal zone (Fig. 3.9A). The relationship between myonuclei content and fibre diameter was fitted with the following second order polynomial equation: Myonuclei cm^{-1} = 322.72 - 5.81 (fibre diameter) + 0.2964 (fibre diameter)^2 (Adj-R^2=0.76; n=251; P<0.01) (Fig. 3.9B). The number of nuclei per cm^{-1} increased from 300 at 20 μm to 1750 at 80 μm.

3.4.6 Myogenic progenitor cells

MPCs were identified using a specific antibody to Pax7 (Fig 3.10A), and those MPCs that were committed to differentiation by an antibody to Fox K1-α (Fig. 3.10B). The densities of $Pax7^+$ and Fox K1-α^+ cells decreased by 2-fold as SL increased from 10.0 to 33.0 mm.

3.5 Discussion

3.5.1 SH drives a continuous production of slow muscle fibres

Previous studies have showed that slow muscle fibres were recruited by SH based on the identification of germinal growth zones over a partial cross-sectional area of slow muscle and/or range of body sizes (Barresi, 2001; Johnston et al., 2004a). In this chapter, new evidence is provided that SH in slow muscle relies on the three different germinal zones arising sequentially to generate multiple waves of muscle fibre recruitment during ontogeny. The spatial and temporal patterns of new fibre generation originating from SG1-SG3 suggest that a greater complexity of SH exists in slow muscle. This work should facilitate future studies on the mechanism of postembryonic slow muscle development and growth.

3.5.2 MH is the predominant mechanism for increasing the number of fast muscle fibres in zebrafish

Unlike in slow muscle where recruited fibres were produced mainly through SH, muscle fibre recruitment in fast muscle of zebrafish involved both SH and MH. The identification of MH in zebrafish is perhaps the most interesting finding in the present study. MH, which is the final phase of muscle fibre recruitment in teleost fast muscle, has been widely reported across species, particularly in fish with large final body sizes (reviewed in Chapter 1, section 1.4.5). In Atlantic salmon, a large fish species that can grow up to 1m in length, MH can account for up to 95% of the FFN (Johnston et al., 2003b). It has traditionally been thought that MH plays a less

important role in postembryonic muscle fibre recruitment in small teleosts. For example, MH is completely absent in Guppy, which do not grow larger than 4.0 cm (Veggetti et al., 1993). MH was also found to be absent in certain Antarctic and sub-Antarctic notothenioid fish, which have evolved very large diameter muscle teleosts as an adaptive metabolic response to living in cold environments (Johnston et al., 2003a). Here, MH accounted for up 70% of FFN in zebrafish and was the main postembryonic mechanism for fibre production. While this thesis was in preparation, a report was published describing MH in zebrafish larvae of 6.0 mm SL although this study was only descriptive and did not measure the contribution of MH to fibre production (Patterson et al., 2008).

3.5.3 The origins of new muscle fibres

Barresi et al., (2001) first demonstrated in zebrafish embryos that SH in slow muscle begins after segmentation and is regulated by a mechanism independent of the Hedgehog signalling required for embryonic slow muscle development (Barresi et al., 2000; Blagden et al., 1997; Du et al., 1997; Wolff et al., 2003). They also showed that fibres formed by SH were distinct from the adaxial cells (Barresi et al., 2001). Recently, significant progress has been made in understanding SH of fast muscle using cell labelling and lineages studies in zebrafish embryos (Hollway et al., 2007; Stellabotte et al., 2007) and pearlfish (Marschallinger et al., 2009). Following the whole somite rotation, MPCs are derived from the anterior somite compartment and become rearranged as a cell layer external to the single layer of slow muscle fibres. This cell layer later gives rise to new fast fibres by SH (Hollway et al., 2007; Stellabotte et al., 2007). Although the origin of the MPCs

involved in MH has yet to be determined by cell labelling studies in any teleost species, the temporal and spatial distribution of pax7^{+} cells suggest they many contribute to MH (Hollway et al., 2007; present study). In the early larvae, pax7^{+} cells were largely restricted to the ECL and they were also found within the deeper myotome in larve and adult zebrafish (Hollway et al., 2007; the present study). This is consistent with an inward migration of Pax7^{+} cells from the ECL that become myotomal MPCs distributed within the myotome.

3.5.4 Role of MPCs during postembryonic growth

The nature of the MPCs responsible for the processes of myotube formation and hypertrophic growth is unknown. Pax7 and Foxk1-α are transcription factors vital for the maintenance of myogenic cells (Bassel-Buby et al. 1994; Seale et al., 2000; Hawke and Garry, 2001). Here, the densities of MPCs immunopositive for these proteins decreased with increasing fish size. However, there was no strong correlation between their density and muscle fibre recruitment in the zebrafish. Similar results were reported in Arctic charr (*Salvelinus alpinus*) (Johnston et al., 2004a), suggesting that neither maker is specific for the founder myoblasts that intiate myotube formation. By counting the number of nuclei in isolated fast muscle fibres, the number of nuclei was observed to increase from 300 cm^{-1} at 20 μm to 2700 cm^{-1} at 80 μm. As a large number of nuclei are required for the expansion of individual muscle fibres, the majority of MPCs might provide nuclei for hypertrophic growth and nuclear turnover.

3.5.5 Zebrafish is an ideal model for postembryonic muscle growth

In teleosts, postembryonic muscle growth is mainly investigated in large aquaculture species due to their economic value. However, the relative large body size and/or long life span of these species make it difficult to address several important questions regarding postembryonic muscle growth. Zebrafish has been the principal teleost model particularly for embryonic myogenesis owing to many powerful and innovative tools available (Chapter 1, section 1.1.3). However, it is yet to be adopted as a teleost model for postembryonic muscle. Here postembryonic muscle growth of zebrafish was characterised across a complete life span, demonstrating similar patterns of hyperplastic and hypertrophic growth as for those large aquaculture species. Therefore, zebrafish can be proposed as an excellent model for the cellular mechanisms of myogenesis in teleosts in general. Coupling cellular results to its available genome resources will be essential in future studies to elucidate the mechanisms underlying postembryonic muscle fibre recruitment in teleosts.

3.6 Figures

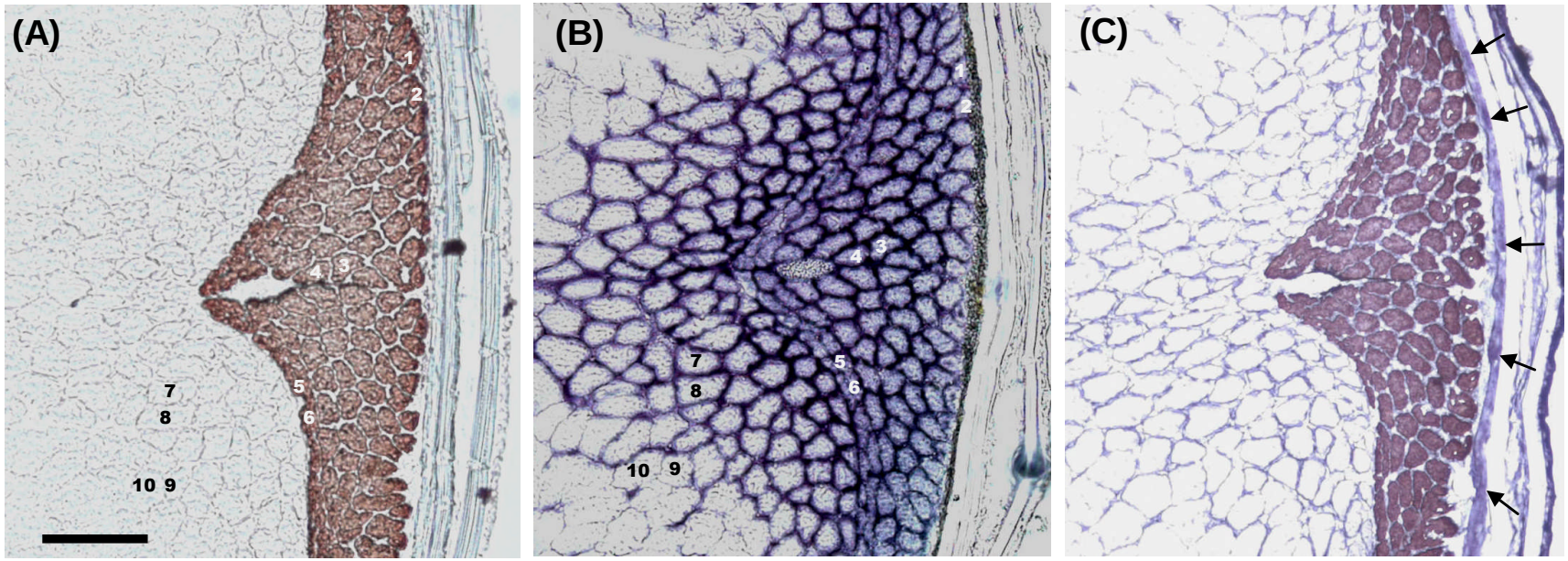

Fig 3.1 Illustration of muscle fibre composition from serial myotomal cross-sections of adult zebrafish (25.0 mm SL). (A) Slow muscle fibres (in red) were distinguished by staining with S58 antibody. (B) Intermediate and fast muscle fibres were further distinguished from $S58^{-}$ muscle fibres by comparing their SDHase activities. (C) Slow muscle fibres were laterally flanked by a layer of $Pax7^{+}$ cells representing the external cells (arrows). Scale bar = 100 μm. Digits indicate the identical fibres from (A) and (B) Slow muscle fibre (1, 2, 3, 4, 5, 6), intermediate muscle fibre (7, 8) and fast muscle (9, 10).

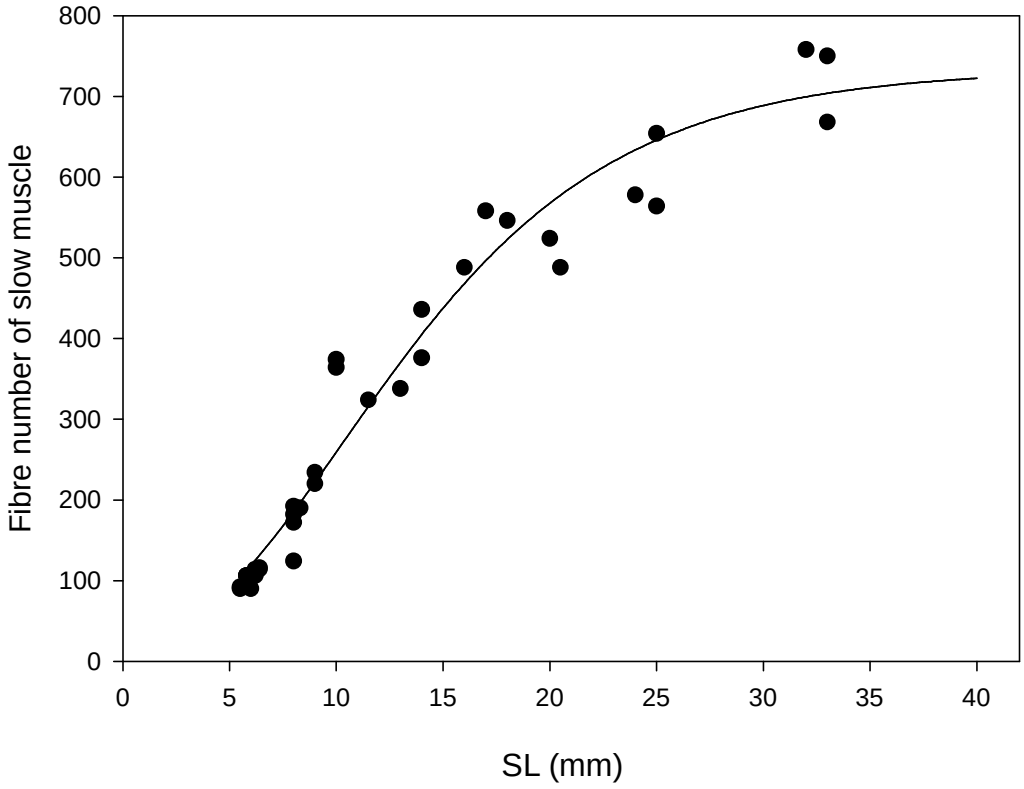

Fig. 3.2 The relationship between the number of slow muscle fibres and SL. A non-linear regression was fitted with a Gompertz equation (Adj-R^2=0.97; N=35, P<0.01).

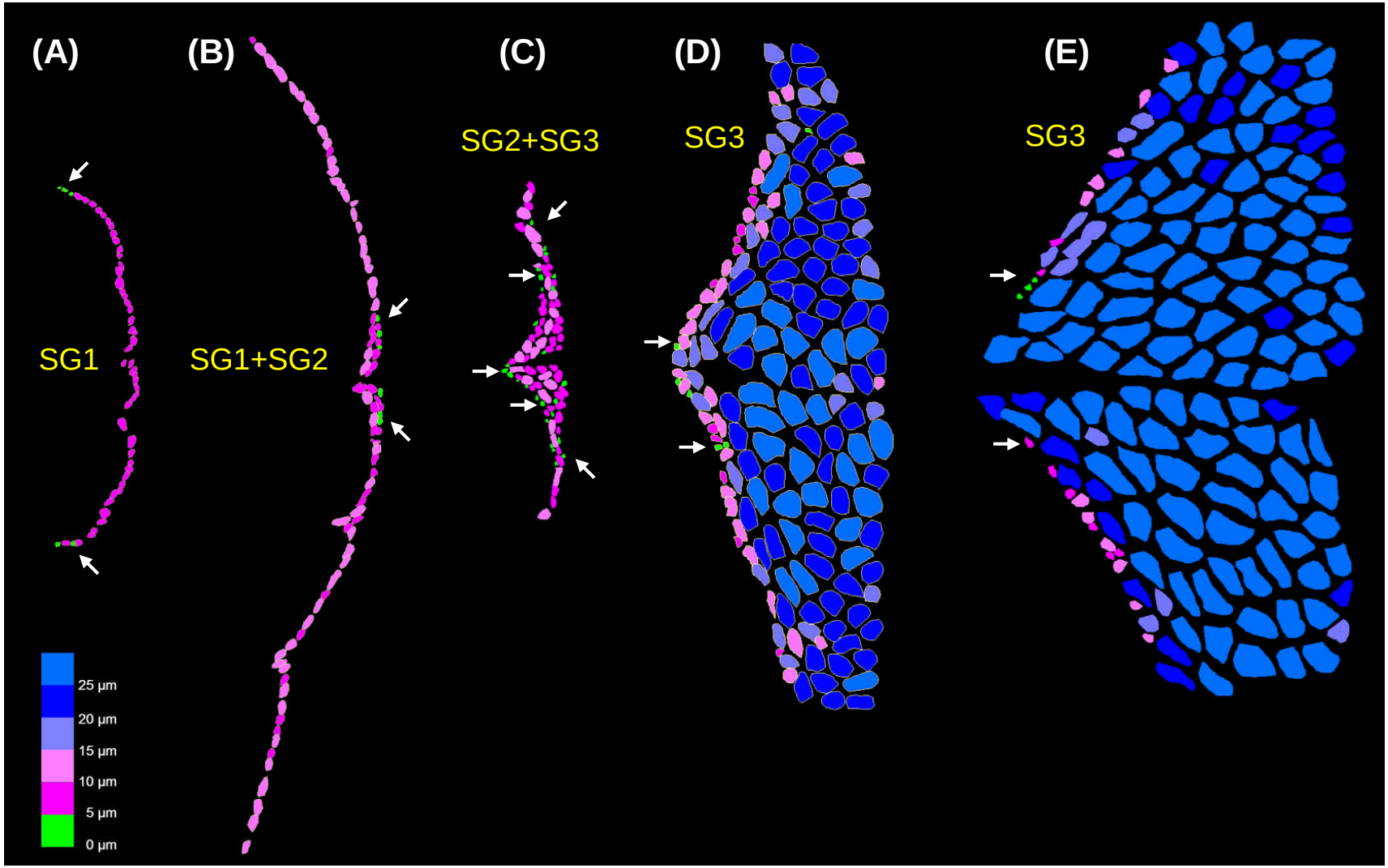
(A)
(B)
(C)
(D)
(E)
SG1
SG1+SG2
SG2+SG3
SG3
SG3
25 µm
20 µm
15 µm
10 µm
5 µm
0 µm

Fig. 3.3 Zones of fibre recruitment in slow muscle of zebrafish representing the period from hatching to late adulthood. All muscle fibres stained with S58 muscle fibre were further divided into 6 different colour groups based on their fibre diameter. New muscle fibres were firstly identified from the germinal zone at the dorsal and ventral myotomes (SG1), in larvae of 5.8 mm SL (A). A second zone (SG2) was identified in the outer region adjacent to the HS in late larvae of 7.0 mm SL (B). A third zone (SG3) was evident in the inner region adjacent to HS in juvenile of 10.0 mm SL (C). SG3 remained active and SG2 became exhausted in early adult of 20.0 mm SL (D). Newly formed fibres were only from SG3 in late adult stages (35.0 mm SL) (E). The arrows indicate the newly formed fibres.

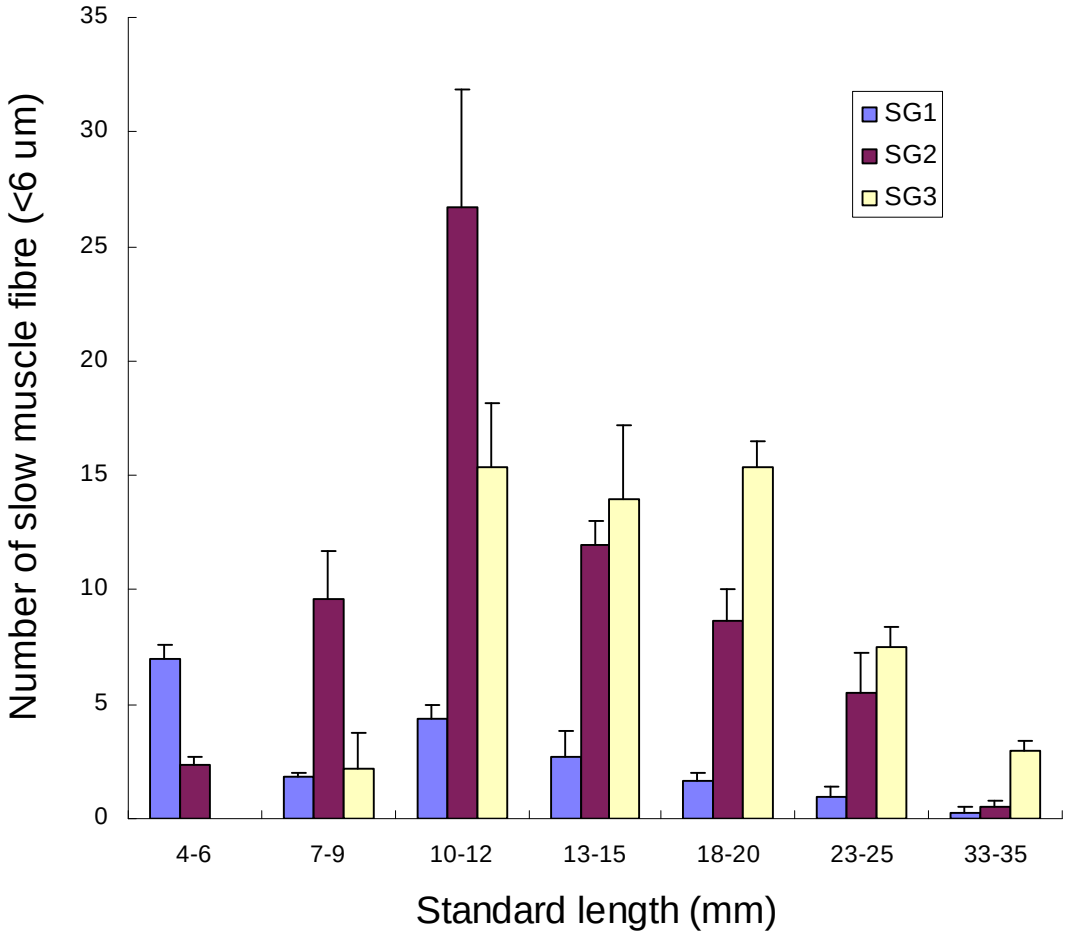

Fig. 3.4 Quantification of the relative contribution of new muscle fibres from three germinal zones (SG1, SG2, SG3) in slow muscle of zebrafish at different size ranges. A muscle fibre diameter of < 6 μm was considered a newly formed muscle fibres. Each size group contained measurements from 3-5 fish. Error bars represent the mean + s.e.m.

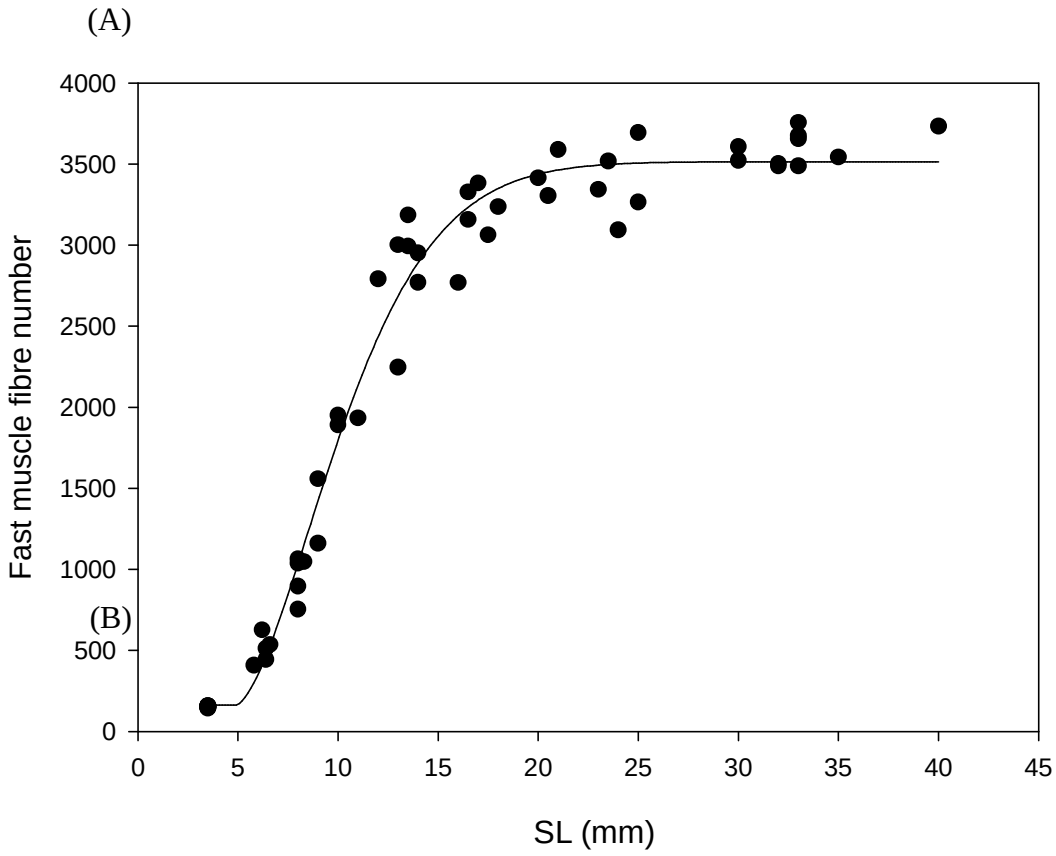

Fig. 3.5 The relationship between the number of fast muscle fibres and SL established by fitting a Gompertz equation (N=53 Adj-R^2=0.98)

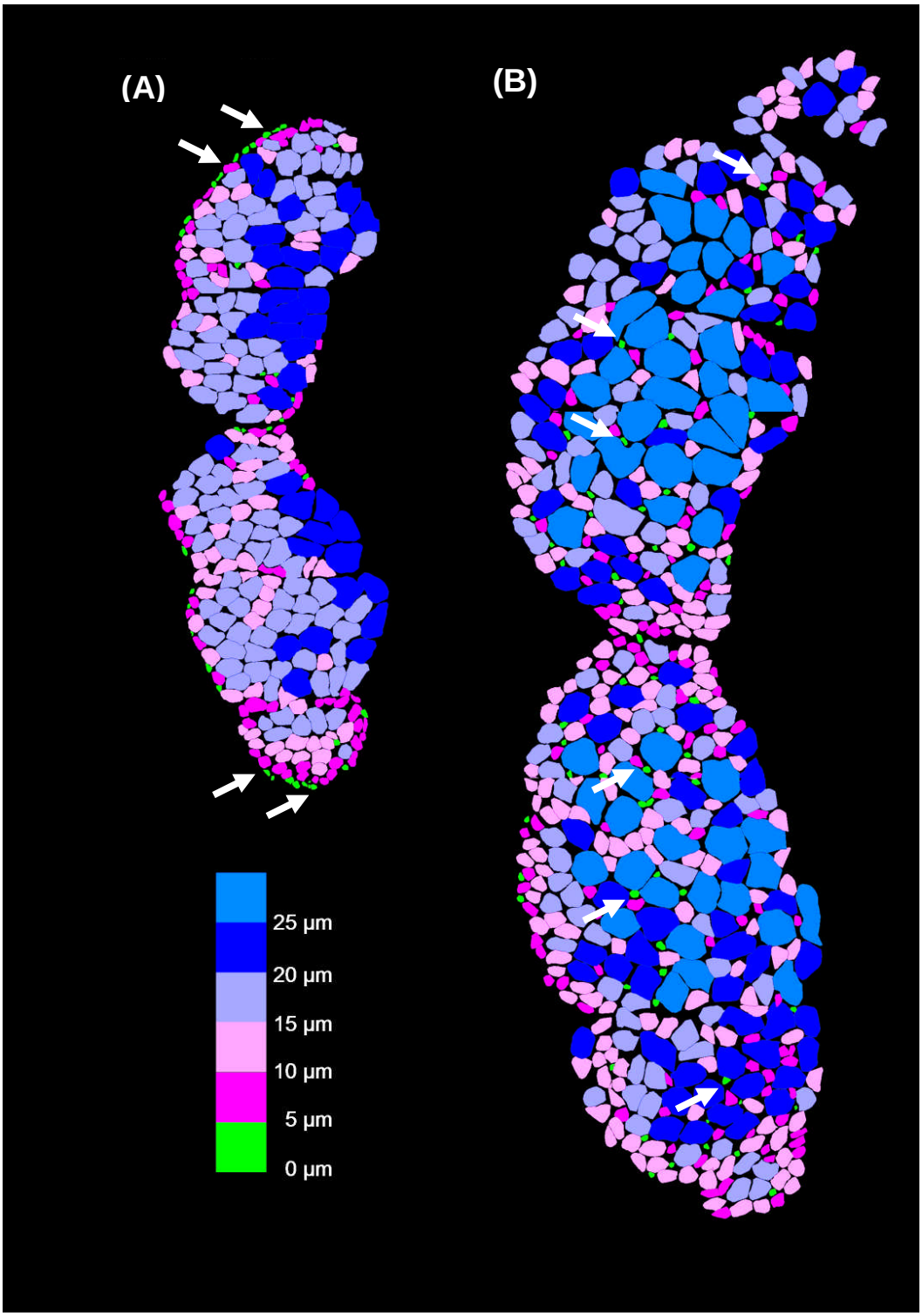
(A)
(B)
25 µm
20 µm
15 µm
10 µm
5 µm
0 µm

Fig. 3.6 Schematic diagram showing zones of muscle fibre recruitment in the fast myotomal muscle. All muscle fibres were divided into 6 different colour groups based on their diameter (<5μm; 6-10μm; 11-15μm; 16-20μm; 21-25μm; >25μm). SH was first identified as small diameter fibres (indicated by white arrows) mainly restricted to germinal zones at dorsal and ventral regions of the myotome in fish of 6.0 mm SL (A). The onset of MH was identified by small diameter muscle fibres (indicated by white arrows) on the surface of existing fibres throughout the myotome in fish of 10 mm SL (B).

(B).

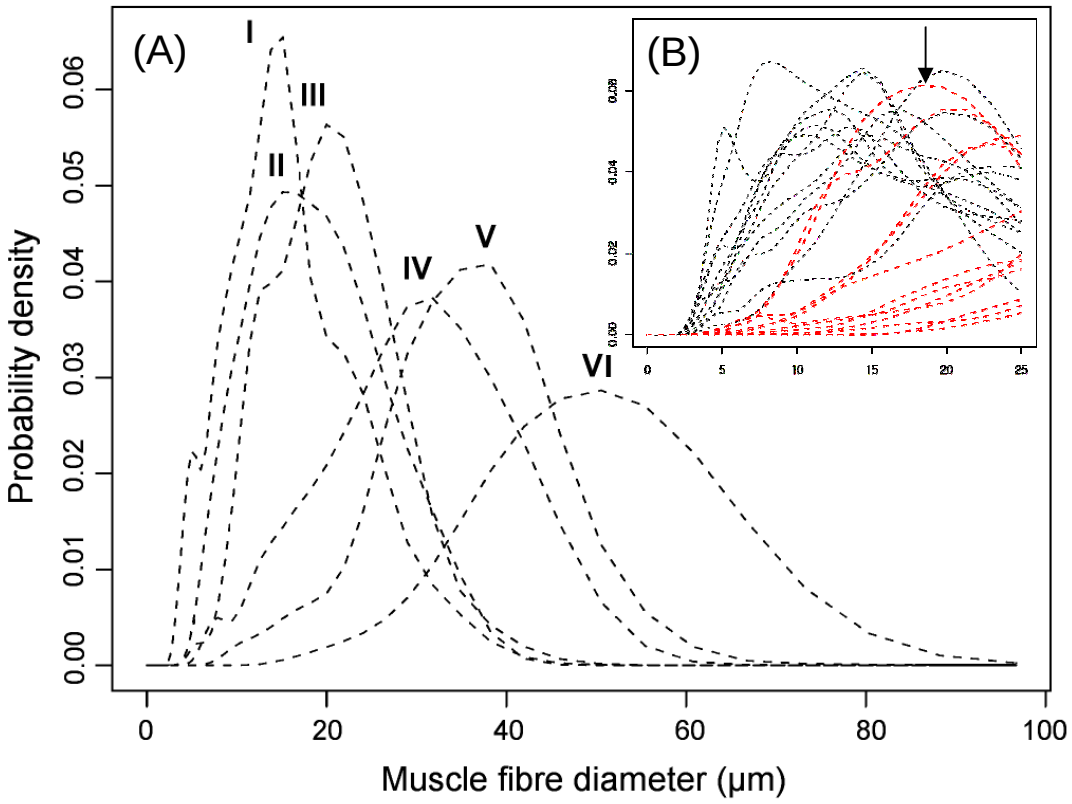

Fig. 3.7 (A) Smooth probability density function fitted to measurements of fast fibre diameter for fish ranging in size from 8.0-35.0 mm SL (Curves for 6 individual fish were selected to show probability density function at: I: 8 mm SL; II: 12 mm SL; III: 16 mm SL; IV: 20 mm SL; V: 25 mm SL; VI: 35 mm SL). Each dashed curve represents the probability density function of an individual fish. The probability density of relatively small muscle fibres diameter (<20μm) remained higher in fish less than 20mm SL (I, II, III) compared to fish larger 20 mm SL (IV, V, VI). (B) An expanded view of the probability distribution for muscle fibre ranging from 0-25 μm in diameter. The red dashed lines represent the fish without newly formed muscle fibres (4.5-5.0 μm in diameter). An arrow indicates the smallest fish (17 mm SL) where new fast muscle fibres (4.5-5.0 μm in diameter) were absent.

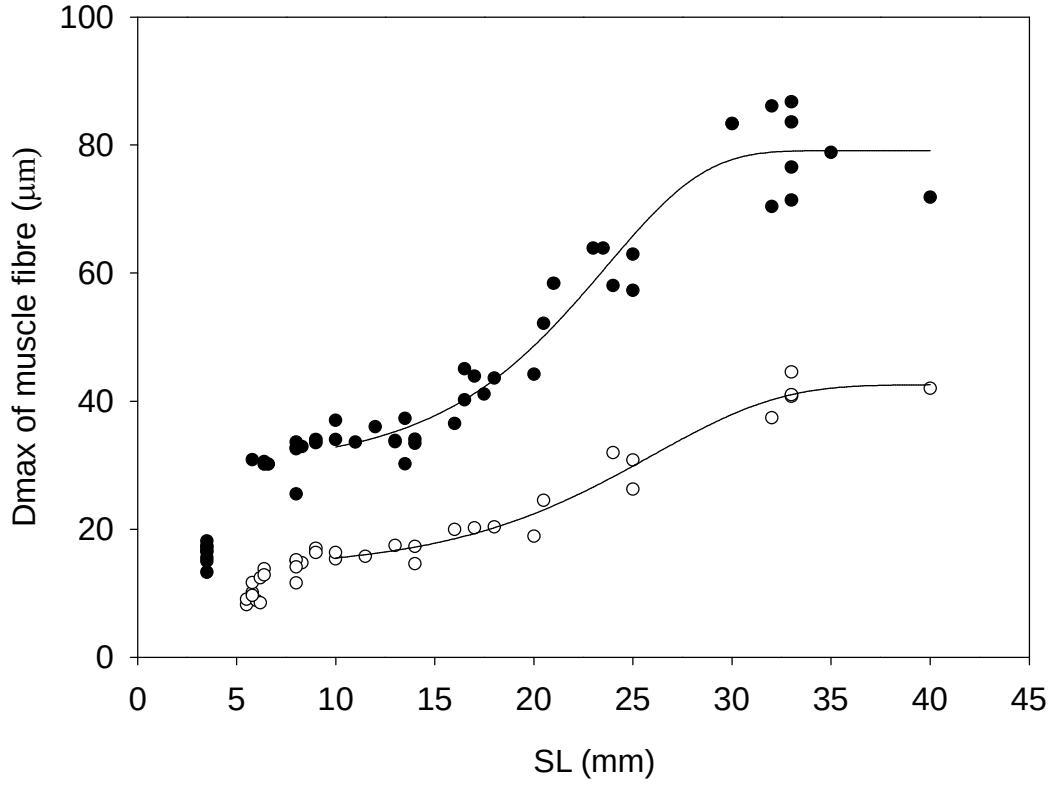

Fig. 3.8 The relationship between Dmax of fast (open circles) and slow (closed circles) muscle fibre and SL. A nonlinear regression was fitted to fish of 8-40 mm SL (Slow muscle, Adj-R^2=0.93 n=18, P<0.001; Fast muscle: Log_{10} Dmax = (Adj-R^2=0.93; n=33, P<0.001).

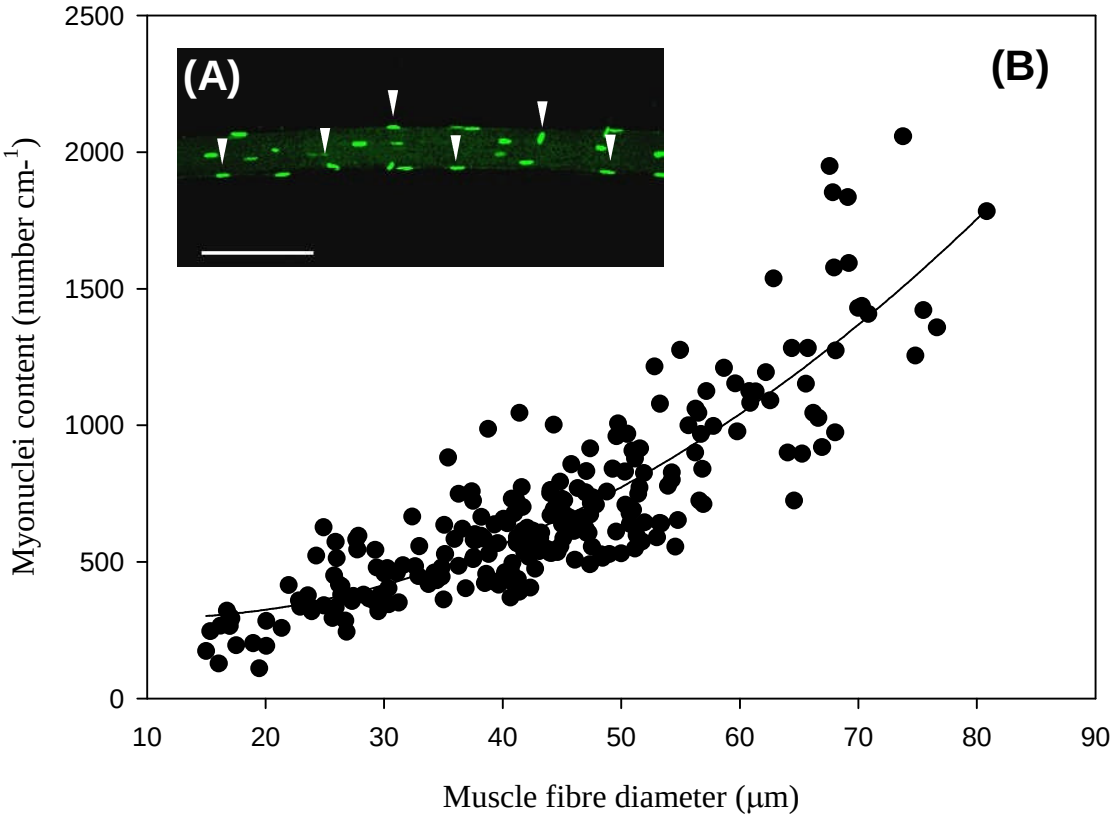

Fig. 3.9 Isolated single fibres from fast myotomal muscle stained with SYTOX green to visualize the myonuclei. (A) Example of a confocal image constructed by a z-series of 2 µm sections through a single fast muscle fibre. (B) The relationship between muscle fibre diameter (µm) and the number of nuclei per cm^{-1} in a single fast muscle fibre. A second order polynomial with the following equations. Myonuclei cm^{-1} = 322.72 -5.81 (fibre diameter) + 0.2964 (fibre diameter)^2 (Adj-R^2=0.76; n=251; P<0.0001). The arrows indicate the individual nuclei. Scale bar=100µm.

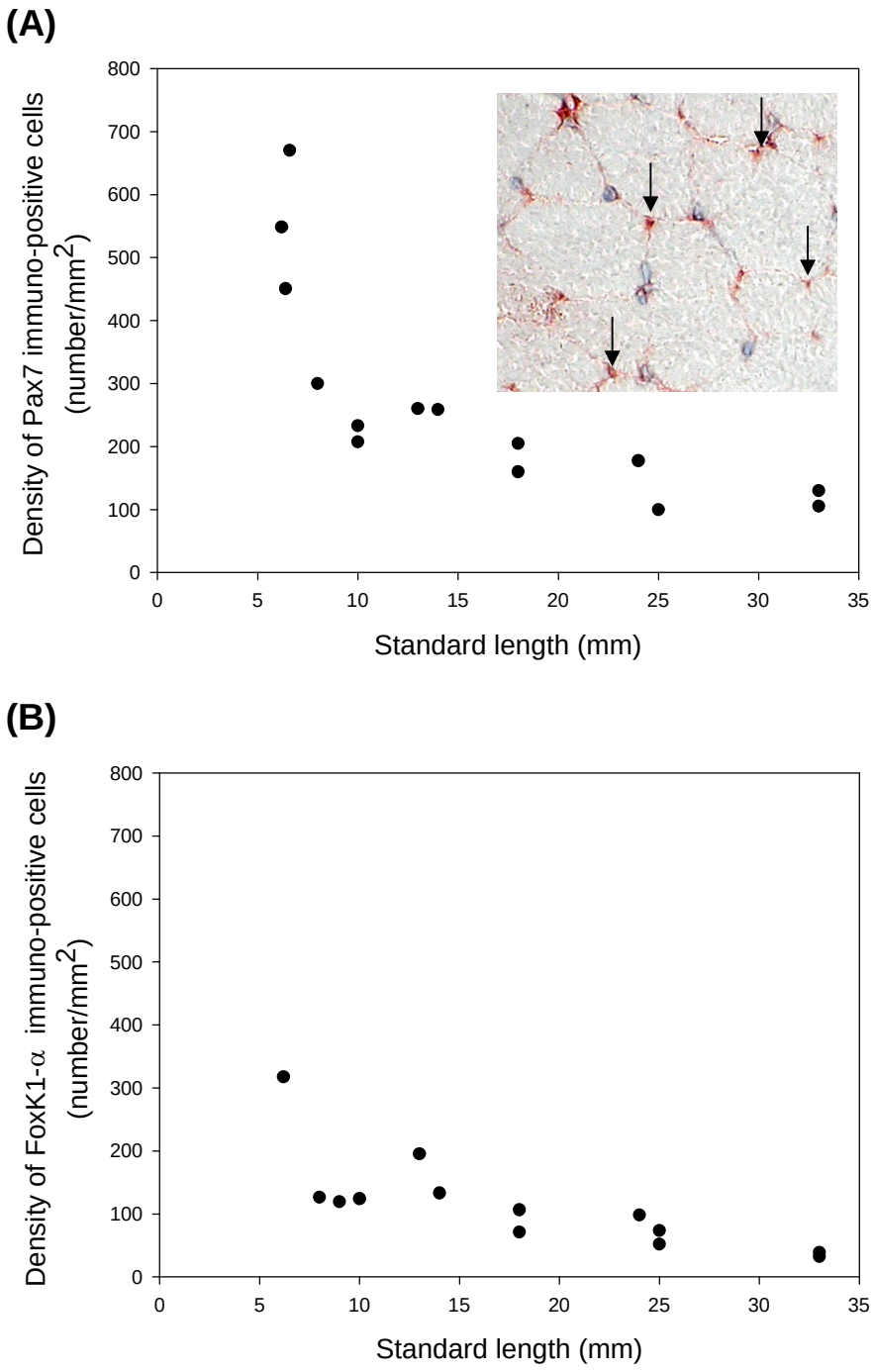

Fig. 3.10 The relationship between fish standard length and the density of presumptive MPCs immuno-positive for (A) Pax7 and (B) FoxK1-α protein in fast myotomal muscle. Inserted image represents an example field with arrows marking MPC stained with Pax7s.

Chapter 4.0 Characterisation of a *myospryn* orthologue and its expression in relation to muscle growth in zebrafish

4.1 Abstract

Myospryn is a gene also known as *cmya5* (cardiomyopathy associated 5) that was later renamed on the basis of its restriction to striated muscles and by the presence of a SPRY domain at its the C terminus. Here, a 5279 bp full-length *myospryn* ORF (open reading frame) was cloned and characterised in zebrafish. Comparative genomic analyses indicated that myospyrn arose in and is restricted to the vertebrates. While zebrafish *myospyrn* is markedly shorter than mammalian orthologues, its protein still contained all the same functional domains, and its gene has a similar intron-exon structure. Further, gene order was well conserved in myospyrn-containing genomic neighborhoods of different vertebrates. *In situ* hybridisation showed that *myospryn* was restricted to the embryonic myotome. In adults, its transcripts were mainly limited to tissue containing striated muscle fibres. In postembryonic zebrafish, *myospryn* was up-regulated concomitant to the cessation of fast muscle fibre production. Specifically, its expression level was lowest when hyperplasia was most active (8-10 mm SL) before being up-regulated as fibre production slowed (15-17 mm SL) and peaking at the body length when fibre production ceased (20-25, 26-30, 33-35 mm SL) to a maximum 3-fold difference. These results indicate a putative role for zebrafish myospryn in regulating myogenesis, particularly as a specific regulator of muscle fibre production.

4.2 Introduction

Myospryn is a gene that was identified in a human cardiac muscle library as a partial cDNA named *cmya5* (cardiomyopathy associated 5) (Walker, 2001). It was later renamed as *myospryn*. In mammals, it codes a costamere protein with a defined role in hypertrophy and atrophy-related conditions. In mice, *myospryn* encodes a costamere protein (~3790 A.A) expressed at the sarcolemma and sarcoplasm of muscle fibres co-localized with binding partners including dysbindin (Benson et al., 2004), α-actinin-2 (Durham et al., 2006), desmin (Kouloumenta et al., 2007), and dystrophin (Reynolds et al., 2008). *Myospryn* was down-regulated in *mef2A* knock-out mice with cardiac abnormalities (Naya et al., 2002), as well as in the muscle of DMD (Duchenne muscular dystrophy) patients (Tkatchenko et al., 2001) and was up-regulated in an experimental model of muscle hypertrophy (Kemp et al., 2001). Recent studies on the protein kinase (PKA) signal transduction pathway indicated that myospyrn is an anchoring protein serving as a PKA substrate at the costametric region of stratified muscle (Reynolds et al., 2007). In dystrophin-deficient muscle, myospryn was found to mislocalise with dystrophin resulting in aberrant PKA signaling (Reynolds et al. 2008). This evidence suggests that *myospryn* plays a vital role in mammalian myogenesis.

Almost no data exists on teleost *myospryn* genes. In the tiger pufferfish, a partial putative myospryn orthologue was identified to be specifically expressed in fast muscle fibres and relatively up-regulated by 25-fold in fast muscles of a 3.4-kg fish where myotube production had been switched off in comparission to fast muscles of a 190-g fish where hyperplasia was active (Fernandes et al., 2005). *In silico*

analysis also showed that pufferfish *myospryn* contained several conserved domains shared with mammalian orthologues. Other than these results, teleost myospryn also remains uncharacterised.

Accordingly, the aim of this chapter was to obtain a full-length cDNA of zebrafish *myospryn* and to perform comparative genomic analyses with other metazoan orthologues to gain insight into its potential functions. The second aim was to perform *in vivo* expression analyses of *myospryn* in embryos, across different adult tissues and in relation to the model of postembryonic muscle fibre recruitment established in an earlier chapter (Chapter 3).

4.3 Material and Methods

4.3.1 In silico identification of a myospryn orthologue in zebrafish

A partial pufferfish *myospryn* orthologue sequence (*FRC258*) (Accession number CK829660) was used as a probe in TBLASTN similarity searches to identify the putative zebrafish orthologue in NCBI (http://www.ncbi.nlm.nih.gov/BLAST/), Uniprot (http://expasy.uniprot.org/) and Ensembl (http://www.ensembl.org/) databases.

4.3.2 Fish collection and sample preparation

The fish were from the same group of F2 zebrafish as described for the growth experiment in Chater2, section 2.2. Tissue samples of brain, heart, liver, ovary, skin, spleen, slow muscle, and fast muscle were collected from 2-10 adult fish (~25 mm SL) and pooled before RNA extraction.

Pure fast muscle dissections were sampled from zebrafish of 6 different body length ranges, including 8-10, 11-13 and 15-17 mm SL corresponding to the active phase of muscle fibre production (myotube +) and 20-25, 26-30 and 31-35 mm SL corresponding to the stage where muscle fibre production ceased (myotube -). For fish less than 20 mm SL, each replicate represented 8 individuals. From 20 to 30 mm SL, each replicate was from 2 fish. For fish > 31 mm SL, replicates were from individual fish. All tissue samples were stored in RNA later solution (Ambion).

4.3.3 RNA isolation and cDNA synthesis

Total RNA was isolated as described in Chapter 2 (section 2.4.2-2.4.4) from each sample using Tri-reagent (Sigma) following the manufactuers instructions.

4.3.4 Cloning and sequencing of myospryn cDNA

Detailed procedures for cloning and sequencing are described in Chapter 2 (section 2.4.7 and 2.4.8). Different sets of primers were designed to amplify various fragments of *myospyrn* by RT-PCR that together represented a complete coding sequence (Fig 4.1).

4.3.5 Sequence alignment

The C-terminal containing conserved domains of *myospryn* from pufferfish, stickleback, medaka, zebrafish, frog, chicken, mouse and human (Table 4.2) were aligned with the web server of T-coffee (Notredame et al., 2000) with a strategy including lalign and Clustal W alignment options.

4.3.6 Comparison of shared synteny of myospryn containing genomic regions

Syntenic maps for *myospryn* and its surrounding genes were constructed manually using data extracted from Ensembl database Release 55 (www.ensembl.org) genome assembles, considering the strand orientation and chromosomal position.

4.3.7 Quantitative Real-time PCR (qPCR)

The expression of *myospryn* and elongation factor 1 alpha (*ef-1α*), beta-action (β-actin), and 18S rRNA was measured using qPCR across the sampling points described in section 2.4. Detail procedure was described in Chapter 2 (Section 2.4.10). Primer pairs used to amplify the selected candidate genes are listed in Table 4.1. Each amplicon was performed in reprelicate in 96-well plates (Applied Biosystems) under the following thermocycling conditions: 15 min at 95 °C for initial activation and then 40 cycles of 15 s at 94 °C, 30 s at 56 °C and 30 s at 72 °C. During Only during confirmation products were sequenced. cDNA dilution series and dissociation analysis were also performed.

Ct values analysed using Genex, v. 4.4.2 (MultiD Analyses AB, Göteborg, Sweden), and corrected for differences in amplification efficiencies calculated from the cDNA dilution series. Genorm (Vandesompele et al., 2002) and Normfinder (Andersen et al., 2004) were used to examine the stability of reference and experimental genes. These programs indicated that *ef-1α* and *beta-actin* were most stable among those tested and together should be used for normalisation. Ct values for *myospryn* were accordingly normalised by Genex using both *ef-1α* and *beta-actin* and relative *myospryn* transcript abundance in each sample was placed on a scale of 0-1. A natural log transformation was performed on the *myospryn* relative expression values to bring the data closer to a normal distribution (Anderson-Darling A squared value = 0.256, p=0.705) and to ensure homogeneity in data variances (Levene's test Statistic =1.493, p=0.221). Thus, the natural log transformed data was suitable for parametric statistics. A one-way ANOVA was

performed in Minitab v13.2 (Minitab Inc.) using Fisher's individual error rate test with an error rate of 0.05 to establish statistical differences in mean relative expression values between sampling stages.

4.3.8 RT-PCR-based analysis of tissue expression

The profile of *myospryn* mRNA across different zebrafish tissues was assessed using RT-PCR as described in Chapter 2 (Section 2.4.8). First strand cDNA was synthesised (as previous described in Chapter 2, Section 2.4.7) from RNA samples derived from the tissues described in Section 4.3.2. These cDNAs were used as a templates to amplify *myospryn* and *EF1α* products with primer described in Table 4.1 using following thermocycling conditions: 5 min at 95 °C for denature and then 30 cycles of 15 s at 94 °C, 30 s at 56 °C and 30 s at 72 °C and 1 cycle of 5 min at 72 °C. No reverse-transcriptase or no-template controls were also included.

4.3.9 Whole-mount in situ hybridisation

Whole-mount *in situ* hybridisation was performed as described in Chapter 2 (section 2.4.13) with a minor modification. Embryos were staged according to a standard criteria (Kimmel et al., 1995). An 1124-bp amplicon of partial zebrafish *myospryn* was amplified by PCR with primers detail in Table 4.1 as described in Chapter 2 (section 2.4.8) All other details, including probe synthesis, *in situ* hybridisation method, embryos processing, imaging was as described in Chapter 2 (section 2.4.13)

4.4 Results

4.4.1 Identification of a zebrafish myospryn gene

BLAST screening public databases with the translated transcript of *FRC258*, retrieved highly significant hits to *myospryn*-like sequences in zebrafish (GeneBank Accession number: NM_001079985) and other vertebrate species (Table 4.2). *Myospryn* was not identified in the genome of any non-vertebrate metazoan species examined. A full-length muscle-derived ORF of zebrafish *myospryn* (GeneBank Accession number: EF141827) was obtained using a PCR strategy following by cloning and sequencing (Fig. 4.1).

4.4.2 Genomic organization and protein characterisation of myospryn in zebrafish

The zebrafish orthologue of *myospryn* was located on Chromosome 16 (42.15-42.19 Mb) (Ensembl release version 55) and, like mammal sequences, comprised 13 exons and 12 introns. As for mammals, the second exon (3574 bp) was comparatively larger than others (Fig. 4.2A). SMART (Simple Modular Architecture Research Tool) demonstrated that full *myospryn* sequence included an ORF of 5277 bp encoding a protein of 1759 A.A. Three functional domains, a B-box coiled-coli (BBC) domain, a region containing fibronectin type III (FN3) repeats, and a SPla and the RYanodine Receptor (SPRY) domain. Each of these was present on a relatively small fragment (~500 A.A) of poly-peptide sequence close to the C-terminal (Fig 4.2.B). Additionally, a phosphorylatioin site was also reveled in zebrafish myospryn (residues 316-331) by ScanProsite (de Castro et al.,

2006)

4.4.3 Sequence alignment analysis of myospryn

Sequence alignment revealed that the *myospryn* protein was approximately twice as long in human (4069 a.a) and mouse (3739 a.a) than zebrafish (1759 a.a). Sequence similarities of 40% were observed by aligning solely the C-terminal domain of myospryn orthologues from mammals (human, mouse), birds (chicken), amphibians (frog), and teleosts (medaka, stickleback, zebrafish, tetraodon, takifugu) (Fig. 4.3). While this region is relatively short (500~600 A.A) for all species examined, the complete functional motifs were present, as in zebrafish (Fig. 4.3).

4.4.4 Conserved gene order surrounding myospryn across the vertebrates

The organisation of the genomic region containing *myospryn* was well-conserved across vertebrate species (Fig 4.4). Numerous genes, including *homer 1* (Homer homolog 1) and *papd4* (PAP associated domain containing 4), *cdk7* (Cyclin-dependent kinase 7), *mtx3* (Metaxin 3), *serinc5* (Serine incorporator 5), and *thbs4* (Thrombospondin-4 precursor) consistently appeared in conserved order relative to *myospryn*. In zebrafish, *cdk7*, *mtx3*, *serinc5*, and *thbs4* were found as a group retaining synteny with other vertebrates, but on a distinct chromosome to the *myospryn* chromosome (Chr 5) (Fig. 4.4). These results provide evidence that the characterised *myospryn* sequence of zebrafish is a true orthologue of *myospryn* from mammals and those identified in other vertebrates (Fig. 4.4).

4.4.5 Localisation of myospryn transcripts during zebrafish development

During embryonic stages, *myospryn* accumulated specifically in the somites (Fig. 4.5A). Cross-sections revealed that *myospryn* was expressed in the myotome compartment (Fig. 4.5B). In adult tissues, *myospryn* was detected after 30 RT-PCR cycles solely in tissue containing striated muscle fibres, plus ovary (Fig. 4.5D). *EF1α* transcripts were constant across all tissues (Fig. 4.5C).

4.4.6 Expression of myospryn across a time course representing active or inactive muscle fibre recruitment

Myospryn transcripts were quantified by qPCR in fast muscle of zebrafish from three myotube (+) stages (8-10, 11-13 and 14-17 mm SL) and three myotube (-) stages (20-25, 25-30 and 35-40). *myospryn* transcript abundance generally increased with body length (Fig. 4.6). The relative expression of *myospryn* abundance was respectively 2.5, 2.3 and 2.8 fold greater in fish of 20-25, 25-30 and 31-35 mm SL than fish of 8-10 mm SL stage (Fig. 4.6) where myotube production was most highly active (all statistically different, $P<0.05$). Interestingly, relative *myospryn* abundance was also significantly greater ($P<0.05$) in 14-17 mm SL where myotube production was evident, but slower (Fig. 4.6). There was no significant difference in the relative transcript abundance of *myospryn* between fish of 11-13, 15-17, 20-25, 26-30 and 31-35 mm SL ($P<0.05$) barring 11-13 and 20-25 mm SL ($P<0.05$) (Fig. 4.6). It should also be noted that a higher variation in relative expression abundance was found in larger fish from myotube (-) stages (Fig. 4.6).

4.5 Discussion

4.5.1 Characterisation of myospryn in zebrafish

The intron-exon structure of *myospryn* in zebrafish was similar to that of mammals (Durham et al., 2006). In addition, three distinct domains, BBC, FN3, and SPRY, previously identified in human and mouse myospryn (Benson, et al., 2004; Durham et al., 2006) were present across vertebrates including zebrafish, indicating function conservation. Yeast two-hybrid screens, GST-pull down, and immuno-precipitation experiments have demonstrated that the domain-containing regions of myospryn served as binding sites for interactions with various proteins. For example, the BBC domain binds dysbidin (Benson, et al., 2004), the BBC, FN3 and SPRY domains bind α-actin (Durham et al., 2006), the SPRY domain binds desmin (Kouloumenta et al., 2007) as well as the RIIα subunit of protein kinase A (PKA) (Reynolds et al., 2007, 2008), and the FN3 and SPRY domains binds dystrophin (Reynolds et al., 2008). It is also interesting that the N-terminal of myospryn, which is variable among vertebrate lineages, is uncharacterised in functional terms. Further studies will be required to characterise its functional role particularly in relation to the significance of the large sequence length difference between zebrafish and mammals.

4.5.2 Vertebrate myospryn orthologues are located within a conserved syntenic region.

In 9 vertebrate species from all major lineages, *myospryn* was located in a highly

conserved syntenic region containing only a limited number of gene inversions and translocations across all species examined. Highly conserved regions of synteny often contain developmentally important genes (Sandelin et al. 2004; Wolff et al. 2005). Furthermore, it has been hypothesized that gene order is retained during evolution as a way of controlling the regulation of the genes involved through shared cis-acting elements (MacKenzie et al. 2004; Ahituv et al. 2005; Goode et al. 2005; Kleinjan and van Heyningen 2005; Gomez-Skarmeta et al. 2006). There is evidence that genes in the syntenic *myospryn* region could share a similar function. For example, *Homer* plays a vital role in skeletal muscle function since its-knockout in mice resulted in a dystrophic phenotype and reduced muscle fibre force generation (Stiber et al., 2008). Thus, it is plausible to suggest that an interaction exists between the protein products of *homer1* and *myospryn* and their conserved genomic proximity allows co-regulation of their genes at transcriptional levels.

4.5.3 Transcriptional evidence supports a role for myospryn in regulating muscle development

Zebrafish *myospryn* was almost exclusively muscle-specific in both embryonic and postembryonic stages, similar to previous findings from mouse (Benson et al., 2004; and Durham et al., 2006). In tiger pufferfish, *myospryn* was differentially expressed between two stages where fibre production was active or had ceased. (Fernandes, et al., 2005). However, this simple experimental design means the up-regulation of *myospryn* after myotube production ceases may also have been due to other physiological aspects related to body size. Here, its expression was

examined over a more comprehensive range of body sizes. It is most strongly expressed at myotube (-) stages compared to the point where myotube production was maximal suggesting that it may regulate muscle fibre production. Since zebrafish at the myotube (–) stage grows solely by hypertrophy, *myospryn* may specifically regulate hypertrophic growth or be part of a genetic pathway inhibiting myotube formation. Functional characterisation is required to explore such scenarios. A simple future study would be its “known-down” in zebrafish with a morpholino followed by characterisation of the muscle fibre phenotype and localisation of orthologues of its mammalian binding partners.

Table 4.1 Primer sequences used for *myospryn* characterisation.

Gene	Primer Sequence (5'-3')	Use
myospryn		
FWD1	CGAAATGGACCGTGCTGTG	SA, WIH
FWD2	CAGACCTCTATGAGG ACGCAATAGG	SA
FWD3	AATCAAGGACACAACTATCACAAC	SA
FWD4	AGGGTGGATAA AGGCAAGACTG	SA
FWD5	CGGAGGAGCTTGATTATG	SA
FWD6	CTCAGAGGAGTACAGA GTGACGG	SA, qPCR
REV1	CTCCATCATCTGAGTCAGAGCATC	SA, WIH
REV2	TCCTCAACTACAGCAAGTGTTTCTC	SA
REV3	CATCTCCAGAGCTTGATCTGGCAG	SA
REV4	TGATCACTGGGACAGAGG	SA, qPCR
REV5	CGTGGGCCTTGTAAACTAGCA	SA
ef1-α		
FWD	CTTCAACGCTCAGGTCATCATCC	RT-PCR, qPCR
REV	GCTTCTTGCCAGAACGACGG	RT-PCR, qPCR
β-actin		
FWD	CCGTGACATCAAGGAGAAGCT	qPCR
REV	TCGTGGATACCGCAAGATTCC	qPCR
18S rRNA		
FWD	The 18S primer pair were obtained from a commercial kit (QuantumRNA™ Universal 18S Internal Standard, Ambion).	qPCR
REV		qPCR

SA: Sequence Assembly; WH: Whole mount *in situ* hybridisation;

Table 4.2 List of gene IDs for the studied *myospryn* orthologues in vertebrates.

Species	Ensembl ID
Human (*Homo sapiens*)	ENSG00000164309
Mouse (*Mus musculus*)	ENSMUSG00000047419
Chicken (*Gallus gallus*)	ENSGALG00000014809
Frog (*Xenopus tropicalis*)	ENSXETG00000000515
Zebrafish (*Danio rerio*)	ENSDARG00000061379
Medaka (*Oryzias latipes*)	ENSORLG00000008983
Stickleback (*Gasterosteus aculeatus*)	ENSGACG00000009895
Takifugu (*Takifugu rubripes*)	ENSTRUG00000009392
Tetraodon (*Tetraodon nigroviridis*)	ENSTNIG00000015411

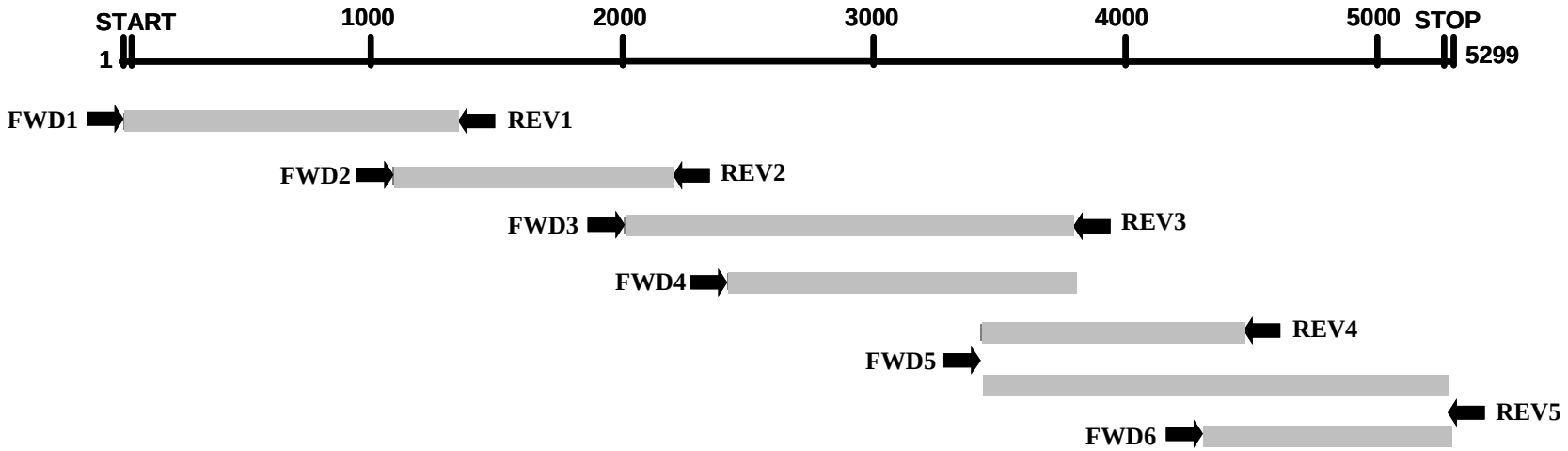

Fig. 4.1 Strategy for cloning and sequencing a full-length *myospryn* cDNA in zebrafish. Overlapped sequence fragments (gray) were amplified using different sets of primers (arrows) as shown in Table 4.1 and assembled into a contig coding a full-length *myospryn* cDNA.

(A)

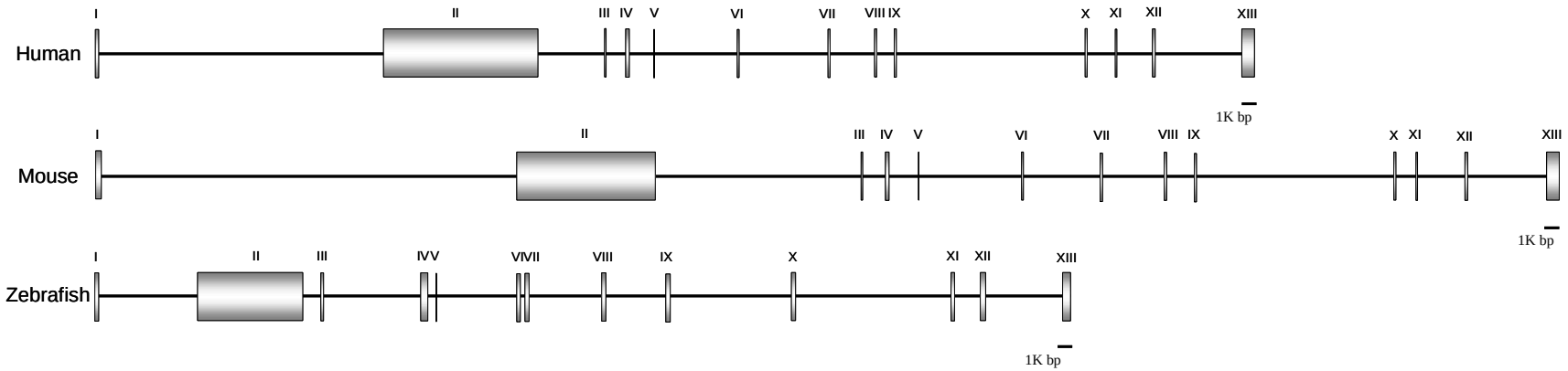
Human
I
II
III
IV
V
VI
VII
VIII
IX
X
XI
XII
XIII
1K bp
Mouse
I
II
III
IV
V
VI
VII
VIII
IX
X
XI
XII
XIII
1K bp
Zebrafish
I
II
III
IVV
VIVII
VIII
IX
X
XI
XII
XIII
1K bp

(B)

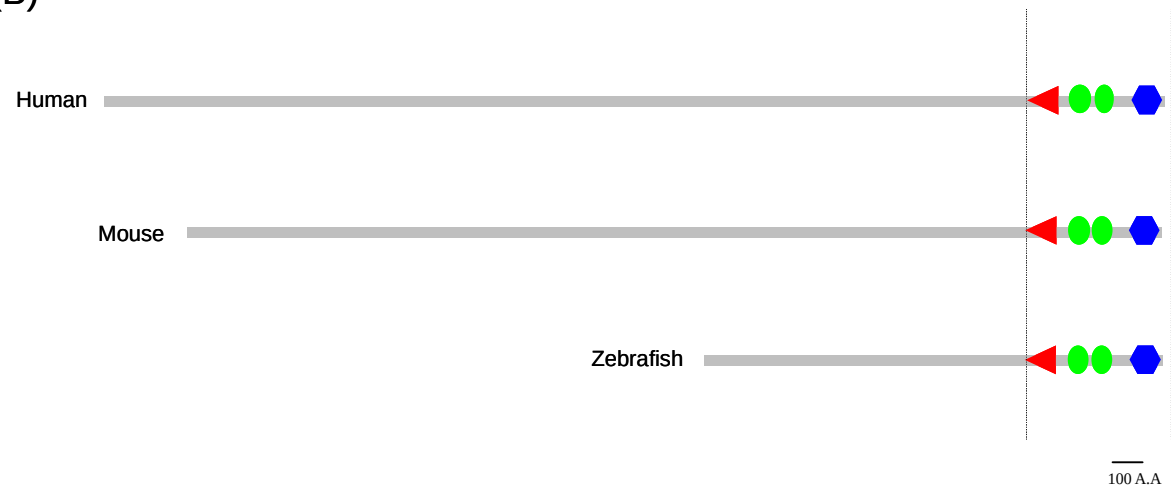
Human
Mouse
Zebrafish
100 A.A

(C)

```
  1
ATGGACCGTGCTGTGAAAGGGGAATGTGAGGGGGCTGAACCAGAGATGGAGGAACTGCAGGACGTGGGCTCTGGAATAATGGATATGGGCGACGAGGAGGAGATTGAGGAACTTCATAAA
  1      M  D  R  A  V  K  G  E  C  E  G  A  E  P  E  M  E.....................................................................

AGCTTAAAGGAAGCTGTGCAAGATCCATCTGTGAAGCCTAAACTACAGTGTCTGATGGTGGACCCATCCTTCTCCATGGTGACAGTGCAGAGCGAGGACAGTGGGATCGTATGGGAGACTGCTT
CAAGCAGATGCTCTACTCCATGGGCTTCAGAGGGAAGCTCGCCCTCTGAACAGTACAGCCTAGAAGGTTCTGGCACACAGGGGAATATTGTAATTATAATGGACGAAGACAGAATTAAGAGGAA
GAAAACAAGCAGCAGAGGCAAGCTGGGTGAAAGGTTTAAAAAGTCAGGCTCCAGAGTGCCAAAAAGTCGGGTGGGTGAGGAAAGACCTGCGATGATAGAGGTAGCCCTGCCGAATATACGACCT
GAAAGTAGTGAGGATGATCTCTCTGCTGTTAGCAAGGATCAAGATCTCTTTAGTTTAGTATCGGAGGGTTTTGAAATACTCAATATTGTCGTACCTTCAAAGCTCGCTACAGTAGATGAGGAAG
ATAGCACTGAACTGACAGAAAATTTAGCCTACTTGGATAATACCCCAAAGATAAAATCCAAACCTAAGCATGAACCTTTAGAAGCAAATGGTTATTGTGTGAGCTCAGAAGCTAACGAAATAAA
GCAAAATGAAAGCTTGAATGATTCATCCCAGATCTCAGATGATAAACAATCCAAAAAAGATGAAACTCAAATGGACTATCTTGAAAAATTCACACTGTTAGATGAGCAGGCACCTAGTGATGGA
CTTGCACTGACAGAAAATCTTGTAGCAGAAGTGACTGTCCAGCCAGAGGTACCTCCGGCGAATCAGAAAGAATCAAAAGCAGATGAAGCCATTGAGGAGGATTCCTTTGTGATCATTAGCGATG
TTGAAATCGCAGGTGAACTTCTCGATGAAGTCTTCTACGGAAGTAAATCCAATGCAGAGCCTGTAGTGCCTCAAGAACATGGACGAATCACAAGACAGAGCTCTAAATCTTTAAAAGAAAGTGG
ATCAGTCTTATTTGGGAGTCAGGAATGTATTCTCACACCTGTTTACCTTCCAACTGGACCACCAAAGATCATTGATCAAGTCCTACTTGAGGAACCACGAGCAATGTCCTTCCATTACTCAGAC
CTCTATGAGGACGCAATAGGAGACCGGAAGAAGGAAGATGAATTCTCTGATACTGAGAGTGTAGTTTCTGAGAGGTCCTTCAAAAGAAGATGCTCTGACTCAGATGATGGAGATGGATATTTGG
AGAAGTTCACTCTGAAAGATGAAACACCAGCAGCTGCACTTGTACCCGAGGACAAAGGGAAGGTAGATGGGGGGATGTTAGTATGGCCACAAAGTAAATTTGAACTTACCGGATGTTTGGAAAG
AGCACAAGAAGAAAGCGATGAAGTAACTGTTGAACAACAGTGTCCACAGGATAAAAATGAAAGTGAAGCGAAGTGTGAGTCCACAGGGTGTTGTTCAAATGGACACTGTGGTCCGGAAATTCAA
CCAAAGGTGGAAGTAATCATTAAAGAAAAAGTCATATCGGATGACTTGGTTGCAAAGCATAGAAGGGAAGATATCAAGCCATGTGATATCACTGTCAGAATCAAGGACACAACTATCACAACTA
AAAGTGAGTCTGATGACAAACACCCTCCACAGGTGGTTGAGCCTAAAAACAAAACCACTAATAAAGAAGAACATGGTAGACAAAAACCAAAAGGTCTGACTGCTCGTATTGAAGTACCAAGGAG
TTTAGAGCATGAAGATGTTAGTAAAACTAAGGATGAACTTGAAATTCTTTCTAAAACAAAGATCTCAGAGAATATACAGGTTGAGATACCACATGAAGCTGAAAAAGTTAGGGTTTCTAAGGAC
AGCATAGGGAAAAATAATAAATCACCTGATGTCATTACTGACATTCAGAAAACGAATATGATTACAAAATTTGACAAAGGAGAGAAGGACGAAACACAGATGCAGAGCAAACTTCTAGACAAAG
ATAAAATTCAAAGGGTGGATAAAGGCAAGACTGAAATTGTAAAAAACCAAGCACCAGAAATATTTGCTCAAAAGGTTATCAGTATCAAAGAAACACCAACAGATAAAACAGAGCTTCCAAAAGC
TAAAGAACTACCAAGAGTAGAAAAAGAGGACAAACCTTTAAAAGAAACTTCTAAGGCTTCTGGAGTAAAACATTCTGCAAAATCCAGAGAAATAGATTCTCTAGTGCACCAAAAAGGAGAAACA
CTTGCTGTAGTTGAGGAGAAAGTAAGTGAAGGATTAACACCCAAGTCAGAGAAACATGAGAAAGTAATTGACATTATTGGAGCAGTGCAAGAGGTCGATGCACAAATCAATAGTATAGAAGTGT
TAGCAGAAATTAAAAAGAAGCCAGAGTCTAACATTACTGCAGTTCTCAGAGGATCAGAGCAATCACATTCAAGTAAAATAGTTACAACAACCACTGAGCTTCTGACTAAACCTGAGATTACAAA
TGAGACGAAAATGCCCCCAGAACTAGAAAATGATTCCAGCTCAGCAAACAATAAAGCCAAAGAGGACATTTATGTAGATAGACCTACAGCTGAGATACCAATCCTGAAACAAGGTCTGGAAAAG
CAAAAGAAACTTATTTACATACCTGAGATTGAACCTGAGGTCACAAAAAAGCTAGAACAAGTTGAGGAAATCAAGGTAGATGGTGTAGAGAAATCAAACAAGAAGGCAGAAATCACACAAGAGC
CTGTTCAGGAGGAGATACCTTCTGAGAACAGAGCAAAAACTGAGATTGAAGACATAGTTGAGTCAAGGCAAGAATGTAGCTTGTCGGTTAATGAAAAGGAGACATCTGTTCCAGAAGTCACAGA
GAACAAGAGTATAACCGCAGACATAGAGGACTCTTCAAAAGTAAGACTGTCATCTGTTGTACCAACAAAGGAGGTAGAATTCGAAGAACATAGTAAAATAAACGATGTAACCACAGAGATACCT
GTCAAAGAGAATTCTGAGATTAAGATTTTACCTCTAGCATCAACATTAGAGAAAGGAAAGAAAACTCAGATTGAAGATATATCAGATTTACCGGAACCCATCTCACCTCCTCCACAAGTTGATG
AAGAAGACTCCTCCGTGATGAGAGTTTCACCATTAGAGCCAGAAGATAGTAAAAAAGCTTATGAAGAAATACATGGAGGAGGAATAAGCCTAAGTAAGAATAAAGGTGTCTTCTCGTTATTGCG
AAGCTACACACCTCAAGAGGACCTCTCGGCCTTGAGCTTTGACCCAGATGTGCAGCGGGACATTGCGGAGGAGCTTGATTATGAGATGATCGATGAACAAGAGGCAAAACAGTCTGAACAAGCA
AGAACTGAGGATGGGAAAATTTGCCTGCCAGATCAAGCTCTGGAGATGGGCTTTGAATTTGTTGAGGATTTAGACAGTGCCCAGTTGGCGGATGAACTTGAAGAGGATGTAGAAATTCAACCAA
TGGATGCA
```

```
3601    TTCTGCCTTGATTGTCTGTGCCCAATACTGCTGAGTGAGGCTGAACATCAAAATCATAAGGTGGCTTCTCTGGAAGAGGCCTTCGACAGTATGAAGAAAAGACTAAGTGAAATGATATCA
1201     ..........................L  L  S  E  A  E  H  Q  N  H  K  V  A  S  L  E  E  A  F  D  S  M  K  K  R  L  S  E  M  I  S
3721    GTTTTGCAGTCAAGATCAGAAAATATCGAAGACTTTGTGTCTGAGCTTGAGGTGGCATACAACACAGTGGAGGAGAACTATAATGATTGTGAGAAGACCATAAAGGTACACAATGAGGAG
1241     V  L  Q  S  R  S  E  N  I  E  D  F  V  S  E  L  E  V  A  Y  N  T  V  E  E  N  Y  N  D  C  E  K  T  I  K  V  H  N  E  E
3841    GAGCTGAAGCTAGTGATGGATCAGTATAATGAGATGTCCCAGGCCATGGAGGAGCAGAAAAAGGCCAGACTGGAGCAGTTGTACGACCAGATTGTGTCGTTCCAAGAGAATATCGACAAG
1281     E  L  K  L  V  M  D  Q  Y  N  E  M  S  Q  A  M  E  E  Q  K  K  A  R  L  E  Q  L  Y  D  Q  I  V  S  F  Q  E  N  I  D  K
3961    GCCAAGGAAACTTTGGAGACAACAGCCAAGGAGGAAGAAGAGACGGATCCGCTTACGTTTATTTCTAAATCAAAAGACATCAGTATGAGGTTGAATACAGCTTTGGAATCCACCATGTCA
1321     A  K  E  T  L  E  T  T  A  K  E  E  E  E  T  D  P  L  T  F  I  S  K  S  K  D  I  S  M  R  L  N  T  A  L  E  S  T  M  S
4081    CTTGAACTTGGTCCACGAGGCCTGCTGGTTTTTGAGGATTACGCCAAGGGCAAGTCAGGCAATCAGGGGAAAAACAGACAAGCCATTCCAGTGCCTCAAAAACCACATCTTCAGCCACAG
1361     L  E  L  G  P  R  G  L  L  V  F  E  D  Y  A  K  G  K  S  G  N  Q  G  K  N  R  Q  A  I  P  V  P  Q  K  P  H  L  Q  P  Q
4201    GAGGCCAATTCTGCAACCAGCACTTCAGTCACTGTGTACTGGAGAGTCAACGAAGATGACATTATCGACTGCTTCCAAGTCTACTGTATGGAAGAGCCACAAGGAGCTATCTCAGAGGAG
1401     E  A  N  S  A  T  S  T  S  V  T  V  Y  W  R  V  N  E  D  D  I  I  D  C  F  Q  V  Y  C  M  E  E  P  Q  G  A  I  S  E  E
4321    TACAGAGTGACGGTGAAGGAGAGCTACTGTAATCTAGAGGAGCTGGAACCTGATAAGTGTTATAAAGTGTGGGTGATGGCGGTAAACTACACAGGCTGCAGCATGCCAAGCGAGAGACTA
1441     Y  R  V  T  V  K  E  S  Y  C  N  L  E  E  L  E  P  D  K  C  Y  K  V  W  V  M  A  V  N  Y  T  G  C  S  M  P  S  E  R  L
4441    CCCTTCAAAACAGCTCCCTCTGTCCCAGTGATCAACACAGAGCAGTGCACAGTGCTTTGGGACAGTGCCACGCTGCGGTGGAGCTCCGTTCAGCCCAGCGCTGTGGACAGCTTCACTCTG
1481     P  F  K  T  A  P  S  V  P  V  I  N  T  E  Q  C  T  V  L  W  D  S  A  T  L  R  W  S  S  V  Q  P  S  A  V  D  S  F  T  I
4561    GAGTACTGCCGACAATATGCCTGTGAGAGAGAGGGACTCAGATCCATATCAGGGATAAAAGGCTATGAGCAGAGGGTCCTTCTTCAGCCCAATGAAAATTACCTCTTCTACATCAAATCA
1521     E  Y  C  R  Q  Y  A  C  E  R  E  G  L  R  S  I  S  G  I  K  G  Y  E  Q  R  V  L  L  Q  P  N  E  N  Y  L  F  Y  I  K  S
4681    GTGAACGCCGGAGGGTCCAGTGAACAGAGCGAGGCGGCCCTCATCTCCACCAGAGGTACGAGATTCCACTTCCTCAGAGAATCAGCGCACTCTGTGCTGAAGGTTTCAGAGGACAGGAAC
1561     V  N  A  G  G  S  S  E  Q  S  E  A  A  L  I  S  T  R  G  T  R  F  H  F  L  R  E  S  A  H  S  V  L  K  V  S  E  D  R  N
4801    TCAGTGGAGTACCCACACGACACCTACAACAAGATGTCCTCAGTCATAGATTGTCCATCAGTTATGGGGGAGATTTTACAATCGAATGGCTATTACTACTGGGAGACAGAGGTGTCGAGA
1601     S  V  E  Y  P  H  D  T  Y  N  K  M  S  S  V  I  D  C  P  S  V  M  G  E  I  L  Q  S  N  G  Y  Y  Y  W  E  T  E  V  S  R
4921    TGCAAAGCGTACCGCATCGGCATTGCATATCAAACTACATCACAAACCAGGACACTGGGAGAGGACAGCGCCTCCTGGTGTCTGCACTGCGTACCCACATCTATAAGCTGCAGGTTTGAG
1641     C  K  A  Y  R  I  G  I  A  Y  Q  T  T  S  Q  T  R  T  L  G  E  D  S  A  S  W  C  L  H  C  V  P  T  S  I  S  C  R  F  E
5041    CTTCTTCATGAGCGTGTGGAGTCTGATATCTTTGTGACGGACATCCCGGCGCGGATCGGTACCTTGTTGGACTACAGCCAGGGTTGCCTCTTCTTCTTTAATGCTCAAAGCGGCCAGGTT
1681     L  L  H  E  R  V  E  S  D  I  F  V  T  D  I  P  A  R  I  G  T  L  L  D  Y  S  Q  G  C  L  F  F  F  N  A  Q  S  G  Q  V
5161    TTGGGCAGTTTTCAGCACAAATTCGCTCAGCCCTGCCACCCGGTGTTTGTCCTGGAGCAGCCGGGGAATCTGGAGCTGAAAATGACCATGGAGGTGCCTGAGTTAGTTAAGCACTGCTAG
1721     L  G  S  F  Q  H  K  F  A  Q  P  C  H  P  V  F  V  L  E  Q  P  G  N  L  E  L  K  M  T  M  E  V  P  E  L  V  K  H
```

Fig 4.2 Characteristion of the zebrafish *myospryn* gene. (A) The intron-exon structure of *myospryn* in human, mouse and zebrafish. (B) Conserved functional domains (BBC, FN3, SPRY) of *myospryn* proteins in human, mouse and zebrafish. (C) cDNA of *myospryn* and its deduced peptide sequence where the domain-containing regions are shaded red (BBC), green (FN3), or blue (SPRY). The diagram is scaled.

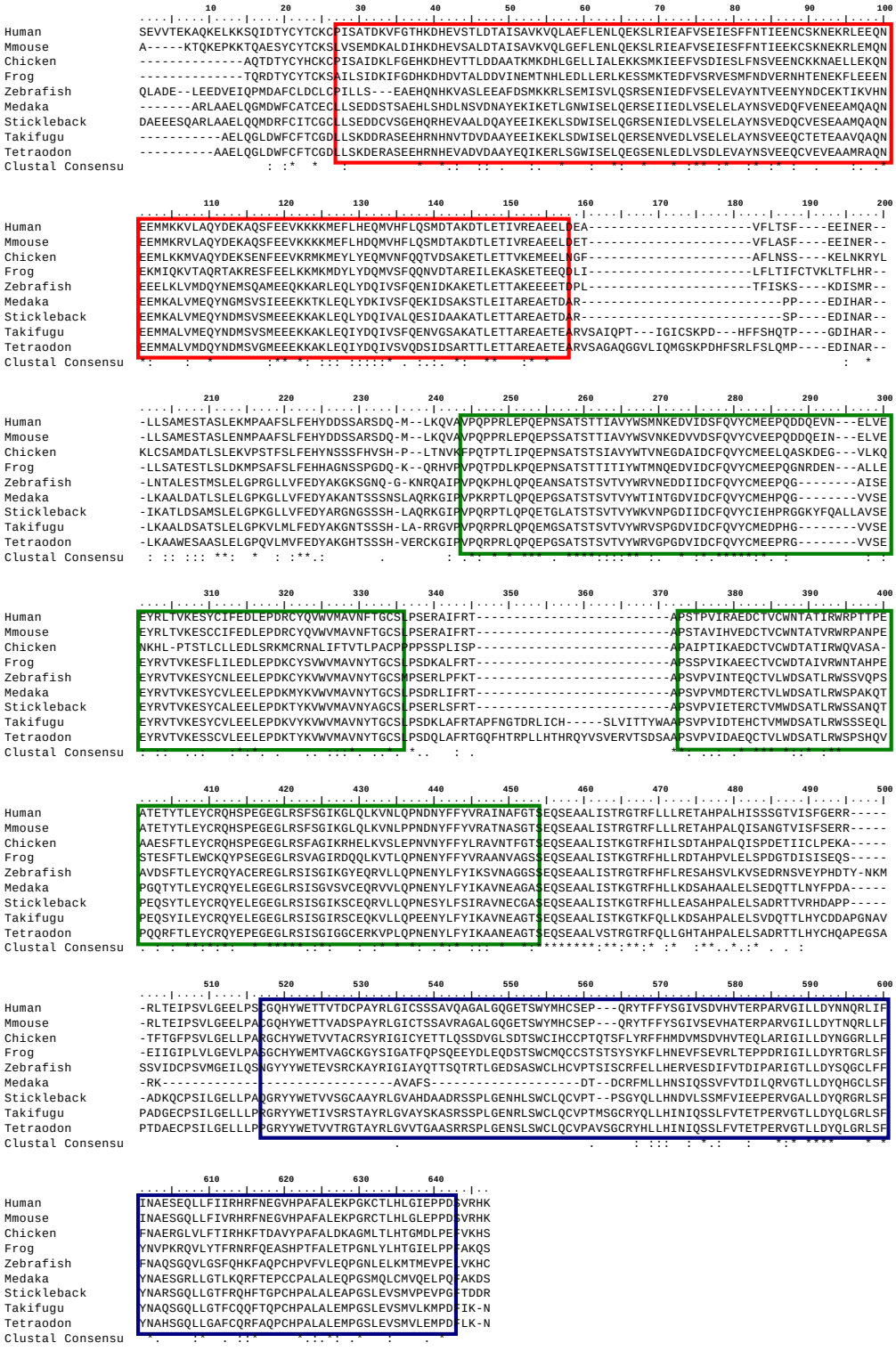

Fig. 4.3 Multiple alignment of the conserved domain containing region of vertebrate myospryn orthologues (eg., zebrafish: residues 1219-1753). In the consensus sequence, identical residues, conserved and semi-conserved substitutions are indicated by asterisks, colons, and dots, respectively. Funtional domains are boxed in red (BBC), green (FN3), and blue (SPRY).

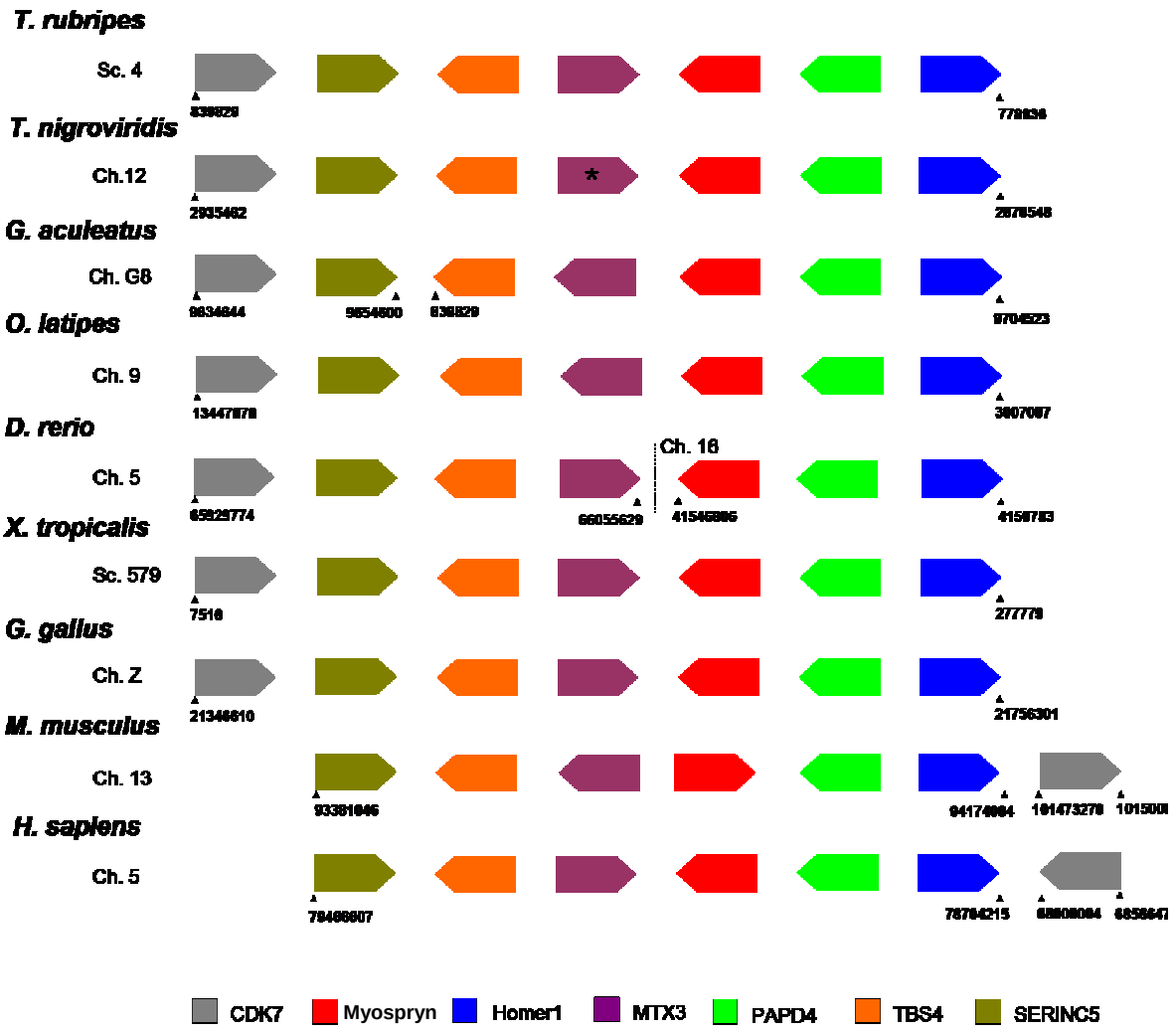

Fig. 4.4 Syntenic region of *myospryn* in various vertebrate species. Arrowheads indicate genes orientated in the direction of sense strand transcription. Chromosomes (Ch) or Scaffolds (Sc) are shown along with the first and last nucleotides numbered in Ensembl database.

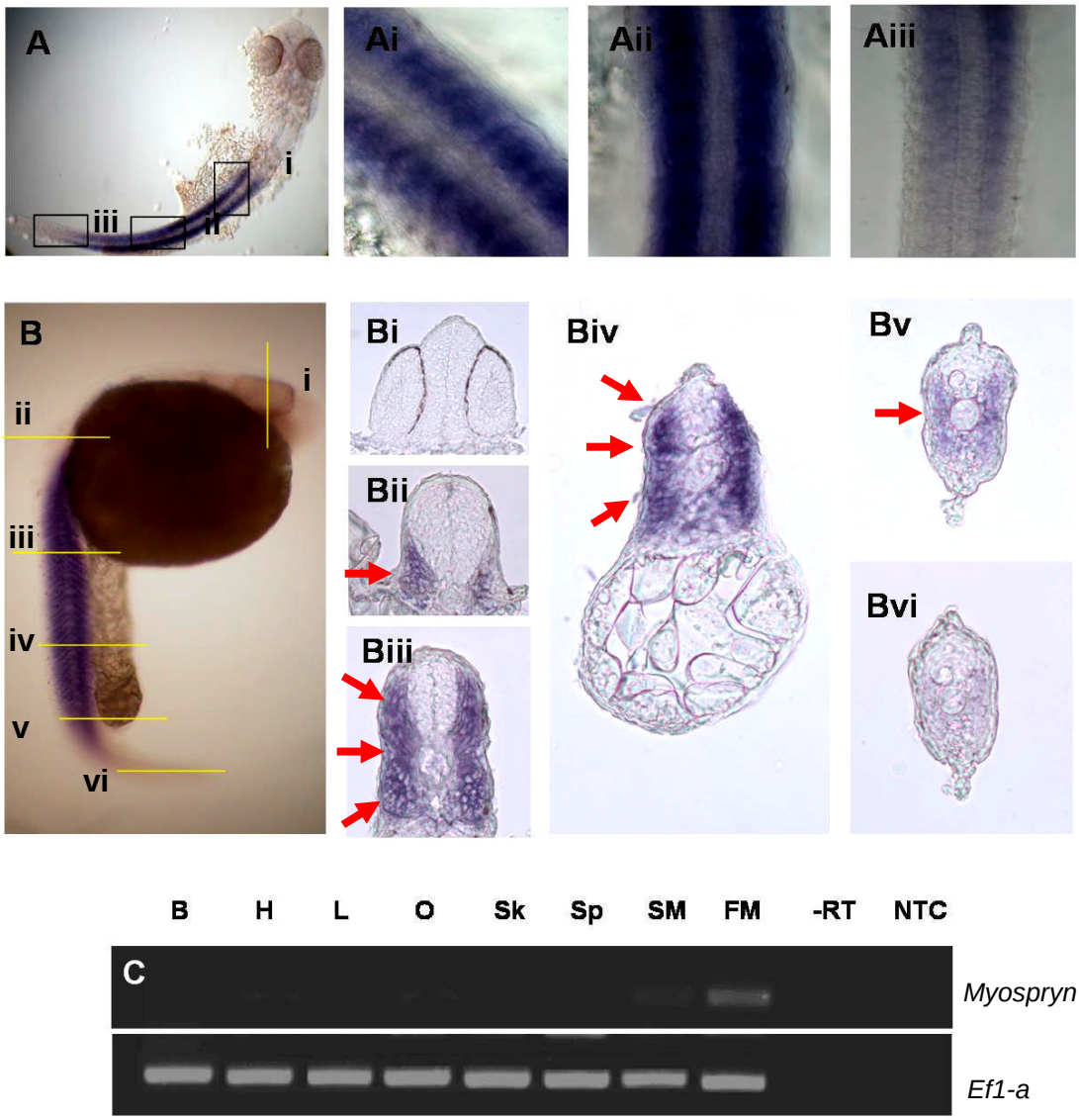

Fig. 4.5 mRNA expression of zebrafish *myospryn* throughout ontogeny. (A) Dorsal view of *myospryn* expression in zebrafish embryo (prim-5 stage: The advancing end of the lateral line primordium overlies myotome (somite) 5). Expanded images of the somites are provided from the anterior to posterior axis (Ai, Aii, Aiii). (B) Lateral view of *myospryn* expression in zebrafish embryos revealed by a series of cross-sections (Bi, Bii, Biii, Biv, Bv). Arrows indicate *myospryn* expression specifically in the myotomes. (C) RT-PCR showing the expression of *myospryn* in the brain (B), heart (H), liver (L), ovary (O), skin (SK), spleen (SP), slow muscle (SM) and fast muscle (FM) of adult zebrafish (~25 mm SL). –RTs (no reverse transcriptase) and NTCs (no template control) produced no amplification.

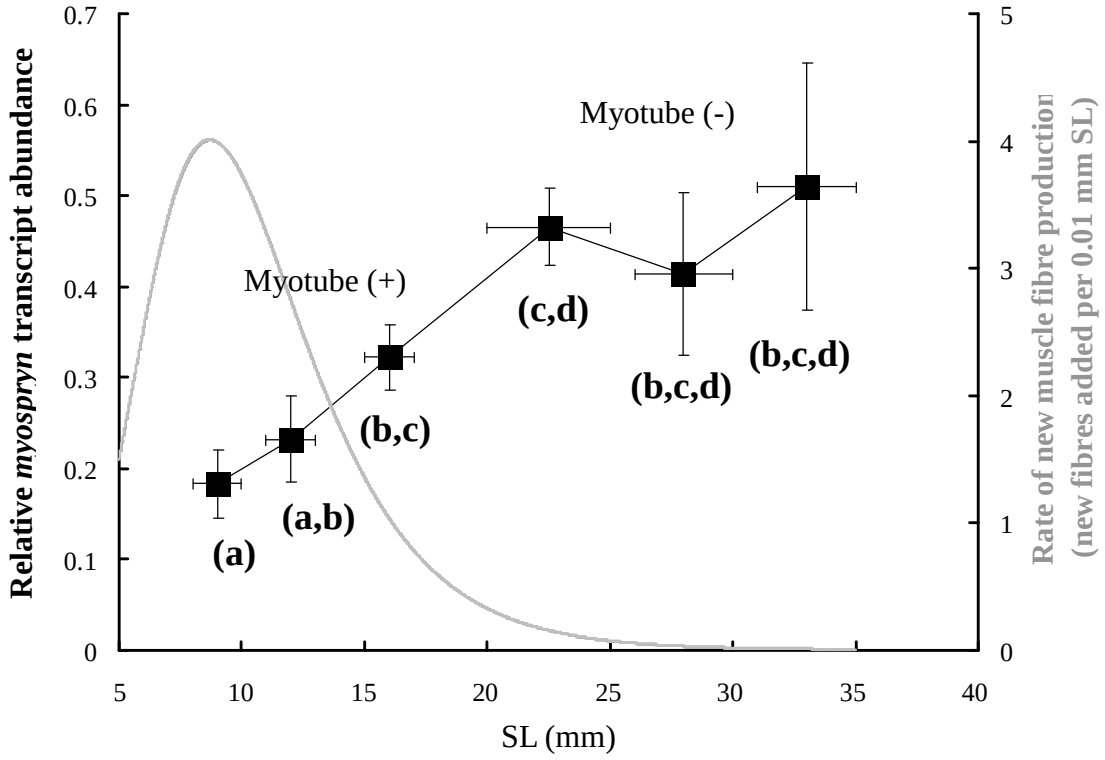

Fig 4.6 The left y axix shows *myospryn* transcript abundance normalized to *beta-actin* and *ef1-α* in fast muscle of zebrafish over 6 different body sizes representing 3 myotube + and 3 myotube - stages. On the right y axis, the rate of muscle fibre production is shown. This was estimated from the Gompertz model as described in Chapter 7. Different letters mark significant differences in the relative expression of *myospyrn* ($p<0.05$). Values represent means ± s.e.m (N=6). The grey line represents the rate of new muscle fibre production.

Chapter 5.0 Genomic characterisation of zebrafish conserved edge expressed protein (cee) and its expression in relation to muscle fibre production.

5.1 Abstract

FRC386 was a gene candidate strongly up-regulated concurrent to the cessation of myotube formation in fast muscle of tiger pufferfish and has been renamed as cee based on its expression pattern in Atlantic salmon. As for most eukaryotes, *cee* was found as a single-copy gene that did not form part of any wider gene family and its protein encompasses a single conserved domain (DUF410) of unknown function. Strong shared synteny existed between the genomic neighborhoods containing cee across tetrapod vertebrates, albeit this was disrupted in teleosts and invertebrates. Using the same model of zebrafish muscle fibre recruitment as for myospryn, *cee* was similarly shown to be at its lowest relative level when hyperplasia was most active and was markedly up-regulated concomitant to the cessation of muscle fibre recruitment. However, its transcripts were also distributed across different tissues, indicating a role in various physiological processes, not only associated with myotube production.

5.2 Introduction

Four gene candidates, namely *FRC258*, *FRC386*, *FRC405* and *FRC586* were up-regulated by 5-25 fold in fast muscle of tiger pufferfish in the myotube (-) compared to myotube (+) growth phenotype (Fernandes et al., 2005). Of these four gene candidates, *FRC386* was the orthologue of a novel gene that was recently named as *cee* (conserved edge expressed protein) according to experimental evidence provided by the genomic, evolutionary, and expressional analyses (Fernandes et al., 2008).

Cee was an ancient gene arising approximately 1.6–1.8 billion years ago that existed as a single-copy gene in most eukaryotic genomes and was highly conserved sharing >80% of amino acid identity across vertebrates (Fernandes et al., 2008). Low dN/dS ratios of *cee* coding sequence (0.02–0.09) suggested its encoded protein was under strong purifying selection (Fernandes et al., 2008). Whole-mount *in situ* hybridisation of Atlantic salmon embryos using the *cee* cRNA probe further revealed cee transcripts were largely restricted to the surfaces of specific developing tissues and organ (Fernandes et al., 2008; Macqueen, 2008).

The first aim of this chapter was to identify a *cee* orthologue in zebrafish and characterize its gene structure and genomic neighbourhood. The second aim was to examine the tissue specific expression of *cee* in zebrafish. The final aim was to profile *cee* transcripts across an earlier established model of muscle fibre recruitment in order to confirm whether its expression was associated with the transition from hyperplastic growth to hypertrophic growth in fast muscle.

5.3 Material and Methods

5.3.1 Fish collection and sample preparation

All the fish were from the same group of F2 zebrafish as described previously (Chapter 3). Tissue samples were the same as described in Chapter 4 (section 4.1.1). Additional sample preparations for pure fast muscle from zebrafish of 6 different body length ranges, including 8-10, 11-13 and 15-17 mm SL for myotube + stages and 20-25, 26-30 and 31-35 mm SL for (myotube - stages) were also performed as described (section 4.1.1)

5.3.2 RNA isolation and cDNA synthesis

Total RNA was isolated from the tissue described above and used as templates to synthesis cDNA for the RT-PCR and qPCR assays following the same procedure as in Chapter 2 (section 2.4.2-2.4.4).

5.3.3 Comparison of shared synteny of cee containing genomic regions

Syntenic maps for *cee* and its surrounding genes in yeast (*Saccharomyces cerevisiae*), round worm (*Caenorhabditis elegans*), sea squirt (*Ciona intestinalis*), fruit fly (*Drosophila melanogaster*), zebrafish (*D. rerio*), stickleback (*G. aculeatus*), medaka (*O. latipes*), tiger pufferfish (*T. rubripes*), african clawed frog (*X. tropicalis*), Chicken (*G. gallus*), mouse (*M. musculus*), and human (*H. sapiens*) were constructed manually using data extracted from Ensembl Release 54

(http://www.ensembl.org) genome assemblies observing the strand orientation and relative chromosomal position.

5.3.4 Quantitative Real-time PCR (qPCR)

The expression of *cee* and three reference genes (*β-actin, ef1α, 18S rRNA*) across the transition between myotube (+) and myotube (-) stages was measued using qPCR assay as described previously (Chapter 2, section 2.4.12). Primer information for qPCR assay was shown in Table 5.1. Data analysis of qPCR results was peformed as described in Chapter 4 (section 4.3.7).

5.3.5 RT-PCR-based analysis of tissue expression

Tissue distribution of *cee* mRNA across zebrafish tissues was assessed using RT-PCR assay performed as described for *myospryn* (Chapter 4, section 4.3.8).

5.4 Results

5.4.1 Identification and characterisation of zebrafish cee

The full-length cDNA sequence of zebrafish *cee* orthologue was identified in NCBI (BC049494) and Ensembl (ENSDARG00000024398) databases following BLAST screens (tblasn) with the sequence of *FRC386* from tiger pufferfish (CK829928). The translated sequence of *cee* revealed a 996 bp ORF encoding a 331 A.A. putative protein. Zebrafish *cee* was located at position 9608,380–9652,194 of chromosome 12 and comprised 9 exons and 8 introns with one uknown function domain (DUF410) within its polypeptide sequence (Fig. 5.1A). The intron-exon structure of *cee* was highly conserved across the vertebrates (Fig. 5.1B). *Cee* was identified as a single gene that did not form part of a wider gene family. Further, alternative splicing variants were predicted in some mammalian *cee* orthologues, including human (ENSG00000239857), mouse (ENSMUSG00000025858) and cow (*Bos taurus*) (ENSBTAG00000026191), but not in other vertebrate lineages.

5.4.2 Comparison of the genomic neighborhood of cee in different vetebrates

Comparison of the chromosomal regions containing *cee* in various eukaryote lineages indicated that strong shared synteny existed between teleosts, barring some gene inversions and intra-chromosomal translocations (Fig. 5.2A). While some common genes were conserved in the genomic neighbourhood of *cee* from teleosts, tunicates and invertebrates, synteny was less conserved (Fig. 5.2A). In

tetrapods, the genomic neighborhood of *cee* was very different to that observed in teleosts and strong synteny was evident between mammals, birds and amphibians (Fig. 5.2B). In zebrafish, *cee* was flanked by genes coding interstitial retinol-binding protein (*rbp3*, BC060944), growth/differentiation factor 2 precursor (*gdf2*, NC_007123), a novel gene associated with esophageal cancer in humans (*C16orf62*), josephin domain-containing 1 (*josd1*, NM_001098181) and the ATP-dependent DNA helicase 2 subunit 1 (*xrcc6*, NM_199904) (Fig. 5.2A).

5.4.3 Tissue distribution of cee transcripts in zebrafish

Cee was expressed ubiquitously across all of the tissues examined in adult zebrafish althought its expression was relatively strong in brain, ovary, and spleen compared to the other tissues (Fig. 5.3).

5.4.4 Expression of cee across an established model of muscle fibre recruitment

To determine if *cee* was differentially expressed in fast muscle between the myotube (+) and myotube (-) growth phenotypes, its transcript profile was measured over the same model used for *myospryn* in Chapter 4. As shown in Fig. 5.4, the relative *cee* transcript abundance remained similar during myotube (+) stages with no statistical differences between fish of 8-10, 11-13, 15-17 mm SL (ANOVA, $p>0.05$). Similarly, while more variable, there were no statistical differences in relative *cee* transcript abundance between myotube (-) stages (ANOVA, $p<0.05$). However, *cee* was significantly up-regulated at myotube (-) stages to a maximum of 1.5-2 fold compared to 8-10 mm SL, where myotube

formation was most active. A higher variation in relative expression abundance was found in larger fish from myotube (-) stage, particularly for the 26-30 mm SL stages.

5.5 Discussion

5.5.1 Cee is a highly conserved gene

As an ancient and highly conserved eukaryotic gene, it is unexpected that *cee* was only recently characterised (Fernandes et al., 2008). It is interesting that *cee* was identified as a single copy gene in almost all eukaryotes since many genes are commonly found in large families, after gene or genome duplication events, which are common and vital mechanism leading to genomic complexity during evolution (Ohno et al., 1970; Zhang, 2003). For example, there is strong evidence that two rounds of WGD occurred in a chordate ancestor (Putnam et al., 2008) and additional rounds in a common teleost ancestor (Jaillon et al., 2004) and again in certain teleost lineages (Allendorf and Thorgaard, 1984). Thus, it is very likely that *cee* has been duplicated many times during vertebrate evolution, but each time one paralogue was lost. This implies there is strong selective pressure for *cee* to remain as single copy gene that is easily regulated. The ratio of nonsynonymous (change amino acid, dN) and synonymous (do not change (silent) amino acid, dS) substitutions between DNA sequences is an indicator of selection pressure at the protein level and can be used to determine whether a gene is under positive (dn/ds >1), neutral (dn/ds = 1), or purifying selection (dn/ds <1) (Yang and Nielsen, 2000). Thus, low dN/dS ratios of *cee* coding sequence (0.02–0.09) provided the evidence that its encoded protein was under strong purifying selection (Fernandes et al., 2008). Further, the general absence of splicing of vertebrate *cee* genes (except certain mammals), plus its broad tissue distribution (Fig. 5.3, Macqueen, 2008) suggests that a single *cee* protein product will be present in many tissues for most

vertebrate species.

5.5.2 Cee is functionally uncharacterised

No protein function for *cee* is known despite its remarkable evolutionary conservation (Fernandes et al., 2008; Macqueen, 2008; this chapter). DUF (domains of unknown function) families refer to those protein domains without any characterised functions although they can be grouped into families based on sequence similarity (Schultz et al., 1998; Jaroszewski et al., 2009). Notably, a conserved domain (DUF410) was found to be consistently present in *cee* orthologues (Fernandes et al., 2008; Macqueen, 2008; this chapter). Current evidence is largely limited to high-throughput functional studies on lower eukaryotes and basal metazoans. In yeast, *cee* is located in the cytoplasm (Huh et al., 2003) where its protein physically interacts with mdy2 (Mating-deficient protein 2) (Fleischer et al., 2006) and get3 (Golgi to ER traffic protein 3) (Ito et al., 2001). Myd2, which contains a UBL (ubiquitin-like) domain, is required for efficient mating (Hu et al., 2006). Get3, an ATPase subunit of the GET complex, is involved in transporting proteins from the Golgi apparatus to the endoplasmic reticulum as well as resisting heat and metal stress (Shen et al., 2003). While targeted deletion of *cee* is not lethal for yeast, these mutants are sensitive to treatments with the antifungal compound nystatin at 5 generations showing reduced growth (Giaever et al., 2001). Knockdown of *cee* in *C. elegans* using RNA interference resulted in growth retardation (Kamath et al., 2003; Simmer et al., 2003). These data suggest that *cee* is likely a positive regulator of growth. Considering the marked sequence difference between *cee* orthologues from

invertebrates and vertebrates, there could be additional functional roles for *cee* in vertebrates (Fernandes et al., 2008). Notably, microarray experiments listed in the Array Express database (http://www.ebi.ac.uk/microarray-as/aer) identified *cee* as a significantly and differentially expressed gene regulated by several human diseases, including Huntington disease and various type of cancer.

5.5.3 Cee exhibits a broad range tissue distribution in zebrafish

Zebrafish *cee* mRNA transcripts were widely expressed in different tissues as reported in adult Atlantic salmon (Macqueen, 2008). Further, *cee* mRNA was widely expressed in a range of developing organs and tissues of salmon embryos, including the eye, gut, otoliths, neuron and optic rectum (Fernandes et al., 2008; Macqueen, 2008). Given its complex tissue distribution, *cee* is probably involved in broad biological processes and not limited to muscle development as suggested earlier for *myospryn* (Chapter 4).

5.5.4 Cee is up-regulated concurrent to the cessation of muscle fibre recruitment

The expression of *cee* in fast muscle of zebrafish is regulated by the transition from hyperplastic to hypertrophic growth phenotypes in fast muscle of zebrafish. The maximum 2-fold up-regulation in myotube (-) stages relative to the time when hyperplasia was most active indicates a potential role for *cee* in governing processes related to myotube development. In salmon embryos, cee was expressed concomitantly with pax7 and MRFs in the ECL and lateral myotomal compartment, respectively (Fernandes et al., 2008; Macqueen, 2008), suggesting a potential role

in embryonic muscle growth where fibre production is active. However, it is unclear that how this embryonic phenotype relates to the postembryonic expression pattern in the present study. Functional characterisation of *cee* through a tissue culture model of myogenesis and/or morpholino-knockdown in embryos are required to gain more insights into its biological role.

Table 5.1 Primer details for this chapter.

Gene	Sense primer	Anti-sense primer	Product
Cee	ACAAGACAAGTGCACTGGTGG	AGTGATGGTTGATACTGCTCGC	175 bp
EF-1α	CTTCAACGCTCAGGTCATCATCC	GCTTCTTGCCAGAACGACGG	143 bp
B-actin	CCGTGACATCAAGGAGAAGCT	TCGTGGATACCGCAAGATTCC	201.bp
18s rRNA	*	*	143 bp

*: The 18S primer pair were obtained from a commercial kit (QuantumRNA™ Universal 18S Internal Standard, Ambion).

(A)

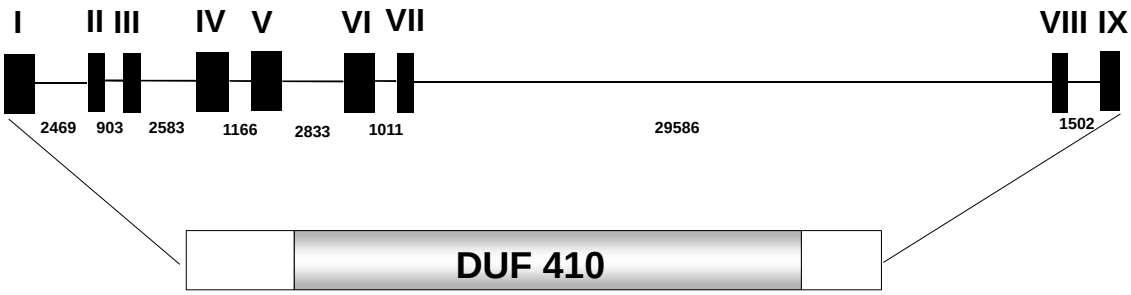

(B)

Takifugu rubripes (scaffold 3)

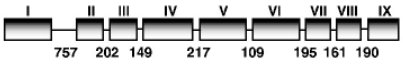

Xenopus tropicalis (scaffold 850)

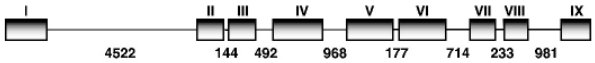

Gallus gallus (chromosome 14)

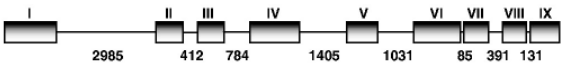

Ornithorhynchus anatinus (ultracontig 333)

Homo sapiens (chromosome 7)

Fig. 5.1 (A) The intron-exon organisation and functional domain (DUF410) of zebrafish *cee*. (B) Conservation of intron-exon structure of cee from a wider range of vertebrates (adapted from Fernandes et al., 2008; Macqueen, 2008).

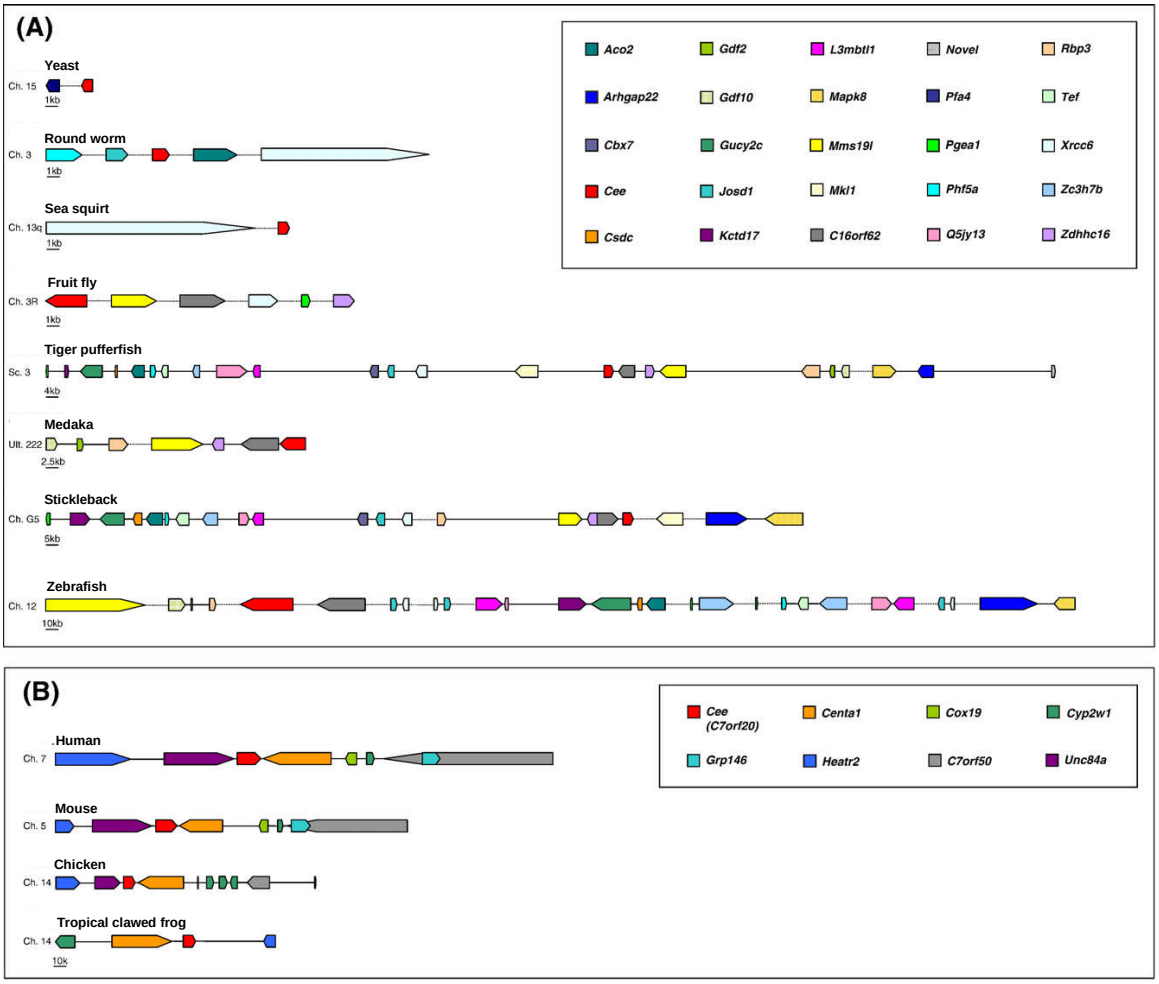

Fig. 5.2 Genomic neighbourhood of *cee* across eukaryotes (A) Genomic neighbourhood of *cee* in zebrafish and its orthologues in a range of eukaryotes. (B) Diagram of the genes surrounding *cee* in tetrapod vertebrates, illustrating the strong conservation of gene order. Genes are color coded and represented by block arrows that reflect their sense strand orientation in the genome and are scaled by exon size. Intergenic regions are not represented to scale.

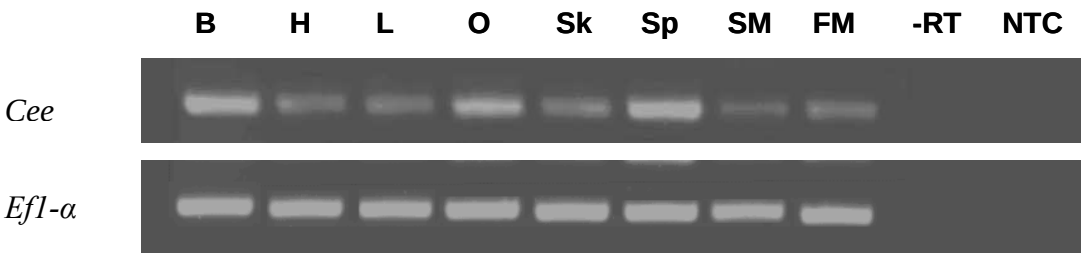

Fig. 5.3 RT-PCR-based assay demonstrating the prescence of *cee* transcripts in brain (B), heart (H), liver (L), ovary, (O), skin (SK), spleen (SP), slow muscle (SM) and fast muscle (FM) of adult zebrafish (~25 mm SL). –RT (no reverse transcriptase) and NTC (no template control) produced no amplification.

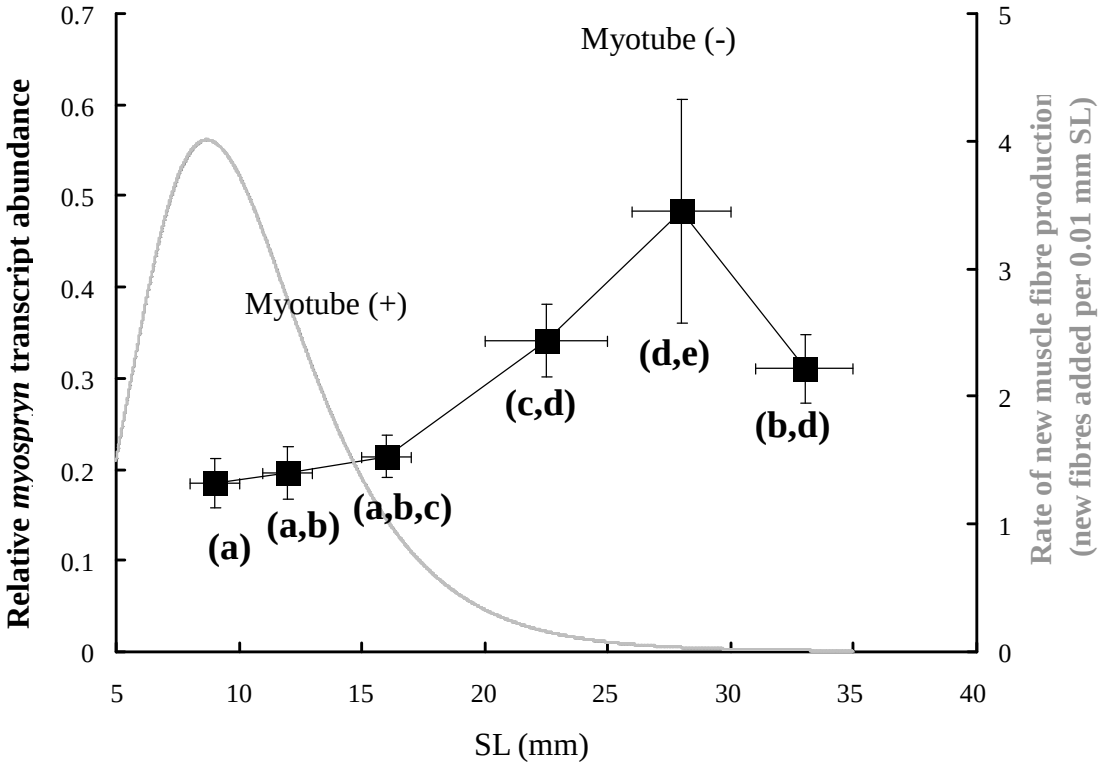

Fig. 5.4 Relative *cee* transcript abundance normalized to β-actin and ef1-α in fast muscle of zebrafish over 6 different body sizes representing 3 myotube + and 3 myotube - stages. Different letters mark significant differences in relative abundance ($p<0.05$). Values represent means ± s.e.m (N=6). The grey curve line represents the rate of new muscle fibre production estimated from Gompertz equation described in Chapter 7.

Chapter 6.0 Genome-wide expression profiling as a tool to discover genes regulating postembryonic muscle fibre production in zebrafish.

6.1 Abstract

In chapter 3 of this thesis, zebrafish was demonstrated to be an excellent model to examine cellular mechanisms of postembryonic muscle growth. In the present study, its genome sequence and available genomic tools were exploited with a genome wide screen for genes associated with the transition from hyperplastic to hypertrophic muscle growth. A whole-genome microarray identified 87 genes that were found to be consistently (8 replicates per phenotype), significantly ($P<0.05$) and differentially (>1.5 fold) expressed in fast muscle between myotube + (8-10 mm SL) and myotube - (~25mm SL). 37 and 50 of these genes were respectively up-regulated and down-regulated during myotube + and myotube - stage. Gene ontology (GO) analysis indicated that catalytic activity and binding were the major molecular functions for the majority of both up-regulated and down-regulated gene candidates that metabolism was the major biological process. KEGG analysis provided another insight into the pathways containing candidate genes. 15 and 5 genes were up-regulated and down-regulated by more than 4 times in myotube + stage, respectively. The significance and possible role of these differentially expressed gene candidates during postembryonic muscle growth is discussed.

6.2 Introduction

Teleost fishes produce new muscle fibres during much of their life span (Weatherley et al., 1988) whereas in mammals all the muscle fibres required for growth are produced before birth and subsequent growth is mainly by fibre hypertrophy alone (Rowe and Goldspink, 1969). Thus, teleosts represent an ideal vertebrate model to examine the cellular and molecular mechanisms underlying postembryonic muscle fibre production.

While most work has focused on the cellular basis of teleost muscle fibre production (reviewed in Johnston, 2006), current understandings on the molecular basis of muscle fibre production is relatively poor. Fernandes et al. (2005) used suppression subtractive hybridisation (SSH) in model teleost tiger pufferfish to identify 11 fast muscle genes that were differentially expressed in fast muscle of myotube (+) and myotube (-) stage. However, the genomic wide transcriptome associated with muscle fibre production phenotype is largely unknown. Microarray technology has emerged as a powerful genetic tool for investigating the global expression profile of genes and has been applied increasingly to address various aspects of fish physiology, particularly in zebrafish (Mathavan et al., 2005; Douglas et al., 2006; Goetz and Mackenzie, 2008).

Cellular basis of muscle fibre prodcuion in zebrafish has been characterised in previous chapter (Chapter 3). In this chapter, differences in genome wide transcriptome profiles were further identified with a robust statistical approach after employing a zebrafish whole genome microarray with myotube (+) and

myotube (-) samples. This approach coupled with bioinformatics provided insight into pathways potentially involved in myotube production.

6.3. Materials and Methods

6. 3.1 Fish collection and tissue sampling

All the fish in the present study were from the same group of F2 zebrafish that were maintained for the normal growth experiment as described in Chapter 3. The epaxial fast muscle were collected from fish of 8-10 mm SL and 20-25 mm SL representing myotube (+) and myotube (-), respectively, according to the standard dissecting procedure (Chapter 2., section 2.2.3). To obtain a sufficient amount of total RNA, pooled fast muscle tissues from 10 fish (8-10 mm SL) and 2 fish (20-25 mm SL) were collected for each individual sample preparation. 8 independent samples were prepared for both muscle fibre hyperplastic and hypertrophic growth stages. All tissue samples were stored in RNA later solution (Ambion) and kept at -20 °C until use.

6.3.2. Total RNA extraction

Total RNA was isolated using the mirVana miRNA Isolation Kit (Ambion) according to the manufacture's instructions. The quality and quantity of isolated total RNA samples were analysed using a NanoDrop spectrophotometer (Thermo Fisher Scientific). Isolated total RNA samples were stored at -80 °C until further processing.

6.3.3 Microarray analysis

Genome wide differences in gene expression of fast muscle representing myotube (+) and myotube (-) growth stages were investigated using a 1x44K zebrafish oligo microarray (G2518A, Agilent Technologies, Santa Clara, CA, USA) performed by a microarray service provider (University Health Network, Toronto, On, Canada). RNA samples from myotube (+) and myotube (–) growth stages were labeled with Cy3 for myotube (+) and Cy5 for myotube (-) fluorescent dyes using AGILENT Low RNA Input Fluorescent Linear Amplification Kit (version 5.5). Fluorescent labeled RNA from each of 8 replicate sample were hybridised to the arrays. Signals on the arrays were detected and scanned using the Gene pix4000A/B scanners. Scan resolution is set at 10 μ and PTM is set between 350 to 700 V. Images extracted from the arrays were further processed and analysed using Gene spring software (Aglient Technologies, Mississauga, Ontario). Data are analyzed by first subtracting the background and then normalization. The background is determined using a regression-based background mapping method. The regression is performed on 5% to 25% of the lowest intensity data points excluding blank spots. Raw data matrix is then subtracted by the background matrix. Normalization is carried out using a LOWESS (Locally-weighted Regression) method on the background-subtracted data. Data was filtered based both on the fold-change of ±1.5 and on confidence with a *P*-value ≤0.05. Fold-change in expression was calculated from the average signal intensity of each group and mRNAs with a fold-change ≥1.5 were selected for further consideration. BLAST searches were performed using the nucleotide sequence of the probe for differentially expressed genes to identify them in the ENSEMBL, NCBI, and ZFIN databases.

6.3.4 GO (Gene ontology) annotation and classification

GO annotation of differentially expressed genes was investigated by searching relevant information in the ZFIN and AMIGO (http://amigo.geneontology.org) databases (Carbon et al., 2009). GO slim was further perform to categorise the differentially expressed gene candidates using CateGOrizer (Hu et al., 2008) (http://www.animalgenome.org/bioinfo/tools/catego/index.html).

6.3.5 KEGG analysis

Differentially expressed gene candidates were analysed using the KEGG database (http://www.genome.jp/kegg/) (Kanehisa et al., 2008). Interesting genes annotated by KEGG database were assigned a KO (KEGG Orthology) number.

6.4 Results

6.4.1 Identification of candidate genes differentially expressed between myotube (+) and myotube (-)

There were 35 (Table 6.1) and 50 (Table 6.2) non-redundant gene candidates significantly ($p<0.05$) up-regulated by more than 1.5 time in all replicate groups obtained from fast muscle of myotube (+) and myotube (-) stages. There were 4 paralogues of fast skeletal muscle myosin heavy polypeptide, including *myhz1a*, *myhz1b*, *myhz1c* and *myhz2* strongly regulated by 8-fold in myotube (+) phenotype. 15 other candidate genes were up-regulated by more than 4 times in the myotube (+) phenotype. 16 gene candidates were up-regulated in fast muscle by 2-4 times. Of 50 down-regulated gene candidates (Table 6.2), parvalbumin 4 (*pvalb4*), beta-2-microglobulin (*b2m*), creatine kinase, sarcomeric mitochondrial precursor (*ckmt2*), and two orthologue genes of complement component 4A (*C4A*) and G0/G1 switch protein2 (*cbm*), were down-regulated by more than 4 times in fast muscle of myotube (+) phenotype. 31 and 14 candidate genes were down-regulated by 2-4 and less than 2 fold in myotube (+) phenotype, respectively.

6.4.2 GO classification of differentially expressed genes

All differentially expressed genes were annotated by molecular function, biological process, and cellular component according to the GO terms (Table 6.3 and Table 6.4). All gene candidates with known GO terms were further grouped and summarised according to GO slim terms. The majority of GO terms assigned to

genes up-regulated in myotube (+) phenotype were involved in two molecular functions, namely catalytic activity (27%) and binding (23%) (Fig. 6.1A). These genes were mainly involved in biological processes such as metabolism (21%) and development (11%) (Fig. 6.1B) and were mostly found to be located in the cell (36%), intracellular region (28%), cytoskeleton (11%), or cytoplasm (10%) according to the annotation of cellular component (Fig. 6.1C). Similarly, for gene down-regulated in myotube (+) phenotype, catalytic activity (27%) and binding (23%) were the major molecular functions assigned by GO terms (Fig. 6.2A). Again, metabolism (29%) was the major biological process for most of these genes (Fig. 6.2B) and they were predicted to localized to the cell (35%), intracellular regions (23%) or cytoplasm (17%) (Fig. 6.2C).

6.4.3 KEGG classification of differentially expressed genes

To provide insight into the genetic network containing the differentially expressed genes, a KEGG analysis was performed. As for the GO analysis, some genes had no assigned pathway and/or protein family information (Table 6.5 and Table 6.6). All gene candidates were further grouped based on the pathway to which they might contribute or are involved with (Fig. 6.3 and Fig. 6.4.). The majority of up-regulated gene in myotube (+) were catergorised in pathway for metabolism pathway, including tyrosine metabolism as well as the cellular process such as tight junctions (Fig. 6.3). The majority of down-regulated genes in myotube (+) phenotype were catergorised in metabolism pathways, including glycolysis, gluconeogensis and oxidative phosphorylation. In addition, these genes were also linked to human disease pathways such as Alzheimer’s disease, Parkinson’s, and

Huntington’s disease (Fig. 6.4).

6.5 Discussion

6.5.1 A complex transcriptional network is involved in the transition from myotube (+) to myotube (-) phenotype

In the present study, a robust approach demonstrated a global expression profile of genes associated with postembryonic fast muscle fibre production of zebrafish. Notably, relatively few differentially expressed gene candidates were identified in the present study compared to the large number typically reported from other microarray experiments (Mathavan et al., 2005; Douglas et al., 2006; Goetz and Mackenzie, 2008). This could be partially due to the fact that the determination of gene candidates in the present study was based on the microarray data from 8 replicates. While the validation of microarray results was not performed in the present study, it is notable that 15 out of 16 of these genes were validated in an associated with the transition from myotube (+) to myotube (-) growth phenotypes (Johnston et al., 2009).

Additionally, GO annotation of differentially expressed genes also reveled various molecular function and biological processes were involved in the transition from myotube (+) to myotube (-) phenotype. In general, the majority of genes differentially expressed in both myotube (+) and myotube (-) phenotype were classified into similar GO categories. For example, the catalytic activity and binding were major molecular functions for genes differentially expressed in both myotube (+) and myotube (-) of fast muscle phenotype in zebrafish. Similar findings also have been shown in pufferfish where 70% of differentially expressed

genes were involved in the catalytic activity and binding (Fernandes et al., 2008). KEGG analysis also indicated the majority of differentially genes were involved in metabolism pathways as suggested by the GO classification, providing new insights into the pathways regulating the myotube production. However, it is also notable that various aspects of muscle phenotype can be correlated with changes in body size, such as the maximum tail-beat frequency (contraction duration per cycle) and aerobic metabolic capacity (James et al., 1998; Davies and Moyes, 2007). Thus, genes differentially expressed between myotube (+) and myotube (-) stage may not solely account for the regulation of myotube formation.

6.5.2. Characterisation of genes up-regulated in myotube (+) phenotype

15 genes were present as strong candidates since they exhibited a 4-19 fold up-regulation in myotube (+) phenotype. Among these genes, four fast-skeletal myosin heavy chain isoforms, were most abundant in myotube (+) phenotype with 8-19 fold up-regulation. These genes have previously been shown to be specific to nascent small diameter muscle fibres in common carp (*Cyprinus carpio* L.) (Ennion et al., 1999), pearlfish (*Rutilus meidingeri*) (Steinbacher et al., 2006) and zebrafish (Johnston et al., 2009). Interestingly, three *myhz2* genes are orientated in tandem cluster that evolved independently in different species (zebrafish, stickleback, medaka and human) (Johnston et al., 2009). Thus, there may be some selective advantage to having multiple fast muscle myosin heavy chain genes in close proximity for tight transcriptional control. Furthermore, their huge down-regulation concurrent to the cessation of muscle fibre recruitment (Johnston et al., 2009 and this chapter) suggest they could be excellent markers for muscle

hyperplasia.

zgc:153704, an uncharacterised paralogue of prostaglandin D2 synthase (*ptgds*) was up-regulated 9-fold during postembryonic fast muscle fibre production. Differential expression analysis of the regeneration of the zebrafish caudal fin revealed *ptgds* was induced 4 days postamputation (Padhi et al., 2004). Characterisation of zebrafish *ptgds* suggested its ability to bind lipophilic molecules such as retinoic acid and thyroxine (Fujimori et al., 2006). Notably, retinoic acid has been shown to regulate myogenesis by *in vitro* (Alric et al., 1998) and *in vivo* studies (Hamade, et al., 2006).

Three actin-binding proteins, including troponin I skeletal, fast 2a.4 (*tnni2a.4*), *zgc:114184* (homologue of troponin T3, skeletal, fast muscle (*tnnt3*) and thymosin, beta (*tmsb*), were found to be up-regulated by 5-7 fold in myotube + phenotypes. Troponin and tropomyosin are binding proteins localised along polymerized actin and essential for calcium-mediated regulation of skeletal and cardiac muscle contraction through their coordinated expression patterns (Farah and Reinach, 1995; Filatov et al., 1999; Gordon et al., 2000). Troponin is a complex consisting of three subunits, including TnC, the Ca^{+2}-binding subunit (troponin C), the inhibitory subunit (troponin I) and tropomyosin-binding subunit (troponin T). Members of three troponin gene families (troponinI, troponinT, troponinC) have been demostrated to be transcriptionally coactivated during skeletal myoblast differentiation and independent control in heart and skeletal muscles (Bucher et al., 1988). *Troponin I2* (*tnni2*) is a member of troponin I gene family that specifically expressed in fast skeletal muscle (Bucher et al., 1988). Interestingly, at least 6 *tnni2*

paralogues has been identified from zebrafish, including 4 tandem *tnni2* copies on Chromosome 25 (*tnni2a.1, tnni2a.2, tnni2a.3* and *tnni2a.4*) and 2 extra copies on Chromosome 7 (*tnni2b.*1 and *tnni2b.2*). These *tnni2* genes are located within genomic regions containing *myod* in teleosts sharing synteny with other vertebrates (Fernandes et al., 2007; Macqueen and Johnston, 2008). It is interesting that only *tnni2a.4* was associated with myotube (+) phenotype. Considering this distinct diversity of tnni2 paralogues in teleosts, it suggests a complex pattern of transcriptional regulation of the different *tnni2* genes in teleosts compared to mammals, where there is only one tnni2 gene. It is tempting to speculate that this could be related to the more complex postembryonic fibre recruitment phenotype in teleosts.

Beta-thymosin (*tmsb*) encodes a protein that binds monomeric actin and is expressed in differentiating skeletal muscle of zebrafish (Roth et al., 1999), indicating a possible role in the formation of new differentiating muscle fibres.

Tyrosinase-related protein 1 (*tyrp1*) is a vital enzyme required for melanin synthesis and specifically expressed in melanocyte-rich tissues such as skin, hair, bulbs and eyes (del Marmol and Beermann, 1996). Its up-regulation in the myotube + phenotype may reflect inadvertent contamination of muscle tissues with melanocyte, considering the small size of larval samples (<10 mm). However, the up-regulation of 4-hydroxyphenylpyruvate dioxygenase (*hpd*) and fumarylacetoacetate hydrolase (*fah*) whose protein are involved in the tyrosine metabolism pathway, implies a potential involvement of tyrosine metabolism is required for postembryonic muscle fibre production.

Fibromodulin (*fmod*) is an extracellular matrix protein produced by collagen-rich tissues and was differentially regulated between two pig breeds with different growth rates and fibre numbers (Tang et al., 2007). Specifically, *fmod* was significantly up-regulated at 90 days post coitus (dpc), in pig strain with a high FFN during a phase of new muscle fibre production. Differential expression of *fmod* is also reported to regulate collagen fibrillogenesis in developing mouse tendons (Ezura et al., 2000).

SRY-box containing gene 11a (*sox11a*) is one of two zebrafish *sox11* paralogues, the other is *sox11b*. These two *sox11* paralogues exhibits both overlapping and non-overlapping expression patterns (de Martino et al., 2000). The *sox11a* orthologue of rainbow trout (Oncorhynchus mykiss) was regulated in skeletal muscle at different nutrition status (Rescan et al., 2007). The mammalian *sox11* paralogue activated *myogenin* in C2C12 myoblasts (Schmidt et al. 2003). These results support a role for sox11 in regulating myotube formation and muscle growth.

Frizzled homolog 8a (*fzd8a*) is a member of the frizzled gene family that encodes seven transmembrane domain proteins which function as the receptors for the wnt family of signaling proteins (Kim et al., 1998). While *fzd8a* is known to be mainly expressed in brain, neuron, and spinal cord (Kim et al., 1998; Kim et al., 2002; Kim et al., 2008), its up-regulation in myotube (+) phenotype implies a potential role in myotube production by signaling to the wnt signalling pathway, which is a known regulator of myogenesis (Cossu1 and Borello, 1999).

6.5.3. Characterisation of genes down-regulated at myotube (+) phenotyp

Postembryonic muscle growth of zebrafish relies on hypertrophic growth alone when muscle fibre production stops (Chapter 3). Thus, the up-regulation of these genes at myotube (-) stage might reflect involvements in inhibition of muscle fibre production and/or promotion of muscle fibre hypertrophy. However, it is difficult to distinguish whether these expression pattern are related to other features linked to body size since numerous aspects of muscle phenotype can be correlated with changes in body size such as the maximum tail-beat frequency (contraction duration per cycle) and aerobic metabolic capacity (James et al., 1998; Davies and Moyes, 2007). Parvalbumin is a calcium-binding protein abundant in fast muscle of teleost fishes appearing as various isoforms in muscle of varying phenotypes (Wilwert et al., 2005). In zebrafish, more than 9 parvalbumin isoforms were reported (Friedberg, 2005) although their exact expression patterns of functions have not been reported. In other species, the expression of parvalbumin genes is correlated with the relaxation rate of muscle, suggesting a role related to swimming activity (Wilwert et al., 2005; Coughlin et al., 2007). Brownridge et al., (2009) demostrated the expression of eight parvalbumin isoforms commonly show a correlation with mechanical properties of different muscle fibres, including the relaxation time and contractile force. Changes in parvalbumin isoform expression may therefore allow adaptive change in muscle mechanical properties in response to varying functional demands and environmental stimuli (Brownridge et al., 2009).

Beta-2 microglobulin (*b2m*) and complement component 4a (*c4a*) are both well-known to be classified as immuno-related genes. B2m is a component of MHC class I molecules that functions in the folding, peptide binding and surface display of class I antigens (Yu et al., 2009). The protein products of *c4a* is an anaphylatoxin produced as part of the activation of the complement system that is able to trigger degranulation of endothelial cells, mast cells or phagocytes, which produce a local inflammatory response (Hugli, 1986). Notably, the latest study indicates macrophages, the white blood cells known for engulfing and eliminating bacteria and other infectious agents, also play a vital role in injured-muscle regeneration (Ruffell et al., 2009). It is also noted that *c4a* is also one of immune response genes previously found to have differential gene expression in the rat soleus muscle during early work overload-induced hypertrophy (Carson et al., 2002). These evidences seem imply the important role of immuno system in regulating muscle growth.

Creatine kinase, mitochondrial 2 sarcomeric (*ckmt2*), also named as mitochondrial creatine kinase (*mtck*), is a member of mitochondrial creatine kinase gene family that is responsible for transferring high energy phosphate from mitochondria to the cytosolic carrier, and creatine (Payne and Strauss, 1994). It was down-regulated in hindlimb muscle of dystrophin-deficient (mdx) mice, suggesting an association with the atrophy of muscle fibre (Porter et al., 2002). Considering ckmt2 is found to be down-regulated both in atrophied muscle fibres (Porter et al., 2002) and myotube (+) stages, it is likely that ckmt2 is involved in the regulation of muscle atrophy and hypertrophy.

6.5.4 Further thoughts on transcriptional regulation of postembryonic muscle fibre production

While the present work has provide a genome-wide profile of genes involved in the transition from myotube (+) to myotube (-) growth phase. It is also worth noted that the short non-coding RNA molecules, e.g. micorRNAs, have been shown to play important regulatory roles in animals and plants by targeting mRNAs for the translational repression and degradation (Bartel, 2004). Although the exact function of microRNAs largely remains to be determined, the expression of microRNAs has been related to various processes associated with development and diseases (Alvarez-Garcia and Miska, 2005; Kloosterman and Plasterk, 2006). Differential expression of microRNAs in fast muscle of zebrafish were recently investigated (Johnston et al., 2009). Interestingly, some of these differentially expressed microRNAs were found to potentially target some of mRNAs reported in the present study (Chapter 6) according to the computational evidence (Johnston et al., 2009). Although further experimental validation are still required to confirm whether these putative matches of microRNAs and mRNAs are positive or not, it is plausible to propose the hypothesis that the co-regulation of these microRNAs and mRNAs might be involved in postembryonic muscle fibre production.

Table 6.1 List of genes up-regulated in myotube (+) phenotype of zebrafish (see appendix I for the full information)

Name of gene	Full descriptioon	Fold (S/B)	Genomic location	Ensembl Gene ID	Gene bank ID	Zfin ID
1. *myhz1-1*	myosin, heavy polypeptide 1, skeletal muscle Fast skeletal myosin heavy chain 4 (Fragment)	18.9 ± 1.3	Chr5: 24070649-24080528	ENSDARG00000067990	NM_001115089	ZDB-GENE-000322-5
2. *myhz1-2*	myosin, heavy polypeptide 1, skeletal muscle Fast skeletal myosin heavy chain 3 (Fragment)	15.0 ± 1.1	Chr5: 24052882-24063763	ENSDARG00000067995	NM_001115089	ZDB-GENE-000322-5
3. *myhz1-3*	myosin, heavy polypeptide 1, skeletal muscle similar to myosin, heavy polypeptide 2, fast muscle specific	11.1 ± 0.6	Chr5: 24033981-24045796	ENSDARG00000067997	NM_001115089	ZDB-GENE-000322-5
4. *zgc:153704*	homologue of prostaglandin D2 synthase	9.9 ± 1.4	Scaffold Zv7_NA792: 274459-279743	ENSDARG00000045979	NM_001076726	ZDB-GENE-040625-119
5. *myhz2*	myosin, heavy polypeptide 2, fast muscle specific (myhz2)	8.0 ± 0.5	Chr5: 23978407-23989516	ENSDARG00000012944	NM_152982	ZDB-GENE-060929-1114
6. *tnni2a.4*	troponin I, skeletal, fast 2a.4 (tnni2a.4)	7.4 ± 1.2	Chr25: 26710679-26728999	ENSDARG00000029069	NM_001009901	ZDB-GENE-020604-1
7. *tmsb*	thymosin, beta (tmsb)	7.7 ± 1.5	Chr21: 24234030-24236677	ENSDARG00000054911	NM_205581	ZDB-GENE-040808-62
8. *hpd*	4-hydroxyphenylpyruvate dioxygenase (hpd)	6.5 ± 1.3	Chr8: 32602449-32612721	ENSDARG00000044935	NM_001003742	ZDB-GENE-040718-249
9. *tyrp1b*	tyrosinase-related protein 1b (tyrp1b)	6.3 ± 1.1	Chr1: 15214369-15227582	ENSDARG00000056151	NM_001002749	ZDB-GENE-050626-97
10. *zgc:114184*	homologue of troponin T3, skeletal, fast muscle	5.4 ± 1.4	Chr25: 11031343-11041768	ENSDARG00000002988	NM_001025179	ZDB-GENE-030131-1091
11. *fah*	fumarylacetoacetate hydrolase (fumarylacetoacetase) (fah)	4.3 ± 1.0	Chr7: 6008060-6061451	ENSDARG00000039743	NM_199601	ZDB-GENE-041008-23
12. *zgc:113456*	homologue of fibromodulin	4.3 ± 1.0	Chr11: 20662672-20668550	ENSDARG00000044895	NM_001030072	ZDB-GENE-980526-395
13. *sox11a*	SRY-box containing gene 11a (sox11a)	4.1 ± 0.4	Chr17: 24045754-24046818	ENSDARG00000070947	NM_131336	ZDB-GENE-000616-6
14. *myf5*	myogenic factor 5	4.0 ± 0.5	Chr4: 28965953-28969805	ENSDARG00000007277	NM_131576	ZDB-GENE-000328-3
15. *fzd8a*	frizzled homolog 8a (fzd8a)	4.0 ± 0.6	Chr24: 3779283-3781339	ENSDARG00000039743	NM_130918	ZDB-GENE-050417-267
16. *zgc:112098*	homologue of Alpha-actin-1 (acta1)	3.7 ± 0.3	Chr1: 50336119-50343694	ENSDARG00000036371	NM_001017750	ZDB-GENE-041105-7

NA: Not available; S: Myotube (+) stage fish; B: Myotube (-) stage fish.

Table 6.2 List of genes down-regulated in myotube (+) phenotype of zebrafish (see appendix I for the full information)

Name of gene	Full descriptioon	Fold change (B/S)	Genomic Location	Ensembl Gene ID	Gene bank ID	Zfin ID
1. *pvalb4*	Parvalbumin 4 (pvalb4)	8.3 ± 0.8	Chr3: 50024614-50034269	ENSDARG00000024433	BC064896	ZDB-GENE-040625-48
2. *b2m*	Beta-2-microglobulin (b2m)	7.8 ± 0.9	Chr4: 13283923-13285961	ENSDARG00000053136	NM_131163	ZDB-GENE-980526-88
3. *zgc:56085*	hypothetical LOC568476 (LOC568476) similar to G0/G1 switch protein2	7.3 ± 1.7	Ch23: 37933392-37938006	NA	NM_001128743	NA
4. *c4a*	Complement C4-B Precursor (Basic complement C4)	6.6 ± 1.2	Chr15: 940695-969452	ENSDARG00000015065	BC146727	ZDB-GENE-030131-5697
5. *ckmt2*	Creatine kinase, sarcomeric mitochondrial Precursor (CKMT2)	4.8 ± 0.4	Chr10: 1901087-1910627	ENSDARG00000069615	NM_199816	ZDB-GENE-030131-5717
6. *ppp1r3c*	Protein phosphatase 1 regulatory subunit 3C (PPP1R3C)	3.8 ± 0.5	Chr17: 21423924-21426422	ENSDARG00000071005	NM_001002376	ZDB-GENE-040718-70
7. *gapdh*	Glyceraldehyde-3-phosphate dehydrogenase (gapdh)	3.4 ± 0.2	Chr16: 12907456-12912394	ENSDARG00000043457	NM_001115114	ZDB-GENE-030115-1
8. *ckm*	Creatine kinase M-type (CKM)	2.8 ± 0.3	Chr15: 22502296-22505544	ENSDARG00000040565	NM_001105683	ZDB-GENE-040426-2128
9. *mt-coI*	Cytochrome c oxidase I, mitochondrial (mt-co1)	2.8 ± 0.3	ChrMT: 6425-7975	ENSDARG00000063905	AY996924	ZDB-GENE-011205-14
10. *hif1an*	Hypoxia-inducible factor 1, alpha subunit inhibitor	2.8 ± 0.3	Chr13: 29424259-29451841	ENSDARG00000031915	NM_201496	ZDB-GENE-030826-19
11. *anxa2a*	annexin A2a (anxa2a)	2.6 ±0.6	Chr25: 28116676-28130724	ENSDARG00000003216	NM_181761	ZDB-GENE-030131-4282
12. *c4-2*	Similar to complement C4-2	2.8 ± 0.6	Chr16: 12390233-12423943	ENSDARG00000038424	XM_001334604	NA
13. *cd9l*	CD9 antigen, like (cd9l)	2.6 ± 0.3	Chr4: 3079683-3103645	ENSDARG00000016691	NM_213428	ZDB-GENE-040426-2768
14. *iclp1*	Invariant chain-like protein 1 (iclp1)	2.6 ± 0.3	Chr14: 55625650-55639921	ENSDART00000026021	NM_131590	ZDB-GENE-000901-1
15. *ak1*	Adenylate kinase isoenzyme 1 (AK1)	2.5 ± 0.3	Chr5: 69265030-69287238	ENSDARG00000001950	NM_001003993	ZDB-GENE-040822-37
16. *ldha*	lactate dehydrogenase A4 (ldha)	2.5 ± 0.2	Chr25: 22370104-22378455	ENSDARG00000040856	NM_131246	ZDB-GENE-991026-5

NA: Not available S: Myotube (+) stage fish; B: Myotube (-) stage fish.

Table 6.3 GO annotation of genes up-regulated in myotube (+) phenotype of zebrafish (see appendix I for the full information)

Name of gene	Molecular function	Biological process	Cellular component
1. *myhz1-1*	GO:0005524 ATP binding GO:0003779 actin binding GO:0003774 motor activity GO:0000166 nucleotide binding	GO:0001757 somite specification GO:0006941 striated muscle contraction	GO:0016459 myosin complex GO:0005863 striated muscle thick filament
2. *myhz1-2*	GO:0005524 ATP binding GO:0003779 actin binding GO:0003774 motor activity GO:0000166 nucleotide binding	GO:0001757 somite specification GO:0006941 striated muscle contraction	GO:0016459 myosin complex GO:0005863 striated muscle thick filament
3. *myhz1-3*	GO:0005524 ATP binding GO:0003779 actin binding GO:0003774 motor activity GO:0000166 nucleotide binding	GO:0001757 somite specification GO:0006941 striated muscle contraction	GO:0016459 myosin complex GO:0005863 striated muscle thick filament
4. *zgc:153704*	GO:0005488 binding GO:0005215 transporter activity	GO:0006629 lipid metabolic process GO:0006810 transport	GO:0005576 extracellular region
5. *myhz2*	GO:0005524 ATP binding GO:0003779 actin binding GO:0003774 motor activity GO:0000166 nucleotide binding	GO:0006950 response to stress GO:0006941 striated muscle contraction	GO:0016459 myosin complex GO:0005863 striated muscle thick filament
6. *tnni2a.4*	NA	NA	NA
7. *tmsb*	GO:0003779 actin binding	GO:0030036 actin cytoskeleton organization GO:0007010 cytoskeleton organization GO:0042989 sequestering of actin monomers	GO:0005737 cytoplasm GO:0005856 cytoskeleton
8. *hpd*	GO:0003868 4-hydroxyphenylpyruvate dioxygenase activity GO:0016702 oxidoreductase activity, acting on single donors	GO:0009072 aromatic amino acid family metabolic process	NA

NA: Not available

Table 6.4 GO annotation of genes down-regulated in myotube (+) phenotype of zebrafish (see appendix I for the full information)

Name of gene	Molecular function	Biological process	Cellular component
1. *pvalb4*	GO:0005509 calcium ion binding		
2. *b2m*	NA	GO:0006955 immune response GO:0002474 antigen processing and presentation of peptide antigen via MHC class I	GO:0042612 MHC class I protein complex GO:0005576 extracellular region
3. *zgc:56085*	NA	NA	NA
4. *c4a*	GO:0004866 endopeptidase inhibitor activity	NA	GO:0005576 extracellular region
5. *ckmt2*	GO:0003824 catalytic activity GO:0016301 kinase activity GO:0016772 transferase activity, transferring phosphorus-containing groups	NA	NA
6. *ppp1r3c*	NA	NA	NA
7. *gapdh*	GO:0004365 glyceraldehyde-3-phosphate dehydrogenase (phosphorylating) activity GO:0051287 NAD binding	GO:0008943 glyceraldehyde-3-phosphate dehydrogenase activity	GO:0006006 glucose metabolic process
8. *ckm*	GO:0003824 catalytic activity GO:0016301 kinase activity GO:0016772 transferase activity, transferring phosphorus-containing groups	NA	NA

NA: Not available

Table 6.5 KEGG annotation of genes up-regulated in myotube (+) phenotype of zebrafish (see appendix I for the full information)

Name of gene	KEGG Orthology	KEGG Pathway	KEGG brite
1. *myhz1-1*	K10352	ko04530 Tight junction	ko04812 Cytoskeleton proteins
2. *myhz1-2*	K10352	ko04530 Tight junction	ko04812 Cytoskeleton proteins
3. *myhz1-3*	K10352	ko04530 Tight junction	ko04812 Cytoskeleton proteins
4. *zgc:153704*	K01830	ko00590 Arachidonic acid metabolism	ko01000 Enzymes
5. *myhz2*	K10352	ko04530 Tight junction	ko04812 Cytoskeleton proteins
6. *tnni2a.4*	K10371	NA	ko04812 Cytoskeleton proteins
7. *tmsb*	K05764	ko04810 Regulation of actin cytoskeleton	ko00001 KEGG Orthology (KO)
8. *hpd*	K00457	ko00350 Tyrosine metabolism	NA
		ko00360 Phenylalanine metabolism	
9. *tyrp1b*	K00506	ko00350 Tyrosine metabolism	ko01000 Enzymes
		ko04916 Melanogenesis	NA
10. *zgc:114184*	K10372	NA	ko04812 Cytoskeleton proteins
11. *fah*	K01555	ko00350 Tyrosine metabolism	ko01000 Enzymes
		ko00643 Styrene degradation	
12. *zgc:113456*	K08121	NA	ko00535 Proteoglycans
13. *sox11a*	K09268	NA	ko03000 Transcription factors
14. *myf5*	K09064	NA	ko03000 Transcription factors
15. *fzd8a*	K02534	ko04310 Wnt signaling pathway	ko04000 Receptors and Channels
		ko04916 Melanogenesis	
		ko05210 Colorectal cancer	
		ko05217 Basal cell carcinoma	
16. *zgc:112098*	K10354	ko05110 Vibrio cholerae infection	ko04812 Cytoskeleton proteins

NA: Not available

Table 6.6 KEGG annotation of genes up-regulated in myotube (+) phenotype of zebrafish (see appendix I for the full information)

Name of gene	KEGG Orthology	KEGG Pathway	KEGG brite
1. *pvalb4*	NA	NA	NA
2. *b2m*	K08055	ko04612 Antigen processing and presentation	NA
3. *zgc:56085*	NA	NA	NA
4. *c4a*	K03989	ko04610 Complement and coagulation cascades	NA
		ko05322 Systemic lupus erythematosus	NA
5. *ckmt2*	K00933	ko00330 Arginine and proline metabolism	NA
6. *ppp1r3c*	K07189	ko04910 Insulin signaling pathway	
7. *gapdh*	K00134	ko00010 Glycolysis / Gluconeogenesis	Enzymes
		ko05010 Alzheimer's disease	
		ko05040 Huntington's disease	
		ko05050 Dentatorubropallidoluysian atrophy (DRPLA)	
8. *ckm*	K00933	ko00330 Arginine and proline metabolism	Enzymes
9. *mt-coI*	K02256	ko00190 Oxidative phosphorylation	Enzymes
		ko05010 Alzheimer's disease	
		ko05012 Parkinson's disease	
10. *hif1an*	K00476	NA	Enzymes
11. *anxa2a*	NA	NA	NA
12. *c4-2*	NA	NA	NA
13. *cd9l*	K06460	ko04640 Hematopoietic cell lineage	Cellular antigens
14. *iclp1*	K06505	ko04612 Antigen processing and presentation	Cellular antigens, Proteoglycans
		ko00535 Proteoglycans	
		ko04090 Cellular antigens	
15. *ak1*	K00939	ko00230 Purine metabolism	Enzymes
16. *ldha*	K00016	ko00010 Glycolysis / Gluconeogenesis	Enzymes
		ko00620 Pyruvate metabolism	
		ko00640 Propanoate metabolism	
		ko00272 Cysteine metabolism	
17. *mpz*	K06770	ko04514 Cell adhesion molecules (CAMs)	Cell adhesion molecules (CAMs), CAM
18. *rgs5*	NA	NA	NA

NA: Not available

(A)

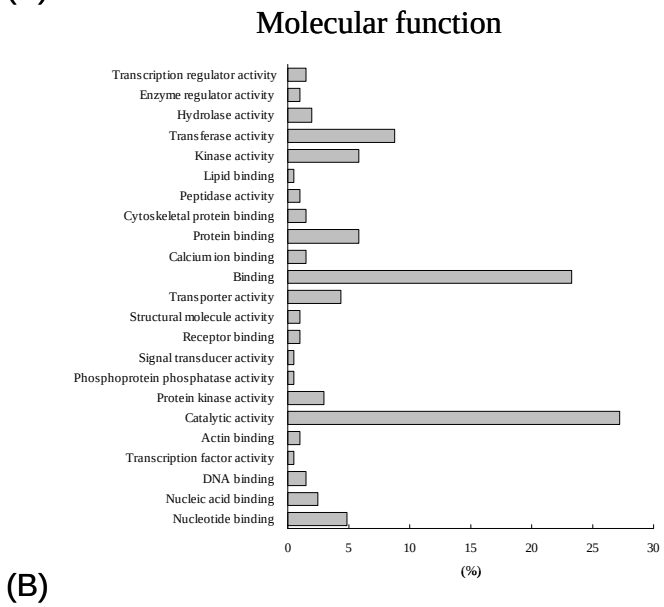

(B)

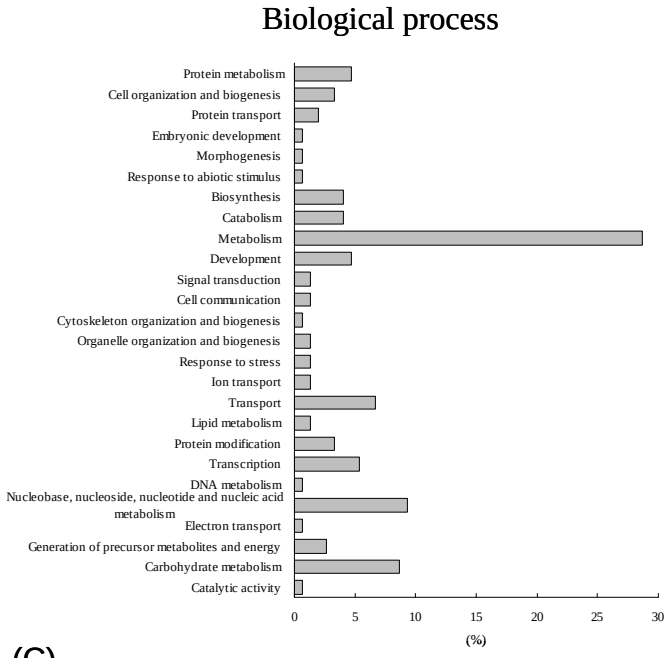

(C)

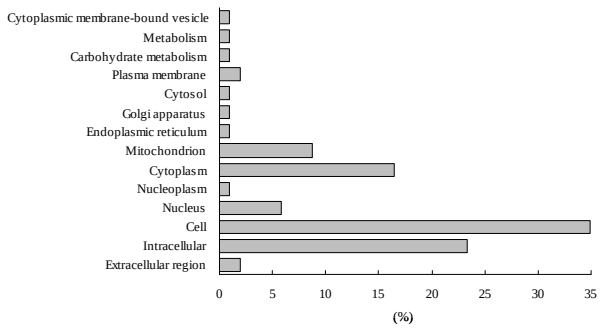

Fig. 6.1 GO slim classification, including (A) molecular function, (B) biological process, and (C) cellular component, of gene candidates up-regulated in the myotube (+) phenotype of zebrafish.

(A)

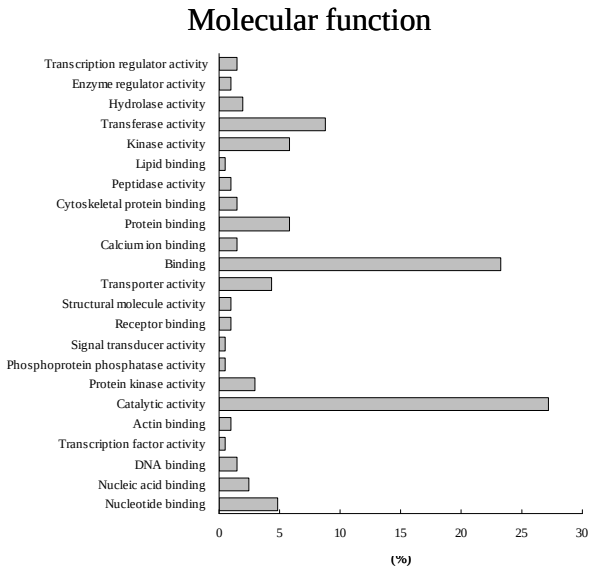

(B)

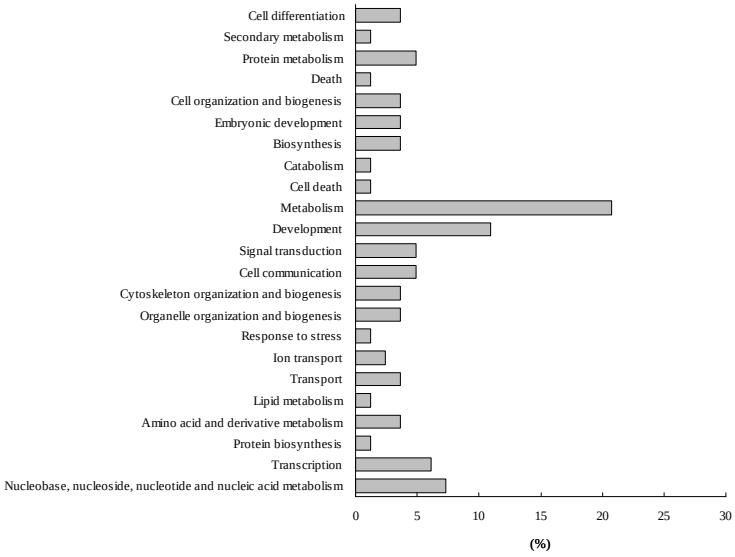

(C)

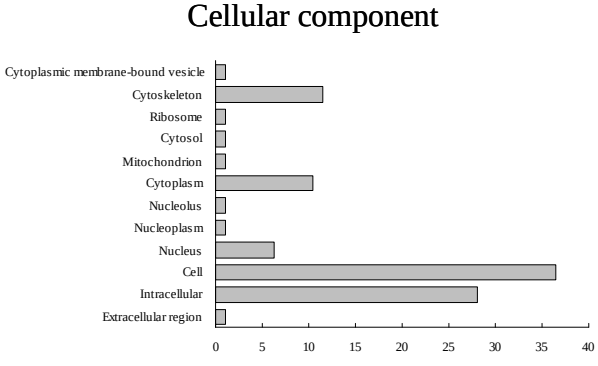

Fig. 6.2 GO slim classification, including (A) molecular function, (B) biological process, and (C) cellular component, of gene candidates down-regulated in the myotube (+) phenotype of zebrafish.

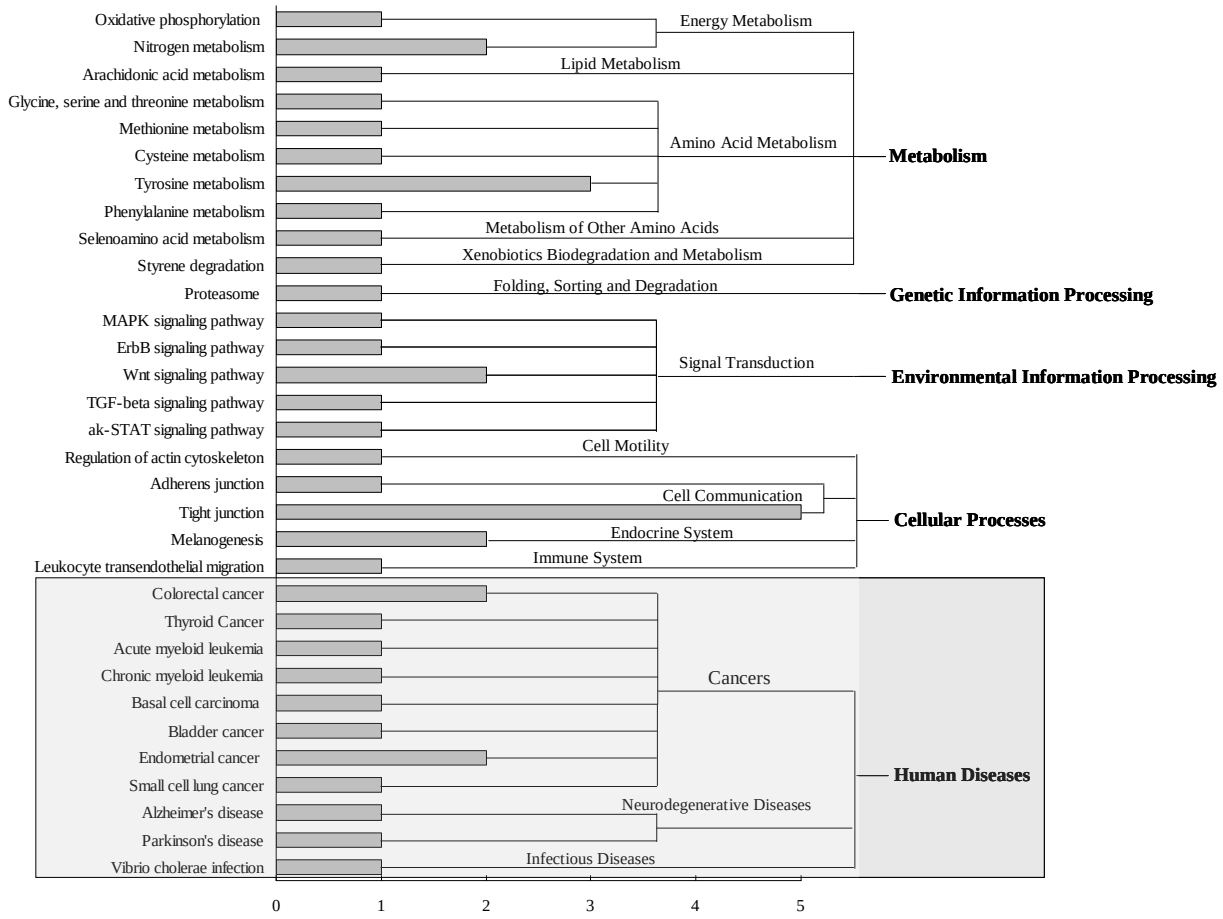

Fig. 6.3 KEGG pathway classification of genes candidates up-regulated (1.5 fold, $P<0.05$) in the myotube (+) phenotype of zebrafish. Pathways catergorised as human diseases were marked with an enclosed grey box.

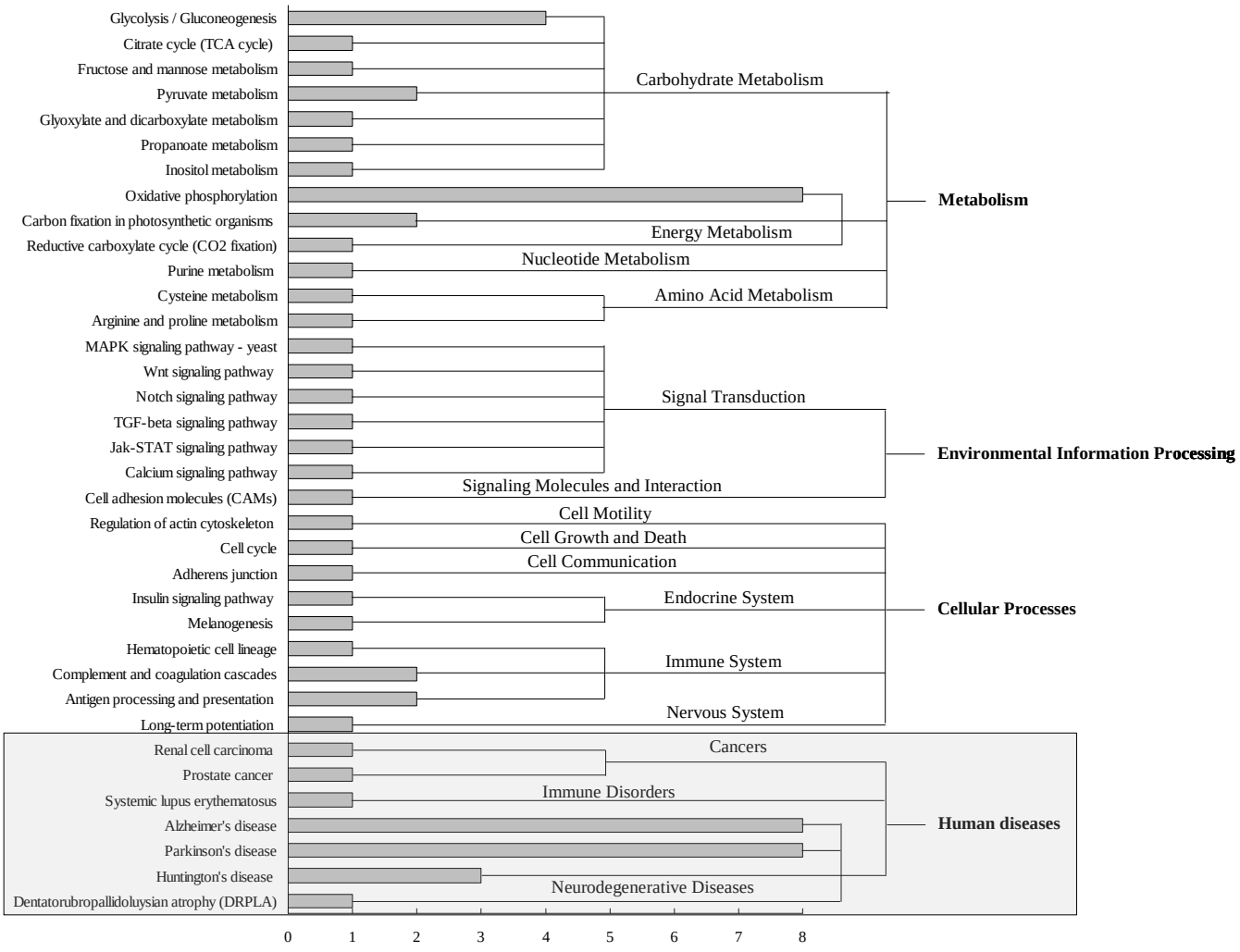

Fig. 6.4 KEGG pathway classification of gene candidates down-regulated in the myotube (+) phenotype of zebrafish. Pathways catergorised as human diseases were marked with an enclosed grey box.

Chapter 7.0 Developmental plasticity of muscle fibre recruitment to temperature in zebrafish.

7.1 Abstract

Developmental plasticity of muscle fibre recruitment to embryonic and parental temperature treatment was investigated in zebrafish over a complete size range (5.0-40.0 mm SL). Fertilized embryos were incubated at either 22, 26, 28, 31, or 35 °C until hatching. A Gompertz model was used to estimate the final fibre number (FFN) in fast muscle. FNN for 26°C treatments (3545 ± 36) was significantly higher ($P<0.01$) than that for 22°C (2995 ± 43) and 31°C (2995 ± 43) treatments. FFN was reached at 19.0 mm SL for 22°C, 21.0 mm SL for 26°C, and 17.5 mm SL for 31°C. Similar results were obtained using the absence of small muscle fibre (<10 μm diameter) as a criteria for the end of fibre recruitment. Examination of the fast myotomes during ontogeny also showed that relative timing of stratified hyperplasia (SH) and mosaic hyperplasia (MH) with respect to SL varied with embryonic temperature. The frequency distribution of muscle fibre diameters was also significantly altered by embryonic temperature treatments. These results demonstrated that embryonic temperature can induce both transient and persistent changes to the postembryonic muscle fibre phenotype. A further comparison of fish incubated at a wide range of embryonic temperature treatments (22, 26, 28, 31, 35°C) indicated that FFN was greatest at 26°C by up to 17% compared to other treatments. This suggests 26°C could be near the optimum for FFN across the reaction norm for this strain of zebrafish. In addition, parental temperature regime was also found to induce a persistent alternation to FFN although its impact was

less marked (~6%) than for embryonic temperature treatments. In conclusion, zebrafish appears to be an excellent model for examining developmental plasticity of muscle fibre recruitment to temperature.

7.2 Introduction

The effects of embryonic temperature treatments on fish have been well-documented in many teleost species, including both transient and persistent alternations of the fish phenotypes. (review in Chapter 1 section 1.6.2).

Embryonic temperature has a pervasive effect on muscle fibre production in teleosts (review in Johnston, 2006). In this chapter, the influences of embryonic temperature on the life-long post-embryonic muscle fibre phenotype were examined, including SH and MH phases established to be present in Chapter 3. Unlike in those large and commercially relevant species such as Atlantic salmon where an equivalent study would be time-consuming and expensive due to rearing costs this study took advantage of the zebrafish model with its short life span and small body size, allowing detailed studies on interactions between environmental temperature and adult muscle phenotype.

Additonally, it has been suggested that developmental plasticity of some phenotypes can be induced in the offspring rather than in the parents (review in Chapter 1 section 1.6.3). Therefore, it is very likely that developmental plasticity of muscle fibre recruitment in fish offsprings can be induced subjected to temperature shifts experienced by their parents.

The aim of the present study were as follows: to establish the body length where fibre production ceased for 3 embryonic temperature treatments; to determine the relative contribution of SH and MH for muscle fibre production for 3 embryonic

temperature; to examine the FFN reaction norm across a wide range of embryonic temperature treatments and finally to examine, for the first time, if parental temperature could also affect the muscle fibre recruitment in offspring.

7.3 Material and Methods

7.3.1 Selection and maintenance of spawning fish groups

A single broodstock comprising 15 females and 8 males zebrafish (same strain described in section 2.2.1) was established and maintained in a freshwater re-circulation system at 26-27 °C (12h dark: 12h light photoperiod). Females and males were kept separately and fed twice daily with bloodworm to enhance their breeding condition. Sexes were mixed every third day producing 600-1,000 embryos per spawning. Two extra broodstocks, each consisting of 8 female and 6 male zebrafish, were prepared as described above for the parental temperature experiments except each broodstock was first acclimated to either 22 and 31 °C for at least 2 weeks before spawning.

7.3.2 Embryo collection and temperature treatments

Fertilized embryos (1-4 cell stage) from the broodstock for the embryonic experiments were rinsed with distilled water and randomly transferred to triplicate 250 ml containers maintained at 22, 26, 28, 31 or 35 °C. Embryos from all individual broodstocks for the parental experiments were collected separately and maintained at a constant temperature (26 °C).

7.3.3 Maintaining and sampling of offspring

After hatching larvae were transferred to duplicate tanks (of increasing size as the

fish grew) maintained at a common temperature of 26-27 °C (12h light:12h dark). All offspring were initially fed 80-200 μm size fry food (ZM Ltd, Winchester, UK) and later proprietary flakes. Fish were sacrificed and morphological measurements were taken as described in Chapter 2 (section 2.2.3).

7.3.4 Muscle cellularity

All sections used for morphological analysis were prepared as described in Chapter 2 (section 2.3). Sections were stained with Meyer's hematoxylin, succinic dehydrogenase and the S58 antibody to distinguish slow, intermediate and fast muscle fibre types as described in Chapter 2 (section 2.3.2-2.3.4). Sections were photographed and the total cross-sectional area of fast muscle was digitized as described in Chapter 2 (section 2.3). The cross-sectional areas of individual fast fibres were measured from section stained with hematoxylin. Fibre number (FN) was estimated as previously as described in Chapter 3 (section 3.3.3)..

7.3.5 Determination of FFN for different temperature treatments

Two methods were used to estimate the FFN of fast muscle in adult fish. A direct estimate was obtained by the criteria that fish with <0.1% of fibres less than 10 μm diameter had stopped hyperplasia. Alternatively, three different asymptotic curves (logistic, von Bertalanfyy and Gompertz) were fitted to the entire data set for each embryonic temperature treatment. Models were fitted with a weighted variance function using the nlme library in R (see Pinheiro and Bates, 2000). Akaike's Information Criteria identified the Gompertz curve as the best model. An even

better fit was obtained if embryonic temperature treatment was allowed to affect the slope as well as the asymptote of the relationship between FN and SL (equation 1).

$$FN_{ij} = Tempasymp_j \times \exp(-\exp(\beta - Temprate_j \times SL_{ij}))$$

where i and j index the ith datum within treatment group $_j$. Tempasymp $_j$, β and Temprate $_j$ are parameters to be estimated with Temprate $_j$ reflecting the rate at which the asymptote is reached and Tempasymp $_j$ the asymptote associated with each factor level j.

7.3.6 Statistics analysis

A natural log transformation was performed on the FFN for both embryonic and parental temperature treatment groups in order to bring the data close to a normal distribution (Anderson-Darling test) and to ensure homogeneity in data variances (Levene's test). Thus, the natural log transformation data was suitable for parametric statistics. A one-way ANOVA was performed in Minitab v13.2 (Minitab Inc.) using Fisher's individual error rate test with an error rate of 0.05 to establish statistical differences in mean relative expression values between sampling stages.

7.4.Results

7.4.1 Embryonic temperature and embryogenesis

The rate of embryogenesis was inversely correlated with embryonic temperature. Embryos hatched at approximately 120, 96, 72, 56, and 48 hours post-fertilization at 22, 26, 28, 31, or 35 °C, respectively. High mortality and a high incidence of abnormal development (>70%) were observed in embryos incubated at extremes of the range. Deformed larvae were humanely killed and not included in experiments.

7.4.2 Parental temperature and embryogenesis

There was no correlation between the rate of embryogenesis and parental temperature. All embryos hatched at the same time (~96 hours post-fertilization) when incubated at a constant temperature (26°C) regardless of parental temperature (24, 26, 31 °C).

7.4.3 The relationship between FN and body length under different embryonic temperature treatments

A modified Gompertz curve was selected as the optimal model for the relationship between FN and fish length (Fig. 7.1). In this model the relationship between FN and fish length varied with embryonic temperature. At any given SL in zebrafish hatched at 31 °C, FN was greater than that of fish hatched at 22 °C and 26 °C prior to reaching their asymptote (i.e. FFN). According to the Gompertz model for 22,

26, 31 °C embryonic treatments, zebrafish reached a FFN of 2995, 3545 and 3010 at 22.0, 23.0, and 18.2 mm SL (Table 7.1). This was highly comparable to the empirical measure (Table 7.1)

7.4.4 Pattern of postembryonic fibre recruitment in fast muscle under different embryonic temperature treatments

The relative timing and contribution of SH and MH with respect to fish length varied with embryonic temperature. In fish larvae of ~6.5 mm SL, SH was identified in fast muscle for both 22°C and 31°C treatments (Fig. 7.2A, B). In addition to SH, MH was evident in zebrafish of ~6.5 mm SL for 31°C treatments (Fig. 7.2B). Both SH and MH was evident in fish of ~8.0 mm SL for both 22 and 31 °C treatments (Fig 7.3A, B). However, at this time a large number of new fibres formed by SH were present in 22°C (Fig. 7.3A). In contrast, SH had seemingly ceased at this time at 31°C and the majority of new fibres were present through MH (Fig. 7.3B). Examining the myotomes of adult fish (~20.0 mm SL) showed that the relative timing for reaching FFN (i.e. cessation of muscle fibre production) with respect to SL varied with embryonic temperature (Fig. 7.4). Specifically, nascent muscle fibres (<10 μm) were completely absent in fish of ~20.0 mm SL for both 22 and 31°C treatments and all existing muscle fibres were larger than 20 μm in diameter. However, some small muscle fibre classes (6-10 and 11-15 μm) were observed at this body size of fish from 26 °C treatments.

7.4.5 Frequency distribution of fast muscle fibre diameters

The frequency distribution of fast muscle fibre diameters was investigated for three embryonic temperature treatments over 8 different size class of diameter (Fig 7.5). The smallest class of muscle fibres (<10μm) appeared until 19.0-21.0 mm SL for 22 °C treatments, 24.0-26.0 mm SL for 26 °C treatments, and 16.0-18.0 mm SL for 31 °C treatments.

7.4.6 The reaction norm for adult FFN in response to embryonic temperature treatments

A further study was performed to estimate FFN of fish incubated at a broader embryonic temperature range (22, 26, 28, 31, and 35 °C). FFN of fast muscle estimated by the empirical approach was highest for the 26°C treatments, to a maximum level of 17% compared to the other temperature treatments ($P<0.05$) (Fig 7.6).

7.4.7 FFN in fast muscle and parental temperature treatment

FNN was 3433 for 24 °C, 3559 for 26°C, and 3290 for 31°C. FFN for 24 °C and 26 °C treatments was significantly higher than 31°C treatments ($P<0.05$)(Fig. 7.7).

7.5 Discussion

7.5.1 Manipulating embryonic temperature solely during embryogenesis induces a persistent effect on FNN

Very few studies have determined the long-term consequences of embryonic temperature for muscle growth in adult stages of fish (e.g. Johnston et al., 2004a; Macqueen et al., 2008; López-Albors et al., 2008). Macqueen et al. (2008) incubated Atlantic salmon embryos at 2, 5, 8 or 10 °C until the completion of eye pigmentation and then transferred them to constant rearing conditions, leading to a maximal FFN at 5 °C that was 17% greater than for other treatments. However, it took approximately ~36 months to complete the rearing experiments in Atlantic salmon due to its relative long life span. In the present study, adult zebrafish phenotypes were observed with a similar maximal FFN difference (17%) induced by a similar broad range of embryonic temperature treatments. However, the experiment took only 3 months to complete, nicely demonstrating the utility of the zebrafish model.

7.5.2 The trade-off between the rate and duration of muscle fibre recruitment

Embryonic temperature affected the pattern of postembryonic fibre recruitment in zebrafish evidenced by several measured parameters. For example, the rate of fibre recruitment, relative timing and contribution of SH and MH, frequency distribution of fibre diameters and the minimum body length of fish reaching FFN were all dependent on embryonic temperature. Interestingly, these results suggest that there

was a tradeoff between the rate and duration of fibre recruitment. While fish from the 31°C treatment initially exhibited a faster fibre recruitment rate than 22 and 26°C treatments, FFN was reached at a lower SL. Conversely, fish reared at 26°C exhibit fibre recruitment at a slower rate than the 31°C treatment, but until a greater SL was reached, meaning the FFN was significantly larger in the end. The 22°C reared fish had a lower rate of recruitment than 26 and 31°C, and its duration was midway between other treatments, meaning FFN was the lowest observed. Thus, there seems to be an optimal temperature range to maximise final fibre number as previously suggested (Macqueen et al., 2008).

7.5.3 Possible mechanism for the developmental plasticity of muscle fibre recruitment to embryonic temperature

Cells derived from the *pax3*/*7* expressing external cell layer (ECL) have been shown to form fast muscle fibres at the lateral myotome in late embryo and larval stages (Hollway et al., 2007; Stellabotte et al., 2007). Since the ECL persisted into adulthood it might function to provide some or all of the myogenic progenitor cells required for juvenile and adult growth (Hollway et al., 2007; Stellabotte et al., 2007). Functional studies revealed that the *pax3*/*pax7* expressing external cells in zebrafish embryos were regulated by fibroblast growth factors and myogenic regulatory factor genes (Groves et al., 2005; Feng, et al., 2006; Hammond et al., 2007). For example, knock-down of *myod* and *myf5* by morpholino in zebrafish embryos resulted in an increase in the number of *pax3*/*7* expressing external cells on the lateral surface of the somite (Hammond et al., 2007). Macqueen et al., (2007) has demonstrated shifts in embryonic temperature could either advance or retard

the mRNA expression of MRFs in Atlantic salmon embryos during embryogenesis. Macqueen at al., (2008) suggested that the temporal shifts in MRFs have the potential to affect the number of external cells, which could impact the number of MPC available for postembryonic muscle growth. However, future studies are required to clarify the potential mechanism described above, most importantly, to establish the relative contribution of the ECL to FFN (Macqueen et al., 2008).

7.5.4 Parental temperature can also alter to muscle phenotype

A change in FFN induced by parental temperature is very interesting and has not been reported in any teleost before. FFN for the 31 °C parental treatments was approximately 6% less compared to the 26 °C treatments. However, this was lower than that induced by embryonic temperature (17%), suggesting parental temperature was less scope to modify subsequent muscle development. However, with the study design employed, the small notable differences in FFN could also reflect genetic variation due to the limited broodstock. Using the same breeding stock to produce offspring acclimated at different parental temperature conditions could control this factor in any future experiments.

Table 7.1 Determination of FFN and the SL where FFN was reached in zebrafish reared at different embryonic temperatures (22, 26, and 31˚C) during embryogenesis and then reared at a common temperature for the rest of life cycle. Results from a modified Gompertz model and a biological observation are shown.

Temp	FFN of fast muscle		SL at which FFN was reached (mm)	
	Model (Mean ± SE)	Observation (Mean ± SE)	Model	Observation
22˚C	2995 ± 43	3009 ± 28 (n= 15)	22.0	19.0
26˚C	3545 ± 36	3559 ± 35 (n= 15)*	23.0	21.0
31˚C	3130 ± 43	3081 ± 35 (n= 18)	18.2	17.5

Asterisk indicates a significant difference ($P<0.05$, ANOVA).

(A)

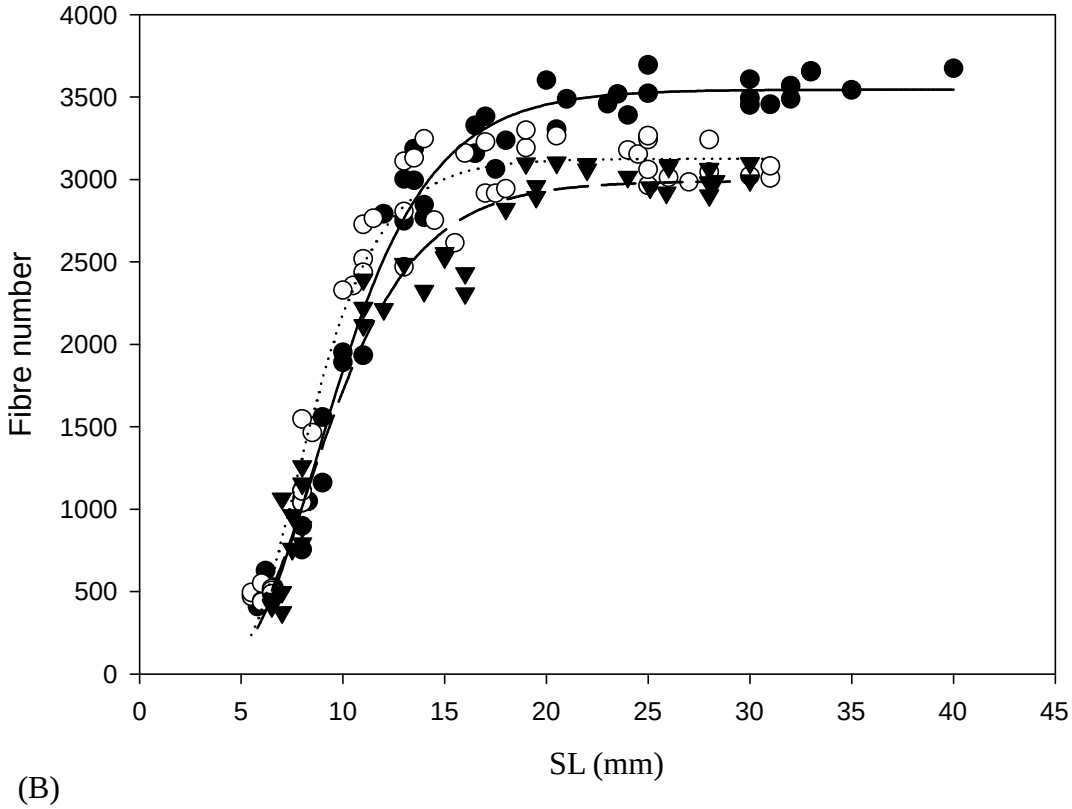
Fibre number
4000
3500
3000
2500
2000
1500
1000
500
0
0
5
10
15
20
25
30
35
40
45
SL (mm)

(B)

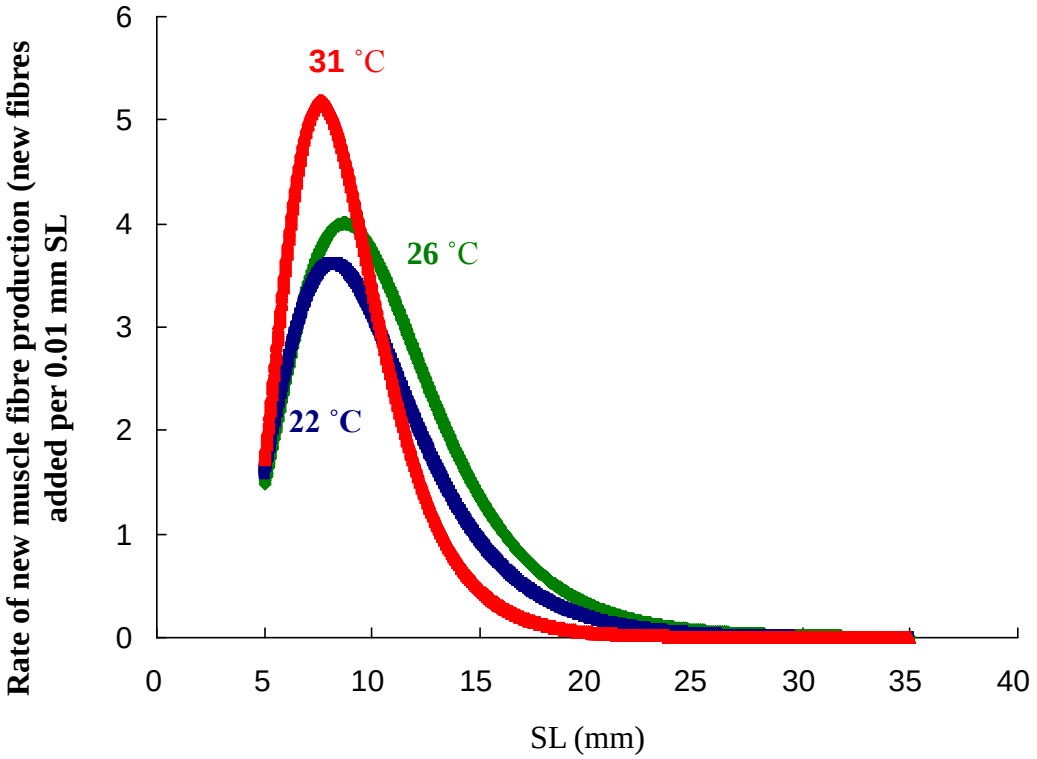
Rate of new muscle fibre production (new fibres added per 0.01 mm SL
6
5
4
3
2
1
0
31 ˚C
26 ˚C
22 ˚C
0
5
10
15
20
25
30
35
40
SL (mm)

Fig 7.1 Model for postembryonic muscle fibre recruitment in zebrafish reared at the different embryonic temperature treatments (22, 26, 31 °C). (A) A modified Gompertz curve was selected to fit the relationship between FN and SL. Filled-triangle corresponds to the 22˚C treatment, filled-circles to the 26˚C treatment and open-circles to the 31˚C treatment. Points represent the data and the lines (broken for 22˚C, solid for 26˚C, dotted for 31˚C) represent the fitted curve. (B) The rate of new muscle fibre production estimated from the above Gompertz curve.

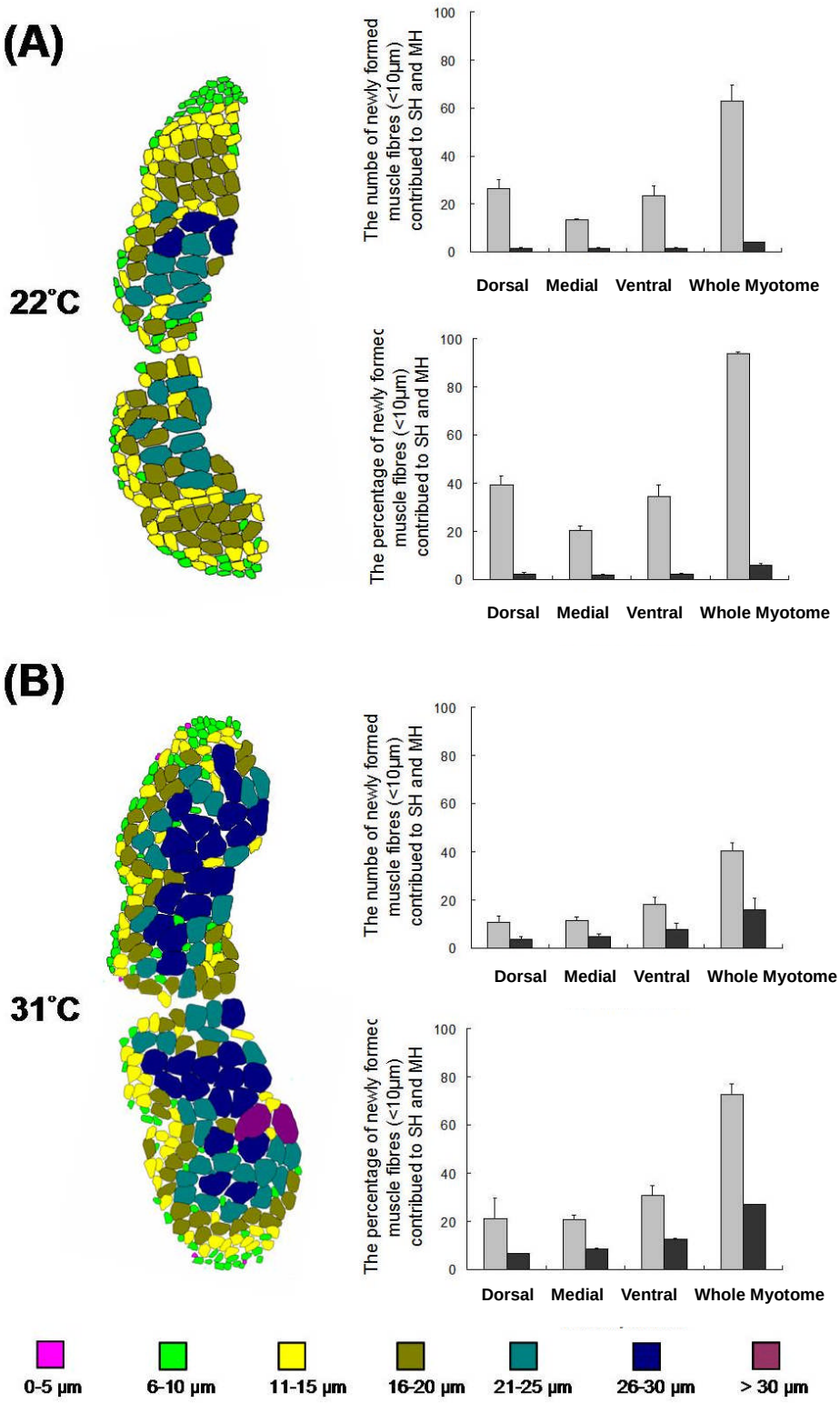
(A)
22°C
The numbe of newly formed muscle fibres (<10μm) contribued to SH and MH
100
80
60
40
20
0
Dorsal
Medial
Ventral
Whole Myotome
The percentage of newly formec muscle fibres (<10μm) contribued to SH and MH
100
80
60
40
20
0
Dorsal
Medial
Ventral
Whole Myotome
(B)
31°C
The numbe of newly formed muscle fibres (<10μm) contribued to SH and MH
100
80
60
40
20
0
Dorsal
Medial
Ventral
Whole Myotome
The percentage of newly formec muscle fibres (<10μm) contribued to SH and MH
100
80
60
40
20
0
Dorsal
Medial
Ventral
Whole Myotome
0-5 μm
6-10 μm
11-15 μm
16-20 μm
21-25 μm
26-30 μm
> 30 μm

Fig 7.2. Representative myotomal cross-sections of larval zebrafish (6.5 mm SL) reared at (A) 22˚C and (B) 31 ˚C during embryonic growth. Graphs to the right of each cross section indicate the proportion of new fibre production from SH and MH in dorsal, medial, ventral and whole regions of the myotome. Individual muscle fibres are classified into different size classes and presented by different colours. Grey and black columns represent new fibres formed by SH and MH. Values represent means ± s.e.m (N=3-5).

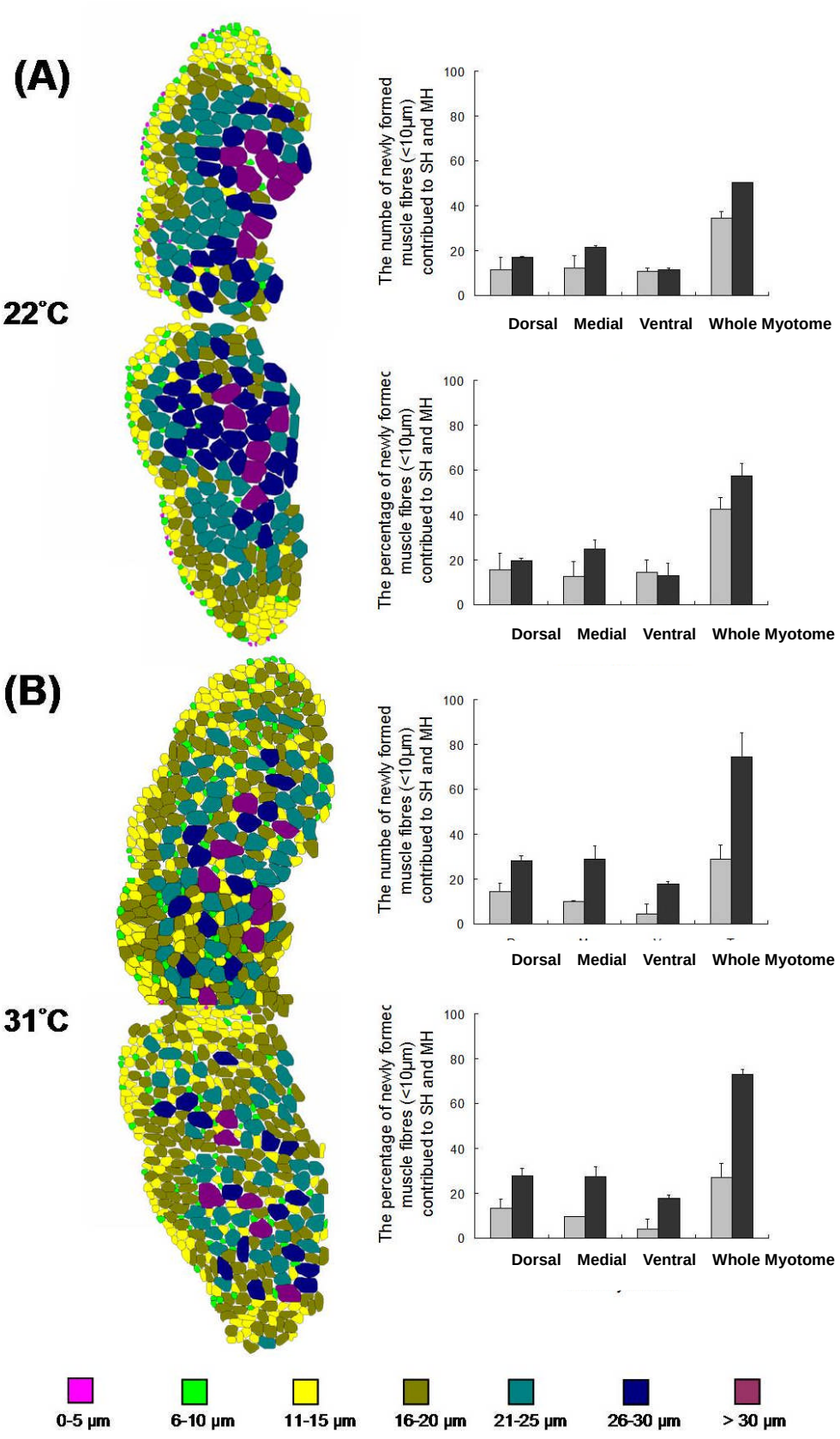
(A)
22°C
The numbe of newly formed muscle fibres (<10μm) contribued to SH and MH
100
80
60
40
20
0
Dorsal
Medial
Ventral
Whole Myotome
The percentage of newly formec muscle fibres (<10μm) contribued to SH and MH
(B)
31°C
0-5 μm
6-10 μm
11-15 μm
16-20 μm
21-25 μm
26-30 μm
> 30 μm

Fig 7.3. Representative myotomal cross-sections of juvenile zebrafish (8.0 mm SL) reared at (A) 22˚C and (B) 31 ˚C during embryonic growth. Graphs to the right of each cross section indicate the proportion of new fibre production from SH and MH in dorsal, medial, ventral and whole regions of the myotome. Individual muscle fibres are classified into different size classes and presented by different colour. Grey and black columns represent new fibres formed by SH and MH. Values represent means ± s.e.m. (N=3-5)

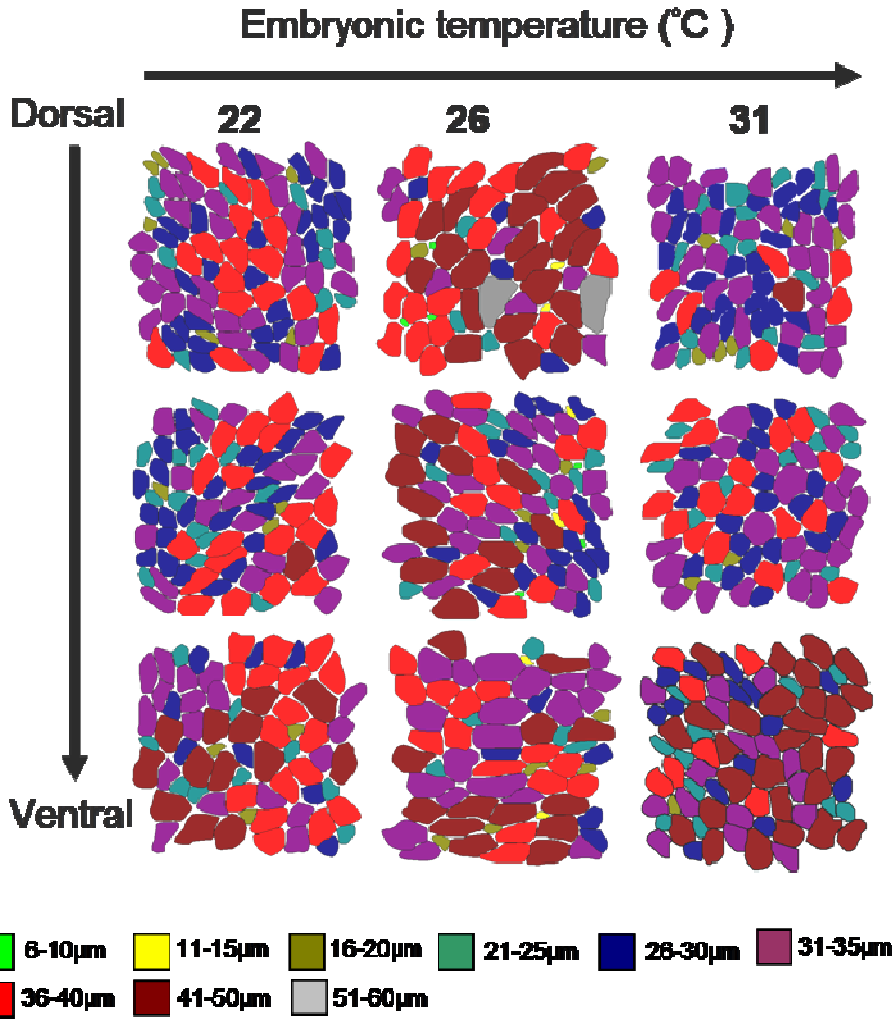

Fig 7.4 Representative cross-sections of myotomes of adult zebrafish (20 mm SL) reared at three embryonic temperatures. Individual muscle fibres are classified by size in different colours.

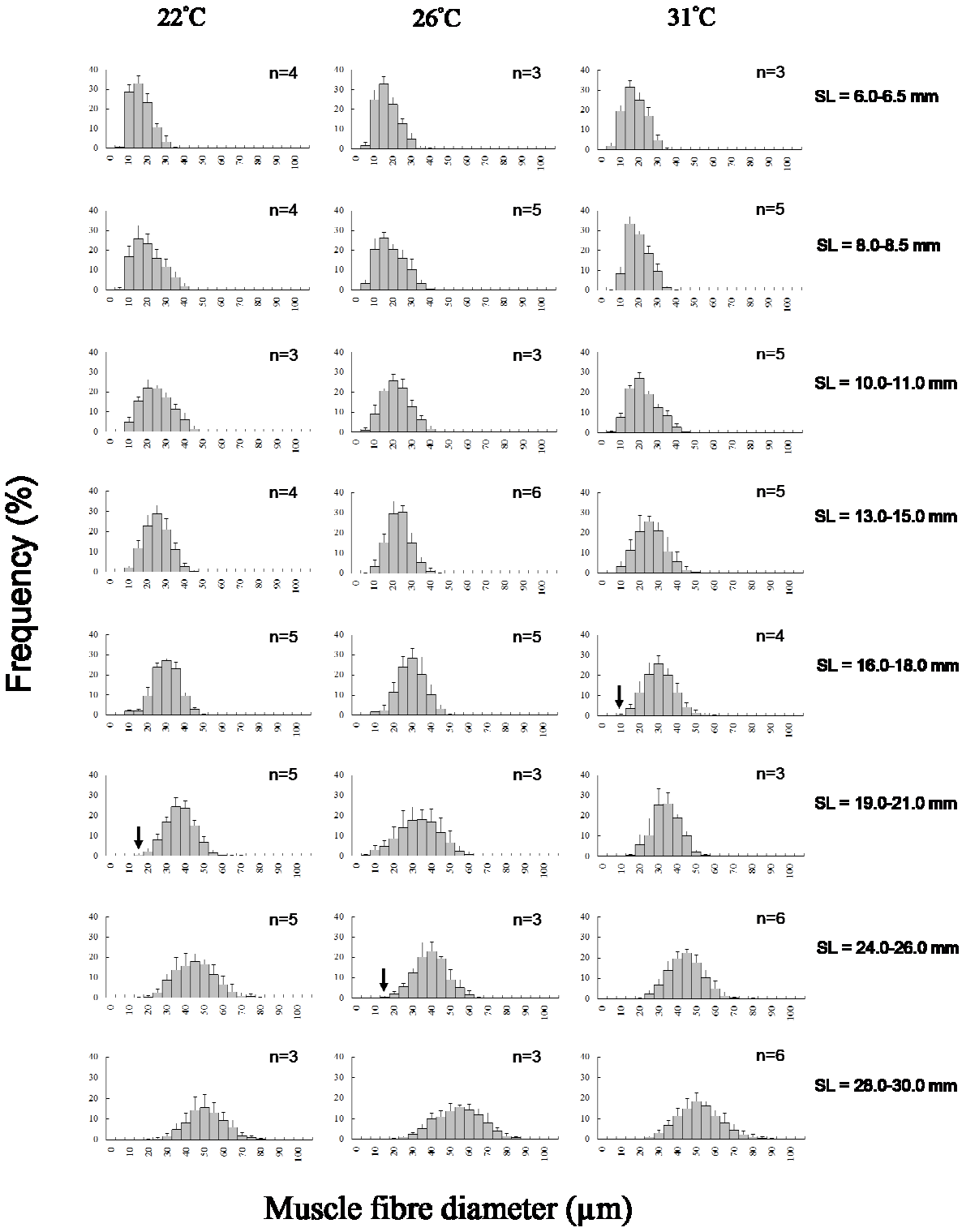

Fig 7.5 Frequency distribution of fibre diameters for three embryonic temperature treatments over 8 size classes. The arrow indicates the absence of new muscle fibre population (<10µm). Values represent means ± s.e.m

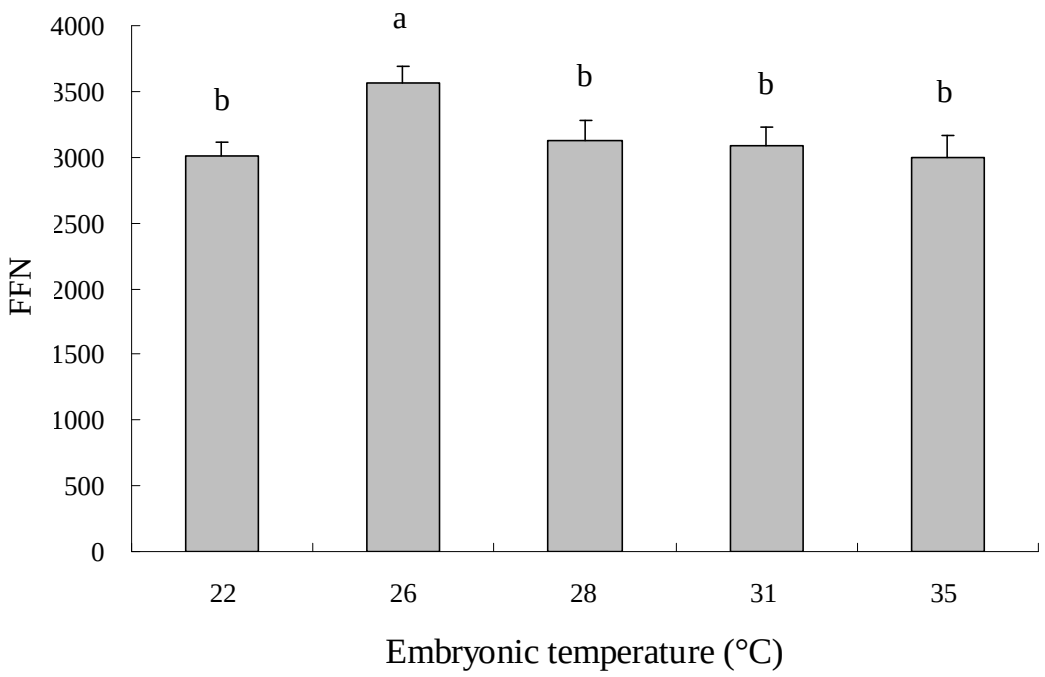

Fig 7.6 Influence of embryonic temperature (22, 26, 28, 31, 35 °C) on zebrafish FFN. Different letters mark the significant difference on final total number of fast muscle fibre between treatments ($p<0.05$, ANOVA). Values represent means ± s.e.m (N=15, 18, ,8, 15 and 9 for 22, 26, 28, 31,and 35 °C treatments, respectively)

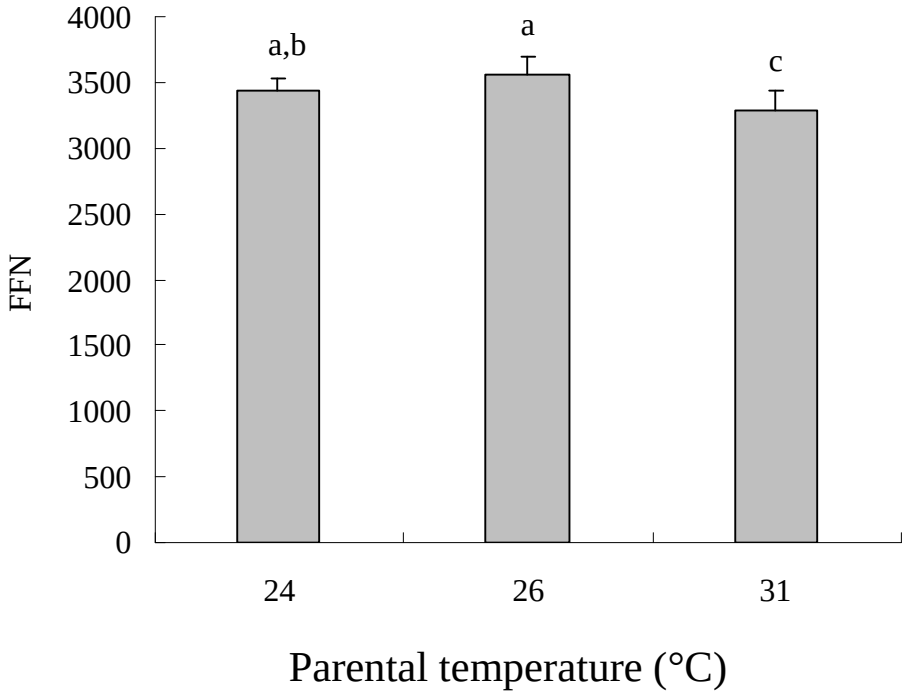

Fig 7.7 Influence of parental temperature (24, 26, 31°C) on zebrafish FFN. Different letters mark significant differences on FFN between treatments ($p<0.05$, ANOVA). Values represent means ± s.e.m (N=8, 15, and 11 for 24, 26, and 31 °C treatments, respectively).

Chapter 8.0 General Discussion

8.1 Cellular mechanism of postembryonic muscle fibre recruitment in fast and slow muscle

SH (SH) has been observed in all teleost species where larval myogenesis was studied whereas mosaic hyperplasia (MH) has been reported to be reduced or completely absent in certain species with a relatively small maximum body size (Rowlerson and Veggetti, 2001; Biga and Goetz, 2005). In striking contrast to previous reports (Biga and Goetz, 2005), this thesis clearly showed that MH is active in fast muscle of zebrafish, accounting for nearly three-quarters of the final fibre number (FFN) (Chapter 3). This finding suggests it might be an oversimplification of the true biological situation to conclude the absence or presence of MH solely by the maximum body size of a given fish. This is exemplified by the study of Johnston et al., (2003a) that discovered a more than 10-fold difference in final FN between two notothenioid fishes, *C. aceratus* and *E. maclovinus*. Although they had a similar maximum body length (~85 cm), MH was absent in *C. aceratus*, which had an unusual large fibre diameter as an adaptation to altered metabolic constraints concomitant to its polar existence (Johnston et al., 2003a). A plausible hypothesis is that while both SH and MH were present in the ancestral condition, SH is a fundamental way of increasing FN for all teleosts but MH has been secondarily retained or repressed subject to physiological and/or metabolic requirements of different lineages. A comprehensive comparison of SH and MH in teleost species across many distinct lineages and a wide range of body size would be be required to test this hypothesis. Nevertheless, the identification of

MH provides strong evidence that it is feasible to use zebrafish as a model for investigating the mechanism of MH in teleosts.

The importance of the external cell layer (ECL) for postembryonic muscle growth was highlighted in Chapter 1. There is now strong evidence that the MPCs required for SH of fast muscle are originally sourced from this structure during embryonic (Hollway et al., 2007; Stellabotte et al., 2007) and postembryonic stages (Steinbacher et al., 2006, 2008; Marschallinger et al., 2009). However, it is still unclear whether the MPCs required for MH are also sourced from the ECL. Notably, the activation of MH in fast muscle was coincident with the appearance of Pax7 expressing cells within the myotomes, which were otherwise mainly restricted to the ECL (Chapter 3; Hollway et al., 2007). This supports a mechanism where MPCs derived from the ECL can directly migrate into the deeper myotome region to give rise to MH (Hollway et al., 2007; Macqueen, 2008). If this is the case, it will need to be determined whether MPCs derived from the ECL and used for MH are different from those used for SH. Future cell tracing and lineages studies are required to address these issues.

Three overlapping waves of SH were shown to sequentially give rise to an increase of FN in slow muscle of zebrafish (Chapter 3). Previous work showed a distinct origin for these new fibres from the embryonic slow muscle (Barresi et al., 2001). While the identity of the founding MPC populations remains unclear it is plausible to suggest they are contributed by the ECL, as seen for SH of fast muscle. However, no study that used cell-tracing methods to track MPCs derived from the anterior somite compartment observed any contribution to the slow muscle fibres (e.g.

Hollway et al., 2007; Stellabotte et al., 2007). Considering that FN of slow muscle is much lower than for fast muscle, it might be expected that if anterior somite cells were directly contributing to the postembryonic slow muscle, then these cells would represent only a small proportion of the total population, making them difficult to trace. Alternatively, it is also possible that only daughter MPCs that have originated by cell division of founder ECL cells contribute to slow muscle. Interestingly, three different slow muscle-specific myosin heavy chains genes (*smhc1*, *smhc2*, *smhc3*) expressed in craniofacial and myotomal slow muscle of zebrafish were recently shown to require different signal pathways (Elworthy et al., 2008). The expression patterns of these three *smhc* genes are strikingly similar to the patterns of slow muscle formation described in Chapter 3. Thus, it is plausible to suggest that three distinct phases of slow muscle SH are perhaps sourced from different MPCs populations derived from the ECL and/or are regulated by separate signalling pathways.

8.2 Molecular regulation of postembryonic muscle fibre recruitment

Very few studies have attempted to investigate the molecular regulation of postembryonic muscle fibre recruitment in teleosts (Fernandes et al., 2005; Johnston et al., 2009; this thesis in Chapter 4, 5, 6). Zebrafish orthologues of two pufferfish genes (*myospryn* and *cee*) that were up-regulated at body sizes where hyperplasia had ceased (Fernandes et al., 2005) also had transcript expression patterns associated with the cessation of postembryonic muscle fibre recruitment in zebrafish (Chapter 4 and 5). *Myospryn* is a muscle-specific gene and may be

involved in muscle hypertrophy since it is up-regulated in zebrafish fast muscle growing solely by hypertrophy and is least transcriptionally abundant at stages where hyperplasia is most active (Chapter 5). This finding is consistent with mammalian studies (Reynolds et al., 2008). Zebrafish can thus be proposed as an alternative experimental model for investigating *myospryn*-associated muscle dystrophy. As a highly conserved single-copy gene present across eukaryotic organisms, current understanding of the functional role of *cee* is extremely poor. Given the expression of *cee* in various tissues (Macqueen, 2008; Chapter 5), its functional characterisation will likely reveal additional roles than in muscle growth.

The first genome-wide profile of genes regulating postembryonic muscle fibre recruitment using a microarray was presented in this thesis (Chapter 6) and was also recently published (Johnston et al., 2009). 85 differentially expressed genes reported here could be used as reference candidates for investigating the regulation of postembryonic muscle fibre recruitment in zebrafish or other teleost species. Among these differentially expressed genes, fast muscle-specific MyHC genes are particularly interesting candidates for further studies since they are effectively switched off when hyperplasia stops and are only expressed in newly formed fast muscle fibres of zebrafish (Johnston et al., 2009). Notably, a comparative analysis of these differentially expressed MyHC genes revealed they were arranged in a tandem of six genes, possibly derived from lineage-specific duplication (Johnston et al., 2009). Interestingly, while five out of six of these tandem genes were switched off when hyperplasia ceased, one was up-regulated, suggesting a high level of regulatory complexity in this region of the zebrafish genome. Given these

MyHC genes are true molecular markers for the cessation of new fibre recruitment, it would be interesting to understand their regulation during the different phases of myogenesis. Furthermore, it would also be interesting to investigate the promoter regions of these MyHC genes since they may hold clues to the underlying regulation of hyperplasia in muscle. In this regard, it might be interesting to determine if any of the transcription factors identified as differentially expressed on the microarray can bind to the promoters of these MyHC genes.

It is also noteworthy that post-transcriptional regulation of protein-coding genes by small non-coding genes (microRNAs) is a known additional level of complexity underlying gene expression and regulation during development (Carrington and Ambros, 2003; Alvarez-Garcia and Miska, 2005). A number of microRNAs are known to be muscle-specific (e.g. miR-1, miR-133 and miR-206) and interact with evolutionarily conserved transcriptional networks regulating myogenesis (Rao et al., 2006). Interestingly, several microRNAs were also shown to be differentially expressed between growth stages where myotube production was active or had ceased (Johnston et al., 2009). Furthermore, the reciprocal expression of differentially expressed protein-coding genes and microRNAs strongly supported a potential role of these microRNAs in the regulation of muscle fibre production by interacting with their targeted genes (Johnston et al., 2009).

Finally, it is difficult to rule out that some differentially expressed genes reported in this work might regulate changes in body length rather than fibre recruitment. Baird et al., (2008) have recently demonstrated a rapid and applicable genetic mapping approach for identifying genes related to the loss of lateral plate armor in

stickleback using sequenced restriction-site associated DNA (RAD) markers (Baird et al., 2008). Interestingly, recent work performed in our groups revealed a significant difference in the maximum body size and FFN of laboratory zebrafish examined in this thesis and the progeny of wild zebrafish (Professor Ian A. Johnston, personal communication). Thus, the molecular regulation of postembryonic muscle growth independent from the body size issue could be investigated by mapping quantitative trait loci (QTL) between high and low FFN strains of zebrafish. Alternatively, the latest launch of wild-strain zebrafish sequencing project (Table 1.2, Project ID: 38201) would also allow the investigation of genes associated with muscle fibre production through the comparison of laboratory and wild strain zebrafish genomes.

8.3 Implications of developmental plasticity of postembryonic muscle fibre recruitment

The plasticity of muscle fibre number in response to various environmental stimuli (e.g. light, temperature) has highlighted the potential ecological significance of developmental plasticity of muscle growth in teleosts (Johnston, 2006). Johnston et al., (2003b) proposed an optimum fibre number hypothesis to interpret the interaction between muscle cellularity and environmental factors. This hypothesis considers that there is a trade-off between the increase in diffusional constraints associated with expanding muscle fibre diameter (muscle hypertrophy) vs. the extra energy cost for ionic homeostasis when increasing muscle fibre number (muscle hyperplasia) under a given energy budget (Johnston et al., 2003b). In light of this hypothesis, plasticity of muscle fibre number can be thought as the fitness

consequence of energy allocation and muscle cellularity. Indeed, new evidence has been shown here that the trajectory of muscle fibre recruitment patterns from larval to adult zebrafish varied with respect to embryonic temperature (Chapter 7), leading to an altered FFN phenotypes as previously shown for large salmonid species (Johnston et al., 2004a; Macqueen et al., 2008). The next step is to determine the fitness consequence of this plasticity such as basal metabolic rate, immune responses and swimming ability associated with foraging/escape behaviours, etc. This would expand our knowledge on the ecological significance of developmental plasticity of muscle fibre recruitment. Furthermore, it would also be interesting to determine if an optimal FFN is established at a cost to other measurable morphological traits e.g. brain size, gut morphology, etc.

From the perspective of cell biology, the present work implies that cell populations for postembryonic growth are strongly modified during embryogenesis subject to signalling events regulated by temperature and these effects are life-long. The anterior-somite compartment and its derived ECL are most promising candidates for future investigation. A simple initial experiment would be to measure whether the densities of Pax7-expressing MPCs derived from the anterior-somite compartment vary with embryonic temperature.

8.4 Final words

In the past few decades, zebrafish has emerged as an important genetic and developmental experimental model for addressing various fundamental biological questions. Studies with zebrafish have also facilitated a dramatic progress in our

understanding of fundamental fish biology. From a perspective of myogenesis, zebrafish has been routinely used for studies of the underlying embryonic mechanisms. Based on results from this thesis, zebrafish has vast potential for studying muscle growth in adult teleosts.

Chapter 9.0 References

Agrawal, A. A., Laforsch, C. and Tollrian, R. (1999). Transgenerational induction of defences in animals and plants. *Nature* **401**, 60-63.

Ahituv, N., Prabhakar, S., Rubin, E. M. and Couronne, O. (2005). Mapping cis-regulatory domains in the human genome using multi-species conservation of synteny. *Human Molecular Genetics* **14**, 3057-3063.

Alestrom, P., Holter, J. L. and Nourizadeh-Lillabadi, R. (2006). Zebrafish in functional genomics and aquatic biomedicine. *Trends in Biotechnology* **24**, 15-21.

Alexander, R. (1969). The orientation of muscle fibres in the myomeres of fishes. *Journal of the Marine Biological Association of the United Kingdom* **49**, 263–290.

Alric, S., Froeschle, A., Piquemal, D., Carnac, G. and Bonnieu, A. (1998). Functional specificity of the two retinoic acid receptor RAR and RXR families in myogenesis. *Oncogene* **16**, 273-282.

Altringham, J. D. and Ellerby, D. J. (1999). Fish swimming: Patterns in muscle function. *Journal of Experimental Biology* **202**, 3397-3403.

Altringham, J. D. and Johnston, I. A. (1982). The pca-tension and force-velocity characteristics of skinned fibers isolated from fish fast and slow muscles. *Journal of Physiology* **333**, 421-449.

Altringham, J. D., Wardle, C. S. and Smith, C. I. (1993). Myotomal muscle function at different locations in the body of a swimming fish. *Journal of Experimental Biology* **182**, 191-206.

Altschul, S. F., Gish, W., Miller, W., Myers, E. W. and Lipman, D. J. (1990). Basic local alignment search tool. *Journal of Molecular Biology* **215**, 403-410.

Alvarez-Garcia, I. and Miska, E. A. (2005). MicroRNA functions in animal development and human disease. *Development* **132**, 4653-4662.

Amores, A., Force, A., Yan, Y. L., Joly, L., Amemiya, C., Fritz, A., Ho, R. K., Langeland, J., Prince, V., Wang, Y. L. et al. (1998). Zebrafish hox clusters and vertebrate genome evolution. *Science* **282**, 1711-1714.

Amsterdam, A. and Hopkins, N. (2006). Mutagenesis strategies in zebrafish for identifying genes involved in development and disease. *Trends in Genetics* **22**, 473-478.

Andersen, C. L., Jensen, J. L. and Orntoft, T. F. (2004). Normalization of real-time quantitative reverse transcription-PCR data: A model-based variance estimation approach to identify genes suited for normalization, applied to bladder and colon cancer data sets. *Cancer research* **64**, 5245-5250.

Aparicio, S., Chapman, J., Stupka, E., Putnam, N., Chia, J., Dehal, P., Christoffels, A., Rash, S., Hoon, S., Smit, A. et al. (2002). Whole-genome shotgun assembly and analysis of the genome of *Fugu rubripes*. *Science* **297**, 1301-1310.

Baird, N. A., Etter, P. D., Atwood, T. S., Currey, M. C., Shiver, A. L., Lewis, Z. A., Selker, E. U., Cresko, W. A. and Johnson, E. A. (2008). Rapid SNP Discovery and Genetic Mapping Using Sequenced RAD Markers. *PLoS One* **3**, e3376.

Barbazuk, W. B., Korf, I., Kadavi, C., Heyen, J., Tate, S., Wun, E., Bedell, J. A., McPherson, J. D. and Johnson, S. L. (2000). The syntenic relationship of the zebrafish and human genomes. *Genome Research* **10**, 1351-1358.

Barresi, M. J. F., D'Angelo, J. A., Hernandez, L. P. and Devoto, S. H. (2001). Distinct mechanisms regulate slow-muscle development. *Current Biology* **11**, 1432-1438.

Barresi, M. J. F., Stickney, H. L. and Devoto, S. H. (2000). The zebrafish slow-muscle-omitted gene product is required for Hedgehog signal transduction and the development of slow muscle identity. *Development* **127**, 2189-2199.

Bartel, D. P. (2004). MicroRNAs: Genomics, biogenesis, mechanism, and function. *Cell* **116**, 281-297.

Basselduby, R., Hernandez, M. D., Yang, Q., Rochelle, J. M., Seldin, M. F. and Williams, R. S. (1994). Myocyte nuclear factor, a novel winged-helix transcription factor under both developmental and neural regulation in striated myocytes. *Molecular and Cellular Biology* **14**, 4596-4605.

Bell, M. and Foster, S. (1994). The evolutionary biology of the threespine stickleback.USA: Oxford University Press.

Bell, A. M. and Stamps, J. A. (2004). Development of behavioural differences between individuals and populations of sticklebacks, *Gasterosteus aculeatus*. *Animal Behaviour* **68**, 1339-1348.

Benson, M. A., Tinsley, C. L. and Blake, D. J. (2004). Myospryn is a novel binding partner for dysbindin in muscle. *Journal of Biological Chemistry* **279**, 10450-10458.

Biga, P. R. and Goetz, F. W. (2006). Zebrafish and giant danio as models for muscle growth: determinate vs. indeterminate growth as determined by morphometric analysis. *American Journal of Physiology-Regulatory Integrative and Comparative Physiology* **291**, 1327-1337.

Blagden, C. S., Currie, P. D., Ingham, P. W. and Hughes, S. M. (1997). Notochord induction of zebrafish slow muscle mediated by Sonic hedgehog. *Genes & Development* **11**, 2163-2175.

Bone, Q. (1966). On the function of the two types of myotomal muscle fibre in elasmobranch fish. *Journal of the Marine Biological Association of the United*

Kingdom **46**, 321-349.

Brenner, S., Elgar, G., Sandford, R., Macrae, A., Venkatesh, B. and Aparicio, S. (1993). Characterization of the Pufferfish (Fugu) Genome as a Compact Model Vertebrate Genome. *Nature* **366**, 265-268.

Brownridge, P., de Mello, L. V., Peters, M., McLean, L., Claydon, A., Cossins, A. R., Whitfield, P. D. and Young, I. S. (2009). Regional variation in parvalbumin isoform expression correlates with muscle performance in common carp (*Cyprinus carpio*). *Journal of Experimental Biology* **212**, 184-193.

Bucher, E. A., Maisonpierre, P. C., Konieczny, S. F. and Emerson, C. P. (1988). Expression of the troponin complex genes - transcriptional coactivation during myoblast differentiation and independent control in heart and skeletal-muscles. *Molecular and Cellular Biology* **8**, 4134-4142.

Carbon, S., Ireland, A., Mungall, C. J., Shu, S., Marshall, B., Lewis, S., Hub, A. and Grp, W. P. W. (2009). AmiGO: online access to ontology and annotation data. *Bioinformatics* **25**, 288-289.

Carrington, J. C. and Ambros, V. (2003). Role of microRNAs in plant and animal development. *Science* **301**, 336-338.

Carson, J. A., Nettleton, D. and Reecy, J. M. (2002). Differential gene expression in the rat soleus muscle during early work overload-induced hypertrophy. *FASEB Journal* **16**, 207-209.

Coughlin, D. J., Solomon, S. and Wilwert, J. L. (2007). Parvalbumin expression in trout swimming muscle correlates with relaxation rate. *Comparative Biochemistry and Physiology a-Molecular & Integrative Physiology* **147**, 1074-1082.

Coutelle, O., Blagden, C. S., Hampson, R., Halai, C., Rigby, P. W. J. and Hughes, S. M. (2001). Hedgehog signalling is required for maintenance of myf5

and myoD expression and timely terminal differentiation in zebrafish adaxial myogenesis. *Developmental Biology* **236**, 136-150.

CrnogoracJurcevic, T., Brown, J. R., Lehrach, H. and Schalkwyk, L. C. (1997). *Tetraodon fluviatilis*, a new puffer fish model for genome studies. *Genomics* **41**, 177-184.

Crow, M. T. and Stockdale, F. E. (1986). The developmental program of fast myosin heavy-chain expression in avian skeletal-muscles. *Developmental Biology* **118**, 333-342.

Currie, P. D. and Ingham, P. W. (1996). Induction of a specific muscle cell type by a hedgehog-like protein in zebrafish. *Nature* **382**, 452-455.

Davies, R. and Moyes, C. D. (2007). Allometric scaling in centrarchid fish: origins of intra- and inter-specific variation in oxidative and glycolytic enzyme levels in muscle. *Journal of Experimental Biology* **210**, 3798-3804.

de Martino, S., Yan, Y. L., Jowett, T., Postlethwait, J. H., Varga, Z. M., Ashworth, A. and Austin, C. A. (2000). Expression of sox11 gene duplicates in zebrafish suggests the reciprocal loss of ancestral gene expression patterns in development. *Developmental Dynamics* **217**, 279-292.

Dehal, P. and Boore, J. L. (2005). Two rounds of whole genome duplication in the ancestral vertebrate. *PLoS Biology* **3**, 1700-1708.

delMarmol, V. and Beermann, F. (1996). Tyrosinase and related proteins in mammalian pigmentation. *FEBS Letters* **381**, 165-168.

Devoto, S. H., Melancon, E., Eisen, J. S. and Westerfield, M. (1996). Identification of separate slow and fast muscle precursor cells in vivo, prior to somite formation. *Development* **122**, 3371-3380.

Devoto, S. H., Stoiber, W., Hammond, C. L., Steinbacher, P., Haslett, J. R.,

Barresi, M. J. F., Patterson, S. E., Adiarte, E. G. and Hughes, S. M. (2006). Generality of vertebrate developmental patterns: evidence for a dermomyotome in fish. *Evolution & development* **8**, 101-110.

Dosch, R., Wagner, D. S., Mintzer, K. A., Runke, G., Wiemelt, A. P. and Mullins, M. C. (2004). Maternal control of vertebrate development before the midblastula transition: Mutants from the zebrafish I. *Developmental Cell* **6**, 771-780.

Douglas, S. E. (2006). Microarray studies of gene expression in fish. *Journal of Integrative Biology* **10**, 474-489.

Driever, W., SolnicaKrezel, L., Schier, A. F., Neuhauss, S. C. F., Malicki, J., Stemple, D. L., Stainier, D. Y. R., Zwartkruis, F., Abdelilah, S., Rangini, Z. et al. (1996). A genetic screen for mutations affecting embryogenesis in zebrafish. *Development* **123**, 37-46.

Du, S. J., Devoto, S. H., Westerfield, M. and Moon, R. T. (1997). Positive and negative regulation of muscle cell identity by members of the hedgehog and TGF-beta gene families. *Journal of Cell Biology* **139**, 145-156.

Durham, J. T., Brand, O. M., Arnold, M., Reynolds, J. G., Muthukumar, L., Weiler, H., Richardson, J. A. and Naya, F. J. (2006). Myospryn is a direct transcriptional target for MEF2A that encodes a striated muscle, alpha-actinin-interacting, costamere-localized protein. *Journal of Biological Chemistry* **281**, 6841-6849.

Egginton, S. and Sidell, B. D. (1989). Thermal-Acclimation Induces Adaptive-Changes in Subcellular Structure of Fish Skeletal-Muscle. *American Journal of Physiology* **256**, R1-R9.

Ekker, S. C., Ungar, A. R., Greenstein, P., Vonkessler, D. P., Porter, J. A., Moon, R. T. and Beachy, P. A. (1995). Patterning activities of vertebrate hedgehog proteins in the developing eye and brain. *Current Biology* **5**, 944-955.

Elworthy, S., Hargrave, M., Knight, R., Mebus, K. and Ingham, P. W. (2008). Expression of multiple slow myosin heavy chain genes reveals a diversity of zebrafish slow twitch muscle fibres with differing requirements for Hedgehog and Prdm1 activity. *Development* **135**, 2115-2126.

Engeszer, R., Patterson, L., Rao, A. and Parichy, D. (2007). Zebrafish in the wild: a review of natural history and new notes from the field. *Zebrafish* **4**, 21-40.

Ennion, S., Wilkes, D., Gauvry, L., Alami-Durante, H. and Goldspink, G. (1999). Identification and expression analysis of two developmentally regulated myosin heavy chain gene transcripts in carp (*Cyprinus carpio*). *Journal of Experimental Biology* **202**, 1081-1090.

Ezura, Y., Chakravarti, S., Oldberg, A., Chervoneva, I. and Birk, D. E. (2000). Differential expression of lumican and fibromodulin regulate collagen fibrillogenesis in developing mouse tendons. *Journal of Cell Biology* **151**, 779-787.

FAO. (2006). The State of World Fisheries and Aquaculture, Rome, Italy.

FAO. (2008). The State of World Fisheries and Aquaculture, Rome, Italy.

Farah, C. S. and Reinach, F. C. (1995). The troponin complex and regulation of muscle-contraction. *FASEB Journal* **9**, 755-767.

Feng, X. S., Adiarte, E. G. and Devoto, S. H. (2006). Hedgehog acts directly on the zebrafish dermomyotome to promote myogenic differentiation. *Developmental Biology* **300**, 736-746.

Fernandes, J. M. O., Kinghorn, J. R. and Johnston, I. A. (2007). Differential regulation of multiple alternatively spliced transcripts of MyoD. *Gene* **391**, 178-185.

Fernandes, J. M. O., Mackenzie, M. G., Elgar, G., Suzuki, Y., Watabe, S., Kinghorn, J. R. and Johnston, I. A. (2005). A genomic approach to reveal novel

genes associated with myotube formation in the model teleost, *Takifugu rubripes*. *Physiological Genomics* **22**, 327-338.

Fernandes, J. M. O., Macqueen, D. J., Lee, H. T. and Johnston, I. A. (2008). Genomic, evolutionary, and expression analyses of cee, an ancient gene involved in normal growth and development. *Genomics* **91**, 315-325.

Filatov, V. L., Katrukha, A. G., Bulargina, T. V. and Gusev, N. B. (1999). Troponin: Structure, properties, and mechanism of functioning. *Biochemistry-Moscow* **64**, 969-985.

Fleischer, T. C., Weaver, C. M., McAfee, K. J., Jennings, J. L. and Link, A. J. (2006). Systematic identification and functional screens of uncharacterized proteins associated with eukaryotic ribosomal complexes. *Genes & Development* **20**, 1294-1307.

Forejt, J. and Trachtulec, Z. (2000). Mouse chromosome 17. *Mammalian Genome* **11**, 956-957.

Friedberg, F. (2005). Parvalbumin isoforms in zebrafish. *Molecular Biology Reports* **32**, 167-175.

Fujimori, K., Inui, T., Uodome, N., Kadoyama, K., Aritake, K. and Urade, Y. (2006). Zebrafish and chicken lipocalin-type prostaglandin D synthase homologues: Conservation of mammalian gene structure and binding ability for lipophilic molecules, and difference in expression profile and enzyme activity. *Gene* **375**, 14-25.

Furutani-Seiki, M. and Wittbrodt, J. (2004). Medaka and zebrafish, an evolutionary twin study. *Mechanisms of Development* **121**, 629-637.

Galloway, T. F., Kjorsvik, E. and Kryvi, H. (1998). Effect of temperature on viability and axial muscle development in embryos and yolk sac larvae of the Northeast Arctic cod (*Gadus morhua*). *Marine Biology* **132**, 559-567.

Gates, M. A., Kim, L., Egan, E. S., Cardozo, T., Sirotkin, H. I., Dougan, S. T., Lashkari, D., Abagyan, R., Schier, A. F. and Talbot, W. S. (1999). A genetic linkage map for zebrafish: Comparative analysis and localization of genes and expressed sequences. *Genome Research* **9**, 334-347.

Giaever, G., Chu, A. M., Ni, L., Connelly, C., Riles, L., Veronneau, S., Dow, S., Lucau-Danila, A., Anderson, K., Andre, B. et al. (2002). Functional profiling of the *Saccharomyces cerevisiae* genome. *Nature* **418**, 387-391.

Gibert, P., Moreteau, B. and David, J. R. (2000). Developmental constraints on an adaptive plasticity: reaction norms of pigmentation in adult segments of *Drosophila melanogaster*. *Evolution & Development* **2**, 249-260.

Goetz, F. W. and MacKenzie, S. (2008). Functional genomics with microarrays in fish biology and fisheries. *Fish and Fisheries* **9**, 378-395.

Gomez-Skarmeta, J. L., Lenhard, B. and Becker, T. S. (2006). New technologies, new findings, and new concepts in the study of vertebrate cis-regulatory sequences. *Developmental Dynamics* **235**, 870-885.

Goode, D. K., Snell, P., Smith, S. F., Cooke, J. E. and Elgar, G. (2005). Highly conserved regulatory elements around the SHH gene may contribute to the maintenance of conserved synteny across human chromosome 7q36.3. *Genomics* **86**, 172-181.

Gordon, A. M., Homsher, E. and Regnier, M. (2000). Regulation of contraction in striated muscle. *Physiological Reviews* **80**, 853-924.

Gotthard, K. and Nylin, S. (1995). Adaptive plasticity and plasticity as an adaptation: a selective review of plasticity in animal morphology and life-history. *Oikos* **74**, 3-17.

Greer-Walker, M. and Pull, G. A. (1975). Survey of red and white muscle in

marine fish. *Journal of Fish Biology* **7**, 295-300.

Gros, J., Manceau, M., Thome, V. and Marcelle, C. (2005). A common somitic origin for embryonic muscle progenitors and satellite cells. *Nature* **435**, 954-958.

Groves, J. A., Hammond, C. L. and Hughes, S. M. (2005). Fgf8 drives myogenic progression of a novel lateral fast muscle fibre population in zebrafish. *Development* **132**, 4211-4222.

Guindon, S. and Gascuel, O. (2003). A simple, fast, and accurate algorithm to estimate large phylogenies by maximum likelihood. *Systematic Biology* **52**, 696-704.

Guyon, J. R., Steffen, L. S., Howell, M. H., Pusack, T. J., Lawrence, C. and Kunkel, L. M. (2007). Modeling human muscle disease in zebrafish. *Biochimica Et Biophysica Acta-Molecular Basis of Disease* **1772**, 205-215.

Haffter, P., Granato, M., Brand, M., Mullins, M. C., Hammerschmidt, M., Kane, D. A., Odenthal, J., vanEeden, F. J. M., Jiang, Y. J., Heisenberg, C. P. et al. (1996). The identification of genes with unique and essential functions in the development of the zebrafish, *Danio rerio*. *Development* **123**, 1-36.

Hamade, A., Deries, M., Begemann, G., Bally-Cuif, L., Genet, C., Sabatier, F., Bonnieu, A. and Cousin, X. (2006). Retinoic acid activates myogenesis in vivo through Fgf8 signalling. *Developmental Biology* **289**, 127-140.

Hammerschmidt, M., Pelegri, F., Mullins, M. C., Kane, D. A., Brand, M., vanEeden, F. J. M., FurutaniSeiki, M., Granato, M., Haffter, P., Heisenberg, C. P. et al. (1996). Mutations affecting morphogenesis during gastrulation and tail formation in the zebrafish, *Danio rerio*. *Development* **123**, 143-151.

Hammond, C. L., Hinits, Y., Osborn, D. P. S., Minchin, J. E. N., Tettamanti, G. and Hughes, S. M. (2007). Signals and myogenic regulatory factors restrict pax3 and pax7 expression to dermomyotome-like tissue in zebrafish. *Developmental*

Biology **302**, 504-521.

Hawke, T. J. and Geary, D. J. (2001). Myogenic satellite cells: physiology to molecular biology.. *Journal of Applied Physiology* **91**, 534-551.

Hedges, S. B. and Kumar, S. (2002). Vertebrate genomes compared. *Science* **297**, 1283-1285.

Henry, C. A. and Amacher, S. L. (2004). Zebrafish slow muscle cell migration induces a wave of fast muscle morphogenesis. *Developmental Cell* **7**, 917-923.

Hill, J. and Johnston, I. A. (1997). Temperature and neural development of the Atlantic herring (*Clupea harengus* L). *Comparative Biochemistry and Physiology a-Physiology* **117**, 457-462.

Hoegg, S., Brinkmann, H., Taylor, J. S. and Meyer, A. (2004). Phylogenetic timing of the fish-specific genome duplication correlates with the diversification of teleost fish. *Journal of Molecular Evolution* **59**, 190-203.

Hollway, G. E., Bryson-Richardson, R. J., Berger, S., Cole, N. J., Hall, T. E. and Currie, P. D. (2007). Whole-somite rotation generates muscle progenitor cell compartments in the developing zebrafish embryo. *Developmental Cell* **12**, 207-219.

Hu, Z., Potthoff, B., Hollenberg, C. P. and Ramezani-Rad, M. (2006). Mdy2, a ubiquitin-like (UBL)-domain protein, is required for efficient mating in *Saccharomyces cerevisiae*. *Journal of Cell Science* **119**, 326-338.

Hu, Z.-L., Bao, J. and Reecy, J. (2008). CateGOrizer: a web-based program to batch analyze gene ontology classification categories. *Online Journal of Bioinformatics* **9**, 108-112.

Hugli, T. (1986). Biochemistry and biology of anaphylatoxins. *Complement (Basel, Switzerland)* **3**, 111.

Huh, W. K., Falvo, J. V., Gerke, L. C., Carroll, A. S., Howson, R. W., Weissman, J. S. and O'Shea, E. K. (2003). Global analysis of protein localization in budding yeast. *Nature* **425**, 686-691.

Ito, T., Chiba, T., Ozawa, R., Yoshida, M., Hattori, M. and Sakaki, Y. (2001). A comprehensive two-hybrid analysis to explore the yeast protein interactome. *Proceedings of the National Academy of Sciences of the United States of America* **98**, 4569-4574.

Jaillon, O., Aury, J. M., Brunet, F., Petit, J. L., Stange-Thomann, N., Mauceli, E., Bouneau, L., Fischer, C., Ozouf-Costaz, C., Bernot, A. et al. (2004). Genome duplication in the teleost fish *Tetraodon nigroviridis* reveals the early vertebrate proto-karyotype. *Nature* **431**, 946-957.

James, R. S., Cole, N. J., Davies, M. L. F. and Johnston, I. A. (1998). Scaling of intrinsic contractile properties and myofibrillar protein composition of fast muscle in the fish *Myoxocephalus scorpius* L. *Journal of Experimental Biology* **201**, 901-912.

Jaroszewski, L., Li, Z. W., Krishna, S. S., Bakolitsa, C., Wooley, J., Deacon, A. M., Wilson, I. A. and Godzik, A. (2009). Exploration of uncharted regions of the protein universe. *PLoS Biology* **7**, e1000205.

Johnston, I. A. (1982). Capillarisation, oxygen diffusion distances and mitochondrial content of carp muscles following acclimation to summer and winter temperatures. *Cell and Tissue Research* **222**, 325-337.

Johnston, I. A. (1993). Temperature Influences Muscle Differentiation and the Relative Timing of Organogenesis in Herring (*Clupea harengus*) Larvae. *Marine Biology* **116**, 363-379.

Johnston, I. A. (1999). Muscle development and growth: potential implications for flesh quality in fish. *Aquaculture* **177**, 99-115.

Johnston, I. A. (2006). Environment and plasticity of myogenesis in teleost fish. *Journal of Experimental Biology* **209**, 2249-2264.

Johnston, I. A., Abercromby, M., Vieira, V. L. A., Sigursteindottir, R. J., Kristjansson, B. K., Sibthorpe, D. and Skulason, S. (2004a). Rapid evolution of muscle fibre number in post-glacial populations of Arctic charr *Salvelinus alpinus*. *Journal of Experimental Biology* **207**, 4343-4360.

Johnston, I. A., Alderson, R., Sandham, C., Dingwall, A., Mitchell, D., Selkirk, C., Nickell, D., Baker, R., Robertson, B., Whyte, D. et al. (2000). Muscle fibre density in relation to the colour and texture of smoked Atlantic salmon (*Salmo salar* L.). *Aquaculture* **189**, 335-349.

Johnston, I. A., Cole, N. J., Abercromby, M. and Vieira, V. L. A. (1998). Embryonic temperature modulates muscle growth characteristics in larval and juvenile herring. *Journal of Experimental Biology* **201**, 623-646.

Johnston, I. A., Cole, N. J., Vieira, V. L. A. and Davidson, I. (1997). Temperature and developmental plasticity of muscle phenotype in herring larvae. *Journal of Experimental Biology* **200**, 849-868.

Johnston, I. A., Davison, W. and Goldspink, G. (1977). Energy metabolism of carp swimming muscles. *Journal of Comparative Physiology* **114**, 203-216.

Johnston, I. A., Fernandez, D. A., Calvo, J., Vieira, V. L. A., North, A. W., Abercromby, M. and Garland, T. (2003a). Reduction in muscle fibre number during the adaptive radiation of notothenioid fishes: a phylogenetic perspective. *Journal of Experimental Biology* **206**, 2595-2609.

Johnston, I. A. and Hall, T. E. (2004). Mechanisms of muscle development and responses to temperature change in fish larvae. *Development of Form and Function in Fishes and the Question of Larval Adaptation* **40**, 85-116.

Johnston, I. A., Lee, H. T., Macqueen, D. J., Paranthaman, K., Kawashima, C.,

Anwar, A., Kinghorn, J. R. and Dalmay, T. (2009). Embryonic temperature affects muscle fibre recruitment in adult zebrafish: genome-wide changes in gene and microRNA expression associated with the transition from hyperplastic to hypertrophic growth phenotypes. *Journal of Experimental Biology* **212**, 1781-1793.

Johnston, I. A., Li, X. J., Vieira, V. L. A., Nickell, D., Dingwall, A., Alderson, R., Campbell, P. and Bickerdike, R. (2006). Muscle and flesh quality traits in wild and farmed Atlantic salmon. *Aquaculture* **256**, 323-336.

Johnston, I. A., Manthri, S., Alderson, R., Smart, A., Campbell, P., Nickell, D., Robertson, B., Paxton, C. G. M. and Burt, M. L. (2003b). Freshwater environment affects growth rate and muscle fibre recruitment in seawater stages of Atlantic salmon (*Salmo salar* L.). *Journal of Experimental Biology* **206**, 1337-1351.

Johnston, I. A., Manthri, S., Bickerdike, R., Dingwall, A., Luijkx, R., Campbell, P., Nickell, D. and Alderson, R. (2004b). Growth performance, muscle structure and flesh quality in out-of-season Atlantic salmon (*Salmo salar*) smolts reared under two different photoperiod regimes. *Aquaculture* **237**, 281-300.

Johnston, I. A., Manthri, S., Smart, A., Campbell, P., Nickell, D. and Alderson, R. (2003c). Plasticity of muscle fibre number in seawater stages of Atlantic salmon in response to photoperiod manipulation. *Journal of Experimental Biology* **206**, 3425-3435.

Johnston, I. A. and McLay, H. A. (1997). Temperature and family effects on muscle cellularity at hatch and first feeding in Atlantic salmon (*Salmo salar* L). *Canadian Journal of Zoology-Revue Canadienne De Zoologie* **75**, 64-74.

Johnston, I. A. and Salamonski, J. (1984). Power output and force-velocity relationship of red and white muscle fibres from the Pacific blue marlin (*Makaira nigricans*). *Journal of Experimental Biology* **111**, 171.

Johnston, I. A., Strugnell, G., McCracken, M. L. and Johnstone, R. (1999). Muscle growth and development in normal-sex-ratio and all-female diploid and triploid Atlantic salmon. *Journal of Experimental Biology* **202**, 1991-2016.

Kamath, R. S., Fraser, A. G., Dong, Y., Poulin, G., Durbin, R., Gotta, M., Kanapin, A., Le Bot, N., Moreno, S., Sohrmann, M. et al. (2003). Systematic functional analysis of the *Caenorhabditis elegans* genome using RNAi. *Nature* **421**, 231-237.

Kanehisa, M., Goto, S., Hattori, M., Aoki-Kinoshita, K. F., Itoh, M., Kawashima, S., Katayama, T., Araki, M. and Hirakawa, M. (2006). From genomics to chemical genomics: new developments in KEGG. *Nucleic Acids Research* **34**, D354-D357.

Kasahara, M., Naruse, K., Sasaki, S., Nakatani, Y., Qu, W., Ahsan, B., Yamada, T., Nagayasu, Y., Doi, K., Kasai, Y. et al. (2007). The medaka draft genome and insights into vertebrate genome evolution. *Nature* **447**, 714-719.

Kemp, T. J., Sadusky, T. J., Simon, M., Brown, R., Eastwood, M., Sassoon, D. A. and Coulton, G. R. (2001). Identification of a novel stretch-responsive skeletal muscle gene (Smpx). *Genomics* **72**, 260-271.

Kim, S., Kim, S. H., Kim, H., Chung, A. Y., Cha, Y. I., Kim, C. H., Huh, T. L. and Park, H. C. (2008). Frizzled 8a Function Is Required for Oligodendrocyte Development in the Zebrafish Spinal Cord. *Developmental Dynamics* **237**, 3324-3331.

Kim, S. H., Shin, J., Park, H. C., Yeo, S. Y., Hong, S. K., Han, S. T., Rhee, M., Kim, C. H., Chitnis, A. B. and Huh, T. L. (2002). Specification of an anterior neuroectoderm patterning by Frizzled8a-mediated Wnt8b signalling during late gastrulation in zebrafish. *Development* **129**, 4443-4455.

Kimmel, C. B., Ballard, W. W., Kimmel, S. R., Ullmann, B. and Schilling, T. F. (1995). Stages of Embryonic-Development of the Zebrafish. *Developmental*

Dynamics **203**, 253-310.

Kimmel, C. B., Warga, R. M. and Schilling, T. F. (1990). Origin and Organization of the Zebrafish Fate Map. *Development* **108**, 581-594.

Kleinjan, D. A. and van Heyningen, V. (2005). Long-range control of gene expression: Emerging mechanisms and disruption in disease. *American Journal of Human Genetics* **76**, 8-32.

Kloosterman, W. P. and Plasterk, R. H. A. (2006). The diverse functions of MicroRNAs in animal development and disease. *Developmental Cell* **11**, 441-450.

Kouloumenta, A., Mavroidis, M. and Capetanaki, Y. (2007). Proper perinuclear localization of the TRIM-like protein myospryn requires its binding partner desmin. *Journal of Biological Chemistry* **282**, 35211-35221.

Lagomarsino, I. V. and Conover, D. O. (1993). Variation in Environmental and Genotypic Sex-Determining Mechanisms across a Latitudinal Gradient in the Fish, *Evolution* **47**, 487-494.

Langfeld, K. S., Altringham, J. D. and Johnston, I. A. (1989). Temperature and the force-velocity relationship of live muscle fibres from the teleost *Myoxocephalus scorpius*. *Journal of Experimental Biology* **144**, 437.

Lassar, A. B. and Munsterberg, A. E. (1996). The role of positive and negative signals in somite patterning. *Current Opinion in Neurobiology* **6**, 57-63.

Letunic, I., Doerks, T. and Bork, P. (2009). SMART 6: recent updates and new developments. *Nucleic Acids Research* **37**, D229-D232.

Lindeman, R. E. and Pelegri, F. (2010). Vertebrate maternal-effect genes: Insights into fertilization, early cleavage divisions, and germ cell determinant localization from studies in the zebrafish. *Molecular Reproduction and Development* **77**, 299-313.

Lopez-Albors, O., Abdel, I., Periago, M. J., Ayala, M. D., Alcazar, A. G., Gracia, C. M., Nathanailides, C. and Vazquez, J. M. (2008). Temperature influence on the white muscle growth dynamics of the sea bass *Dicentrarchus labrax*, L. Flesh quality implications at commercial size. *Aquaculture* **277**, 39-51.

MacKenzie, A., Miller, K. A. and Collinson, J. M. (2004). Is there a functional link between gene interdigitation and multi-species conservation of synteny blocks? *Bioessays* **26**, 1217-1224.

Macqueen, D. J. (2008). Embryonic temperature and the genes regulating myogenesis in teleosts, Doctoral dissertation. St. Andrews, Scotland: University of St. Andrews.

Macqueen, D. J. and Johnston, I. A. (2008). An Update on MyoD Evolution in Teleosts and a Proposed Consensus Nomenclature to Accommodate the Tetraploidization of Different Vertebrate Genomes. *PLoS One* **3**, e1567.

Macqueen, D. J., Robb, D. and Johnston, I. A. (2007). Temperature influences the coordinated expression of myogenic regulatory factors during embryonic myogenesis in Atlantic salmon (*Salmo salar* L.). *Journal of Experimental Biology* **210**, 2781-2794.

Macqueen, D. J., Robb, D. H. F., Olsen, T., Melstveit, L., Paxton, C. G. M. and Johnston, I. A. (2008). Temperature until the 'eyed stage' of embryogenesis programmes the growth trajectory and muscle phenotype of adult Atlantic salmon. *Biology Letters* **4**, 294-298.

Marler, P. and Nelson, D. A. (1993). Action-Based Learning - a New Form of Developmental Plasticity in Bird Song. *Netherlands Journal of Zoology* **43**, 91-103.

Marschallinger, J., Obermayer, A., Sanger, A. M., Stoiber, W. and Steinbacher, P. (2009). Postembryonic fast muscle growth of teleost fish depends

upon a nonuniformly distributed population of mitotically active pax7^{+} precursor cells. *Developmental Dynamics* **238**, 2442-2448.

Martell, D. J. and Kieffer, J. D. (2007). Persistent effects of incubation temperature on muscle development in larval haddock (*Melanogrammus aeglefinus* L.). *Journal of Experimental Biology* **210**, 1170-1182.

Mathavan, S., Lee, S. G. P., Mak, A., Miller, L. D., Murthy, K. R. K., Govindarajan, K. R., Tong, Y., Wu, Y. L., Lam, S. H., Yang, H. et al. (2005). Transcriptome analysis of zebrafish embryogenesis using microarrays. *PLOS Genetics* **1**, 260-276.

McClure, M. M., McIntyre, P. B. and McCune, A. R. (2006). Notes on the natural diet and habitat of eight danionin fishes, including the zebrafish *Danio rerio*. *Journal of Fish Biology* **69**, 553-570.

Meyer, A. and Schartl, M. (1999). Gene and genome duplications in vertebrates: the one-to-four (-to-eight in fish) rule and the evolution of novel gene functions. *Current Opinion in Cell Biology* **11**, 699-704.

Meyer, A. and Van de Peer, Y. (2005). From 2R to 3R: evidence for a fish-specific genome duplication (FSGD). *Bioessays* **27**, 937-945.

Miller, W., Makova, K. D., Nekrutenko, A. and Hardison, R. C. (2004). Comparative genomics. *Annual Review of Genomics and Human Genetics* **5**, 15-56.

Mitani, H., Kamei, Y., Fukamachi, S., Oda, S., Sasaki, T., Asakawa, S., Todo, T. and Shimizu, N. (2006). The medaka genome: Why we need multiple fish models in vertebrate functional genomics. *Genome Dynamics* **2**, 165.

Mousseau, T. and Fox, C. (1998). Maternal effects as adaptations. U.S.A: Oxford University Press.

Mulley, J. and Holland, P. (2004). Comparative genomics - Small genome, big insights. *Nature* **431**, 916-917.

Mungpakdee, S., Seo, H. C., Angotzi, A. R., Dong, X. J., Akalin, A. and Chourrout, D. (2008). Differential evolution of the 13 Atlantic salmon Hox clusters. *Molecular Biology and Evolution* **25**, 1333-1343.

Nakagami, H., Kikuchi, Y., Katsuya, T., Morishita, R., Akasaka, H., Saitoh, S., Rakugi, H., Kaneda, Y., Shimamoto, K. and Ogihara, T. (2007). Gene polymorphism of myospryn (cardiomyopathy-associated 5) is associated with left ventricular wall thickness in patients with hypertension. *Hypertension Research* **30**, 1239-1246.

Naya, F. J., Black, B. L., Wu, H., Bassel-Duby, R., Richardson, J. A., Hill, J. A. and Olson, E. N. (2002). Mitochondrial deficiency and cardiac sudden death in mice lacking the MEF2A transcription factor. *Nature Medicine* **8**, 1303-1309.

Nelson, J. (1994). Fishes of the world. New York, U.S.A: Wiley

Nelson, J. (2006). Fishes of the world. New York, U.S.A: Wiley.

Newman, R. (1992). Adaptive plasticity in amphibian metamorphosis. *BioScience* **42**, 671-678.

Notredame, C., Higgins, D. G. and Heringa, J. (2000). T-Coffee: A novel method for fast and accurate multiple sequence alignment. *Journal of Molecular Biology* **302**, 205-217.

Ohno, S. (1970). Evolution by gene duplication. New York, U.S.A.: Springer-Verlag.

Padhi, B. K., Joly, L., Tellis, P., Smith, A., Nanjappa, P., Chevrette, M., Ekker, M. and Akimenko, M. A. (2004). Screen for genes differentially expressed during regeneration of the zebrafish caudal fin. *Developmental Dynamics* **231**, 527-541.

Patruno, M., Radaelli, G., Mascarello, F. and Carnevali, M. D. C. (1998). Muscle growth in response to changing demands of functions in the teleost *Sparus aurata* (L.) during development from hatching to juvenile. *Anatomy and Embryology* **198**, 487-504.

Patterson, S. E., Mook, L. B. and Devoto, S. H. (2008). Growth in the larval zebrafish pectoral fin and trunk musculature. *Developmental Dynamics* **237**, 307-315.

Payne, R. M. and Strauss, A. W. (1994). Expression of the Mitochondrial Creatine-Kinase Genes. *Molecular and Cellular Biochemistry* **133**, 235-243.

Pebusque, M. J., Coulier, F., Birnbaum, D. and Pontarotti, P. (1998). Ancient large-scale genome duplications: Phylogenetic and linkage analyses shed light on chordate genome evolution. *Molecular Biology and Evolution* **15**, 1145-1159.

Pelegri, F., Dekens, M. P. S., Schulte-Merker, S., Maischein, H. M., Weiler, C. and Nusslein-Volhard, C. (2004). Identification of recessive maternal-effect mutations in the zebrafish using a gynogenesis-based method. *Developmental Dynamics* **231**, 324-335.

Periago, M., Ayala, M., Lopez-Albors, O., Abdel, I., Martinez, C., Garcia-Alcazar, A., Ros, G. and Gil, F. (2005). Muscle cellularity and flesh quality of wild and farmed sea bass, *Dicentrarchus labrax* L. *Aquaculture* **249**, 175-188.

Pfaffl, M. W., Horgan, G. W. and Dempfle, L. (2002). Relative expression software tool (REST (c)) for group-wise comparison and statistical analysis of relative expression results in real-time PCR. *Nucleic Acids Research* **30**, e36.

Pinheiro, J. and Bates, D. (2000). Mixed-effects models in S and S-PLUS New York, U.S.A.: Springer-Verlag.

Porter, J. D., Khanna, S., Kaminski, H. J., Rao, J. S., Merriam, A. P., Richmonds, C. R., Leahy, P., Li, J. J., Guo, W. and Andrade, F. H. (2002). A chronic inflammatory response dominates the skeletal muscle molecular signature in dystrophin-deficient mdx mice. *Human Molecular Genetics* **11**, 263-272.

Postlethwait, J. H., Woods, I. G., Ngo-Hazelett, P., Yan, Y. L., Kelly, P. D., Chu, F., Huang, H., Hill-Force, A. and Talbot, W. S. (2000). Zebrafish comparative genomics and the origins of vertebrate chromosomes. *Genome Research* **10**, 1890-1902.

Pourquie, O. (2001). Vertebrate somitogenesis. *Annual Review of Cell and Developmental Biology* **17**, 311-350.

Price, T. D., Qvarnstrom, A. and Irwin, D. E. (2003). The role of phenotypic plasticity in driving genetic evolution. *Proceedings of the Royal Society of London Series B-Biological Sciences* **270**, 1433-1440.

Prince, V. E., Joly, L., Ekker, M. and Ho, R. K. (1998). Zebrafish hox genes: genomic organization and modified colinear expression patterns in the trunk. *Development* **125**, 407-420.

Prusky, G. T. and Douglas, R. M. (2003). Developmental plasticity of mouse visual acuity. *European Journal of Neuroscience* **17**, 167-173.

Putnam, N. H., Butts, T., Ferrier, D. E. K., Furlong, R. F., Hellsten, U., Kawashima, T., Robinson-Rechavi, M., Shoguchi, E., Terry, A., Yu, J. K. et al. (2008). The amphioxus genome and the evolution of the chordate karyotype. *Nature* **453**, 1064-U3.

Rao, P. K., Kumar, R. M., Farkhondeh, M., Baskerville, S. and Lodish, H. F. (2006). Myogenic factors that regulate expression of muscle-specific, microRNAs. *Proceedings of the National Academy of Sciences of the United States of America* **103**, 8721-8726.

Relaix, F., Rocancourt, D., Mansouri, A. and Buckingham, M. (2005). A Pax3/Pax7-dependent population of skeletal muscle progenitor cells. *Nature* **435**, 948-953.

Rescan, P. Y., Montfort, J., Ralliere, C., Le Cam, A., Esquerre, D. and Hugot, K. (2007). Dynamic gene expression in fish muscle during recovery growth induced by a fasting-refeeding schedule. *BMC Genomics* **8**, -.

Reynolds, J. G., McCalmon, S. A., Donaghey, J. A. and Naya, F. J. (2008). Deregulated protein kinase A signaling and myospryn expression in muscular dystrophy. *Journal of Biological Chemistry* **283**, 8070-8074.

Reynolds, J. G., McCalmon, S. A., Tomczyk, T. and Naya, F. J. (2007). Identification and mapping of protein kinase A binding sites in the costameric protein myospryn. *Biochimica Et Biophysica Acta-Molecular Cell Research* **1773**, 891-902.

Rome, L. C., Loughna, P. T. and Goldspink, G. (1984). Muscle-fiber activity in carp as a function of swimming speed and muscle temperature. *American Journal of Physiology* **247**, R272-R279.

Rome, L. C. and Sosnicki, A. A. (1990). The influence of temperature on mechanics of red muscle in carp. *Journal of Physiology-London* **427**, 151-169.

Roth, L. W. A., Bormann, P., Bonnet, A. and Reinhard, E. (1999). beta-thymosin is required for axonal tract formation in developing zebrafish brain. *Development* **126**, 1365-1374.

Rowe, R. and Goldspink, G. (1969). Muscle fibre growth in five different muscles in both sexes of mice. *Journal of Anatomy* **104**, 519.

Rowlerson, A., Mascarello, F., Radaelli, G. and Veggetti, A. (1995). Differentiation and growth of muscle in the fish *Sparus Aurata* (L) .II. Hyperplastic and hypertrophic growth of lateral muscle from hatching to adult.

Journal of Muscle Research and Cell Motility **16**, 223-236.

Rowlerson, A., Radaelli, G., Mascarello, F. and Veggetti, A. (1997). Regeneration of skeletal muscle in two teleost fish: *Sparus aurata* and *Brachydanio rerio*. *Cell and Tissue Research* **289**, 311-322.

Rowlerson, A. and Veggetti, A. (2001). Cellular mechanisms of post-embryonic muscle growth in aquaculture species. *Fish physiology* **18**, 103-140.

Roy, R. L., Kim, J. A., Grossman, E. J., Bekmezian, A., Talmadge, R. J., Zhong, H. and Edgerton, V. R. (2000). Persistence of myosin heavy chain-based fiber types in innervated but silenced rat fast muscle. *Muscle & Nerve* **23**, 735-747.

Ruffell, D., Mourkioti, F., Gambardella, A., Kirstetter, P., Lopez, R. G., Rosenthal, N. and Nerlov, C. (2009). A CREB-C/EBP beta cascade induces M2 macrophage-specific gene expression and promotes muscle injury repair. *Proceedings of the National Academy of Sciences of the United States of America* **106**, 17475-17480.

Russell, L. and Forsdyke, D. R. (1991). A human putative lymphocyte g0/g1 switch gene containing a cpg-rich island encodes a small basic-protein with the potential to be phosphorylated. *DNA and Cell Biology* **10**, 581-591.

Sandelin, A., Bailey, P., Bruce, S., Engstrom, P. G., Klos, J. M., Wasserman, W. W., Ericson, J. and Lenhard, B. (2004). Arrays of ultraconserved non-coding regions span the loci of key developmental genes in vertebrate genomes. *BMC Genomics* **5**, 99.

Sanger, A. and Stoiber, W. (2001). Muscle fiber diversity and plasticity. *Fish Physiology* **18**, 187-250.

Sarparanta, J. (2008). Biology of myospryn: what's known? *Journal of Muscle Research and Cell Motility* **29**, 177-180.

Schauerte, H. E., van Eeden, F. J. M., Fricke, C., Odenthal, J., Strahle, U. and Haffter, P. (1998). Sonic hedgehog is not required for the induction of medial floor plate cells in the zebrafish. *Development* **125**, 2983-2993.

Schmidt, K., Glaser, G., Wernig, A., Wegner, M. and Rosorius, O. (2003). Sox8 is a specific marker for muscle satellite cells and inhibits myogenesis. *Journal of Biological Chemistry* **278**, 29769-29775.

Schultz, J., Milpetz, F., Bork, P. and Ponting, C. P. (1998). SMART, a simple modular architecture research tool: Identification of signaling domains. *Proceedings of the National Academy of Sciences of the United States of America* **95**, 5857-5864.

Seale, P., Sabourin, L. A., Girgis-Gabardo, A., Mansouri, A., Gruss, P. and Rudnicki, M. A. (2000). Pax7 is required for the specification of myogenic satellite cells. *Cell* **102**, 777-786.

Shen, J., Hsu, C. M., Kang, B. K., Rosen, B. P. and Bhattacharjee, H. (2003). The *Saccharomyces cerevisiae* Arr4p is involved in metal and heat tolerance. *Biometals* **16**, 369-378.

Shine, R. (2005). Life-history evolution in reptiles. *Annual Review of Ecology Evolution and Systematics* **36**, 23-46.

Simmer, F., Moorman, C., van der Linden, A. M., Kuijk, E., van den Berghe, P. V. E., Kamath, R. S., Fraser, A. G., Ahringer, J. and Plasterk, R. H. A. (2003). Genome-wide RNAi of *C-elegans* using the hypersensitive rrf-3 strain reveals novel gene functions. *PLoS Biology* **1**, 77-84.

Skromne, I. and Prince, V. (2008). Current perspectives in zebrafish reverse genetics: moving forward. *Developmental Dynamics* **237**, 861-882.

Smith-Gill, S. J. (1983). Developmental plasticity: developmental conversion versus phenotypic modulation. *Integrative and Comparative Biology* **23**, 47.

Spence, R., Fatema, M. K., Reichard, M., Huq, K. A., Wahab, M. A., Ahmed, Z. F. and Smith, C. (2006). The distribution and habitat preferences of the zebrafish in Bangladesh. *Journal of Fish Biology* **69**, 1435-1448.

Spence, R., Gerlach, G., Lawrence, C. and Smith, C. (2008). The behaviour and ecology of the zebrafish, Danio rerio. *Biological Reviews* **83**, 13-34.

Sprague, J., Bayraktaroglu, L., Clements, D., Conlin, T., Fashena, D., Frazer, K., Haendel, M., Howe, D. G., Mani, P., Ramachandran, S. et al. (2006). The Zebrafish Information Network: the zebrafish model organism database. *Nucleic Acids Research* **34**, D581-D585.

Sprague, J., Doerry, E., Douglas, S., Westerfield, M. and Grp, Z. (2001). The Zebrafish Information Network (ZFIN): a resource for genetic, genomic and developmental research. *Nucleic Acids Research* **29**, 87-90.

Stearns, S. C. (1989). The Evolutionary Significance of Phenotypic Plasticity - Phenotypic Sources of Variation among Organisms Can Be Described by Developmental Switches and Reaction Norms. *BioScience* **39**, 436-445.

Steinbacher, P., Haslett, J. R., Obermayer, A., Marschallinger, J., Bauer, H. C., Sanger, A. M. and Stoiber, W. (2007). MyoD and Myogenin expression during myogenic phases in Brown trout: A precocious onset of mosaic hyperplasia is a prerequisite for fast somatic growth. *Developmental Dynamics* **236**, 1106-1114.

Steinbacher, P., Haslett, J. R., Six, M., Gollmann, H. P., Sanger, A. M. and Stoiber, W. (2006). Phases of myogenic cell activation and possible role of dermomyotome cells in teleost muscle formation. *Developmental Dynamics* **235**, 3132-3143.

Steinbacher, P., Stadlmayr, V., Marschallinger, J., Sanger, A. M. and Stoiber, W. (2008). Lateral Fast Muscle Fibers Originate From the Posterior Lip of the

Teleost Dermomyotome. *Developmental Dynamics* **237**, 3233-3239.

Steinke, D., Salzburger, W. and Meyer, A. (2006). Novel relationships among ten fish model species revealed based on a phylogenomic analysis using ESTs. *Journal of Molecular Evolution* **62**, 772-784.

Stellabotte, F. and Devoto, S. H. (2007). The teleost dermomyotome. *Developmental Dynamics* **236**, 2432-2443.

Stellabotte, F., Dobbs-McAuliffe, B., Fernandez, D. A., Feng, X. S. and Devoto, S. H. (2007). Dynamic somite cell rearrangements lead to distinct waves of myotome growth. *Development* **134**, 1253-1257.

Stevenson, E. J., Giresi, P. G., Koncarevic, A. and Kandarian, S. C. (2003). Global analysis of gene expression patterns during disuse atrophy in rat skeletal muscle. *Journal of Physiology-London* **551**, 33-48.

Stiber, J. A., Zhang, Z. S., Burch, J., Eu, J. P., Zhang, S., Truskey, G. A., Seth, M., Yamaguchi, N., Meissner, G., Shah, R. et al. (2008). Mice lacking homer 1 exhibit a skeletal myopathy characterized by abnormal transient receptor potential channel activity. *Molecular and Cellular Biology* **28**, 2637-2647.

Stickney, H. L., Barresi, M. J. F. and Devoto, S. H. (2000). Somite development in zebrafish. *Developmental Dynamics* **219**, 287-303.

Sultan, S. E. (2000). Phenotypic plasticity for plant development, function and life history. *Trends in Plant Science* **5**, 537-542.

Tang, Z. L., Li, Y., Wan, P., Li, X. P., Zhao, S. H., Liu, B., Fan, B., Zhu, M. J., Yu, M. and Li, K. (2007). LongSAGE analysis of skeletal muscle at three prenatal stages in Tongcheng and Landrace pigs. *Genome Biology* **8**, R115.

Taylor, J. S., Van de Peer, Y., Braasch, I. and Meyer, A. (2001). Comparative genomics provides evidence for an ancient genome duplication event in fish.

Philosophical Transactions of the Royal Society of London Series B-Biological Sciences **356**, 1661-1679.

Thisse, C., Thisse, B., Schilling, T. F. and Postlethwait, J. H. (1993). Structure of the zebrafish snail1 gene and its expression in wild-type, spadetail and no tail mutant embryos. *Development* **119**, 1203-1215.

Tkatchenko, A. V., Pietu, G., Cros, N., Gannoun-Zaki, L., Auffray, C., Leger, J. J. and Dechesne, C. A. (2001). Identification of altered gene expression in skeletal muscles from Duchenne muscular dystrophy patients. *Neuromuscular Disorders* **11**, 269-277.

van der Ven, P. F. M., Wiesner, S., Salmikangas, P., Auerbach, D., Himmel, M., Kempa, S., Hayess, K., Pacholsky, D., Taivainen, A., Schroder, R. et al. (2000). Indications for a novel muscular dystrophy pathway: gamma-filamin, the muscle-specific filamin isoform, interacts with myotilin. *Journal of Cell Biology* **151**, 235-247.

van Raamsdonk, W., Mos, W., Smit-Onel, M. J., van der Laarse, W. J. and Fehres, R. (1983). The development of the spinal motor column in relation to the myotomal muscle fibers in the zebrafish (*Brachydanio rerio*). I. Posthatching development. *Anatomy and embryology* **167**, 125-39.

Vandesompele, J., De Preter, K., Pattyn, F., Poppe, B., Van Roy, N., De Paepe, A. and Speleman, F. (2002). Accurate normalization of real-time quantitative RT-PCR data by geometric averaging of multiple internal control genes. *Genome Biology* **3**.

Veggetti, A., Mascarello, F., Scapolo, P. A., Rowlerson, A. and Carnevali, M. D. C. (1993). Muscle Growth and Myosin Isoform Transitions during Development of a Small Teleost Fish, Poecilia-Reticulata (Peters) (Atheriniformes, Poeciliidae) - a Histochemical, Immunohistochemical, Ultrastructural and Morphometric Study. *Anatomy and Embryology (Berl)* **187**, 353-361.

Venkatesh, B. and Yap, W. H. (2005). Comparative genomics using fugu: a tool for the identification of conserved vertebrate cis-regulatory elements. *Bioessays* **27**, 100-107.

Venter JC, Adams MD, Myers EW, Li PW, Mural RJ, Sutton GG, Smith HO, Yandell M, Evans CA, Holt RA, Gocayne JD, Amanatides P, Ballew RM, Huson DH, Wortman JR, Zhang Q, Kodira CD, Zheng XQH, Chen L, Skupski M, Subramanian G, Thomas PD, Zhang JH, Miklos GLG, Nelson C, Broder S, Clark AG, Nadeau C, McKusick VA, Zinder N, Levine AJ, Roberts RJ, Simon M, Slayman C, Hunkapiller M, Bolanos R, Delcher A, Dew I, Fasulo D, Flanigan M, Florea L, Halpern A, Hannenhalli S, Kravitz S, Levy S, Mobarry C, Reinert K, Remington K, Abu-Threideh J, Beasley E, Biddick K, Bonazzi V, Brandon R, Cargill M, Chandramouliswaran I, Charlab R, Chaturvedi K, Deng ZM, Di Francesco V, Dunn P, Eilbeck K, Evangelista C, Gabrielian AE, Gan W, Ge WM, Gong FC, Gu ZP, Guan P, Heiman TJ, Higgins ME, Ji RR, Ke ZX, Ketchum KA, Lai ZW, Lei YD, Li ZY, Li JY, Liang Y, Lin XY, Lu F, Merkulov GV, Milshina N, Moore HM, Naik AK, Narayan VA, Neelam B, Nusskern D, Rusch DB, Salzberg S, Shao W, Shue BX, Sun JT, Wang ZY, Wang AH, Wang X, Wang J, Wei MH, Wides R, Xiao CL, Yan CH, Yao A, Ye J, Zhan M, Zhang WQ, Zhang HY, Zhao Q, Zheng LS, Zhong F, Zhong WY, Zhu SPC, Zhao SY, Gilbert D, Baumhueter S, Spier G, Carter C, Cravchik A, Woodage T, Ali F, An HJ, Awe A, Baldwin D, Baden H, Barnstead M, Barrow I, Beeson K, Busam D, Carver A, Center A, Cheng ML, Curry L, Danaher S, Davenport L, Desilets R, Dietz S, Dodson K, Doup L, Ferriera S, Garg N, Gluecksmann A, Hart B, Haynes J, Haynes C, Heiner C, Hladun S, Hostin D, Houck J, Howland T, Ibegwam C, Johnson J, Kalush F, Kline L, Koduru S, Love A, Mann F, May D, McCawley S, McIntosh T, McMullen I, Moy M, Moy L, Murphy B, Nelson K, Pfannkoch C, Pratts E, Puri V, Qureshi H, Reardon M, Rodriguez R, Rogers YH, Romblad D, Ruhfel B, Scott R, Sitter C, Smallwood M, Stewart E, Strong R, Suh E, Thomas R, Tint NN, Tse S, Vech C, Wang G, Wetter J, Williams S, Williams M, Windsor S, Winn-Deen E, Wolfe K, Zaveri J, Zaveri K, Abril JF, Guigo R, Campbell MJ, Sjolander KV, Karlak B, Kejariwal A, Mi HY, Lazareva B, Hatton T, Narechania A, Diemer K, Muruganujan A, Guo N, Sato S, Bafna V,

Istrail S, Lippert R, Schwartz R, Walenz B, Yooseph S, Allen D, Basu A, Baxendale J, Blick L, Caminha M, Carnes-Stine J, Caulk P, Chiang YH, Coyne M, Dahlke C, Mays AD, Dombroski M, Donnelly M, Ely D, Esparham S, Fosler C, Gire H, Glanowski S, Glasser K, Glodek A, Gorokhov M, Graham K, Gropman B, Harris M, Heil J, Henderson S, Hoover J, Jennings D, Jordan C, Jordan J, Kasha J, Kagan L, Kraft C, Levitsky A, Lewis M, Liu XJ, Lopez J, Ma D, Majoros W, McDaniel J, Murphy S, Newman M, Nguyen T, Nguyen N, Nodell M, Pan S, Peck J, Peterson M, Rowe W, Sanders R, Scott J, Simpson M, Smith T, Sprague A, Stockwell T, Turner R, Venter E, Wang M, Wen MY, Wu D, Wu M, Xia A, Zandieh A & Zhu XH. (2001). The sequence of the human genome. *Science* **291**, 1304.

Vieira, V. L. A. and Johnston, I. A. (1992). Influence of Temperature on Muscle-Fiber Development in Larvae of the Herring *Clupea Harengus*. *Marine Biology* **112**, 333-341.

Wagner, D. S., Dosch, R., Mintzer, K. A., Wiemelt, A. P. and Mullins, M. C. (2004). Maternal control of development at the midblastula transition and beyond: Mutants from the zebrafish II. *Developmental Cell* **6**, 781-790.

Walker, M. G. (2001). Pharmaceutical target identification by gene expression analysis. *Mini-Reviews in Medicinal Chemistry* **1**, 197-205.

Waterman, R. E. (1969). Development of the lateral musculature in the teleost, (*Brachydanio rerio*): A fine structural study. *American Journal of Anatomy* **125**, 457-493.

Weatherley, A. H. and Gill, H. S. (1985). Dynamics of Increase in Muscle-Fibers in Fishes in Relation to Size and Growth. *Experientia* **41**, 353-354.

Weatherley, A. H., Gill, H. S. and Lobo, A. F. (1988). Recruitment and maximal diameter of axial muscle fibres in teleosts and their relationship to somatic growth and ultimate size. *Journal of Fish Biology* **33**, 851-859.

Weinberg, E. S., Allende, M. L., Kelly, C. S., Abdelhamid, A., Murakami, T., Andermann, P., Doerre, O. G., Grunwald, D. J. and Riggleman, B. (1996). Developmental regulation of zebrafish MyoD in wild-type, no tail and spadetail embryos. *Development* **122**, 271-280.

West-Eberhard, M. (2003). Developmental plasticity and evolution. USA: Oxford University Press.

Wheelan, S. J., Church, D. M. and Ostell, J. M. (2001). Spidey: A tool for mRNA-to-genomic alignments. *Genome Research* **11**, 1952-1957.

White, R. M., Sessa, A., Burke, C., Bowman, T., LeBlanc, J., Ceol, C., Bourque, C., Dovey, M., Goessling, W., Burns, C. E. et al. (2008). Transparent adult zebrafish as a tool for in vivo transplantation analysis. *Cell Stem Cell* **2**, 183-189.

Wilwert, J. L., Madhoun, N. M. and Coughlin, D. J. (2006). Parvalbumin correlates with relaxation rate in the swimming muscle of sheepshead and kingfish. *Journal of Experimental Biology* **209**, 227-237.

Wittbrodt, J., Shima, A. and Schartl, M. (2002). Medaka - A model organism from the Far East. *Nature Reviews Genetics* **3**, 53-64.

Wolff, C., Roy, S. and Ingham, P. W. (2003). Multiple muscle cell identities induced by distinct levels and timing of hedgehog activity in the zebrafish embryo. *Current Biology* **13**, 1169-1181.

Woods, I. G., Wilson, C., Friedlander, B., Chang, P., Reyes, D. K., Nix, R., Kelly, P. D., Chu, F., Postlethwait, J. H. and Talbot, W. S. (2005). The zebrafish gene map defines ancestral vertebrate chromosomes. *Genome Research* **15**, 1307-1314.

Woolfe, A., Goodson, M., Goode, D. K., Snell, P., McEwen, G. K., Vavouri, T., Smith, S. F., North, P., Callaway, H., Kelly, K. et al. (2005). Highly conserved

non-coding sequences are associated with vertebrate development. *PLoS Biology* **3**, 116-130.

Yu, S. H., Chen, X. H. and Ao, J. Q. (2009). Molecular characterization and expression analysis of beta(2)-microglobulin in large yellow croaker *Pseudosciaena crocea*. *Molecular Biology Reports* **36**, 1715-1723.

Zhang, G. X., Swank, D. M. and Rome, L. C. (1996). Quantitative distribution of muscle fiber types in the scup *Stenotomus chrysops*. *Journal of Morphology* **229**, 71-81.

Zhang, J. Z. (2003). Evolution by gene duplication: an update. *Trends in Ecology & Evolution* **18**, 292-298.

Zheng, X. H., Lu, F., Wang, Z. Y., Hoover, J. and Mural, R. (2005). Using shared genomic synteny and shared protein functions to enhance the identification of orthologous gene pairs. *Bioinformatics* **21**, 703-710.

Zhou, R. J., Cheng, H. H. and Tiersch, T. R. (2001). Differential genome duplication and fish diversity. *Reviews in Fish Biology and Fisheries* **11**, 331-337.

Chapter 10.0 Publication

Fernandes JM, Macqueen DJ, **Lee HT** & Johnston IA. (2008). Genomic, evolutionary, and expression analyses of cee, an ancient gene involved in normal growth and development. *Genomics* **91,** 315-325.

Johnston IA, **Lee HT**, Macqueen DJ, Paranthaman K, Kawashima C, Anwar A, Kinghorn JR & Dalmay T. (2009). Embryonic temperature affects muscle fibre recruitment in adult zebrafish: genome-wide changes in gene and microRNA expression associated with the transition from hyperplastic to hypertrophic growth phenotypes. *Journal of Experimental Biology* **212,** 1781-1793.

AppendixI: Full information for Table 6.1-6.5

Table 6.1 List of genes up-regulated in myotube (+) phenotype of zebrafish

Name of gene	Full descriptioon	Fold (S/B)	Genomic location	Ensembl Gene ID	Gene bank ID	Zfin ID
1. *myhz1-1*	myosin, heavy polypeptide 1, skeletal muscle Fast skeletal myosin heavy chain 4 (Fragment)	18.9 ± 1.3	Chr5: 24070649-24080528	ENSDARG00000067990	NM_001115089	ZDB-GENE-000322-5
2. *myhz1-2*	myosin, heavy polypeptide 1, skeletal muscle Fast skeletal myosin heavy chain 3 (Fragment)	15.0 ± 1.1	Chr5: 24052882-24063763	ENSDARG00000067995	NM_001115089	ZDB-GENE-000322-5
3. *myhz1-3*	myosin, heavy polypeptide 1, skeletal muscle similar to myosin, heavy polypeptide 2, fast muscle specific	11.1 ± 0.6	Chr5: 24033981-24045796	ENSDARG00000067997	NM_001115089	ZDB-GENE-000322-5
4. *zgc:153704*	homologue of prostaglandin D2 synthase	9.9 ± 1.4	Scaffold Zv7_NA792: 274459-279743	ENSDARG00000045979	NM_001076726	ZDB-GENE-040625-119
5. *myhz2*	myosin, heavy polypeptide 2, fast muscle specific (myhz2)	8.0 ± 0.5	Chr5: 23978407-23989516	ENSDARG00000012944	NM_152982	ZDB-GENE-060929-1114
6. *tnni2a.4*	troponin I, skeletal, fast 2a.4 (tnni2a.4)	7.4 ± 1.2	Chr25: 26710679-26728999	ENSDARG00000029069	NM_001009901	ZDB-GENE-020604-1
7. *tmsb*	thymosin, beta (tmsb)	7.7 ± 1.5	Chr21: 24234030-24236677	ENSDARG00000054911	NM_205581	ZDB-GENE-040808-62
8. *hpd*	4-hydroxyphenylpyruvate dioxygenase (hpd)	6.5 ± 1.3	Chr8: 32602449-32612721	ENSDARG00000044935	NM_001003742	ZDB-GENE-040718-249
9. *tyrp1b*	tyrosinase-related protein 1b (tyrp1b)	6.3 ± 1.1	Chr1: 15214369-15227582	ENSDARG00000056151	NM_001002749	ZDB-GENE-050626-97
10. *zgc:114184*	homologue of troponin T3, skeletal, fast muscle	5.4 ± 1.4	Chr25: 11031343-11041768	ENSDARG00000002988	NM_001025179	ZDB-GENE-030131-1091
11. *fah*	fumarylacetoacetate hydrolase (fumarylacetoacetase) (fah)	4.3 ± 1.0	Chr7: 6008060-6061451	ENSDARG00000039743	NM_199601	ZDB-GENE-041008-23
12. *zgc:113456*	homologue of fibromodulin	4.3 ± 1.0	Chr11: 20662672-20668550	ENSDARG00000044895	NM_001030072	ZDB-GENE-980526-395
13. *sox11a*	SRY-box containing gene 11a (sox11a)	4.1 ± 0.4	Chr17: 24045754-24046818	ENSDARG00000070947	NM_131336	ZDB-GENE-000616-6
14. *myf5*	myogenic factor 5	4.0 ± 0.5	Chr4: 28965953-28969805	ENSDARG00000007277	NM_131576	ZDB-GENE-000328-3
15. *fzd8a*	frizzled homolog 8a (fzd8a)	4.0 ± 0.6	Chr24: 3779283-3781339	ENSDARG00000039743	NM_130918	ZDB-GENE-050417-267
16. *zgc:112098*	homologue of Alpha-actin-1 (acta1)	3.7 ± 0.3	Chr1: 50336119-50343694	ENSDARG00000036371	NM_001017750	ZDB-GENE-041105-7

NA: Not available

17. *aspn*	asporin (LRR class 1) (aspn)	3.7 ± 0.4	Chr22: 8085710-8093188	ENSDARG00000045444	NM_131713	ZDB-GENE-030131-7715
18. *cox6a1*	cytochrome c oxidase subunit VIa polypeptide 1 (cox6a1)	3.5 ± 0.4	Chr8: 51808440-51814132	ENSDARG00000044895	NM_001005592	ZDB-GENE-040718-395
19. *slc38a3*	solute carrier family 38, member 3 (slc38a3)	3.5 ± 0.4	Chr8: 22005547-220037135	ENSDARG00000022438	NM_001002648	ZDB-GENE-060804-3
20. *zgc:136591*	Ribosomal protein L22-like 1(rpl22l1) zgc:136591	3.3 ± 0.5	Chr24: 25139398-25143996	ENSDARG00000014587	NM_001045335	ZDB-GENE-030131-774
21. *cth*	cystathionase (cystathionine gamma-lyase) (cth)	3.2 ± 0.4	Chr6: 23316257-23358819	ENSDARG00000010244	NM_212604	ZDB-GENE-040426-1865
23. *hhatla*	hedgehog acyltransferase-like, a (hhatla)	3.1 ± 0.5	Chr2: 17012180-17026431	ENSDARG00000036371	NM_200887	ZDB-GENE-041001-201
24. *smyd2b*	SET and MYND domain containing 2b (smyd2b), transcript variant 2	3.0 ± 0.5	Chr3: 59122046-59138360	ENSDARG00000045695	NM_001045291	ZDB-GENE-990415-162
25. *myca*	myelocytomatosis oncogene a (myca)	2.8 ± 0.2	Chr24: 9243280-9245820	ENSDARG00000039051	NM_131412	ZDB-GENE-040426-1785
26. *fkbp1b*	FK506 binding protein 1b (fkbp1b)	2.8 ± 0.4	Chr20: 47867879-47899760	ENSDARG00000052625	NM_200812	ZDB-GENE-040426-1794
27. *zgc:76872*	zinc finger and BTB domain containing 45	2.7 ±	NA	ENSDARG00000005629	NM_205706	ZDB-GENE-990415-167
28. *atp1b3a*	ATPase, Na+/K+ transporting, beta 3a polypeptide (atp1b3a)	2.6 ± 0.4	Chr2: 12226568-12244519	ENSDARG00000015790	NM_131221	ZDB-GENE-070424-15
29. *zgc:158803*	homologue of LUC7-like 2	2.5 ± 0.2	Chr1: 51679409-51691123	ENSDARG00000019765	NM_001089547	ZDB-GENE-040625-96
30. *psma5*	easome (prosome, macropain) subunit, alpha ty	2.3 ± 0.3	Chr11: 34353504-34361443	ENSDARG00000003526	NM_205708	ZDB-GENE-040718-146
31. *zgc:92347*	Myozenin-1 (myoz1), zgc:92347	2.3 ± 0.2	Chr12: 27189308-27212541	ENSDARG00000071445	NM_001002447	ZDB-GENE-041001-52
31. *ctnna2*	si:rp71-1h10.1, Catenin alpha-2 (ctnna2)	2.2 ± 0.2	Chr1: 41138533-41954484	ENSDARG00000024785	BC131855	ZDB-GENE-040322-1
33. *pdcl3*	Phosducin-like protein 3 (pdcl3)	2.2 ± 0.1	Scaffold Zv7_NA1057: 1991-3276	ENSDARG00000009449	NM_205721	ZDB-GENE-030131-8556
34. *ppia*	eptidylprolyl isomerase A (cyclophilin A) (ppia	2.0 ± 0.2	Chr8: 42049758-42055131	ENSDARG00000009212	NM_212758	ZDB-GENE-040718-454
35. *zgc:92624*	zgc:92624, similar to zinc finger protein 706	1.9 ± 0.1	Chr19: 24944654-24951292	ENSDARG00000056307	NM_205612	NA

NA: Not available

Table 6.2 List of genes down-regulated in myotube (+) phenotype of zebrafish

Name of gene	Full descriptioon	Fold change (B/S)	Genomic Location	Ensembl Gene ID	Gene bank ID	Zfin ID
1. *pvalb4*	Parvalbumin 4 (pvalb4)	8.3 ± 0.8	Chr3: 50024614-50034269	ENSDARG00000024433	BC064896	ZDB-GENE-040625-48
2. *b2m*	Beta-2-microglobulin (b2m)	7.8 ± 0.9	Chr4: 13283923-13285961	ENSDARG00000053136	NM_131163	ZDB-GENE-980526-88
3. *zgc:56085*	hypothetical LOC568476 (LOC568476) similar to G0/G1 switch protein2	7.3 ± 1.7	Ch23: 37933392-37938006	NA	NM_001128743	NA
4. *c4a*	Complement C4-B Precursor (Basic complement C4)	6.6 ± 1.2	Chr15: 940695-969452	ENSDARG00000015065	BC146727	ZDB-GENE-030131-5697
5. *ckmt2*	Creatine kinase, sarcomeric mitochondrial Precursor (CKMT2)	4.8 ± 0.4	Chr10: 1901087-1910627	ENSDARG00000069615	NM_199816	ZDB-GENE-030131-5717
6. *ppp1r3c*	Protein phosphatase 1 regulatory subunit 3C (PPP1R3C)	3.8 ± 0.5	Chr17: 21423924-21426422	ENSDARG00000071005	NM_001002376	ZDB-GENE-040718-70
7. *gapdh*	Glyceraldehyde-3-phosphate dehydrogenase (gapdh)	3.4 ± 0.2	Chr16: 12907456-12912394	ENSDARG00000043457	NM_001115114	ZDB-GENE-030115-1
8. *ckm*	Creatine kinase M-type (CKM)	2.8 ± 0.3	Chr15: 22502296-22505544	ENSDARG00000040565	NM_001105683	ZDB-GENE-040426-2128
9. *mt-coI*	Cytochrome c oxidase I, mitochondrial (mt-co1)	2.8 ± 0.3	ChrMT: 6425-7975	ENSDARG00000063905	AY996924	ZDB-GENE-011205-14
10. *hif1an*	Hypoxia-inducible factor 1, alpha subunit inhibitor	2.8 ± 0.3	Chr13: 29424259-29451841	ENSDARG00000031915	NM_201496	ZDB-GENE-030826-19
11. *anxa2a*	annexin A2a (anxa2a)	2.6 ±0.6	Chr25: 28116676-28130724	ENSDARG00000003216	NM_181761	ZDB-GENE-030131-4282
12. *c4-2*	Similar to complement C4-2	2.8 ± 0.6	Chr16: 12390233-12423943	ENSDARG00000038424	XM_001334604	NA
13. *cd9l*	CD9 antigen, like (cd9l)	2.6 ± 0.3	Chr4: 3079683-3103645	ENSDARG00000016691	NM_213428	ZDB-GENE-040426-2768
14. *iclp1*	Invariant chain-like protein 1 (iclp1)	2.6 ± 0.3	Chr14: 55625650-55639921	ENSDART00000026021	NM_131590	ZDB-GENE-000901-1
15. *ak1*	Adenylate kinase isoenzyme 1 (AK1)	2.5 ± 0.3	Chr5: 69265030-69287238	ENSDARG00000001950	NM_001003993	ZDB-GENE-040822-37
16. *ldha*	lactate dehydrogenase A4 (ldha)	2.5 ± 0.2	Chr25: 22370104-22378455	ENSDARG00000040856	NM_131246	ZDB-GENE-991026-5

17. *mpz*	Myelin protein zero (mpz)	2.5 ± 0.2	Chr2: 40032322-40046088	ENSDARG00000038609	NM_194361	ZDB-GENE-010724-4
18. *rgs5*	Regulator of G-protein signaling 5 (RGS5)	2.5 ± 0.3	Chr6: 51733513-51747191	ENSDARG00000002644	NM_199962	ZDB-GENE-030131-7570
19. *slc25a4*	solute carrier family 25 (mitochondrial carrier; adenine nucleotide translocator), member 4 (slc25a4)	2.4 ± 0.2	Chr1: 13508242-13510586	ENSDARG00000027355	NM_214702	ZDB-GENE-030131-5275
20. *uqcrfs1*	ubiquinol-cytochrome c reductase, Rieske iron-sulfur polypeptide 1 (uqcrfs1)	2.4 ± 0.4	Chr 7: 40936359-40939321	ENSDARG00000007745	NM_001103194	ZDB-GENE-040426-2060
21. *eno3*	enolase 3, (beta, muscle)	2.3 ± 0.2	Chr23: 45063449-45075389	ENSDARG00000039007	NM_214723	ZDB-GENE-031006-5
22. *zgc:109940*	homology of omplement factor D	2.3 ± 0.4	Chr13: 19764908-19768260	ENSDARG00000039579	NM_001020532	ZDB-GENE-050522-411
23. *cox6a2*	Cytochrome c oxidase polypeptide 6A2, mitochondrial Precursor (COX6A2)	2.2 ± 0.2	Chr3: 28763802-28765969	ENSDARG00000054588	NM_001004680	ZDB-GENE-040912-129
24. *mfsd2b*	major facilitator superfamily domain containing 2b (mfsd2b)	2.2 ± 0.3	Chr19: 28048777-28064992	ENSDARG00000035909	NM_001003570	ZDB-GENE-040801-89
25. *necab1*	N-terminal EF-hand calcium binding protein 1 (NECAB1)	2.2 ± 0.3	Chr19: 27410190-27495130	ENSDARG00000056566	NM_001017848	ZDB-GENE-050417-395
26. *wu:fc83c01*	wu:fc83c01 hypothetical protein LOC325488	2.2 ± 0.4	Chr13: 38976293-38990347	ENSDARG00000069047	BC091661	ZDB-GENE-030131-4213
27. *tnk2*	tyrosine kinase, non-receptor, 2 (tnk2)	2.2 ± 0.3	Chr7: 17641382-17660211 Chr7: 17526498-17545327	ENSDARG00000069429 ENSDARG00000069433	NM_001080017	ZDB-GENE-030131-7427
28. *mdh1* b	malate dehydrogenase 1b, NAD (soluble) (mdh1b)	2.1 ± 0.2	Chr17: 2260250-2265062	ENSDARG00000044080	NM_199969	ZDB-GENE-030131-7655
29. *rtn4a*	reticulon 4a (rtn4a), transcript variant 2	2.1 ± 0.2	Chr6: 4869201-4896360	ENSDARG00000044601	NM_001079912	ZDB-GENE-030710-1
30. *agbl5*	ATP/GTP binding protein-like 5	2.0 ± 0.1	Chr4: 500788-521144	ENSDARG00000045900	NM_001004113	ZDB-GENE-040822-29
31. *arl6ip1*	ADP-ribosylation factor-like 6 interacting protein (arl6ip1)	2.0 ± 0.2	Chr3: 28828753-28839814	ENSDARG00000054578	NM_201112	ZDB-GENE-040426-1087
32. *cox5b*	Cytochrome c oxidase subunit 5B, mitochondrial Precursor (cox5b)	2.0 ± 0.2	Chr13: 48499202-48501673	ENSDARG00000068738	NM_001045357	ZDB-GENE-060825-71
33. *crebbpa*	CREB binding protein a (crebbpa)	2.0 ± 0.2	Chr22: 25506771-25557526	ENSDARG00000061308	NM_001089455	ZDB-GENE-050208-439

34. *fgl2*	fibrinogen-like 2 (fgl2)	2.0 ± 0.2	Chr4: 30528333-30531598	ENSDARG00000019861	NM_001025539	ZDB-GENE-030131-9506
35. *zgc:86773*	zgc:86773, Homology of Ras-related protein Rab-1A (rab1a)	2.0 ± 0.1	Chr10: 20919474-20939644	ENSDARG00000056479	NM_001002129	ZDB-GENE-040625-133
36. *scinla*	scinderin like a (scinla)	2.0 ± 0.2	Chr6: 55395786-55408367	ENSDARG00000069983	NM_178131	ZDB-GENE-030131-2005
37. *atp5i*	zgc:171560, Similar to ATP synthase, H+ transporting, mitochondrial F0 complex, subunit E (ATP5I)	1.9 ± 0.2	NA	NA	BC152574	ZDB-GENE-070928-12
38. *cryabb*	crystallin, alpha B, b (cryabb)	1.9 ± 0.1	Chr5: 51144279-51148409	ENSDARG00000052447	NM_001002670	ZDB-GENE-040718-419
39. *hoxc8a*	homeo box C8a (hoxc8a)	1.9 ± 0.1	Chr23: 33748786-33752344 Chr23: 35238088-35241646	ENSDARG00000070346 ENSDARG00000070302	NM_001005771	ZDB-GENE-990415-114
40. *gapdhs*	glyceraldehyde-3-phosphate dehydrogenase, spermatogenic (gapdhs)	1.9 ± 0.1	Chr16: 43604258-43618535	ENSDARG00000039914	NM_213094	ZDB-GENE-020913-1
41. *tpi1b*	triosephosphate isomerase 1b (tpi1b)	1.9 ± 0.1	Chr16: 8903934-8918257	ENSDARG00000040988	NM_153668	ZDB-GENE-020416-4
42. *cdkn3*	cyclin-dependent kinase inhibitor 3 (cdkn3)	1.8 ± 0.1	Chr13: 38159395-38168391	ENSDARG00000039130	BC049021	ZDB-GENE-060427-2
43. *grsf1*	G-rich RNA sequence binding factor 1 (grsf1)	1.8 ± 0.1	Chr5: 37438031-37444859	ENSDARG00000053021	NM_001045852	ZDB-GENE-060825-196
44. *hc*	clathrin, heavy polypeptide a (Hc)	1.8 ± 0.1	Chr10: 22936583-22993396	ENSDARG00000043493		ZDB-GENE-030131-2299
45. *ldb3b*	LIM domain binding 3b (ldb3b)	1.8 ± 0.1	Chr12: 27532954-27572379	ENSDARG00000019202	NM_199858	ZDB-GENE-030131-6032
46. *ndufb2*	NADH dehydrogenase ubiquinone 1 beta subcomplex subunit 2, mitochondrial Precursor (NDUFB2)	1.8 ± 0.1	Chr4: 28228655-28231097	ENSDARG00000045490	NM_200791	ZDB-GENE-040426-1762
47. *uqcrb*	ubiquinol-cytochrome c reductase binding protein (uqcrb), nuclear gene encoding mitochondrial protein	1.8 ± 0.1	Chr19: 41784642-41789972	ENSDARG00000011146	NM_001024442	ZDB-GENE-050522-542
48. *ap2a1*	LOC558153 similar to adaptor-related protein complex 2, alpha 1 subunit (ap2a1)	1.7 ± 0.1	Chr3: 30109198-30142395	ENSDARG00000054320	XP_001922436	NA
49. *stka*	serine/threonine kinase a (stka)	1.7 ± 0.1	Chr4: 2551627-2664560	ENSDARG00000037640	NM_212566	ZDB-GENE-020419-40
50. *atp5f1*	ATP synthase subunit b, mitochondrial Precursor (ATP5F1)	1.6 ± 0.1	Chr8: 23742429-23748206	ENSDARG00000011553	NM_001005960	ZDB-GENE-041010-33

Table 6.3 GO annotation of genes up-regulated in myotube (+) phenotype of zebrafish

Name of gene	Molecular function	Biological process	Cellular component
1. *myhz1-1*	GO:0005524 ATP binding GO:0003779 actin binding GO:0003774 motor activity GO:0000166 nucleotide binding	GO:0001757 somite specification GO:0006941 striated muscle contraction	GO:0016459 myosin complex GO:0005863 striated muscle thick filament
2. *myhz1-2*	GO:0005524 ATP binding GO:0003779 actin binding GO:0003774 motor activity GO:0000166 nucleotide binding	GO:0001757 somite specification GO:0006941 striated muscle contraction	GO:0016459 myosin complex GO:0005863 striated muscle thick filament
3. *myhz1-3*	GO:0005524 ATP binding GO:0003779 actin binding GO:0003774 motor activity GO:0000166 nucleotide binding	GO:0001757 somite specification GO:0006941 striated muscle contraction	GO:0016459 myosin complex GO:0005863 striated muscle thick filament
4. *zgc:153704*	GO:0005488 binding GO:0005215 transporter activity	GO:0006629 lipid metabolic process GO:0006810 transport	GO:0005576 extracellular region
5. *myhz2*	GO:0005524 ATP binding GO:0003779 actin binding GO:0003774 motor activity GO:0000166 nucleotide binding	GO:0006950 response to stress GO:0006941 striated muscle contraction	GO:0016459 myosin complex GO:0005863 striated muscle thick filament
6. *tnni2a.4*	NA	NA	NA
7. *tmsb*	GO:0003779 actin binding	GO:0030036 actin cytoskeleton organization GO:0007010 cytoskeleton organization GO:0042989 sequestering of actin monomers	GO:0005737 cytoplasm GO:0005856 cytoskeleton
8. *hpd*	GO:0003868 4-hydroxyphenylpyruvate dioxygenase activity GO:0016702 oxidoreductase activity, acting on single donors	GO:0009072 aromatic amino acid family metabolic process	NA

9. *tyrp1b*	GO:0005507 copper ion binding GO:0046872 metal ion binding GO:0016491 oxidoreductase activity GO:0016716 oxidoreductase activity, acting on paired donors	GO:0042438 melanin biosynthetic process GO:0008152 metabolic process	GO:0033162 melanosome membrane
10. *zgc:114184*	NA	NA	NA
11. *fah*	GO:0003824 catalytic activity GO:0004334 fumarylacetoacetase activity GO:0016787 hydrolase activity	GO:0009072 aromatic amino acid family metabolic process GO:0008152 metabolic process	
12. *zgc:113456*	NA	NA	NA
13. *sox11a*	GO:0003677 DNA binding	NA	GO:0005634 nucleus
14. *myf5*	GO:0003677 DNA binding GO:0030528 transcription regulator activity	GO:0002074 extraocular skeletal muscle development GO:0007517 muscle development GO:0043282 pharyngeal muscle development GO:0045449 regulation of transcription GO:0006355 regulation of transcription, DNA-dependent GO:0048741 skeletal muscle fiber development	GO:0005730 nucleolus GO:0005654 nucleoplasm GO:0005634 nucleus
15. *fzd8a*	GO:0004930 G-protein coupled receptor activity GO:0004926 non-G-protein coupled 7TM receptor activity GO:0004872 receptor activity GO:0004871 signal transducer activity	GO:0007186 G-protein coupled receptor protein signaling pathway GO:0016055 Wnt receptor signaling pathway GO:0007166 cell surface receptor linked signal transduction GO:0007275 multicellular organismal	GO:0016021 integral to membrane GO:0016020 membrane
16. *zgc:112098*	GO:0005524 ATP binding GO:0005515 protein binding		GO:0005856 cytoskeleton

17. *aspn*	GO:0005515 protein binding	NA	GO:0016020 membrane
18. *cox6a1*	GO:0004129 cytochrome-c oxidase activity GO:0009055 electron carrier activity	NA	GO:0005740 mitochondrial envelope
19. *slc38a3*	NA	NA	GO:0016021 integral to membrane GO:0016020 membrane
20. *zgc:136591*	GO:0003735 structural constituent of ribosome	GO:0006412 translation	GO:0005622 intracellular GO:0005840 ribosome
21. *cth*	GO:0003824 catalytic activity GO:0016829 lyase activity GO:0030170 pyridoxal phosphate binding	GO:0006520 amino acid metabolic process	NA
23. *hhatla*	GO:0008415 acyltransferase activity GO:0016740 transferase activity	NA	GO:0016021 integral to membrane GO:0016020 membrane
24. *smyd2b*	GO:0008270 zinc ion binding		GO:0005634 nucleus
25. *myca*	GO:0003677 DNA binding GO:0003700 transcription factor activity GO:0030528 transcription regulator activity	GO:0045449 regulation of transcription GO:0006355 regulation of transcription, DNA-dependent GO:0006350 transcription	GO:0005634 nucleus
26. *fkbp1b*	GO:0003755 peptidyl-prolyl cis-trans isomerase activity	GO:0006457 protein folding	NA
27. *zgc:76872*	GO:0046872 metal ion binding GO:0003676 nucleic acid binding GO:0005515 protein binding GO:0008270 zinc ion binding	NA	GO:0005622 intracellular

28. *atp1b3a*	GO:0005391 sodium:potassium-exchanging ATPase activity	GO:0006754 ATP biosynthetic process GO:0006813 potassium ion transport GO:0006814 sodium ion transport	GO:0016020 membrane
29. *zgc:158803*			
30. *psma5*	GO:0004175 endopeptidase activity GO:0004298 threonine-type endopeptidase activity	GO:0006511 ubiquitin-dependent protein catabolic process	GO:0005829 cytosol GO:0005839 proteasome core complex GO:0043234 protein complex
31. *zgc:92347*			
31. *ctnna2*	GO:0005198 structural molecule activity	GO:0007155 cell adhesion	GO:0015629 actin cytoskeleton
33. *pdcl3*		GO:0006915 apoptosis	GO:0005737 cytoplasm
34. *ppia*	GO:0016853 isomerase activity GO:0003755 peptidyl-prolyl cis-trans isomerase activity		
35. *zgc:92624*	GO:0008270 zinc ion binding		GO:0005622 intracellular

Table 6.4 GO annotation of genes down-regulated in myotube (+) phenotype of zebrafish

Name of gene	Molecular function	Biological process	Cellular component
1. *pvalb4*	GO:0005509 calcium ion binding		
2. *b2m*	NA	GO:0006955 immune response GO:0002474 antigen processing and presentation of peptide antigen via MHC class I	GO:0042612 MHC class I protein complex GO:0005576 extracellular region
3. *zgc:56085*	NA	NA	NA
4. *c4a*	GO:0004866 endopeptidase inhibitor activity	NA	GO:0005576 extracellular region
5. *ckmt2*	GO:0003824 catalytic activity GO:0016301 kinase activity GO:0016772 transferase activity, transferring phosphorus-containing groups	NA	NA
6. *ppp1r3c*	NA	NA	NA
7. *gapdh*	GO:0004365 glyceraldehyde-3-phosphate dehydrogenase (phosphorylating) activity GO:0051287 NAD binding	GO:0008943 glyceraldehyde-3-phosphate dehydrogenase activity	GO:0006006 glucose metabolic process
8. *ckm*	GO:0003824 catalytic activity GO:0016301 kinase activity GO:0016772 transferase activity, transferring phosphorus-containing groups	NA	NA

9. *mt-coI*	GO:0005506 iron ion binding GO:0004129 cytochrome-c oxidase activity GO:0009055 electron carrier activity GO:0020037 heme binding GO:0005506 iron ion binding GO:0046872 metal ion binding GO:0016491 oxidoreductase activity	GO:0009060 aerobic respiration GO:0022900 electron transport chain GO:0055114 oxidation reduction GO:0046686 response to cadmium ion GO:0051597 response to methylmercury GO:0006810 transport	GO:0016021 integral to membrane GO:0016020 membrane GO:0005743 mitochondrial inner membrane GO:0005746 mitochondrial respiratory chain GO:0005739 mitochondrion
10. *hif1an*	GO:0005506 iron ion binding GO:0046872 metal ion binding GO:0016491 oxidoreductase activity GO:0016702 oxidoreductase activity, acting on single donors with incorporation of molecular oxygen GO:0004597 peptide-aspartate beta-dioxygenase activity	GO:0055114 oxidation reduction GO:0006355 regulation of transcription, DNA-dependent GO:0006350 transcription	GO:0005634 nucleus
11. *anxa2a*	GO:0005509 calcium ion binding GO:0005544 calcium-dependent phospholipid binding GO:0008092 cytoskeletal protein binding GO:0004859 phospholipase inhibitor activity	NA	NA
12. *c4-2*	NA	NA	NA
13. *cd9l*	NA	NA	GO:0016021 integral to membrane GO:0016020 membrane
14. *iclp1*	GO:0042289 MHC class II protein binding	GO:0019882 antigen processing and presentation GO:0006955 immune response GO:0006886 intracellular protein transport	GO:0016020 membrane
15. *ak1*	GO:0005524 ATP binding GO:0004017 adenylate kinase activity GO:0019205 nucleobase, nucleoside, nucleotide kinase activity	GO:0046034 ATP metabolic process GO:0006139 nucleobase, nucleoside, nucleotide and nucleic acid metabolic process	GO:0005737 cytoplasm

16. *ldha*	GO:0004459 L-lactate dehydrogenase activity GO:0005488 binding GO:0003824 catalytic activity GO:0016491 oxidoreductase activity GO:0016616 oxidoreductase activity, acting on the CH-OH group of donors, NAD or NADP as acceptor	GO:0019642 anaerobic glycolysis GO:0005975 carbohydrate metabolic process GO:0044262 cellular carbohydrate metabolic process GO:0006096 glycolysis GO:0008152 metabolic process GO:0055114 oxidation reduction GO:0001666 response to hypoxia	GO:0005737 cytoplasm
17. *mpz*	NA	NA	GO:0016020 membrane
18. *rgs5*	GO:0004871 signal transducer activity	NA	GO:0005575 cellular_component
19. *slc25a4*	GO:0005488 binding GO:0005215 transporter activity	GO:0006839 mitochondrial transport GO:0006810 transport	GO:0016021 integral to membrane GO:0016020 membrane GO:0005743 mitochondrial inner membrane GO:0005739 mitochondrion
20. *uqcrfs1*	GO:0051537 2 iron, 2 sulfur cluster binding GO:0009055 electron carrier activity GO:0016491 oxidoreductase activity GO:0008121 ubiquinol-cytochrome-c reductase activity	GO:0055114 oxidation reduction	GO:0016020 membrane
21. *eno3*	GO:0004634 phosphopyruvate hydratase activity	GO:0006096 glycolysis	GO:0000015 phosphopyruvate hydratase complex
22. *zgc:109940*	GO:0004252 serine-type endopeptidase activity	GO:0006508 proteolysis	GO:0005575 cellular_component
23. *cox6a2*	GO:0004129 cytochrome-c oxidase activity GO:0009055 electron carrier activity	NA	GO:0005740 mitochondrial envelope
24. *mfsd2b*	GO:0005215 transporter activity	GO:0006810 transport	GO:0016021 integral to membrane GO:0016020 membrane

25. *necab1*	GO:0003779 actin binding GO:0005509 calcium ion binding GO:0016491 oxidoreductase activity	GO:0017000 antibiotic biosynthetic process GO:0007010 cytoskeleton organization	GO:0005737 cytoplasm
26. *wu:fc83c01*	GO:0005524 ATP binding GO:0004672 protein kinase activity GO:0004674 protein serine/threonine kinase activity	GO:0006468 protein amino acid phosphorylation	NA
27. *tnk2*	GO:0005524 ATP binding GO:0016301 kinase activity GO:0000166 nucleotide binding GO:0004672 protein kinase activity GO:0004713 protein tyrosine kinase activity GO:0016740 transferase activity	GO:0006468 protein amino acid phosphorylation	GO:0005575 cellular_component
28. *mdh1b*	GO:0030060 L-malate dehydrogenase activity GO:0003824 binding GO:0003824 catalytic activity GO:0016615 malate dehydrogenase activity GO:0016491 oxidoreductase activity GO:0016616 oxidoreductase activity, acting on the CH-OH group of donors, NAD or NADP as acceptor	GO:0005975 carbohydrate metabolic process GO:0044262 cellular carbohydrate metabolic process GO:0006096 glycolysis GO:0006108 malate metabolic process GO:0008152 metabolic process	NA
29. *rtn4a*	NA	NA	GO:0005783 endoplasmic reticulum
30. *agbl5*	GO:0004181 metallocarboxypeptidase activity GO:0008270 zinc ion binding	GO:0006508 proteolysis	GO:0005737 cytoplasm GO:0005634 nucleus
31. *arl6ip1*	NA	NA	NA
32. *cox5b*	GO:0004129 cytochrome-c oxidase activity	NA	GO:0005740 mitochondrial envelope
33. *crebbpa*	GO:0004402 histone acetyltransferase activity GO:0005515 protein binding GO:0003713 transcription coactivator activity GO:0003712 transcription cofactor activity GO:0008270 zinc ion binding	GO:0016573 histone acetylation GO:0045449 regulation of transcription GO:0006355 regulation of transcription, DNA-dependent	GO:0000123 histone acetyltransferase complex GO:0005634 nucleus

34. *fgl2*	GO:0005102 receptor binding	GO:0007165 signal transduction	
35. *zgc:86773*	GO:0005524 ATP binding GO:0005525 GTP binding GO:0000166 nucleotide binding GO:0008134 transcription factor binding	GO:0015031 protein transport GO:0006355 regulation of transcription, DNA-dependent GO:0007264 small GTPase mediated signal transduction	GO:0005622 intracellular
36. *scinla*	GO:0003779 actin binding	GO:0007420 brain development GO:0009953 dorsal/ventral pattern formation GO:0001654 eye development	NA
37. *atp5i*	GO:0015078 hydrogen ion transmembrane transpc	GO:0015986 ATP synthesis coupled proton transp	GO:0000276 mitochondrial proton-transporting ATP synthase complex, coupling factor F(o)
38. *cryabb*	GO:0008168 methyltransferase activity GO:0003676 nucleic acid binding GO:0005212 structural constituent of eye lens GO:0051082 unfolded protein binding	GO:0032259 methylation GO:0009408 response to heat	GO:0005575 cellular_component
39. *hoxc8a*	GO:0003677 DNA binding GO:0043565 sequence-specific DNA binding GO:0003700 transcription factor activity	GO:0035118 embryonic pectoral fin morphogenesis IGI GO:0031018 endocrine pancreas development IGI GO:0007275 multicellular organismal development GO:0045449 regulation of transcription GO:0006355 regulation of transcription, DNA-	GO:0005634 nucleus
40. *gapdhs*	GO:0051287 NAD binding GO:0005488 binding GO:0003824 catalytic activity GO:0004365 glyceraldehyde-3-phosphate dehydrogenase (phosphorylating) activity GO:0008943 glyceraldehyde-3-phosphate dehydrogenase activity	GO:0006006 glucose metabolic process GO:0008152 metabolic process	GO:0005575 cellular_component

41. *tpi1b*	GO:0003824 catalytic activity GO:0016853 isomerase activity GO:0004807 triose-phosphate isomerase activity	GO:0006633 fatty acid biosynthetic process GO:0006094 gluconeogenesis GO:0006096 glycolysis GO:0008610 lipid biosynthetic process GO:0008152 metabolic process GO:0006098 pentose-phosphate shunt	NA
42. *cdkn3*	GO:0016791 phosphatase activity GO:0004725 protein tyrosine phosphatase activity	GO:0016311 dephosphorylation GO:0006470 protein amino acid dephosphorylation	NA
43. *grsf1*	GO:0003676 nucleic acid binding GO:0000166 nucleotide binding	NA	NA
44. *hc*	GO:0005488 binding GO:0005515 protein binding GO:0005198 structural molecule activity	GO:0006886 intracellular protein transport GO:0016192 vesicle-mediated transport	GO:0030132 clathrin coat of coated pit GO:0030130 clathrin coat of trans-Golgi network vesicle
45. *ldb3b*	GO:0005515 protein binding	NA	
46. *ndufb2*	NA	NA	
47. *uqcrb*	GO:0008121 ubiquinol-cytochrome-c reductase ac	GO:0006122 mitochondrial electron transport, ubiquinol to cytochrome c	
48. *ap2a1*	NA	NA	NA
49. *stka*	GO:0005524 ATP binding GO:0016301 kinase activity GO:0000287 magnesium ion binding GO:0046872 metal ion binding GO:0000166 nucleotide binding GO:0004672 protein kinase activity GO:0004674 protein serine/threonine kinase activity GO:0016740 transferase activity	GO:0007275 multicellular organismal development GO:0006468 protein amino acid phosphorylation	GO:0005634 nucleus
50. *atp5f1*	GO:0015078 hydrogen ion transmembrane transporter activity	GO:0015986 ATP synthesis coupled proton transp	GO:0000276 mitochondrial proton-transporting ATP synthase complex, coupling factor F(o)

Table 6.5 KEGG annotation of genes up-regulated in myotube (+) phenotype of zebrafish

Name of gene	KEGG Orthology	KEGG Pathway	KEGG brite
1. *myhz1-1*	K10352	ko04530 Tight junction	ko04812 Cytoskeleton proteins
2. *myhz1-2*	K10352	ko04530 Tight junction	ko04812 Cytoskeleton proteins
3. *myhz1-3*	K10352	ko04530 Tight junction	ko04812 Cytoskeleton proteins
4. *zgc:153704*	K01830	ko00590 Arachidonic acid metabolism	ko01000 Enzymes
5. *myhz2*	K10352	ko04530 Tight junction	ko04812 Cytoskeleton proteins
6. *tnni2a.4*	K10371	NA	ko04812 Cytoskeleton proteins
7. *tmsb*	K05764	ko04810 Regulation of actin cytoskeleton	ko00001 KEGG Orthology (KO)
8. *hpd*	K00457	ko00350 Tyrosine metabolism	NA
		ko00360 Phenylalanine metabolism	
9. *tyrp1b*	K00506	ko00350 Tyrosine metabolism	ko01000 Enzymes
		ko04916 Melanogenesis	NA
10. *zgc:114184*	K10372	NA	ko04812 Cytoskeleton proteins
11. *fah*	K01555	ko00350 Tyrosine metabolism	ko01000 Enzymes
		ko00643 Styrene degradation	
12. *zgc:113456*	K08121	NA	ko00535 Proteoglycans
13. *sox11a*	K09268	NA	ko03000 Transcription factors
14. *myf5*	K09064	NA	ko03000 Transcription factors
15. *fzd8a*	K02534	ko04310 Wnt signaling pathway	ko04000 Receptors and Channels
		ko04916 Melanogenesis	
		ko05210 Colorectal cancer	
		ko05217 Basal cell carcinoma	
16. *zgc:112098*	K10354	ko05110 Vibrio cholerae infection	ko04812 Cytoskeleton proteins

17. *aspn*	K08120	NA	ko00535 Proteoglycans
18. *cox6a1*	K02266	ko00190 Oxidative phosphorylation ko05010 Alzheimer's disease ko05012 Parkinson's disease	ko01000 Enzymes
19. *slc38a3*	NA	NA	NA
20. *zgc:136591*	NA	NA	NA
21. *cth*	K01758	ko00910 Nitrogen metabolism ko00260 Serine and threonine metabolism ko00271 Methionine metabolism ko00272 Cysteine metabolism ko00450 Selenoamino acid metabolism	ko01000 Enzymes
23. *hhatla*	NA	NA	NA
24. *smyd2b*	K11426	NA	NA
25. *myca*	K04377	ko04010 MAPK signaling pathway ko04012 ErbB signaling pathway ko04310 Wnt signaling pathway ko04350 TGF-beta signaling pathway ko04630 Jak-STAT signaling pathway ko05210 Colorectal cancer ko05216 Thyroid Cancer ko05221 Acute myeloid leukemia ko05220 Chronic myeloid leukemia ko05219 Bladder cancer ko05213 Endometrial cancer ko05222 Small cell lung cancer	ko03000 Transcription factors
26. *fkbp1b*	K09568	NA	ko03110 Chaperones and folding catalysts
27. *zgc:76872*	K10516	NA	ko04121 Ubiquitin System

28. *atp1b3a*	K01540	NA	ko04090 Cellular antigens
29. *zgc:158803*	NA	NA	NA
30. *psma5*	K02729	ko03050 Proteasome	ko01002 Peptidases
31. *zgc:92347*	NA	NA	NA
31. *ctnna2*	K05691	ko04520 Adherens junction	ko01000 Enzymes
		ko04530 Tight junction	
		ko04670 Leukocyte transendothelial migration	
		ko05213 Endometrial cancer	
33. *pdcl3*		NA	
34. *ppia*	K01802	NA	ko01000 Enzymes
35. *zgc:92624*	NA	NA	NA

Table 6.6 KEGG annotation of genes down-regulated in myotube (+) phenotype of zebrafish

Name of gene	KEGG Orthology	KEGG Pathway	KEGG brite
1. *pvalb4*	NA	NA	NA
2. *b2m*	K08055	ko04612 Antigen processing and presentation	NA
3. *zgc:56085*	NA	NA	NA
4. *c4a*	K03989	ko04610 Complement and coagulation cascades	NA
		ko05322 Systemic lupus erythematosus	NA
5. *ckmt2*	K00933	ko00330 Arginine and proline metabolism	NA
6. *ppp1r3c*	K07189	ko04910 Insulin signaling pathway	
7. *gapdh*	K00134	ko00010 Glycolysis / Gluconeogenesis	Enzymes
		ko05010 Alzheimer's disease	
		ko05040 Huntington's disease	
		ko05050 Dentatorubropallidoluysian atrophy (DRPLA)	
8. *ckm*	K00933	ko00330 Arginine and proline metabolism	Enzymes
9. *mt-coI*	K02256	ko00190 Oxidative phosphorylation	Enzymes
		ko05010 Alzheimer's disease	
		ko05012 Parkinson's disease	
10. *hif1an*	K00476	NA	Enzymes
11. *anxa2a*	NA	NA	NA
12. *c4-2*	NA	NA	NA
13. *cd9l*	K06460	ko04640 Hematopoietic cell lineage	Cellular antigens
14. *iclp1*	K06505	ko04612 Antigen processing and presentation	Cellular antigens, Proteoglycans
		ko00535 Proteoglycans	
		ko04090 Cellular antigens	
15. *ak1*	K00939	ko00230 Purine metabolism	Enzymes
16. *ldha*	K00016	ko00010 Glycolysis / Gluconeogenesis	Enzymes
		ko00620 Pyruvate metabolism	
		ko00640 Propanoate metabolism	
		ko00272 Cysteine metabolism	
17. *mpz*	K06770	ko04514 Cell adhesion molecules (CAMs)	Cell adhesion molecules (CAMs), CAM
18. *rgs5*	NA	NA	NA

19. *slc25a4*	K05863	ko04020 Calcium signaling pathway	NA
		ko05012 Parkinson's disease	
20. *uqcrfs1*	K00411	ko00190 Oxidative phosphorylation	Enzymes
		ko05010 Alzheimer's disease	
		ko05012 Parkinson's disease	
21. *eno3*	K01689	ko00010 Glycolysis / Gluconeogenesis	Enzymes
22. *zgc:109940*	K01334	ko04610 Complement and coagulation cascades	Enzymes, Peptidases
23. *cox6a2*	K02266	ko00190 Oxidative phosphorylation	Enzymes
		ko05010 Alzheimer's disease	
		ko05012 Parkinson's disease	
24. *mfsd2b*	NA	NA	NA
25. *necab1*	NA	NA	NA
26. *wu:fc83c01*	K11230	ko04011 MAPK signaling pathway - yeast	Enzymes, Protein kinases
27. *tnk2*	K08252	NA	Enzymes
28. *mdh1b*	K00026	ko00710 Carbon fixation in photosynthetic	Enzymes
		ko00620 Pyruvate metabolism	
		ko00720 Reductive carboxylate cycle (CO2	NA
		ko00630 Glyoxylate and dicarboxylate	NA
		ko00020 Citrate cycle (TCA cycle)	NA
29. *rtn4a*	NA	NA	
30. *agbl5*	NA	NA	
31. *arl6ip1*	NA	NA	
32. *cox5b*	K02265	ko00190 Oxidative phosphorylation	Enzymes
33. *crebbpa*	K04498	ko04916 Melanogenesis	Enzymes, Transcription factors
		ko04520 Adherens junction	
		ko04720 Long-term potentiation	
		ko05211 Renal cell carcinoma	
		ko04630 Jak-STAT signaling pathway	
		ko04330 Notch signaling pathway	
		ko05215 Prostate cancer	
		ko04350 TGF-beta signaling pathway	
		ko04910 Insulin signaling pathway	
		ko04310 Wnt signaling pathway	

34. *fgl2*	NA	NA	NA
35. *zgc:86773*	NA		
36. *scinla*	K05768	ko04810 Regulation of actin cytoskeleton	Cytoskeleton proteins
37. *atp5i*	K02129	ko00190 Oxidative phosphorylation	Enzymes
38. *cryabb*	K09542	NA	Chaperones and folding catalysts
39. *hoxc8a*	K09308	NA	Transcription factors
40. *gapdhs*	K10705	NA	Enzymes
41. *tpi1b*	K01803	ko00010 Glycolysis / Gluconeogenesis ko00710 Carbon fixation in photosynthetic ko00051 Fructose and mannose metabolism ko00031 Inositol metabolism	Enzymes
42. *cdkn3*	K01090		Enzymes
43. *grsf1*	NA	NA	
44. *hc*	K04646	ko05040 Huntington's disease	NA
45. *ldb3b*	NA		NA
46. *ndufb2*	K03958	ko00190 Oxidative phosphorylation	Enzymes
47. *uqcrb*	K00417	ko00190 Oxidative phosphorylation ko05010 Alzheimer's disease ko05012 Parkinson's disease	Enzymes
48. *ap2a1*	NA	NA	NA
49. *stka*	K11479		Enzymes, Protein kinases
50. *atp5f1*	K02127	ko00190 Oxidative phosphorylation ko05010 Alzheimer's disease ko05012 Parkinson's disease	Enzymes

AppendixII: List of manufacturers' addresses

Ambion, Cambridgeshire, UK

Applied Biosystems, Cheshire, UK

BDH, Poole, UK

Bioline, London, UK

Bio-Rad, Hertfordshire, UK

Dako UK Ltd, Cambridgeshire, UK

Millipore, Hertfordshire, UK

NanoDrop Technologies, Delaware, USA

New England Biolabs, Hertfordshire, UK

Nikon, Surrey, UK

Promega, Hampshire, UK

Qiagen, West Sussex, UK

Roche, Sussex, UK

Sigma, Dorset, UK

Thermo Electron Corporation, Waltham, Massachusetts, USA

Zeiss, Warwickshire, UK

ZM Ltd, Winchester, UK